Università degli studi di Roma Tor Vergata

facoltà di ingegneria

Dottorato di Ricerca in

Informatica e Ingegneria dell'Automazione

Ciclo XX

Trajectory tracking in switched systems: an internal model principle approach. The elliptical billiard system as a benchmark for theory

Candidato: Relatore:

Alessandro Potini   *Prof. Antonio Tornambè*

Co-relatori: Coordinatore:

Prof. Chaouki T. Abdallah   *Prof. Daniel P. Bovet*

ii

Trajectory tracking in switched systems: an internal model principle approach. The elliptical billiard system as a benchmark for theory

Advisor
Prof. Antonio Tornambè

Coordinator
Prof. Daniel P. Bovet

ii

The most important things in life aren't things

iv

Acknowledgments

Foremost, I would like to express my deep gratitude to my thesis supervisor, Prof. Antonio Tornambè. He has been an advisor and supporter throughout my PhD studies. His instruction and encouragement have been fundamental in both my professional and personal experience.

I also thank the other professors at the "Dipartimento Informatica, Sistemi e Produzione (DISP), University of Rome Tor Vergata ", Prof. Alessandro Astolfi, Dr. Sergio Galeani, Prof. Osvaldo Maria Grasselli, Dr. Francesco Martinelli, Prof. Laura Menini, Prof. Salvatore Nicosia and Prof. Luca Zaccarian for their helpful comments and assistance throughout. I am particularly indebted with Dr. Sergio Galeani. He has long been there to listen and to offer sound and quick advice on both technical and professional matters. Further, this work was greatly improved by the suggestions of Prof. Laura Menini.

Thanks must also go to colleagues and friends at DISP, Giuseppe Viola, Simona Onori, Serena Pani, Claudio Argento, Daniele Carnevale, Fabio Piedimonte, Fulvio Forni for their important support especially during the most tiring moments. We enjoyed our time together. A special thank is due to Giuseppe Viola for his generous understanding of my tedious problems.

My period at " University of New Mexico, Albuquerque " with Prof Chaouki T. Abdallah and Prof. Peter Dorato was particularly enjoyable and instructive. I also thank my friend Joud Khoury for introducing me to the wonderful world of ABQ by night.

Last but not least, I would like to thank girlfriend, the friends and fam-

ily who have always been there, despite the ravages of time and distance. Thanks Cesca for your sweetness and tenderness. Thanks Alessandro, Luca, Alberto, Angelo, Mirko, Christian, Francesco for your real friendship. Thanks Emanuela, Davide, Matteo and Flavio for your affection. Mom and Dad, thanks for everything! Without you nothing makes sense.

Contents

List of Figures

Chapter 1

Introduction

Mechanical systems with impacts are nonsmooth dynamical systems with trajectories possessing intervals of continuity (flow) and points of discontinuity (jumps). Several frameworks for modeling this class of systems have been proposed in the literature including Poincaré map modeling [18, 80, 88, 73], dynamical systems with unilateral constraints [14, 73, 17], measure differential inclusions [60, 59], and many others.

Control problems for systems subject to impacts [14] are of interest in a variety of applications, especially in robotics, e.g., hopping [72] or walking robots [61, 45, 84], juggling robots [18, 17], hammering tasks [46]. Among a number of important stabilization tasks for these systems, the problem of stabilization of rhythmic patterns has received great attention from the engineering and neuroscience community because of its relevance in robotics and nature.

Mechanical systems subject to jumps form a subset of the more general class of dynamical complementary systems (see [40] for an excellent overview on modeling, analysis and control for such systems). The problem of trajectory tracking for such a class of systems has been tackled recently in [16, 15, 9, 69, 70, 65, 56]. In [65] a discontinuous control algorithm is designed to regulate the system onto the constraint surface in finite time using results from nonsmooth Lyapunov theory (see, e.g., [74]). Control of "complete robotic tasks" [58]

including free motion, constrained motion and impacting phases is studied for rigid manipulators in [16, 15, 9, 69, 70]. More precisely, in [16, 15, 9] a control scheme based on "classical" nonlinear controllers (like passivity-based, etc.) adapted to the nonsmoothness of the problem is presented, which ensures stable tracking of some reference trajectories. On the other hand, [69, 70] propose an event-based control-switching strategy that includes a stable discontinuous controller for the transition phases.

A widely used benchmark system for this type of task is the simple, but rich in dynamics, model of a mechanical system with impacts which is referred to as *Birkhoff billiards*. In [56] PD-like control inputs are used to asymptotically stabilize particular periodic trajectories for a planar mechanical system inside a Birkhoff circular billiard, whereas in [33] and [32] a more general tracking problem has been considered for the elliptical billiard system. In [73] and [35] stabilization results for periodic orbits of the controlled wedge billiard are obtained.

Mechanical systems subject to impacts (e.g., billiard systems) are a particular example of *switched systems*. A switched system is a hybrid dynamical system consisting of a family of continuous-time subsystems and a rule that orchestrates the switching between them [53]. The theory of such systems is related to the study of hybrid systems, which has recently attracted considerable attention among control theorists, computer scientists, and practicing engineers. Concerning the stability analysis and control synthesis for this class of systems a lot of work has been done, nevertheless there are very few works on the trajectory tracking problem that have been published to date in the control literature.

In the present work, by using an internal model principle approach, a formal solution to the problem of asymptotically tracking some reference signals for a particular class of *linear* switched systems is obtained. The main topics of the thesis are:

- ***Asymptotic trajectory tracking in the elliptical billiard system***:

a tracking control problem taking into account the hybrid nature of the considered system is properly defined by using notions similar to the *quasi stability* concept proposed in [50] for impulsive differential systems. A switching strategy based on a discontinuous version of the internal model principle is proposed and the control result is formally proved.

- ***Robust asymptotic trajectory tracking in the elliptical billiard system***: the possible presence of uncertainties on the system parameters is considered for the control problem definition and solution. An algorithm for estimating the correct jumps for the dynamical compensator is also given.

- ***Robust asymptotic trajectory tracking in linear switched systems***: in this part an attempt to generalize the results obtained for the billiard system is discussed. At the end, a nonsmooth version of the internal model principle is proposed for a class of switched systems with linear dynamics between the switching events.

Chapter 2

Background material

In this chapter, some background material is reported for the benefits of the reader. Topics reviewed are the classical elliptical billiard system, an overview about hybrid and switched systems and the constrained polynomial interpolation with application to the trajectory planning.

2.1 The classical elliptical billiard system

The notion of billiard system was introduced by Birkhoff [7], and from then on it became a challenging research field, which has attracted the attention of researchers from mathematics, engineering and physics, where billiards are used to investigate the transition from quantum mechanics to classical mechanics [86]. A lot of work has been done to study the properties of trajectories followed by a *free* particle inside *classical* billiards of different shape, that is when no control is exerted on the moving mass (see, e.g., [48]). On the other hand, for their particular dynamical features, *controlled* billiards, that is when control forces acting on the moving body are considered, are a very interesting benchmark (see, e.g., [73, 35, 56]) for studying many control problems as it will be shown in Chapters 3, 4 and 5.

Remark 1. Unless otherwise stated, whenever in Chapter 2 the elliptical bil-

liards is referred to, it is intended as "classical elliptical billiards"; whereas in Chapters 3, 4 and 5, it has to be intended as "controlled elliptical billiards".

In the following, after some preliminaries, the notion of caustic curve is introduced and the Hamilton-Jacobi theory is used to show a fundamental dynamical property of the classical elliptical billiard system. In the last part of this section, important results about the existence and the computation of periodic paths inside the elliptical billiards are given together with some numerical examples.

2.1.1   Preliminaries

Consider a dimensionless body having unitary mass (*particle*), which moves on a horizontal plane, constrained to move inside a convex domain with an ellipse as boundary curve. The particle bounces at the boundary according to the reflection law (i.e., the angle of incidence is equal to the angle of reflection) and follows a straight-line path between two consecutive impacts [7]. This dynamical system is known as *the classical elliptical billiard system* (see Fig. 2.1). Concerning the elliptic boundary, from a geometric point of view,
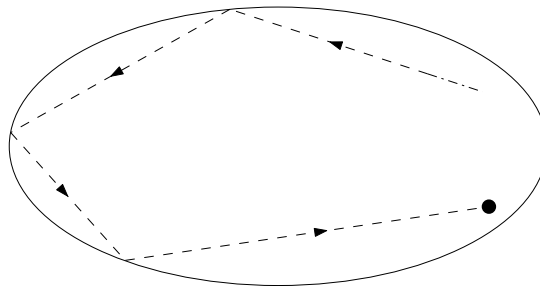
Figure 2.1: The classical elliptical billiard system.

an ellipse is defined as the locus of points whose sum of distances to two given points F_1 and F_2 (called *foci*) is fixed. In the cartesian coordinates, the equation of an ellipse centered at the origin with a and b ($b < a$) the semi-major

and semi-minor axis, respectively, is

$$\frac{x^2}{a^2} + \frac{y^2}{b^2} = 1. \tag{2.1}$$

Such an ellipse has foci with coordinates $(\pm f, 0)$, where $f := \sqrt{a^2 - b^2}$, and eccentricity $e := \frac{f}{a} = \frac{\sqrt{a^2 - b^2}}{a}$ (see Fig. 2.2).
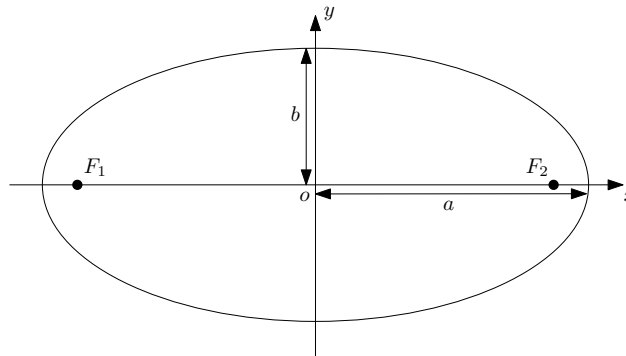
Figure 2.2: Ellipse of equation: $\frac{x^2}{a^2} + \frac{y^2}{b^2} = 1$.

2.1.2 Elliptical billiard paths: the notion of caustic curve

The path described by a particle moving inside an elliptical billiards along straight-lines and reflecting from the boundary according to the reflection law is in general open, and it forms a dense subset of the region bounded by a *caustic* curve and the boundary (see, e.g., [24]). The concept of caustic plays a fundamental role in the study of paths in elliptical billiards.

Definition 1. A *caustic* is a smooth and convex curve inside the billiard table such that if a segment (or its continuation) of a billiard path is tangent to it, then so is every other reflected segment (or its continuation) of the same path.

The following theorem asserts the existence of caustics for each path inside an elliptic billiards.

Theorem 1. *Every segment of a path in an elliptical billiards is always tangent to a unique conic confocal with the given ellipse (the boundary of the billiards) of foci F_1 and F_2. In particular the caustic curve will be:*

- *a confocal ellipse if the initial segment of the billiard path falls outside the foci;*

- *a confocal hyperbole if the initial segment of the billiard path falls between the foci.*

Proof. By following the guidelines given in [52] and [22], the existence of the caustic curve in the case in which it is a confocal and inner ellipse can be proved by simple geometric considerations. In a wholly similar way, a geometric proof can also be given in order to prove the existence of a confocal hyperbole caustic (that is, when the first segment of the billiard path crosses the x-axis between the foci).

Consider two consecutive segments of a billiard path: $\overline{A_0A_1}$ and $\overline{A_1A_2}$ (where α is the angle of incidence, which is equal to the angle of reflection at point A_1), and assume that the first segment intersects the x-axis outside the segment $\overline{F_1F_2}$ (see Fig. 2.3). By considering the optical property of the
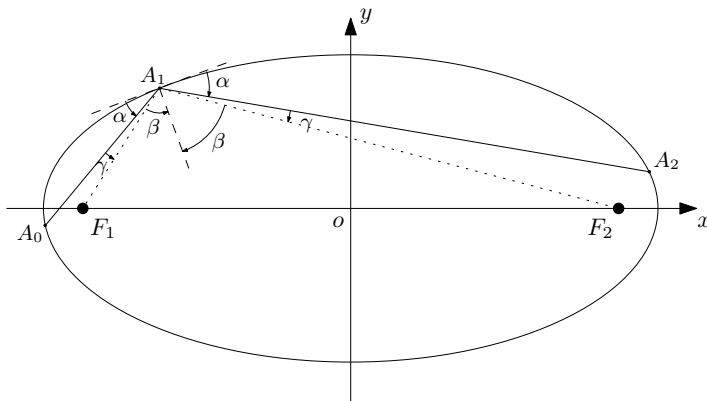
Figure 2.3: The first segment of the billiard path intersects the x-axis outside the foci.

foci of the elliptic boundary (namely, each segment passing through a focus is

always reflected to the other one), the following relation between angles can be shown: $\angle A_0 A_1 F_1 = \angle F_2 A_1 A_2 =: \gamma$, which is depicted in Fig. 2.3, where β is the angle between the segment $\overline{F_2 A_1}$ (or, analogously, $\overline{F_1 A_1}$) and the normal vector with respect to the elliptic boundary at point A_1.

Let F_1' and F_2' be the reflections of the foci F_1 and F_2 with respect to the segments $\overline{A_0 A_1}$ and $\overline{A_1 A_2}$, respectively, and define the point X as the intersection between the segments $\overline{A_0 A_1}$ and $\overline{F_1' F_2}$ (i.e., $X = \overline{A_0 A_1} \cap \overline{F_1' F_2}$), and the point Y as the intersection of $\overline{A_1 A_2}$ with $\overline{F_1 F_2'}$ (i.e., $Y = \overline{A_1 A_2} \cap \overline{F_1 F_2'}$), see Fig. 2.4. By considering an ellipse $\mathcal{E}_1$ confocal with the elliptic boundary
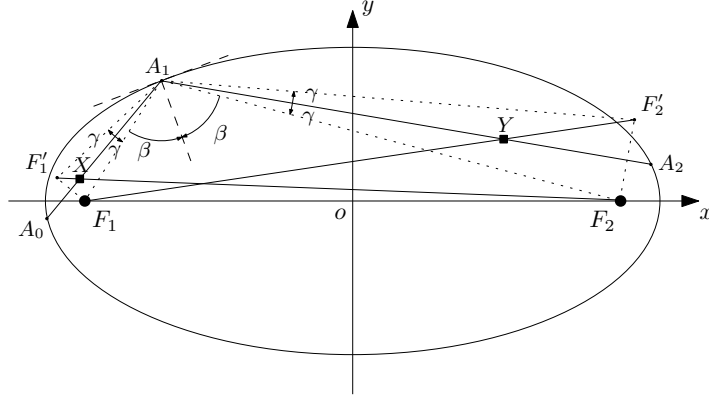
Figure 2.4: Graphical construction of points X and Y.

and tangent to the segment $\overline{A_0 A_1}$, since the angles $\angle F_2 X A_1$ and $\angle F_1 X A_0$ are equal (see Fig. 2.5), it follows that such an ellipse touches the segment $\overline{A_0 A_1}$ exactly at the point X. In the same way, it can be proved that an ellipse $\mathcal{E}_2$ with foci F_1 and F_2 is tangent to the segment $\overline{A_1 A_2}$ at the point Y. In order to complete the proof, it is necessary to show that these two ellipses $\mathcal{E}_1$ and $\mathcal{E}_2$ are actually the same. By the definition of the ellipse, this is equivalent to prove that the points X and Y are both on the same ellipse with foci F_1 and F_2, or, in other words, that $|\overline{F_1 X}| + |\overline{F_2 X}| = |\overline{F_1 Y}| + |\overline{F_2 Y}|$. By construction, this is analogous to show that $|\overline{F_1' F_2}| = |\overline{F_1 F_2'}|$. At this point, one can observe that the triangle $\widehat{F_1 A_1 F_2'}$ is congruent to the triangle $\widehat{F_1' A_1 F_2}$ (see Fig. 2.6),
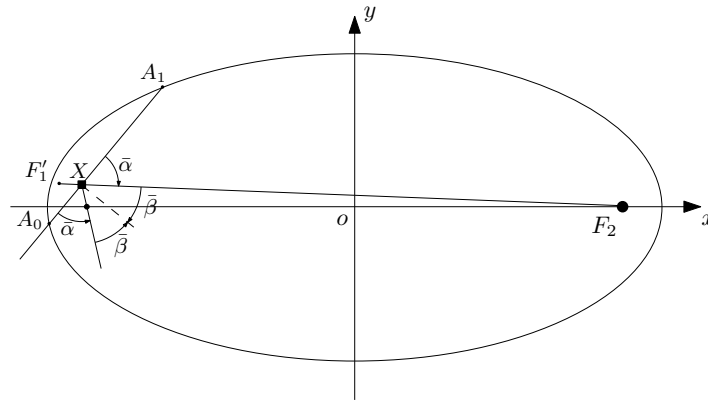
Figure 2.5: An ellipse confocal with the elliptic boundary and tangent to the segment $\overline{A_0 A_1}$ touches such a segment at the point X.

so that $|\overline{F_1' F_2}| = |\overline{F_1 F_2'}|$. With analogous reasonings, one can prove that all reflections of the path are tangent to the same inner ellipse, as shown in Fig. 2.7.   □
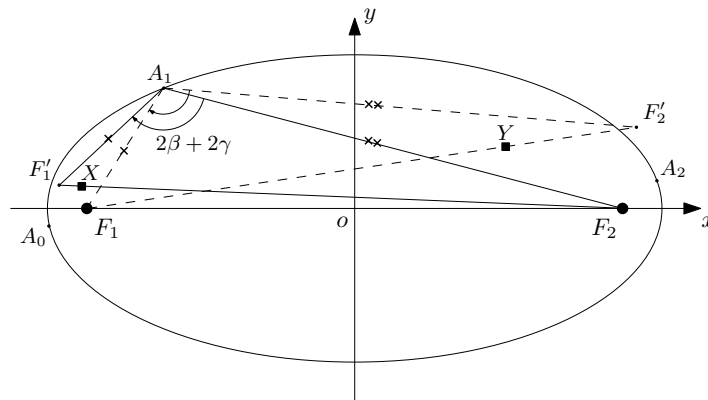
Figure 2.6: Triangle $\widehat{F_1 A_1 F_2'}$ is congruent to the triangle $\widehat{F_1' A_1 F_2}$.

Once the existence of the inner caustic curve has been proved, a path inside an elliptical billiards can be described as a collection of straight-line segments joining on the outer ellipse (the billiard boundary), and tangent to the (inner and confocal) caustic curve. Of particular interest is the case of closed orbits,
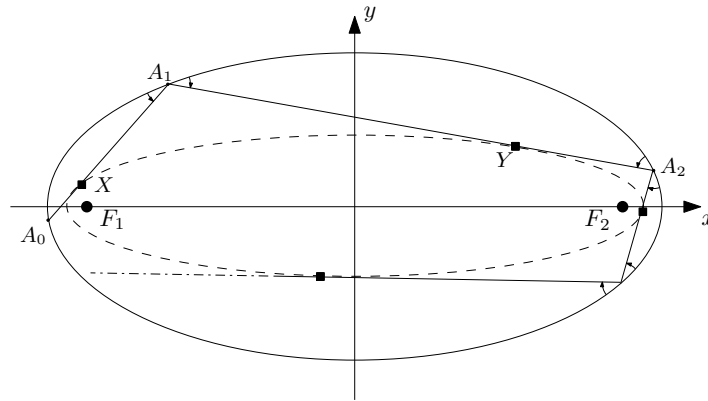
Figure 2.7: The confocal (inner) elliptic caustic curve.

i.e., periodic paths, inside the elliptical billiards, which is the main topic of Section 2.1.4, but first the most important dynamical property of the elliptical billiards is discussed.

2.1.3 Integrability of the elliptical billiard system

In the following, the Hamilton-Jacobi theory is used to show that the system constituted by a dimensionless body of unitary mass (particle) moving inside an elliptical billiards (*the classical elliptical billiard system*) is a Hamiltonian integrable system [79].

Definition 2. A Hamiltonian system with n degrees of freedom is *Hamilton integrable* if it has n constants of motion.

The Hamiltonian approach is used in classical mechanics to describe the motion of a physical system in term of first-order equations of motion in the phase space [36]. The main purpose of the Hamilton-Jacobi method is to find a canonical change of variables which reduces the Hamiltonian function to a form for which the Hamiltonian equations are integrable (e.g., in the plane, the system has two constant of the motion). The canonical transformation of variables is given by a generation function satisfying the Hamilton-Jacobi partial differential equation.

Integrable systems are very rare but they play a fundamental role in physics because only these systems can be solved in a complete analytical form and, moreover, the motion of an integrable system is regular and predictable. An important property of the elliptical billiard system is given by the following result.

Theorem 2. *The elliptical billiard system is an integrable system.*

Proof. In the following, the guidelines given in [24], [22] and [75] are followed. The dynamics of a particle, moving in an elliptical billiard table, between two consecutive bounces (the potential energy is assumed to be zero on the table: $U(\mathbf{q}) = 0$) are completely characterized by its Lagrangian function:

$$L = \frac{1}{2}(\dot{x}^2 + \dot{y}^2). \tag{2.2}$$

The momenta conjugate to x and y are defined as $p_x := \frac{\partial L}{\partial \dot{x}} = \dot{x}$ and $p_y := \frac{\partial L}{\partial \dot{y}} = \dot{y}$ and the Hamiltonian can be computed as $H(\mathbf{q}, \mathbf{p}, t) = \mathbf{q}^T \dot{\mathbf{p}} - L(\mathbf{q}, \dot{\mathbf{q}}, t)$,[1] where $\mathbf{q} := \begin{bmatrix} x & y \end{bmatrix}^T$ is the vector of the generalized coordinates, $\mathbf{p} := \begin{bmatrix} p_x & p_y \end{bmatrix}^T$ is the vector of the conjugate momenta and L is the Lagrangian, so that

$$H = \frac{1}{2}(\dot{p_x}^2 + \dot{p_y}^2). \tag{2.3}$$

By using the elliptical coordinates [85]:

$$\begin{cases} x = f \cosh(\rho)\cos(\theta), \\ y = f \sinh(\rho)\sin(\theta), \end{cases} \tag{2.4}$$

where $f := \sqrt{a^2 - b^2}$ is the semi-focal distance of the elliptic boundary, the curves with $\rho = const$ are ellipses, whereas the curves with $\theta = const$ are hyperboles. Both families of curves are confocal with the elliptical boundary.

---

[1]In this case, the Hamiltonian is equal to the total energy E, i.e., $H = E = T$, where T is the kinetic energy.

As a matter of fact, if $\rho = const$, then

$$
\begin{cases}
x^2 = f^2 \cosh^2(\rho) \cos^2(\theta) \\
y^2 = f^2 \sinh^2(\rho) \sin^2(\theta)
\end{cases}
\Rightarrow
\frac{x^2}{\bar{a}^2} + \frac{y^2}{\bar{b}^2} = \cos^2(\theta) + \sin^2(\theta) = 1, \quad (2.5)
$$

where $\bar{a} := f \cosh(\rho)$ and $\bar{b} := f \sinh(\rho)$. On the other hand, if $\theta = const$, then

$$
\begin{cases}
x^2 = f^2 \cos^2(\theta) \cosh^2(\rho) \\
y^2 = f^2 \sin^2(\theta) \sinh^2(\rho)
\end{cases}
\Rightarrow
\frac{x^2}{\underline{a}^2} - \frac{y^2}{\underline{b}^2} = \cosh^2(\theta) - \sinh^2(\theta) = 1, \quad (2.6)
$$

where $\underline{a} := f \cos(\theta)$ and $\underline{b} := f \sin(\theta)$.

In order to obtain the Lagrangian and the Hamiltonian in terms of the elliptical coordinates, the derivative with respect to time t of (2.4) is taken as follows:

$$
\begin{cases}
\dot{x} = f \sinh(\rho) \cos(\theta)\dot{\rho} - f \cosh(\rho) \sin(\theta)\dot{\theta}, \\
\dot{y} = f \cosh(\rho) \sin(\theta)\dot{\rho} + f \sinh(\rho) \cos(\theta)\dot{\theta},
\end{cases}
\quad (2.7)
$$

so that (2.2) becomes

$$
L = \frac{1}{2} f^2 (\sinh^2(\rho) + \sin^2(\theta))(\dot{\rho}^2 + \dot{\theta}^2). \quad (2.8)
$$

As for the momenta conjugate to ρ and θ, one obtains

$$
p_\rho = \frac{\partial L}{\partial \dot{\rho}} = f^2 (\sinh^2(\rho) + \sin^2(\theta))\dot{\rho} \Rightarrow \dot{\rho} = \frac{p_\rho}{f^2 (\sinh^2(\rho) + \sin^2(\theta))}, \quad (2.9)
$$

$$
p_\theta = \frac{\partial L}{\partial \dot{\theta}} = f^2 (\sinh^2(\rho) + \sin^2(\theta))\dot{\theta} \Rightarrow \dot{\theta} = \frac{p_\theta}{f^2 (\sinh^2(\rho) + \sin^2(\theta))}, \quad (2.10)
$$

and the Hamiltonian becomes

$$
H = \mathbf{p}^T \dot{\mathbf{q}} - L(\rho, \dot{\rho}, \theta, \dot{\theta}) = \frac{p_\rho^2 + p_\theta^2}{2 f^2 (\sinh^2(\rho) + \sin^2(\theta))}, \quad (2.11)
$$

where, with a slight abuse of notation, $\mathbf{q} := \begin{bmatrix} \rho & \theta \end{bmatrix}^T$ and $\mathbf{p} := \begin{bmatrix} p_\rho & p_\theta \end{bmatrix}^T$.

At this point, by introducing the Jacobi variables λ_1 and λ_2 (see, e.g.,

[36, 22]), the ellipse (2.5) characterized by $\rho = const$ can be expressed as

$$\frac{x^2}{A - \lambda_1} + \frac{y^2}{B - \lambda_1} = 1, \tag{2.12}$$

where $A := a^2$ and $B := b^2$. By the definition of $\bar{a}$ and $\bar{b}$ in (2.5), it follows that

$$A - \lambda_1 = \bar{a}^2 = f^2 \cosh^2(\rho), \tag{2.13}$$

$$B - \lambda_1 = \bar{b}^2 = f^2 \sinh^2(\rho). \tag{2.14}$$

Note that if $\lambda_1 = 0$, then (2.12) coincides with the elliptic boundary, whereas if $\lambda_1 = A$, then it coincides with the y-axis;[2] analogously if $\lambda_1 = B$, then it coincides with the x-axis.

In the same way, the hyperbole characterized by $\theta = const$ can be described by

$$\frac{x^2}{A - \lambda_2} + \frac{y^2}{B - \lambda_2} = 1, \tag{2.15}$$

where

$$A - \lambda_2 = \underline{a}^2 = f^2 \cos^2(\theta), \tag{2.16}$$

$$B - \lambda_2 = -\underline{b}^2 = -f^2 \sin^2(\theta). \tag{2.17}$$

Note that if $\lambda_2 = A$, then (2.15) coincides with the y-axis, whereas if $\lambda_2 = B$, then it coincides with the x-axis.

By (2.13) and (2.16), it follows that $A > \lambda_1$, $B > \lambda_1$ and $A > \lambda_2$, $B < \lambda_2$, respectively, so that

$$-\infty < \lambda_1 < B < \lambda_2 < A. \tag{2.18}$$

Note that, the change of variables from (x, y) to (λ_1, λ_2) is not 1-to-1. In

---

[2]In fact,

$$\frac{x^2}{A - \lambda_1} + \frac{y^2}{B - \lambda_1} = 1 \Rightarrow x^2 + \frac{A - \lambda_1}{B - \lambda_1} y^2 = A - \lambda_1,$$

so that substituting $\lambda_1 = A$ implies that $x = 0$, i.e., the equation of the y-axis.

fact, points $(x, y), (x, -y), (-x, y)$ and $(-x, -y)$ are mapped into the same point (λ_1, λ_2) (see (2.12) and (2.15)). However, λ_1 and λ_2 are single-variable function with respect to ρ and θ.

In order to obtain the Lagrangian and the Hamiltonian in terms of λ_1 and λ_2, preliminary computations are necessary. In particular, by using (2.13), one has

$$(A - \lambda_1) + (B - \lambda_1) = f^2(\cosh^2(\rho) + \sin^2(\theta)) = (A - B)(1 + 2\sinh^2(\rho))$$

$$\Updownarrow$$

$$\frac{1}{2}(\frac{A + B - 2\lambda_1}{A - B} - 1) = \sinh^2(\rho)$$

$$\Updownarrow$$

$$\sinh^2(\rho) = \frac{B - \lambda_1}{A - B}, \tag{2.19}$$

where the equation $f^2 = a^2 - b^2 = A - B$ has been used, and by taking the positive square root of (2.19),[3] one obtains

$$\rho = \operatorname{arcsinh}\left(\sqrt{\frac{B - \lambda_1}{A - B}}\right). \tag{2.20}$$

With analogous reasonings, θ can be obtained in terms of λ_2 as follows:

$$(A - \lambda_2) + (B - \lambda_2) = f^2(\cos^2(\theta) - \sin^2(\theta)) = (A - B)(1 - 2\sin^2(\theta))$$

$$\Updownarrow$$

$$-\frac{1}{2}(\frac{A + B - 2\lambda_2}{A - B} - 1) = \sin^2(\theta)$$

$$\Updownarrow$$

$$\sin^2(\theta) = \frac{B - \lambda_2}{B - A}, \tag{2.21}$$

___
[3]Since $\arcsin(-x) = -\arcsin(x)$ and $\operatorname{arcsinh}(-x) = -\operatorname{arcsinh}(x)$, such a particular choice does not affect the computation of L and H.

so that, by taking the positive square root of (2.21), one obtains

$$\theta = \arcsin\left(\sqrt{\frac{B - \lambda_2}{B - A}}\right). \tag{2.22}$$

By using (2.20) and (2.22), also $\dot\rho$ and $\dot\theta$ can be rewritten in terms of λ_1 and λ_2. In particular, as for $\dot\rho$, one has

$$\dot\rho = -\frac{1}{2}\frac{1}{A - B}\frac{1}{\sqrt{1 + \frac{B - \lambda_1}{A - B}}}\frac{1}{\sqrt{\frac{B - \lambda_1}{A - B}}}\dot\lambda_1 = -\frac{1}{2}\frac{1}{A - B}\frac{1}{\sqrt{\frac{A - \lambda_1}{A - B}}}\frac{1}{\sqrt{\frac{B - \lambda_1}{A - B}}}\dot\lambda_1 =$$

$$= -\frac{1}{2}\frac{1}{\sqrt{A - \lambda_1}}\frac{1}{\sqrt{B - \lambda_1}}\dot\lambda_1,$$

so that

$$\dot\rho^2 = \frac{1}{4(A - \lambda_1)(B - \lambda_1)}\dot\lambda_1^2. \tag{2.23}$$

On the other hand, concerning the computation of $\dot\theta$, one has

$$\dot\theta = -\frac{1}{2}\frac{1}{B - A}\frac{1}{\sqrt{1 - \frac{B - \lambda_2}{B - A}}}\frac{1}{\sqrt{\frac{B - \lambda_2}{B - A}}}\dot\lambda_2 = -\frac{1}{2}\frac{1}{B - A}\frac{1}{\sqrt{\frac{-A + \lambda_2}{B - A}}}\frac{1}{\sqrt{\frac{B - \lambda_2}{B - A}}}\dot\lambda_2 =$$

$$= -\frac{1}{2}\frac{1}{\sqrt{-A + \lambda_2}}\frac{1}{\sqrt{B - \lambda_2}}\dot\lambda_2,$$

that is

$$\dot\theta^2 = -\frac{1}{4(A - \lambda_2)(B - \lambda_2)}\dot\lambda_2^2, \tag{2.24}$$

where the following facts: $\frac{d}{dx}\operatorname{arcsinh}(x) = \frac{1}{\sqrt{1 + x^2}}$ and $\frac{d}{dx}\arcsin(x) = \frac{1}{\sqrt{1 - x^2}}$ have been used. Finally, since $(B - \lambda_1) - (B - \lambda_2) = \lambda_2 - \lambda_1 = f^2(\sinh^2(\rho) + \sin^2(\theta))$, the Lagrangian (2.8) with respect to λ_1 and λ_2 is given by

$$L = \frac{1}{2}(\lambda_2 - \lambda_1)\left(\frac{1}{4(A - \lambda_1)(B - \lambda_1)}\dot\lambda_1^2 - \frac{1}{4(A - \lambda_2)(B - \lambda_2)}\dot\lambda_2^2\right) =$$

$$= \frac{1}{2}\left(\frac{\lambda_2 - \lambda_1}{4(A - \lambda_1)(B - \lambda_1)}\dot\lambda_1^2 + \frac{\lambda_1 - \lambda_2}{4(A - \lambda_2)(B - \lambda_2)}\dot\lambda_2^2\right). \tag{2.25}$$

At this point, the momenta conjugate to λ_1 and λ_2 are computed as:

$$p_{\lambda_1} = \frac{\partial L}{\partial \lambda_1} = \frac{\lambda_2 - \lambda_1}{4(A - \lambda_1)(B - \lambda_1)} \dot{\lambda}_1, \qquad (2.26)$$

$$p_{\lambda_2} = \frac{\partial L}{\partial \lambda_2} = \frac{\lambda_1 - \lambda_2}{4(A - \lambda_2)(B - \lambda_2)} \dot{\lambda}_2, \qquad (2.27)$$

and the Hamiltonian with respect to λ_1 and λ_2 is

$$H = \mathbf{p}^T \dot{\mathbf{q}} - L(\lambda_1, \dot{\lambda}_1, \lambda_2, \dot{\lambda}_2) =$$
$$= \frac{1}{2} \left(\frac{4(A - \lambda_1)(B - \lambda_1)}{\lambda_2 - \lambda_1} p_{\lambda_1}^2 + \frac{4(A - \lambda_2)(B - \lambda_2)}{\lambda_1 - \lambda_2} p_{\lambda_2}^2 \right), \qquad (2.28)$$

where $\mathbf{q} := \begin{bmatrix} \lambda_1 & \lambda_2 \end{bmatrix}^T$ and $\mathbf{p} := \begin{bmatrix} p_{\lambda_1} & p_{\lambda_2} \end{bmatrix}^T$.

Now, by introducing the generating function S such that $\mathbf{p} = \frac{\partial S}{\partial \mathbf{q}}$, the Hamiltonian given by (2.28) becomes

$$H(\mathbf{q}, \frac{\partial S}{\partial \mathbf{q}}) =$$
$$= \frac{1}{2} \left(\frac{4(A - \lambda_1)(B - \lambda_1)}{\lambda_2 - \lambda_1} \left(\frac{\partial S}{\partial \lambda_1} \right)^2 + \frac{4(A - \lambda_2)(B - \lambda_2)}{\lambda_1 - \lambda_2} \left(\frac{\partial S}{\partial \lambda_2} \right)^2 \right) =$$
$$= \alpha,$$

so as to obtain the *Hamilton-Jacobi equation* in terms of λ_1 and λ_2, where α denotes the total energy of the system, that is the "first constant of motion". In order to achieve the separation of variables, it is assumed that $S(\lambda_1, \lambda_2) = S_1(\lambda_1) + S_2(\lambda_2)$, so that

$$\frac{1}{2} \left(\frac{4(A - \lambda_1)(B - \lambda_1)}{\lambda_2 - \lambda_1} \left(\frac{\partial S_1}{\partial \lambda_1} \right)^2 + \frac{4(A - \lambda_2)(B - \lambda_2)}{\lambda_1 - \lambda_2} \left(\frac{\partial S_2}{\partial \lambda_2} \right)^2 \right) = \alpha,$$

and multiplying both sides by $\lambda_2 - \lambda_1$ and separating all terms that depend

by λ_1 from the terms that depend by λ_2 imply that

$$2(A-\lambda_1)(B-\lambda_1)\left(\frac{\partial S_1}{\partial \lambda_1}\right)^2 + \alpha\lambda_1 = 2(A-\lambda_2)(B-\lambda_2)\left(\frac{\partial S_2}{\partial \lambda_2}\right)^2 + \alpha\lambda_2. \quad (2.29)$$

Since the left and right sides of (2.29) depend on different functions, it follows that each side have to be a constant

$$2(A-\lambda_i)(B-\lambda_i)\left(\frac{\partial S_i}{\partial \lambda_i}\right)^2 + \alpha\lambda_i = \alpha\alpha', \quad i \in \{1,2\}, \qquad (2.30)$$

where α' (*the separation constant*) represents the " second constant of the motion" . In [75] and [89], it is proved that such a constant of motion coincides with the product of the focal angular momenta, more precisely: $L_1 L_2 = \alpha\alpha'$ (see Fig. 2.8).
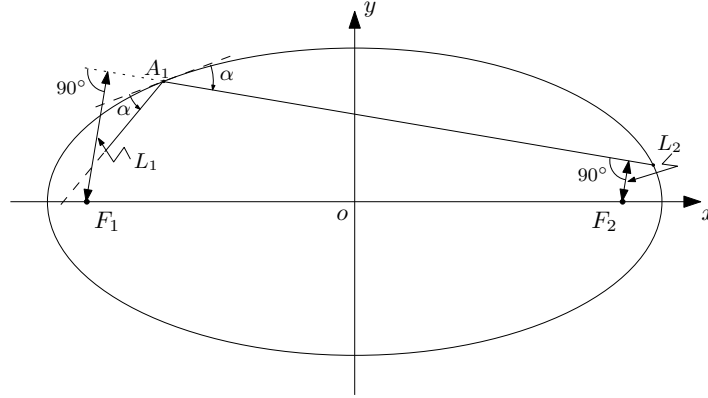
Figure 2.8: The product of the focal angular momenta L_1 and L_2 of an elliptical billiards is conserved.

Since the elliptical billiard system is a two-dimensional system, the existence of two constants of motion implies that it is Hamiltonian integrable. $\quad \square$

2.1.4   Periodic paths: rotational and librational motion

The study of the existence of periodic paths inside an elliptical billiards is strongly related to the Poncelet's closure theorem [68].

Theorem 3. *If a path inscribed in a conic and circumscribed about a second conic (caustic) is closed after N bounces, then all the paths sharing the same caustic conic are also closed after N bounces with the same number of sides and the same perimeter.*

Hence, the problem of finding periodic paths inside an elliptical billiards (*closed Poncelet polygons*) can be turned into the problem of finding particular caustics so that such paths close.

By using (2.30), the momenta conjugate to λ_1 and λ_2 can be computed as:

$$p_1 = \frac{dS_1}{d\lambda_1} = \sqrt{\frac{\alpha(\alpha' - \lambda_1)}{2(A - \lambda_1)(B - \lambda_1)}}, \tag{2.31}$$

$$p_2 = \frac{dS_2}{d\lambda_2} = \sqrt{\frac{\alpha(\alpha' - \lambda_2)}{2(A - \lambda_2)(B - \lambda_2)}}, \tag{2.32}$$

and since p_1 and p_2 are reals, then by (2.18) one has

$$\lambda_1 < \alpha' < \lambda_2,$$

where α' has been defined in Section 2.1.3 and represents the second constant of motion. According to the value of α', there exist two possible (physical) cases, which correspond to two different kinds of motion:

rotational motion: $0 < \lambda_1 < \alpha' < B < \lambda_2 < A$,

librational motion: $0 < \lambda_1 < B < \alpha' < \lambda_2 < A$,

where A and B have been defined in (2.12).

In the first case, the variable λ_1 oscillates between 0 and α' for every bounce with the billiard boundary. In fact, the path of the particle bounces at the boundary at $\lambda_1 = 0$, is tangent to the inner ellipse (caustic) at $\lambda_1 = \alpha'$ and returns to the outer ellipse ($\lambda_1 = 0$) (in this case the path crosses the x-axis outside the foci). The variable λ_2 oscillates between B and A. The path followed by the particle is always outside the foci and tangent to the

inner confocal caustic curve (an ellipse). Such a kind of motion is said to be *rotational* (see Fig. 2.9).

In the other case, the variable λ_2 oscillates between α' and A, which corresponds to the region between two branches of the hyperbole (caustic) $\lambda_2 = \alpha'$ (in this case the path crosses the x-axis ($\lambda_1 = B$) between the foci). The variable λ_1 oscillates now between 0 and B. The path (or its continuation) followed by the particle is always between the foci and tangent to the confocal caustic curve (a hyperbole). Such a kind of motion is said to be *librational* (see Fig. 2.10).

The present result obtained by using the Hamilton-Jacobi theory is consistent with the result discussed in Section 1, where by using a pure geometric approach the existence of two different kinds of caustic curves (which determines two different kinds of motion) was been proved. In both cases, it is important to note that the parameter α' uniquely determines the caustic. Thus, in order to find periodic paths in an elliptical billiards, it is sufficient to determine the particular values of α' such that the orbits close.

Analytic conditions for the closure of Poncelet polygons are obtained by Cayley in the mid-19th century (see [21], but also [51, 39, 5, 75, 22]). The higher-dimensional generalization of these conditions have been recently obtained in [28, 29]. See also [30] for generalizations in several different directions. By following the approach described in [6], the periodic paths of the elliptical billiards can be determined by introducing the action-angle variables of the Hamilton-Jacobi theory (see, e.g., [36]). In particular, it is shown that, the periodic orbits of an integrable system can be found by imposing the condition that the ratio of the angular frequencies (angle variables conjugate to the actions) be a rational number.[4] In the following, classical results giving conditions that guarantee periodic orbits for elliptical billiards in the plane are reported (for the proofs see, e.g., [75, 22]).

---

[4]If the separate frequencies are not rational fractions of each other, the particle will not traverse a closed curve in space but will describe an open *Lissajous figure* [36].

Theorem 4 (rotational motion). *Let $N \in \mathbb{N}$ and $R \in \mathbb{N}$ be the number of reflections and the rotation number (i.e., the number of circuits around the inner caustic) per period, respectively. Then, for all $N > 2$ and $1 \leq R < \frac{N}{2}$ all the orbits characterized by the pair (N, R) share the same caustic curve, which is an ellipse confocal with the elliptical boundary of semi-major axis $a_c = \sqrt{f^2 + \alpha}$ and semi-minor axis $b_c = \sqrt{\alpha}$, where $f = \sqrt{a^2 - b^2}$ and α can be determined by the following condition*

$$F\left(\arcsin\left(\sqrt{\frac{b^2 - \alpha}{b^2}}\right), \frac{f}{\sqrt{f^2 + \alpha}}\right) = \frac{2R}{N} K\left(\frac{f}{\sqrt{f^2 + \alpha}}\right), \qquad (2.33)$$

with $F(\cdot, \cdot)$ and $K(\cdot)$ being the incomplete and complete elliptic integrals of the second kind, respectively (see, e.g., [85, 1]).[5]

Theorem 5 (librational motion). *Let $N \in \mathbb{N}$ and $R \in \mathbb{N}$ be the number of reflections and the libration number (i.e., half the number of touches at the inner caustic) per period, respectively. Then, for all even N and $1 \leq R < \frac{N}{2}$ all the orbits characterized by the pair (N, R) share the same caustic curve, which is a hyperbola confocal with the elliptical boundary of semi-transverse axis $a_c = \sqrt{f^2 + \alpha}$ and semi-conjugate axis $b_c = \sqrt{-\alpha}$, where $f = \sqrt{a^2 - b^2}$ and α can be determined by the following condition*

$$F\left(\arcsin\left(\sqrt{\frac{b^2}{b^2 - \alpha}}\right), \frac{\sqrt{f^2 + \alpha}}{f}\right) = \frac{2R}{N} K\left(\frac{\sqrt{f^2 + \alpha}}{f}\right), \qquad (2.34)$$

with $F(\cdot, \cdot)$ and $K(\cdot)$ being the incomplete and complete elliptic integrals of the second kind, respectively (see, e.g., [85, 1]).

In both cases, the pair (N, R) is usually referred to as *winding number*.

---

[5]The incomplete and the complete elliptic integrals of the second kind are defined as follows:

$$F(\phi, k) = \int_0^\phi \frac{1}{\sqrt{1 - k^2 \sin^2(\theta)}} d\theta, \quad K(k) = F(\frac{\pi}{2}, k) = \int_0^{\frac{\pi}{2}} \frac{1}{\sqrt{1 - k^2 \sin^2(\theta)}} d\theta.$$

Remark 2. By conditions (2.33) and (2.34), it follows that the caustic param-
eter α is independent of the position of the starting vertex, hence moving that
point on the boundary has the effect to rotate the path around the caustic but
its periodicity properties are preserved.

In Fig. 2.9 and 2.10 examples of rotational and librational motion are
reported.
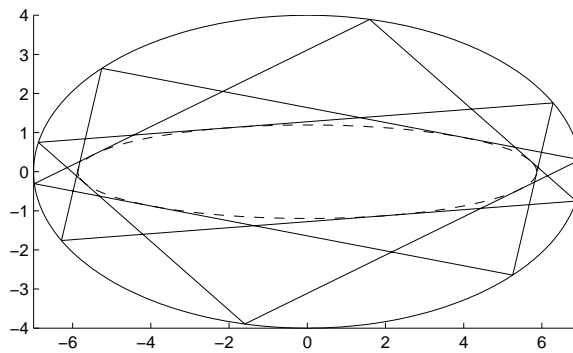
Figure 2.9: Rotational motion: $(N = 10, R = 3)$ and starting vertex on the
ellipse with $\bar{x}_0 = 1.6$.
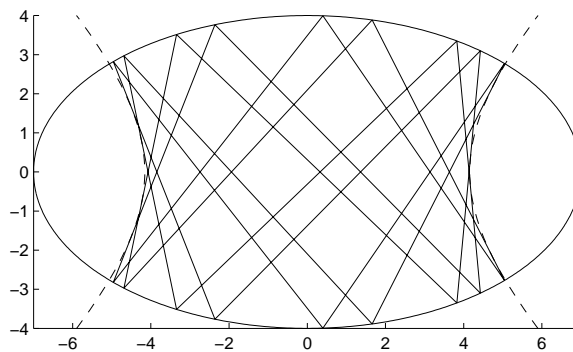
Figure 2.10: Librational motion: $(N = 18, R = 4)$ and starting vertex on the
ellipse with $\bar{x}_0 = 0.4$.

2.2 Overview of Hybrid and Switched Systems

Dynamical systems that are described by an interaction between continuous and discrete dynamics are called *hybrid systems* [53]. Their evolution is generally given by equations of motion containing mixtures of logic, discrete-valued or digital dynamics, and continuous-variable or analog dynamics. The continuous dynamics of such systems may be continuous-time, discrete-time, or mixed (sampled-data). The discrete-variable dynamics of hybrid systems are generally governed by a digital automaton, or input-output transition system with a countable number of states. The continuous and discrete dynamics interact at "event" or "trigger" times when the continuous state hits certain prescribed sets in the continuous state space. Hybrid control systems are control systems that involve both continuous and discrete dynamics and continuous and discrete controls. The continuous dynamics of such a system are usually modeled by a controlled vector field or difference equation. Its hybrid nature is expressed by a dependence on some discrete phenomena, corresponding to discrete states, dynamics, and controls [10]. In Fig. 2.11 a generic scheme of hybrid control system is depicted, where $\mathcal{U}$ and $\mathcal{Y}$ are an input space and an output space, respectively, associated to the continuous dynamics; while $\mathcal{I}$ and $\mathcal{O}$ are an input space and an output space, respectively, associated to the discrete dynamics of the hybrid system (see [2, 11, 63, 71] for further discussion). Continuous dynamics may be represented by a continuous-time control
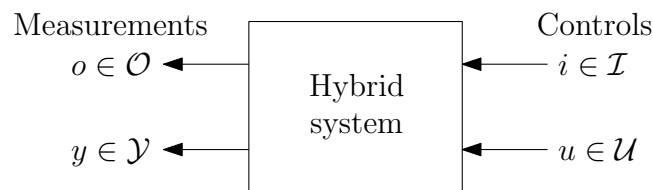
Figure 2.11: Hybrid control system.

system, such as a scalar linear system $\dot{x} = ax + bu$, with state $x \in \mathbb{R}$ and control input $u \in \mathbb{R}$. As an example of discrete dynamics, one can consider a

finite-state automaton, with state q taking values in some finite set $\mathcal{Q}$, where transition between different discrete states are triggered by suitable values of an input variable v. When the input u to the continuous dynamics is some function of the discrete state q and, similarly, the value of the input v to the discrete dynamics is determined by the value of the continuous state x, a hybrid system arises (see Fig. 2.12) [53]. Many (if not most) of the dynamical
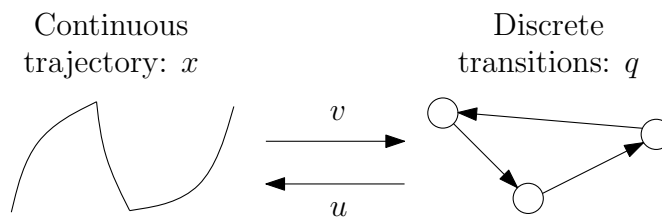
Figure 2.12: Continuous and discrete dynamics in a hybrid system.

systems encountered in practice are of hybrid nature. The following example is borrowed from [13].

Example 1. A very simple model that describes the motion of an automobile might take the form

$$\dot{x}_1 = x_2,$$
$$\dot{x}_2 = f(a, q),$$

where x_1 is the position, x_2 is the velocity, $a \geq 0$ is the acceleration input, and $q \in \{1, 2, 3, 4, 5, -1, 0\}$ is the gear shift position. The function f should be negative and decreasing in a when $q = -1$, negative and independent of a when $q = 0$, and increasing in a, positive for sufficiently large a, and decreasing in q when $q > 0$. In this system, x_1 and x_2 are the continuous states and q is the discrete state. Clearly, the discrete transitions affect the continuous trajectory. In the case of an automatic transmission, the evolution of the continuous state x_2 is in turn used to determine the discrete transitions. In the case of a manual transmission, the discrete transitions are controlled by the driver. It is also natural to consider output variables that depend on both the continuous and the discrete states, such as the engine rotation rate (rpm)

which is a function of x_2 and q.

Continuous-time systems with "isolated" discrete switching events are usually referred to as *switched systems*. A switched system may be obtained from a hybrid system by neglecting the details of the discrete behavior and instead considering all possible switching patterns from a certain class [53]. In other words, a switched system is a hybrid dynamical system consisting of a family of continuous-time subsystems and a rule that orchestrates the switching between them [54]. Switched systems have numerous applications in control of mechanical systems, automotive industry, aircraft and air traffic control, switching power converters, and many other fields (see, e.g., [53]–[67] and the references therein). Some other typical examples of switched system are: thermostat, tank system, bouncing ball, Clegg integrator [87], biological networks [31], chemical process control, engine control (a four-stroke gasoline engine is naturally modeled by using four discrete modes corresponding to the position of the pistons, while combustion and power train dynamics are continuous) [47].

2.2.1   Classification of switching events

In this section, the discrete phenomena that generally arise in hybrid systems are identified. More precisely, switching events in switched systems can be classified into [53]

- State-dependent switching,

- Time-dependent switching,

- Autonomous (uncontrolled) switching,

- Controlled switching.

State-dependent switching

Suppose that the continuous state space (e.g., $\mathbb{R}^n$) is partitioned into a finite or infinite number of *operating regions* by means of a family of *switching surfaces* (or *guards*). In each of these regions, a continuous-time dynamical system (described by differential equations, with or without controls) is given. Whenever the system trajectory hits a switching surface, the continuous state jumps instantaneously to a new value, specified by a *reset map*. In the simplest case, this is a map whose domain is the union of the switching surfaces and whose range is the entire state space, possibly excluding the switching surfaces. The instantaneous jumps of the continuous state are sometimes referred to as *impulse effects*. A special case is when such impulse effects are absent, i.e., the reset map is the identity. This means that the state trajectory is continuous everywhere, although it in general loses differentiability when it passes through a switching surface.

In summary, the system is specified by

- The family of switching surfaces and the resulting operating regions;

- The family of continuous-time subsystems, one for each operating region;

- The reset maps.

Time-dependent switching

Let $\mathbf{f}_p$, $p \in \mathcal{P}$ be a family of functions from $\mathbb{R}^n$ to $\mathbb{R}^n$, where $\mathcal{P}$ is some index set (typically, $\mathcal{P}$ is a subset of a finite-dimensional linear vector space). This gives rise to a family of systems

$$\dot{\mathbf{x}} = \mathbf{f}_p(\mathbf{x}), \quad p \in \mathcal{P}, \tag{2.35}$$

evolving on $\mathbb{R}^n$. The functions $\mathbf{f}_p$ are assumed to be sufficiently regular (at least locally Lipschitz). To define a switched system generated by the such a family, the notion of a *switching signal* has to be introduced.

Definition 3. A switching signal is a piecewise constant function $\sigma : [0, \infty) \rightarrow$ $\mathcal{P}$ with a finite number of discontinuities, which one call the *switching times*, on every bounded time interval and takes a constant value on every interval between two consecutive switching times.

The role of σ is to specify, at each time instant t, the index $\sigma(t) \in \mathcal{P}$ of the *active subsystem*, i.e., the system from the family (2.35) that is currently being followed. It is assumed that σ is continuous from the right everywhere: $\sigma(t) = \lim_{\tau \rightarrow t^+} \sigma(\tau)$ for each $\tau \geq 0$.

Thus a switched system with time-dependent switching can be described by the equation

$$\dot{\mathbf{x}}(t) = \mathbf{f}_{\sigma(t)}(\mathbf{x}(t)). \tag{2.36}$$

Remark 3. It is actually difficult to make a formal distinction between state-dependent and time-dependent switching. If the elements of the index set $\mathcal{P}$ from (2.35) are in 1-to-1 correspondence with the operating regions, and if the systems in these regions are those appearing in (2.35), then every possible trajectory of the system with state-dependent switching is also a solution of the system with time-dependent switching given by (2.36) for a suitable defined switching signal (but not viceversa).

In view of this observation, system with time-dependent switching (2.36) can be used, for example, when the locations of the switching surfaces are unknown.

Autonomous versus Controlled switching

By *autonomous switching*, one means a situation where there is no direct control over the switching mechanism that triggers the discrete events. This category includes systems with state-dependent switching in which locations of the switching surfaces are predetermined, as well as systems with time-dependent switching in which the rule that defines the switching signal is unknown. For example, abrupt changes in system dynamics may be caused by

unpredictable environmental factors or component failures. In contrast with the above, in many situation the switching is actually imposed by the designer in order to achieve a desired behavior of the system. In this case, one has direct control over the switching mechanism (which can be state-dependent or time-dependent) and may adjust it as the system evolves. An *Embedded system*, in which computer software interacts with physical devices, is an important example of system with controlled switching (see Fig. 2.13). It is not easy

measurements

computer
software

physical
device

discrete actions
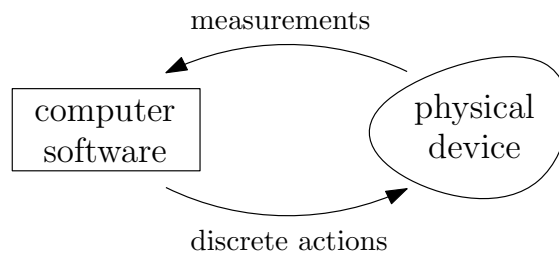
Figure 2.13: A computer-controlled system.

to draw a precise distinction between autonomous and controlled switching, or between state-dependent or time-dependent switching. In a given system, these different types of switching may coexist. In the context of the automobile model discussed in Example 1, automatic transmission corresponds to autonomous state-dependent switching (shifting gears when reaching a certain value of the velocity or rpm), whereas manual transmission corresponds to switching being controlled by the driver.

2.3 Constrained polynomial interpolation

From the theory of non-negative polynomials [64] a very important result (which is a generalization of the Markov-Lukacs theorem) states that a polynomial is non-negative if and only if it satisfies the so-called sum-of-squares decomposition (see, e.g., [42]).

Lemma 1. *A given scalar polynomial $p_i(s)$ of degree q is non-negative along the interval $s \in [s_i, s_f]$ if and only if there exist polynomials $q_{ij}(s), r_{ij}(s)$ of*

degree $m = q/2$ (q even) or $m = (q-1)/2$ (q odd) such that

$$p_i(s) = (s - s_i) \sum_j q_{ij}^2(s) + (s_f - s) \sum_j r_{ij}^2(s). \qquad (2.37)$$

The problem of satisfying the sum-of-squares decomposition (2.37) can be reformulated as a linear matrix inequality (LMI) problem, which can be solved using efficient solvers [76], as follows (see, e.g., [43, 42]).

Lemma 2. *The polynomial non-negativity constraint*

$$p_i(s) = \sum_{j=0}^{q} c_j^i s^j \geq 0, \quad \forall s \in [s_i, s_f],$$

is equivalent to the existence of symmetric and positive semidefinite matrices $\mathbf{Q}_i$ and $\mathbf{R}_i$ of size $m + 1$ with $m = q/2$ (q even) or $m = (q-1)/2$ (q odd), satisfying for any $j = 0, 1, \ldots, q$ the convex LMIs constraints

$$c_j^i = tr(\mathbf{Q}_i(\mathbf{H}_{j-1} - s_i\mathbf{H}_j)) + tr(\mathbf{R}_i(s_f\mathbf{H}_j - \mathbf{H}_{j-1})), \qquad (2.38)$$

where $tr(\mathbf{X})$ denotes the trace of a generic square matrix $\mathbf{X}$ (i.e., the sum of its diagonal elements), and $\mathbf{H}_j$ is the Hankel matrix of dimension $m + 1$ with ones along the $(j + 1)$-th anti-diagonal and zeros elsewhere, that is

$$\mathbf{H}_0 = \begin{bmatrix} 1 & 0 & 0 & \\ 0 & 0 & 0 & \\ 0 & 0 & 0 & \\ & & & \ddots \end{bmatrix}, \quad \mathbf{H}_1 = \begin{bmatrix} 0 & 1 & 0 & \\ 1 & 0 & 0 & \\ 0 & 0 & 0 & \\ & & & \ddots \end{bmatrix},$$

$$\mathbf{H}_2 = \begin{bmatrix} 0 & 0 & 1 & \\ 0 & 1 & 0 & \\ 1 & 0 & 0 & \\ & & & \ddots \end{bmatrix}, \quad \cdots \quad \mathbf{H}_{2m} = \begin{bmatrix} \ddots & & & \\ & 0 & 0 & 0 \\ & 0 & 0 & 0 \\ & 0 & 0 & 1 \end{bmatrix},$$

for $j \in \{0, 1, \ldots, 2m\}$, whereas $\mathbf{H}_j = \mathbf{0}$ for $j < 0$ or $j > 2m$.

Such results have been used recently in order to solve some interesting control problems. In [43], by using results on positive polynomials it is shown that, as soon as distinct negative real closed-loop poles are assigned, satisfying time-domain constraints on closed-loop system signals (such as input amplitude or rate limitations, output overshoot or undershoot) amounts to solving a convex LMI optimization problem when the degree of the polynomial Youla-Kučera parameter (hence the order of the controller) is fixed. In a similar way, results on positive polynomials are also used in [42] where an open-loop trajectory planning problem for linear systems with bound constraints originating from saturations or physical limitations is considered. By using an algebraic approach it is shown that such a control problem can be cast into a constrained polynomial interpolation problem admitting a convex linear matrix inequality (LMI) formulation. In the following, more details about such a result are given.

2.3.1   Application to the trajectory planning

Given a multivariable linear system described by a left coprime polynomial matrix fraction

$$\mathbf{y}(s) = \mathbf{A}_l^{-1}(s)\mathbf{B}_l(s)\mathbf{u}(s), \tag{2.39}$$

in the Laplace domain, where $\mathbf{u}(s)$ and $\mathbf{y}(s)$ are the input and output signals, respectively, and $\mathbf{A}_l(s)$ is non-singular [49], consider the problem to seek a control law $\mathbf{u}(t)$ in the time-domain $[t_q, t_r]$ such that system input $\mathbf{u}(t)$ and output $\mathbf{y}(t)$ together with their derivatives $\mathbf{u}^{(k)}(t)$ and $\mathbf{y}^{(k)}(t)$ satisfy

- **linear constraints:**

$$\begin{aligned} \mathbf{u}^{(k_i)}(t)\big|_{t=t_i} &= \mathbf{u}_i \\ \mathbf{y}^{(k_i)}(t)\big|_{t=t_i} &= \mathbf{y}_i \end{aligned}, \quad i = 1, 2, \ldots, \tag{2.40}$$

where $k_i \geq 0$ are given integers, $t_i \in [t_q, t_r]$ are given real numbers, and

$\mathbf{u}_i$, $\mathbf{y}_i$ are given real vectors;

- **bound constraints:**

$$
\begin{aligned}
\mathbf{u}_i^{low} \leq & \ \mathbf{u}^{(k_i)}(t) \ \leq \mathbf{u}_i^{up} \\
\mathbf{y}_i^{low} \leq & \ \mathbf{y}^{(k_i)}(t) \ \leq \mathbf{y}_i^{up}
\end{aligned} \ , \quad i = 1, 2, \ldots,
$$

where $k_i \geq 0$ are given integers and $\mathbf{u}_i^{low}, \mathbf{u}_i^{up}, \mathbf{y}_i^{low}, \mathbf{y}_i^{up}$ are given real vectors.

By using a right coprime polynomial matrix fraction, linear system (2.39) can be represented as follows:

$$
\mathbf{A}_l^{-1}(s)\mathbf{B}_l(s) = \mathbf{B}_r(s)\mathbf{A}_r^{-1}(s),
$$

where $\mathbf{A}_r(s)$ is nonsingular. Under the coprimeness assumption on the pair $(\mathbf{A}_r(s), \mathbf{B}_r(s))$, there exists a polynomial matrix solution pair $(\mathbf{X}_l(s), \mathbf{Y}_l(s))$ to the Bézout identity

$$
\mathbf{X}_l(s)\mathbf{A}_r(s) + \mathbf{Y}_l(s)\mathbf{B}_r(s) = \mathbf{I},
$$

with $\mathbf{I}$ being the identity matrix. Now, by defining vector

$$
\mathbf{x}(s) := \mathbf{X}_l(s)\mathbf{u}(s) + \mathbf{Y}_l(s)\mathbf{y}(s),
$$

as the internal state, or at output of system (2.39), it follows that all system signals can be represented as linear combinations of signal $\mathbf{x}(t) = \mathcal{L}^{-1}(\mathbf{x}(s))$ and its derivatives. In fact, by virtue of the above Bézout identity, the input and output signals can be obtained as follows:

$$
\mathbf{u}(s) = \mathbf{A}_r(s)\mathbf{x}(s) = \left(\sum_k \mathbf{A}_k s^k \right) \mathbf{x}(s),
$$

$$
\mathbf{y}(s) = \mathbf{B}_r(s)\mathbf{x}(s) = \left(\sum_k \mathbf{B}_k s^k \right) \mathbf{x}(s),
$$

where k is a given integer. As a consequence, algebraic constraints on vectors $\mathbf{y}$ and $\mathbf{u}$ can be translated into algebraic constraints on vector $\mathbf{x}$.

By assuming that $\mathbf{x}(t)$ is a vector polynomial

$$\mathbf{x}(t) = \sum_k \mathbf{x}_k t^k,$$

of given degree, interpolation constraints (2.40) can be written as:

$$\begin{aligned}
\sum_k \mathbf{A}_k \mathbf{x}_k^{(k+k_i)}(t)\Big|_{t=t_i} &= \mathbf{u}_i \\
\sum_k \mathbf{B}_k \mathbf{y}_k^{(k+k_i)}(t)\Big|_{t=t_i} &= \mathbf{y}_i
\end{aligned} \quad , \quad i = 1, 2, \ldots,$$

which are linear constraints on coefficients $\mathbf{x}_k$ of polynomial $\mathbf{x}(t)$. For convenience, they are expressed in matrix form as follows:

$$\mathbf{F}\mathbf{x} = \mathbf{f}, \tag{2.41}$$

where $\mathbf{F}$ is a given matrix, $\mathbf{f}$ is a given vector, and $\mathbf{x}$ denotes the column vector obtained by stacking column vector coefficients $\mathbf{x}_k$. Note that the symbol $\mathbf{x}$ is used indifferently to denote time signal $\mathbf{x}(t)$, its Laplace transform $\mathbf{x}(s)$, and the vector of coefficients $\mathbf{x}_k$. Similarly, bound constraints (2.3.1) can be written as:

$$\begin{aligned}
\mathbf{u}_i^{low} &\leq \sum_k \mathbf{A}_k \mathbf{x}_k^{(k+k_i)}(t) \leq \mathbf{u}_i^{up} \\
\mathbf{y}_i^{low} &\leq \sum_k \mathbf{B}_k \mathbf{y}_k^{(k+k_i)}(t) \leq \mathbf{y}_i^{up}
\end{aligned} \quad , \quad i = 1, 2, \ldots,$$

which can be formulated entrywise as non-negativity constraints

$$\mathbf{g}_i(t) \geq 0, \quad t \in [t_q, t_r], \ i = 1, 2, \ldots. \tag{2.42}$$

on a set of scalar polynomials $\mathbf{g}_i(t)$ whose coefficient vectors $\mathbf{g}_i$ depend linearly on coefficient vector $\mathbf{x}$, i.e.

$$\mathbf{G}_i \mathbf{x} = \mathbf{g}_i, \quad i = 1, 2, \ldots, \tag{2.43}$$

for given matrices $\mathbf{G}_i$.

By using the notation so far introduced, the trajectory planning problem with bound constraints can be cast into the following equivalent constrained polynomial interpolation problem.

Problem 1. *Given matrices* $\mathbf{F}$, $\mathbf{G}_i$ *and vector* $\mathbf{f}$, *and polynomial coefficient vector* $\mathbf{x}$ *satisfying polynomial positivity constraints (2.42), as well as linear constraints (2.41) and (2.43).*

At this point, Lemma 2 can be used in order to rewrite relation (2.42) as an LMI optimization problem and the following result is obtained.

Theorem 6. *Coefficient vector* $\mathbf{x}$ *solves Problem 1 if and only if there exist positive semidefinite symmetric matrices* $\mathbf{Q}_i$, $\mathbf{R}_i$ *solving the LMI problem*

$$\mathbf{Fx} = \mathbf{f},$$

$$\mathbf{G}_i\mathbf{x} = \mathbf{H}(\mathbf{Q}_i, \mathbf{R}_i),$$

where, in order to show the dependence on the decision variables $\mathbf{Q}_i$ *and* $\mathbf{R}_i$, *the set of linear equations (2.38) for* $k = 1, 2, \dots$ *are denoted by* $\mathbf{g}_i = \mathbf{H}(\mathbf{Q}i, \mathbf{R}i)$ *with* $\mathbf{g}_i$ *being the coefficient vector of polynomial* $\mathbf{g}_i(t)$.

Chapter 3

Trajectory definition in the elliptical billiard system

In general terms, a motion planning problem is formulated as two stage planning. First, path planning under kinematic constraints is transformed into a pure geometric problem. Then, combined with dynamic characteristics of the considered system, velocity profiles are generated under (possible) dynamic constraints.

In order to define the class of reference trajectories considered here, in the following, a trajectory planning problem will be properly defined and, by using the theory of non-negativeness polynomials and LMIs techniques, velocity profiles along the desired paths (*closed Poncelet polygons*) are found so as to satisfy some imposed constraints.

3.1 Controlled elliptical billiard system: equations of motion

Consider a dimensionless body having unitary mass (*particle*), which moves on a horizontal plane, on which a Cartesian reference xOy is defined. Let $\mathbf{q}(t) = \begin{bmatrix} x(t) & y(t) \end{bmatrix}^T \in \mathbb{R}^2$ denotes the position of the body at time $t > t_0$,

with $t_0 \in \mathbb{R}$, and let $\mathbf{q}(t)$ be constrained to belong to the following *admissible* region:

$$\mathcal{A} := \left\{ \mathbf{q} \in \mathbb{R}^2 \, : \, f(\mathbf{q}) \leq 0, \quad f(\mathbf{q}) := \frac{x^2}{a^2} + \frac{y^2}{b^2} - 1, \, a, b \in \mathbb{R}^+, \, a > b \right\}, \quad (3.1)$$

that is $f(\mathbf{q}) = 0$ defines an ellipse centered at the origin with a and b being the semi-major and semi-minor axis, respectively. Let the control inputs be two forces $u_x(t)$, $u_y(t) \in \mathbb{R}$, acting directly on the considered body, having directions parallel to the x and y axes, respectively; $u_x(t)$ and $u_y(t)$ are positive when directed as the x and y axes, respectively. It is also assumed that $\mathbf{q}(t)$ and $\dot{\mathbf{q}}(t)$ are measured. The system is completely characterized by: (i) the Lagrangian function

$$\begin{aligned} L_t(\mathbf{q}(t), \dot{\mathbf{q}}(t)) &= T(\mathbf{q}(t), \dot{\mathbf{q}}(t)) - (U(\mathbf{q}(t)) - \mathbf{q}^T(t)\mathbf{E}\mathbf{u}(t)) = \\ &= \frac{1}{2}\dot{\mathbf{q}}^T(t)\dot{\mathbf{q}}(t) + \mathbf{q}^T(t)\mathbf{u}(t) = \\ &= \frac{1}{2}(\dot{x}^2(t) + \dot{y}^2(t)) + u_x(t)x(t) + u_y(t)y(t), \qquad (3.2) \end{aligned}$$

where $T(\mathbf{q}(t))$ denotes the kinetic energy, $U(\mathbf{q}(t))$ is the potential energy due to the conservative forces (which is assumed to be zero on the horizontal billiard plane) and $\mathbf{q}^T(t)\mathbf{E}\mathbf{u}(t)$ is the (*pseudo*)potential energy due to the control forces $\mathbf{u}(t)$. In the case of fully actuated systems, matrix $\mathbf{E}$ coincides with the identity matrix; (ii) the admissible region defined by (3.1) and (iii) nonsmooth, perfectly elastic and without friction impacts.

The method of *the Valentine variables* is used for modeling the considered mechanical system as in [78, 77]. One real-valued Valentine variable $\gamma(t)$ is introduced so that the inequality constraint in (3.1) characterizing the admissible region is transformed into the equality constraint: $f(\mathbf{q}(t)) + \gamma^2(t) = 0$. Since $\gamma(t)$ is taken real, such an equality constraint is completely equivalent to the original inequality constraint. Now, by taking the derivative with respect to time of both sides of the equality constraint, the differential constraint

$(2/a^2)x(t)\dot{x}(t)+(2/b^2)y(t)\dot{y}(t)+2\gamma(t)\dot{\gamma}(t)=0$ is obtained and by starting from the initial conditions $\mathbf{q}(t_0)\in\mathcal{A}$ and $\gamma(t_0)=\sqrt{-f(\mathbf{q}(t_0))}$, such a differential constraint is completely equivalent to the equality constraint.

The actual path of motion can be found by looking for the stationary value of the unconstrained functional $\int_{t_1}^{t_2}\hat{L}\,dt$, where $\hat{L}:=L+\lambda((2/a^2)x\dot{x}+(2/b^2)y\dot{y}+2\gamma\dot{\gamma})$, λ is a Lagrange multiplier and $[t_1,\,t_2]$ is the time interval over which the motion is studied. The stationary value of the unconstrained functional corresponds to the path of motion that is solution (in each (*free-motion*) interval, i.e., an open time interval without impacts) of the following *Euler-Lagrange equations*:

$$\frac{d}{dt}\frac{\partial L}{\partial\dot{\mathbf{q}}}-\frac{\partial L}{\partial\mathbf{q}}+\dot{\lambda}\mathbf{J}(\mathbf{q})=\mathbf{u},\tag{3.3a}$$

$$2\gamma\dot{\lambda}=0,\tag{3.3b}$$

$$\mathbf{J}^T(\mathbf{q})\dot{\mathbf{q}}+2\gamma\dot{\gamma}=0,\tag{3.3c}$$

where $L(\mathbf{q}(t),\dot{\mathbf{q}}(t)):=L_t(\mathbf{q}(t),\dot{\mathbf{q}}(t))-\mathbf{q}^T(t)\mathbf{u}(t)$, $\gamma(t)\in\mathbb{R}^+$ is the Valentine variable and $\lambda(t)\in\mathbb{R}$ is the Lagrange multiplier ($\dot{\lambda}(t)$ has to be understood in the distribution sense) and $\mathbf{J}(\mathbf{q}(t))$ is the gradient vector of $f(\mathbf{q})$ in (3.1), that is

$$\mathbf{J}(\mathbf{q}(t))=\frac{\partial f}{\partial\mathbf{q}}=\frac{\partial}{\partial\mathbf{q}}\left(\frac{x^2}{a^2}+\frac{y^2}{b^2}-1\right)=\begin{bmatrix}\frac{2}{a^2}x\\\frac{2}{b^2}y\end{bmatrix}.\tag{3.4}$$

On the other hand, the impacts can occur only at times $t_i\in\mathbb{R},i\in\mathbb{N}$, where the following *Erdmann-Weierstrass corner conditions* (see, e.g., [55, 8, 82]), which are necessary at corner points where $\mathbf{q}(t)$ is not differentiable (*constrained-motion*), are satisfied

$$\frac{1}{2}\dot{\mathbf{q}}^T(t_i^-)\dot{\mathbf{q}}(t_i^-)=\frac{1}{2}\dot{\mathbf{q}}^T(t_i^+)\dot{\mathbf{q}}(t_i^+),\tag{3.5a}$$

$$\dot{\mathbf{q}}(t_i^-)+\lambda(t_i^-)\mathbf{J}(\mathbf{q}(t_i))=\dot{\mathbf{q}}(t_i^+)+\lambda(t_i^+)\mathbf{J}(\mathbf{q}(t_i)),\tag{3.5b}$$

$$2\gamma(t_i)\dot{\lambda}(t_i^-)=2\gamma(t_i)\dot{\lambda}(t_i^+).\tag{3.5c}$$

Hence, by substituting (3.2) and (3.4) into (3.3) and (3.5), it follows that

$$\ddot{x}(t) + \frac{2}{a^2}\dot{\lambda}(t)x(t) = u_x(t), \tag{3.6a}$$

$$\ddot{y}(t) + \frac{2}{b^2}\dot{\lambda}(t)y(t) = u_y(t), \tag{3.6b}$$

$$2\gamma(t)\dot{\lambda}(t) = 0, \tag{3.6c}$$

$$\frac{2}{a^2}x(t)\dot{x}(t) + \frac{2}{b^2}y(t)\dot{y}(t) + 2\gamma(t)\dot{\gamma}(t) = 0. \tag{3.6d}$$

with the Erdmann-Weierstrass corner conditions given by

$$\dot{x}^2(t_i^-) + \dot{y}^2(t_i^-) = \dot{x}^2(t_i^+) + \dot{y}^2(t_i^+), \tag{3.7a}$$

$$\dot{x}(t_i^-) + \frac{2}{a^2}\lambda(t_i^-)x(t_i) = \dot{x}(t_i^+) + \frac{2}{a^2}\lambda(t_i^+)x(t_i), \tag{3.7b}$$

$$\dot{y}(t_i^-) + \frac{2}{b^2}\lambda(t_i^-)y(t_i) = \dot{y}(t_i^+) + \frac{2}{b^2}\lambda(t_i^+)y(t_i), \tag{3.7c}$$

$$\gamma(t_i)\dot{\lambda}(t_i^-) = \gamma(t_i)\dot{\lambda}(t_i^+). \tag{3.7d}$$

Remark 4. By the definition of the Valentine variable, one has $\gamma^2(t) = -f(\mathbf{q}(t))$ so that $\gamma(t)$ is non-zero whenever the body is located in an interior point of the admissible region $\mathcal{A}$. Hence, in order to satisfy (3.6c), it is necessary that $\dot{\lambda}(t) = 0$ during the free-motion phases. In particular, in absence of impacts, equations (3.6a) and (3.6b) coincide with the classical Euler-Lagrange equations of an unconstrained unitary mass moving on a horizontal plane under the action of the control forces $u_x(t)$ and $u_y(t)$. On the other hand, in classical mechanics, the Erdmann-Weierstrass corner conditions can be interpreted as conservation of momentum and energy across a corner point. In particular, (3.7a) states merely the conservation of the kinetic energy at the impact times.

The initial conditions at the initial time t_0 are

$$x(t_0) = x_0, \quad y(t_0) = y_0,$$
$$\dot{x}(t_0^+) = v_{x,0}, \quad \dot{y}(t_0^+) = v_{y,0},$$
$$\gamma(t_0) = \sqrt{-f(\mathbf{q}(t_0))}, \quad \lambda(t_0^+) = 0.$$

Concerning the initial time t_0, it is required that $(\mathbf{q}(t_0), \dot{\mathbf{q}}(t_0^+)) \in \hat{\mathcal{A}}$, where

$$\hat{\mathcal{A}} := \left\{ (\mathbf{q}, \dot{\mathbf{q}}) \in \mathcal{A} \times \mathbb{R}^2 : \mathbf{J}(\mathbf{q})\dot{\mathbf{q}} \leq 0 \text{ if } f(\mathbf{q}) = 0 \right\}, \tag{3.8}$$

so that, if $\mathbf{q}(t_0)$ is on the boundary, the velocity vector $\dot{\mathbf{q}}(t_0^+)$ points toward the interior of the admissible region.

Definition 4. An impact for the controlled body occurs if, at a given time $t_i > t_0$, one has

$$f(\mathbf{q}(t_i)) = 0, \tag{3.9}$$
$$\mathbf{J}(\mathbf{q}(t_i))\dot{\mathbf{q}}(t_i^-) > 0. \tag{3.10}$$

In particular, (3.9) represents the condition of contact between the particle and the elliptic boundary, whereas (3.10) guarantees that, at the intersection, the path followed by the particle is not tangent to the constraint (*transversality* condition).

In order to guarantees that the particle does not leave the admissible region $\mathcal{A}$ right after an impact, the following condition is required

$$\mathbf{J}(\mathbf{q}(t_i))\dot{\mathbf{q}}(t_i^+) \leq 0, \tag{3.11}$$

so that the Erdmann-Weierstrass corner conditions (3.7) can be solved uniquely in the unknowns $\dot{x}(t_i^+), \dot{y}(t_i^+)$ and $\lambda(t_i^+)$ at an impact time t_i. As a matter of

fact, (3.7b) and (3.7c) can be rewritten, respectively, as

$$\dot{x}(t_i^+) - \dot{x}(t_i^-) = -\frac{2}{a^2} x(t_i) \left(\lambda(t_i^+) - \lambda(t_i^-)\right), \tag{3.12}$$

$$\dot{y}(t_i^+) - \dot{y}(t_i^-) = -\frac{2}{b^2} y(t_i) \left(\lambda(t_i^+) - \lambda(t_i^-)\right), \tag{3.13}$$

so that, by multiplying (3.12) by $a^2 y(t_i)$ and (3.13) by $b^2 x(t_i)$, the discontinuity $\lambda(t_i^+) - \lambda(t_i^-)$ in the Lagrange multiplier can be computed so as to obtain the following two equations in the two unknowns $\dot{x}(t_i^+)$ and $\dot{y}(t_i^+)$

$$a^2 y(t_i) \left(\dot{x}(t_i^+) - \dot{x}(t_i^-)\right) = b^2 x(t_i) \left(\dot{y}(t_i^+) - \dot{y}(t_i^-)\right), \tag{3.14a}$$

$$\dot{x}^2(t_i^-) + \dot{y}^2(t_i^-) = \dot{x}^2(t_i^+) + \dot{y}^2(t_i^+). \tag{3.14b}$$

Solving such a system of equations yields, at each impact time $t_i \geq t_0$, the following results

$$\dot{x}(t_i^+) = \left(\frac{a^4 y^2(t_i) - b^4 x^2(t_i)}{a^4 y^2(t_i) + b^4 x^2(t_i)}\right) \dot{x}(t_i^-) - \left(\frac{2a^2 b^2 x(t_i)y(t_i)}{a^4 y^2(t_i) + b^4 x^2(t_i)}\right) \dot{y}(t_i^-) =$$
$$= C_1(\mathbf{q}(t_i))\dot{x}(t_i^-) + C_2(\mathbf{q}(t_i))\dot{y}(t_i^-), \tag{3.15a}$$

and

$$\dot{y}(t_i^+) = \left(\frac{b^4 x^2(t_i) - a^4 y^2(t_i)}{a^4 y^2(t_i) + b^4 x^2(t_i)}\right) \dot{y}(t_i^-) - \left(\frac{2a^2 b^2 x(t_i)y(t_i)}{a^4 y^2(t_i) + b^4 x^2(t_i)}\right) \dot{x}(t_i^-) =$$
$$= C_2(\mathbf{q}(t_i))\dot{x}(t_i^-) - C_1(\mathbf{q}(t_i))\dot{y}(t_i^-), \tag{3.15b}$$

where $C_1(\mathbf{q}(t_i)) := (a^4 y^2(t_i) - b^4 x^2(t_i))/(a^4 y^2(t_i) + b^4 x^2(t_i))$ and $C_2(\mathbf{q}(t_i)) := (-2a^2 b^2 x(t_i)y(t_i))/(a^4 y^2(t_i) + b^4 x^2(t_i))$. It is important to note that, by (3.4),

(5.3a) and (5.3b), it follows that

$$
\begin{aligned}
\mathbf{J}(\mathbf{q}(t_i))\dot{\mathbf{q}}(t_i^+) &= \left[\begin{array}{cc} \frac{2}{a^2}x(t_i) & \frac{2}{b^2}y(t_i) \end{array} \right] \left[\begin{array}{c} \dot{x}(t_i^+) \\ \dot{y}(t_i^+) \end{array} \right] = \\
&= \frac{2}{a^2}x(t_i)\dot{x}(t_i^+) + \frac{2}{b^2}y(t_i)\dot{y}(t_i^+) = \\
&= -\frac{2}{a^2b^2}\left(b^2 x(t_i)\dot{x}(t_i^-) + a^2 y(t_i)\dot{y}(t_i^-) \right) = \\
&= -\mathbf{J}(\mathbf{q}(t_i))\dot{\mathbf{q}}(t_i^-),
\end{aligned}
\tag{3.16}
$$

so that, requiring condition (3.10) at each impact time guarantees that, right after the impact, condition (3.11) (i.e., $\mathbf{J}(\mathbf{q}(t_i))\dot{\mathbf{q}}(t_i^+) < 0$) is automatically satisfied.

Remark 5. Actually, the system of equations (3.14a) and (3.14b) has also the solution: $\dot{x}(t_i^+) = \dot{x}(t_i^-)$, $\dot{y}(t_i^+) = \dot{y}(t_i^-)$. However, it does not satisfy constraint (3.11), given that $\mathbf{J}(\mathbf{q}(t_i))\dot{\mathbf{q}}(t_i^+) = \mathbf{J}(\mathbf{q}(t_i))\dot{\mathbf{q}}(t_i^-)$ implies that if $\mathbf{J}(\mathbf{q}(t_i))\dot{\mathbf{q}}(t_i^-) > 0$, then $\mathbf{J}(\mathbf{q}(t_i))\dot{\mathbf{q}}(t_i^+) > 0$, which is not physically admissible.

As for the Lagrange multiplier, by substituting (5.3a) into (3.12), one has

$$
\begin{aligned}
\lambda(t_i^+) &= \lambda(t_i^-) + \left(\frac{a^2 b^2}{a^4 y^2(t_i) + b^4 x^2(t_i)} \right)\left(b^2 x(t_i)\dot{x}(t_i^-) + a^2 y(t_i)\dot{y}(t_i^-) \right) = \\
&= \lambda(t_i^-) + \left(\frac{a^2 b^4 x(t_i)}{a^4 y^2(t_i) + b^4 x^2(t_i)} \right)\dot{x}(t_i^-) + \left(\frac{a^4 b^2 y(t)}{a^4 y^2(t_i) + b^4 x^2(t_i)} \right)\dot{y}(t_i^-) = \\
&= \lambda(t_i^-) + C_3(\mathbf{q}(t_i))\dot{x}(t_i^-) + C_4(\mathbf{q}(t_i))\dot{y}(t_i^-),
\end{aligned}
\tag{3.17}
$$

where $C_3(\mathbf{q}(t_i)) := (a^2 b^4 x(t_i))/(a^4 y^2(t_i) + b^4 x^2(t_i))$ and $C_4(\mathbf{q}(t_i)) := (a^4 b^2 y(t_i))/(a^4 y^2(t_i) + b^4 x^2(t_i))$. Note that, at each impact time t_i

$$
\mathbf{J}(\mathbf{q}(t_i))\dot{\mathbf{q}}(t_i^-) = \frac{2}{a^2 b^2}\left(b^2 x(t_i)\dot{x}(t_i^-) + a^2 y(t_i)\dot{y}(t_i^-) \right) > 0
$$

$$
\Downarrow
$$

$$
b^2 x(t_i)\dot{x}(t_i^-) + a^2 y(t_i)\dot{y}(t_i^-) > 0,
\tag{3.18}
$$

so that, by (3.17) and (3.18)

$$\lambda(t_i^+) - \lambda(t_i^-) > 0. \tag{3.19}$$

Since $\dot{\lambda}(t) = 0$ for all $t \neq t_i$ (see Remark 4), it follows that $\lambda(t^+) - \lambda(t^-) = 0$ (i.e., the absence of impacts implies the continuity of $\lambda(t)$, in the case of non-impulsive control inputs).

It is clear that, by using the polar representation of an ellipse, that is

$$\begin{cases} x = a\cos(\theta), \\ y = b\sin(\theta), \end{cases} \tag{3.20}$$

the jump conditions (5.3a) and (5.3b) can be replaced, respectively, by[1]

$$\dot{x}(t_i^+) = \left(\frac{a^2\sin^2(\theta_i) - b^2\cos^2(\theta_i)}{a^2\sin^2(\theta_i) + b^2\cos^2(\theta_i)}\right)\dot{x}(t_i^-) - \left(\frac{ab\sin(2\theta_i)}{a^2\sin^2(\theta_i) + b^2\cos^2(\theta_i)}\right)\dot{y}(t_i^-) =$$
$$= \bar{C}_1(\theta_i)\dot{x}(t_i^-) + \bar{C}_2(\theta_i)\dot{y}(t_i^-), \tag{3.21}$$

and

$$\dot{y}(t_i^+) = \left(\frac{ab\sin(2\theta_i)}{a^2\sin^2(\theta_i) + b^2\cos^2(\theta_i)}\right)\dot{y}(t_i^-) - \left(\frac{a^2\sin^2(\theta_i) - b^2\cos^2(\theta_i)}{a^2\sin^2(\theta_i) + b^2\cos^2(\theta_i)}\right)\dot{x}(t_i^-) =$$
$$= \bar{C}_2(\theta_i)\dot{x}(t_i^-) - \bar{C}_1(\theta_i)\dot{y}(t_i^-), \tag{3.22}$$

where $\bar{C}_1(\theta_i) := (a^2\sin^2(\theta_i) - b^2\cos^2(\theta_i))/(a^2\sin^2(\theta_i) + b^2\cos^2(\theta_i))$ and $\bar{C}_2(\theta_i) := (ab\sin(2\theta_i))/(a^2\sin^2(\theta_i) + b^2\cos^2(\theta_i))$. $\theta_i \in \mathbb{R}$ is the polar angle that the vector from the origin to point $\mathbf{q}(t_i)$ makes with the positive direction of the x-axis (see Fig. 3.1).

---

[1]Time dependence of the polar angle θ is omitted for the sake of readability.
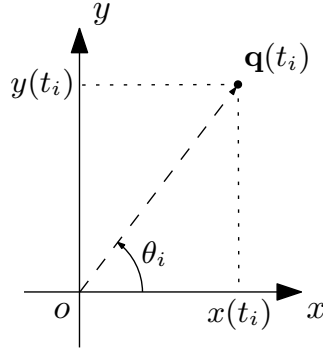
Figure 3.1: Polar representation of an ellipse. The polar angle θ is taken positive when measured counterclockwise.

3.2 The class of reference trajectories

The class of reference trajectories considered hereafter for the elliptical billiard system is characterized by the trajectory planning problem defined below, whose meaning will be clarified later (see Remark 20).

Problem 2. *Find, if any, velocity profiles for a particle moving inside an elliptical billiards along closed Poncelet polygons (see Section 2.1.4) such that*

1. *impacts (in correspondence of polygon vertices) occur at each integer time;*

2. *the Erdmann-Weierstrass corner conditions (3.15) are satisfied at the corner points.*

In the following, first the closed Poncelet polygons for both the cases of rotational and librational motion (see Section 2.1.4) are considered as nominal geometric paths of the reference trajectories. Then, velocity profiles along such nominal paths are computed so as to solve Problem 2.

3.2.1 Nominal paths

Some results on existence and computation of periodic paths inside an elliptical billiards have been reported in Section 2.1.4. Depending on the value

of the second constant of the motion α' in (2.30) two kinds of motion arise: rotational and librational. Geometrically, such a distinction is determined by the intersection of the first billiard path with the x-axis. In particular, if such a segment crosses the x-axis between the foci, then the motion is said to be rotational with an inner confocal ellipse as caustic curve (see Fig. 2.9), otherwise it is said to be librational with a confocal hyperbola as caustic (see Fig. 2.10).

From a geometrical point of view, the path followed by a particle between two consecutive bounces with the boundary can be represented as a straight-line joining two consecutive polygon vertices. The generic segment of a billiard path can be expressed in a parameterized form as

$$\bar{\mathbf{q}}(t) = \bar{\mathbf{q}}_i + l_i(s)\bar{\mathbf{q}}_{i+1}, \tag{3.23}$$

where $\bar{\mathbf{q}}(t) := \begin{bmatrix} \bar{x}(t) & \bar{y}(t) \end{bmatrix}^T$ is the position at time t of a particle moving on the desired path, $\bar{\mathbf{q}}_i := \begin{bmatrix} \bar{x}_i & \bar{y}_i \end{bmatrix}^T$ represents the position of the i-th polygon vertex and $l_i(\cdot) : [0, 1] \to [0, 1]$ determines the velocity profile on the nominal path segment from the vertex i to the vertex $i+1$ (see Fig. 3.2). Theorems 4
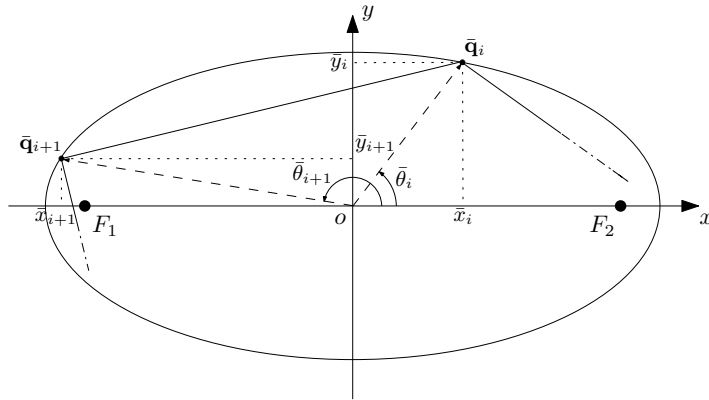
Figure 3.2: A billiard path segment in an elliptical billiards .

and 5 provide operative conditions for the cases of rotational and librational

motion, respectively, for finding closed orbits inside the elliptical billiards .
In particular, conditions (2.33) and (2.34) permit to compute the parameters
characterizing caustic curves, an ellipse and a hyperbola, respectively. Once a
starting vertex is chosen on the elliptical boundary (see Remark 2), the whole
path can be obtained by drawing the first segment tangent to the caustic and
just by applying the reflection law at the vertices. By Definition 1 of the
caustic curve, it is guaranteed that all the path segments are tangent to such
a conic. More precisely, the nominal path can be obtained by following the
steps reported below.

1) **Fix the elliptical boundary:** the semi-major axis a and the semi-minor
   axis b, with $a > b$, are chosen so as to define the boundary of the elliptical
   billiards, which is assumed to be centered at the origin (see Section 2.1.1).

2) **Fix the winding number and the kind of motion:** if the rotational
   motion is considered, then the winding number (N, R) is chosen ac-
   cording to the definition given in Theorem 4. On the other hand, if
   the librational motion is considered, then the winding number (N, R) is
   chosen according to the definition given in Theorem 5.

3) **Find the caustic curve:** consider separately the case of rotational and
   librational motion.

   rotational motion: in this case the caustic curve is an inner ellipse
   confocal with the elliptical boundary (see Section 2.1.2). Solving
   condition (2.33) of Theorem 4, with the parameters instantiated in
   the previous steps, yields the caustic parameter α such that the
   caustic curve is given by

   $$\frac{x^2}{a_c^2} + \frac{y^2}{b_c^2} = 1, \tag{3.24}$$

   where $a_c := \sqrt{f^2 + \alpha}$ and $b_c := \sqrt{\alpha}$ with $f := \sqrt{a^2 - b^2}$ (see Fig.
   3.3).
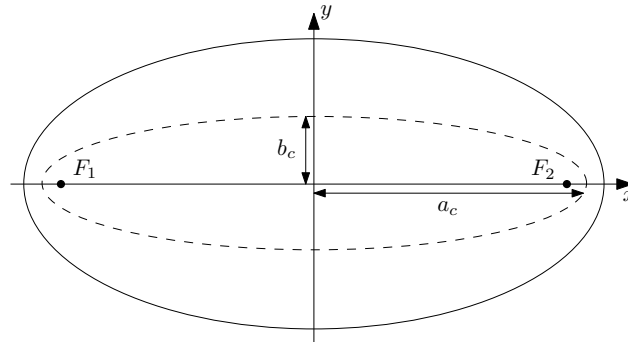
Figure 3.3: Rotational motion caustic curve: a confocal ellipse.

librational motion: in this case the caustic curve is a hyperbola con-
focal with the elliptical boundary (see Section 2.1.2). Solving con-
dition (2.34) of Theorem 5, with the parameters instantiated in the
previous steps, yields the caustic parameter α such that the caustic
curve is given by

$$\frac{x^2}{a_c^2} - \frac{y^2}{b_c^2} = 1, \tag{3.25}$$

where $a_c := \sqrt{f^2 + \alpha}$ and $b_c := \sqrt{-\alpha}$ with $f := \sqrt{a^2 - b^2}$. The
hyperbola asymptotes have equations: $y = \pm \frac{b_c}{a_c} x$ (see Fig. 3.4).
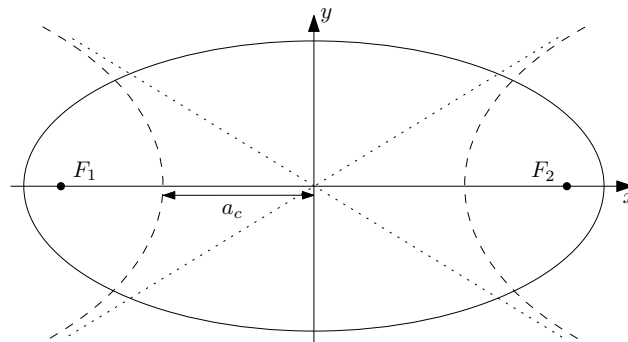
Figure 3.4: Librational motion caustic curve: a confocal hyperbola.

4) Fix the starting vertex: choose the starting point $\bar{\mathbf{q}}_0$ of the nominal
path (closed Poncelet polygon with winding number (N, R)). It is as-

sumed that such a point is a vertex of the reference polygon, i.e., $\bar{\mathbf{q}}_0$ is on the elliptical boundary.

5) **Compute the first billiard path segment:** by Definition 1 of the caustic curve, each segment of the billiard path has to be tangent to the caustic found at Step 4). In view of this fact, the first segment of the reference path can be obtained by drawing a straight line from point $\bar{\mathbf{q}}_0$ to another point $\bar{\mathbf{q}}_1$ on the elliptical boundary in such a way that the segment is tangent to the caustic. More precisely, once that the starting vertex $\bar{\mathbf{q}}_0$ is fixed, the first billiard path segment is completely determined by its slope, whose computation depends on the kind of motion (rotational or librational).

rotational motion: by solving the following system in the unknowns x and y

$$\begin{cases} \dfrac{x^2}{a_c^2} + \dfrac{y^2}{b_c^2} - 1 = 0, \\ y = \bar{y}_1 + m_\perp(x - \bar{x}_1), \end{cases} \tag{3.26}$$

and by imposing the condition of tangency between the straight line and the caustic curve (i.e., system (3.26) has a unique and real solution), the angular coefficient $m_\perp$ is given by[2]

$$m_\perp = \frac{\bar{x}_1 \bar{y}_1 \pm \sqrt{(\bar{x}_1^2 - a_c^2)b_c^2 + b_c^2 \bar{y}_1^2}}{\bar{x}_1^2 - a_c^2}. \tag{3.27}$$

librational motion: by solving the following system in the unknowns x and y

$$\begin{cases} \dfrac{x^2}{a_c^2} - \dfrac{y^2}{b_c^2} - 1 = 0, \\ y = \bar{y}_1 + m_\perp(x - \bar{x}_1), \end{cases} \tag{3.28}$$

and by imposing the condition of tangency between the straight

---

[2]In general, (3.27) (or, analogously, (3.29)) yields two values for $m_\perp$. One can choose arbitrarily between them.

line and the caustic curve (i.e., system (3.28) has a unique and real solution), the angular coefficient $m_\perp$ is given by

$$m_\perp = \frac{\bar{x}_1 \bar{y}_1 \pm \sqrt{(a_c^2 - \bar{x}_1^2)b_c^2 + a_c^2 \bar{y}_1^2}}{\bar{x}_1^2 - a_c^2}. \qquad (3.29)$$

Finally, in order to find point $\bar{\mathbf{q}}_1$ on the elliptical boundary, it is sufficient to solve the following system in the unknowns x and y

$$\begin{cases} \dfrac{x^2}{a^2} + \dfrac{y^2}{b^2} - 1 = 0, \\ y = \bar{y}_1 + m_\perp(x - \bar{x}_1), \end{cases} \qquad (3.30)$$

where $m_\perp$ is computed by either (3.27) or (3.29) for the cases of rotational and librational motion, respectively.

6) **Obtain the whole path:** by starting from point $\bar{\mathbf{q}}_1$, which has been obtained at Step 5), the whole reference path can be obtained by the reflection law. Although reflection is usually introduced as " the angle of incidence is equal to the angle of reflection " this is often difficult to work with. However, the reflection property of the ellipse (i.e., each segment passing through a focus is always reflected to the other one) renders this problem easier to deal with. As a matter of fact, consider a point $\bar{\mathbf{q}} = \begin{bmatrix} \bar{x} & \bar{y} \end{bmatrix}^T$ on the elliptical boundary (2.1), which has foci $\mathbf{F}_1 = \begin{bmatrix} -f & 0 \end{bmatrix}^T$ and $\mathbf{F}_2 = \begin{bmatrix} f & 0 \end{bmatrix}^T$, where $f := \sqrt{a^2 - b^2}$ (see Section 2.1.1). The unit vectors from $\bar{\mathbf{q}}$ to each of the foci are

$$\hat{\mathbf{n}}_1 := \frac{\mathbf{F}_1 - \bar{\mathbf{q}}}{\|\mathbf{F}_1 - \bar{\mathbf{q}}\|}, \quad \hat{\mathbf{n}}_2 := \frac{\mathbf{F}_2 - \bar{\mathbf{q}}}{\|\mathbf{F}_2 - \bar{\mathbf{q}}\|}, \qquad (3.31)$$

and by the reflection property, it follows that each of these vectors makes the same angle with the tangent to the ellipse at $\bar{\mathbf{q}}$. Hence, the normal line to the ellipse coincides with the bisector of the angle they make with the ellipse (see Fig. 3.5). Since they are both of unit length this line is
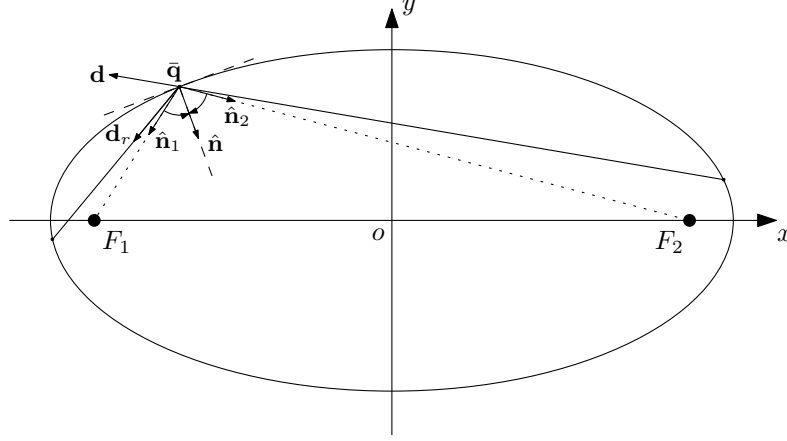
Figure 3.5: Normal line to the ellipse at point $\bar{\mathbf{q}}$.

simply their normalized average, that is

$$\hat{\mathbf{n}} = \frac{\dfrac{\hat{\mathbf{n}}_1 + \hat{\mathbf{n}}_2}{2}}{\left\| \dfrac{\hat{\mathbf{n}}_1 + \hat{\mathbf{n}}_2}{2} \right\|}. \tag{3.32}$$

At this point, if a line with direction $\mathbf{d}$ going through $\bar{\mathbf{q}}$ is considered, then the direction $\mathbf{d}_r$ of its reflection through the tangent line is found by reversing the component of $\mathbf{d}$ in the direction of $\hat{\mathbf{n}}$, whereas the component perpendicular to $\hat{\mathbf{n}}$ remains unchanged (see Fig. 3.5), namely

$$\begin{aligned} \mathbf{d} &= \mathbf{d}_{\hat{\mathbf{n}}_\perp} + \mathbf{d}_{\hat{\mathbf{n}}} \\ \mathbf{d}_r &= \mathbf{d}_{\hat{\mathbf{n}}_\perp} - \mathbf{d}_{\hat{\mathbf{n}}} \end{aligned} \;\Rightarrow\; \mathbf{d}_r = \mathbf{d} - 2\mathbf{d}_{\hat{\mathbf{n}}} = \mathbf{d} - 2 <\mathbf{d}, \hat{\mathbf{n}}> \hat{\mathbf{n}},$$

where $\mathbf{d}_{\hat{\mathbf{n}}_\perp}$ and $\mathbf{d}_{\hat{\mathbf{n}}}$ denote the components of $\mathbf{d}$ perpendicular and parallel to $\hat{\mathbf{n}}$, respectively, whereas $<\mathbf{d}, \hat{\mathbf{n}}> := \mathbf{d}^T \hat{\mathbf{n}}$ denotes the dot product. Hence, in order to find the vertex $\bar{\mathbf{q}}_{i+1}$ starting from vertex $\bar{\mathbf{q}}_i$ and the direction $\mathbf{d}_{i-1}$ of the line joining vertices $\bar{\mathbf{q}}_{i-1}$ and $\bar{\mathbf{q}}_i$, the following algorithm is used

1. Compute direction $\mathbf{d}_i$ of the reflected line at $\bar{\mathbf{q}}_i$:

$$\mathbf{d}_i = \mathbf{d}_{i-1} - 2 < \mathbf{d}_{i-1}, \hat{\mathbf{n}}_i > \hat{\mathbf{n}}_i,$$

   where $\hat{\mathbf{n}}_i$ can be computed by using (3.31) and (3.32) with $\bar{\mathbf{q}} = \bar{\mathbf{q}}_i$.

2. Define the reflected line in a parameterized form as: $\bar{\mathbf{q}}_i + s\mathbf{d}_i$ and solve

$$\left(\frac{x^2}{a^2} + \frac{y^2}{b^2} - 1 = 0 \right) \Big|_{\substack{x=(\bar{\mathbf{q}}_i+s\mathbf{d}_i)[1] \\ y=(\bar{\mathbf{q}}_i+s\mathbf{d}_i)[2]}},$$

   with the nonzero solution denoted by s^*.

3. Find the next vertex $\bar{\mathbf{q}}_{i+1}$ as

$$\bar{\mathbf{q}}_{i+1} = (\bar{\mathbf{q}}_i + s\mathbf{d}_i) \big|_{s=s^*} .$$

By iterating the procedure so far described, all the vertices of the reference path (a polygon inscribed inside the elliptical boundary) can be obtained.

Next section aims at finding velocity profiles along such nominal paths satisfying the constraints defined in Problem 2.

3.2.2   Nominal velocity profiles

In Section 3.2.1, a procedure for obtaining the vertices of a polygon characterized by the winding number (N, R) and the kind of motion, rotational or librational, inscribed inside an elliptical billiards is proposed. In order to completely define the class of reference trajectories, for each integer i, the function $l_i(\cdot)$ in (3.23) has to be chosen so as to solve Problem 2.

Constraint 1: *impacts (in correspondence of polygon vertices) occur at each integer time.*

By considering $\lfloor t \rfloor$ as the largest integer smaller than or equal to t, (3.23) can

be rewritten as

$$\begin{bmatrix} \bar{x}(t) \\ \bar{y}(t) \end{bmatrix} = \begin{bmatrix} \bar{x}_{\lfloor t \rfloor} \\ \bar{y}_{\lfloor t \rfloor} \end{bmatrix} + l_{\lfloor t \rfloor}(t - \lfloor t \rfloor) \begin{bmatrix} \bar{x}_{\lfloor t \rfloor + 1} - \bar{x}_{\lfloor t \rfloor} \\ \bar{y}_{\lfloor t \rfloor + 1} - \bar{y}_{\lfloor t \rfloor} \end{bmatrix}, \tag{3.33}$$

where $\begin{bmatrix} \bar{x}_i & \bar{y}_i \end{bmatrix}^T$ denotes the position of the i-th polygon vertex, which has been computed in Section 3.2.1. In order to guarantee that a particle moving along the desired path (closed Poncelet polygons) hits the boundary (in correspondence with the polygon vertices) at consecutive integer times, functions $l_i(t - i)$ have to meet the following properties

$$l_i(t - i)|_{t=i} = l_i(0) = 0, \tag{3.34a}$$

$$l_i(t - i)|_{t=i+1} = l_i(1) = 1. \tag{3.34b}$$

Moreover, it is also required that for all $t \in [i, i+1]$

$$l_i(t - i) \geq 0, \tag{3.35a}$$

$$l_i(t - i) \leq 1. \tag{3.35b}$$

Remark 6. By the periodicity of the nominal paths, the following facts hold for each integer i

$$\bar{\mathbf{q}}_i = \bar{\mathbf{q}}_{(i \bmod N)}, \tag{3.36}$$

$$l_i(\cdot) = l_{(i \bmod N)}(\cdot), \tag{3.37}$$

where $(i \bmod N) = i - nN$ with $n = \lfloor i/N \rfloor$. In view of this properties, without loss of generality it can be assumed that $i \in \mathcal{I}$, with $\mathcal{I} := \{0, \ldots, N-1\}$, i.e., a single period is taken into account.

Now, by using (3.34), it follows that Constraint 1 is satisfied and the continuity of the trajectory at the corner points (polygon vertices) is guaranteed

for each integer i, that is

$$\bar{x}(t)|_{t=i} = \bar{x}(i) = \bar{x}(i^-) = \bar{x}(i^+) = \bar{x}_i,$$

$$\bar{y}(t)|_{t=i} = \bar{y}(i) = \bar{y}(i^-) = \bar{y}(i^+) = \bar{y}_i.$$

If the polar coordinates (3.20) are considered, then (3.33) becomes

$$\begin{bmatrix} \bar{x}(t) \\ \bar{y}(t) \end{bmatrix} = \begin{bmatrix} a\,\cos(\bar{\theta}_{\lfloor t \rfloor}) \\ b\,\sin(\bar{\theta}_{\lfloor t \rfloor}) \end{bmatrix} + l_{\lfloor t \rfloor}(t - \lfloor t \rfloor) \begin{bmatrix} a\,(\cos(\bar{\theta}_{\lfloor t \rfloor + 1}) - \cos(\bar{\theta}_{\lfloor t \rfloor})) \\ b\,(\sin(\bar{\theta}_{\lfloor t \rfloor + 1}) - \sin(\bar{\theta}_{\lfloor t \rfloor})) \end{bmatrix},$$

which can be rewritten by using the prosthaphaeresis formulas as

$$\begin{bmatrix} \bar{x}(t) \\ \bar{y}(t) \end{bmatrix} = \begin{bmatrix} a\cos(\bar{\theta}_{\lfloor t \rfloor}) \\ b\sin(\bar{\theta}_{\lfloor t \rfloor}) \end{bmatrix} +$$

$$+ l_{\lfloor t \rfloor}(t - \lfloor t \rfloor) \begin{bmatrix} 2\,a\sin(\frac{\bar{\theta}_{\lfloor t \rfloor + 1} - \bar{\theta}_{\lfloor t \rfloor}}{2})\cos(\frac{\pi}{2} + \frac{\bar{\theta}_{\lfloor t \rfloor + 1} + \bar{\theta}_{\lfloor t \rfloor}}{2}) \\ 2\,b\sin(\frac{\bar{\theta}_{\lfloor t \rfloor + 1} - \bar{\theta}_{\lfloor t \rfloor}}{2})\sin(\frac{\pi}{2} + \frac{\bar{\theta}_{\lfloor t \rfloor + 1} + \bar{\theta}_{\lfloor t \rfloor}}{2}) \end{bmatrix}, \quad (3.38)$$

where $\bar{\theta}_i$ is the polar angle relevant to point $\bar{\mathbf{q}}_i$ (see Fig. 3.2).

Constraint 2: *the Erdmann-Weierstrass corner conditions (3.15) are satisfied at the corner points.*

In Section 3.1, the equations of motion during the unconstrained and constrained phases have been obtained for the controlled elliptical billiard system. In particular, at the impact times, (3.15) provide the post-impact velocities, given the pre-impact velocities and the position, under the assumption of perfectly elastic collisions. Note that, if the particle moves along the desired trajectory, then rules (3.15) have to be satisfied at each desired (integer) impact time $\bar{t}_i$ in the nominal coordinates, i.e., $x(t) = \bar{x}(t)$ and $y(t) = \bar{y}(t)$. More precisely, the Erdmann-Weierstrass corner conditions (3.14) expressed in the

nominal coordinates are given by

$$a^2 \bar{y}(i) \left(\dot{\bar{x}}(i^+) - \dot{\bar{x}}(i^-) \right) = b^2 \bar{x}(i) \left(\dot{\bar{y}}(i^+) - \dot{\bar{y}}(i^-) \right), \qquad (3.39a)$$

$$\dot{\bar{x}}^2(i^-) + \dot{\bar{y}}^2(i^-) = \dot{\bar{x}}^2(i^+) + \dot{\bar{y}}^2(i^+). \qquad (3.39b)$$

Substituting (3.23) into (3.39a) and (3.39a) yields

$$a^2 \bar{y}(i) \left(\left. \frac{\partial \bar{x}}{\partial l_{\lfloor t \rfloor}} \right|_{t=i^+} \dot{l}_i(0^+) - \left. \frac{\partial \bar{x}}{\partial l_{\lfloor t \rfloor}} \right|_{t=i^-} \dot{l}_{i-1}(1^-) \right) =$$

$$= b^2 \bar{x}(i) \left(\left. \frac{\partial \bar{y}}{\partial l_{\lfloor t \rfloor}} \right|_{t=i^+} \dot{l}_i(0^+) - \left. \frac{\partial \bar{y}}{\partial l_{\lfloor t \rfloor}} \right|_{t=i^-} \dot{l}_{i-1}(1^-) \right), \quad (3.40a)$$

and

$$\left. \left(\left(\frac{\partial \bar{x}}{\partial l_{\lfloor t \rfloor}} \right)^2 + \left(\frac{\partial \bar{y}}{\partial l_{\lfloor t \rfloor}} \right)^2 \right) \right|_{t=i^-} \dot{l}_{i-1}^2(1^-) =$$

$$= \left. \left(\left(\frac{\partial \bar{x}}{\partial l_{\lfloor t \rfloor}} \right)^2 + \left(\frac{\partial \bar{y}}{\partial l_{\lfloor t \rfloor}} \right)^2 \right) \right|_{t=i^+} \dot{l}_i^2(0^+), \qquad (3.40b)$$

respectively, where the following facts and definitions have been used

$$\dot{\bar{x}}(l_{\lfloor t \rfloor}(t)) = \left. \frac{\partial \bar{x}}{\partial \eta} \right|_{\eta = l_{\lfloor t \rfloor}(t)} \dot{l}_{\lfloor t \rfloor}(t - \lfloor t \rfloor) =: \frac{\partial \bar{x}}{\partial l_{\lfloor t \rfloor}} \dot{l}_{\lfloor t \rfloor}(t - \lfloor t \rfloor),$$

$$\dot{\bar{y}}(l_{\lfloor t \rfloor}(t)) = \left. \frac{\partial \bar{y}}{\partial \eta} \right|_{\eta = l_{\lfloor t \rfloor}(t)} \dot{l}_{\lfloor t \rfloor}(t - \lfloor t \rfloor) =: \frac{\partial \bar{y}}{\partial l_{\lfloor t \rfloor}} \dot{l}_{\lfloor t \rfloor}(t - \lfloor t \rfloor),$$

and

$$(t - \lfloor t \rfloor)|_{t=i^-} = i^- - (i-1) = 0^- + 1 = 1^-,$$

$$(t - \lfloor t \rfloor)|_{t=i^+} = i^+ - i = 0^+.$$

At this point, by substituting (3.33) into (3.40), the following conditions on

the time derivative of functions $l_i(\cdot)$ and $l_{i-1}(\cdot)$ are obtained

$$a^2 \bar{y}_i \left((\bar{x}_{i+1} - \bar{x}_i)\, \dot{l}_i(0^+) - (\bar{x}_i - \bar{x}_{i-1})\, \dot{l}_{i-1}(1^-) \right) =$$
$$= b^2 \bar{x}_i \left((\bar{y}_{i+1} - \bar{y}_i)\, \dot{l}_i(0^+) - (\bar{y}_i - \bar{y}_{i-1})\, \dot{l}_{i-1}(1^-) \right), \qquad (3.41)$$

and

$$\left((\bar{x}_i - \bar{x}_{i-1})^2 + (\bar{y}_i - \bar{y}_{i-1})^2 \right) \dot{l}_{i-1}^2(1^-) =$$
$$= \left((\bar{x}_{i+1} - \bar{x}_i)^2 + (\bar{y}_{i+1} - \bar{y}_i)^2 \right) \dot{l}_i^2(0^+). \qquad (3.42)$$

As seen in Section 3.1, conditions (3.41) and (3.42) can be merged so as to obtain

$$\dot{l}_i(0^+) \begin{bmatrix} \bar{x}_{i+1} - \bar{x}_i \\ \bar{y}_{i+1} - \bar{y}_i \end{bmatrix} =$$
$$= \dot{l}_{i-1}(1^-) \begin{bmatrix} C_1(\bar{\mathbf{q}}(i)) & C_2(\bar{\mathbf{q}}(i)) \\ C_2(\bar{\mathbf{q}}(i)) & -C_1(\bar{\mathbf{q}}(i)) \end{bmatrix} \begin{bmatrix} \bar{x}_i - \bar{x}_{i-1} \\ \bar{y}_i - \bar{y}_{i-1} \end{bmatrix}, \qquad (3.43)$$

where $C_1(\cdot)$ and $C_2(\cdot)$ have been defined in (3.15). Conditions (3.41) and (3.42) (as well as (3.43)) can also be expressed by using the polar representation just considering (3.38) in place of (3.33). For example, the kinetic energy conservation (3.39a) becomes

$$\sin^2 \left(\frac{\bar{\theta}_i - \bar{\theta}_{i-1}}{2} \right) \left(a^2 \sin^2 \left(\frac{\bar{\theta}_i + \bar{\theta}_{i-1}}{2} \right) + b^2 \cos^2 \left(\frac{\bar{\theta}_i + \bar{\theta}_{i-1}}{2} \right) \right) \dot{l}_{i-1}^2(1^-) =$$
$$= \sin^2 \left(\frac{\bar{\theta}_{i+1} - \bar{\theta}_i}{2} \right) \left(a^2 \sin^2 \left(\frac{\bar{\theta}_{i+1} + \bar{\theta}_i}{2} \right) + b^2 \cos^2 \left(\frac{\bar{\theta}_{i+1} + \bar{\theta}_i}{2} \right) \right) \dot{l}_i^2(0^+).$$
$$(3.44)$$

In summary, each function $l_i(\cdot)$, describing the velocity profile along the segment joining the vertices i and $i + 1$ of the reference path, solves Problem 2 if it satisfy conditions (3.34),(3.35) and (3.43). Nevertheless, no assumption

has been made on the "kind" (polynomial, exponential, sinusoidal and so on) of $l_i(\cdot)$. In the next section, by assuming that such functions are polynomials, a procedure based on LMIs techniques is described in order to solve the motion planning problem defined in Problem 2.

3.3 Trajectory planning via constrained polynomial interpolation

In the following, it is shown how the problem of finding velocity profiles that solve Problem 2 can be turned into the problem of satisfying some polynomial non-negative constraints, hence by Lemma 2 (see Section 2.3) into an LMI problem. As a matter of fact, consider the case when the functions $l_i(s)$ in (3.33) are generic polynomials of degree $q \geq 1$ in $s := t - i$

$$l_i(s) = a_q^i s^q + a_{q-1}^i s^{q-1} + \ldots + a_1^i s + a_0^i, \tag{3.45}$$

where $a_j^i \in \mathbb{R}$ for each $j \in \{0, 1, \ldots, q\}$.

Remark 7. Classical studies of trajectories within a billiards assume that the particle moves with constant (says, unitary) velocity until it hits the boundary. Such an assumption implies that each function $l_i(\cdot)$ is chosen such that

$$l_i(t - i) = t - i, \tag{3.46}$$

so that $\dot{l}_i(t - i) = 1$, which corresponds to take $q = 1$ and $a_0^i = 0$, $a_1^i = 1$ in (3.45). In this case, conditions (3.34) and (3.35) are trivially satisfied, however one need to verify also condition (3.42) (or, analogously, (3.44)). In [56], the desired trajectories are constituted by regular polygons (having $N \geq 2$ vertices) inscribed in the circle of unitary radius centered at the origin and having one vertex coincident with the point $\begin{bmatrix} 1 & 0 \end{bmatrix}^T$; it is proved that such a reference trajectory is the path followed by a not actuated (*free*) particle (with constant velocity between impacts) inside the circular billiards and involving

an impact at each integer time (if its initial position and velocity are properly chosen). In fact, a unitary circle centered at the origin can be represented by taking $a = 1$ and $b = 1$ in (2.1), whereas by the regularity of the considered polygons it follows that $\bar{\theta}_i - \bar{\theta}_{i-1} = \bar{\theta}_{i+1} - \bar{\theta}_i = \frac{\pi}{n}$, Therefore, condition (3.44) becomes $\dot{l}_{i-1}^2(1^-) = \dot{l}_i^2(0^+)$, which is satisfied by the hypothesis of constant velocity, i.e. $\dot{l}_i(\cdot) = 1$ for each integer i. On the other hand, in the elliptical billiards a and b are different and the inscribed polygons can be not regular, i.e., $\bar{\theta}_i - \bar{\theta}_{i-1} \neq \bar{\theta}_{i+1} - \bar{\theta}_i$. Therefore, in general, the choice (3.46) of constant velocity along the path does not satisfy condition (3.44) for the conservation of the energy and more general interpolating polynomials, for example the ones defined by (3.45), need to be considered.

As seen in the previous section, in order to solve Problem 2, for each integer $i \in \mathcal{I}$, function $l_i(\cdot)$ have to satisfy

- equality conditions: (3.34) and (3.43);

- inequality conditions: (3.35).

Such a system of equations and inequalities is in general hard to solve. In the following sections, first conditions (3.34), (3.43) and (3.35) will be rewritten in terms of the polynomial coefficients a_j^i and then Lemma 2 (see Section 2.3) will be applied in order to obtain an LMI problem easier to solve.

3.3.1 Inequality constraints

In this section, inequality constraints in the form

$$e_{i,k}^{low} \leq l_i^{(k)}(s) \leq e_{i,k}^{up},$$

are considered, where $k \geq 0$ denotes the derivative order, $s \in [s^i, s^e]$ and $e_{i,k}^{low}, e_{i,k}^{up} \in \mathbb{R}$.

Concerning inequalities (3.35a) and (3.35b), for each integer i guaranteeing $0 \leq l_i(s) \leq 1$ is completely equivalent to guarantee the non-negativeness of

the following polynomials

$$
\begin{aligned}
p_{1,i}(s) &:= l_i(s) \\
p_{2,i}(s) &:= 1 - l_i(s)
\end{aligned}
\quad \Rightarrow \quad
\begin{aligned}
l_i(s) &\geq 0 \;\Leftrightarrow\; p_{1,i}(s) \geq 0 \\
l_i(s) &\leq 1 \;\Leftrightarrow\; p_{2,i}(s) \geq 0
\end{aligned}.
\tag{3.47}
$$

At this point, Lemma 2 permits to reformulate the non-negativeness of polynomials $p_{1,i}(s)$ and $p_{2,i}(s)$ as an LMI problem. In fact, by considering the periodicity of the desired path, the inequalities in (3.47) are satisfied if and only if there exist symmetric and positive semidefinite matrices $\mathbf{Q}_i^1, \mathbf{R}_i^1, \mathbf{Q}_i^2$ and $\mathbf{R}_i^2$ for $i = 0, \ldots, N-1$ such that

$$
\begin{cases}
a_0^i = tr(\mathbf{R}_i^1 \mathbf{H}_0), \\
a_1^i = tr(\mathbf{Q}_i^1 \mathbf{H}_0) + tr(\mathbf{R}_i^1(\mathbf{H}_1 - \mathbf{H}_0)), \\
\vdots \\
a_q^i = tr(\mathbf{Q}_i^1 \mathbf{H}_{q-1}) + tr(\mathbf{R}_i^1(\mathbf{H}_q - \mathbf{H}_{q-1})),
\end{cases}
\tag{3.48}
$$

and

$$
\begin{cases}
a_0^i = 1 - tr(\mathbf{R}_i^2 \mathbf{H}_0), \\
a_1^i = -tr(\mathbf{Q}_i^2 \mathbf{H}_0) - tr(\mathbf{R}_i^2(\mathbf{H}_1 - \mathbf{H}_0)), \\
\vdots \\
a_q^i = -tr(\mathbf{Q}_i^2 \mathbf{H}_{q-1}) - tr(\mathbf{R}_i^2(\mathbf{H}_q - \mathbf{H}_{q-1})),
\end{cases}
\tag{3.49}
$$

where the Hankel matrices $\mathbf{H}_k$ are defined in (2.38). Since the coefficients $a_0^i, a_1^i, \ldots, a_q^i$ in (3.48) and (3.49) are relevant to the same polynomial $l_i(\cdot)$,

one has to guarantee that

$$
\begin{cases}
tr(\mathbf{R}_i^1 \mathbf{H}_0) = 1 + tr(\mathbf{R}_i^2 \mathbf{H}_0), \\
tr(\mathbf{Q}_i^1 \mathbf{H}_0) + tr(\mathbf{R}_i^1(\mathbf{H}_1 - \mathbf{H}_0)) = \\
\qquad\qquad = -(tr(\mathbf{Q}_i^2 \mathbf{H}_0) + tr(\mathbf{R}_i^2(\mathbf{H}_1 - \mathbf{H}_0))), \\
\vdots \\
tr(\mathbf{Q}_i^1 \mathbf{H}_{q-1}) + tr(\mathbf{R}_i^1(\mathbf{H}_q - \mathbf{H}_{q-1})) = \\
\qquad\qquad = -(tr(\mathbf{Q}_i^2 \mathbf{H}_{q-1}) + tr(\mathbf{R}_i^2(\mathbf{H}_q - \mathbf{H}_{q-1}))).
\end{cases}
\tag{3.50}
$$

3.3.2   Equality constraints

In this section, equality constraints in the form

$$
l_i^{(k)}(s)|_{s=s^*} = e_{i,k}^*,
$$

are considered, where $k \geq 0$ denotes the derivative order, $s^* \in [s^i, s^e]$ and $e_{i,k}^* \in \mathbb{R}$.

By using (3.45), conditions (3.34a) and (3.34b) can be given in terms of the polynomial coefficients as

$$
l_k(0) = a_0^i = 0,
\tag{3.51a}
$$

and

$$
l_k(1) = a_q^i + a_{q-1}^i + \cdots + a_1^i + a_0^i = 1,
\tag{3.51b}
$$

respectively. By using $(3.48)^3$, such conditions become

$$l_i(0) = 0 \Leftrightarrow \underbrace{tr(\mathbf{R}_i^1 \mathbf{H}_0)}_{a_0^i} = 0,$$

$$l_i(1) = 1 \Leftrightarrow \underbrace{tr(\mathbf{R}_i^1 \mathbf{H}_0)}_{a_0^i} + \underbrace{tr(\mathbf{Q}_i^1 \mathbf{H}_0) + tr(\mathbf{R}_i^1(\mathbf{H}_1 - \mathbf{H}_0))}_{a_1^i} + \cdots$$

$$\cdots + \underbrace{tr(\mathbf{Q}_i^1 \mathbf{H}_{q-1}) + tr(\mathbf{R}_i^1(\mathbf{H}_q - \mathbf{H}_{q-1}))}_{a_q^i} = 1.$$

As for the corner conditions (3.43), taking the time derivative of function $l_i(\cdot)$ as

$$\dot{l}_i(0^+) = a_1^i,$$

$$\dot{l}_{i-1}(1^-) = q a_q^{i-1} + (q-1) a_{q-1}^{i-1} + \cdots + a_1^{i-1},$$

yields

$$\left(q a_q^{i-1} + (q-1) a_{q-1}^{i-1} + \cdots + a_1^{i-1} \right) \left(C_1(\mathbf{q}(i))(\bar{x}_i - \bar{x}_{i-1}) + C_2(\mathbf{q}(i))(\bar{y}_i - \bar{y}_{i-1}) \right) =$$

$$= a_1^i \left(\bar{x}_{i+1} - \bar{x}_i \right),$$

$$\left(q a_q^{i-1} + (q-1) a_{q-1}^{i-1} + \cdots + a_1^{i-1} \right) \left(C_2(\mathbf{q}(i))(\bar{x}_i - \bar{x}_{i-1}) - C_1(\mathbf{q}(i))(\bar{y}_i - \bar{y}_{i-1}) \right) =$$

$$= a_1^i \left(\bar{y}_{i+1} - \bar{y}_i \right),$$

which can be rewritten in a more compact form as

$$a_1^i h_1(i) = \left(\sum_{j=1}^{q} j a_j^{i-1} \right) h_2(i), \tag{3.52a}$$

---

[3] Once (3.50) is satisfied, the coefficients of $l_i(\cdot)$ can be computed by using (3.48) or (3.49) indifferently.

and

$$a_1^i w_1(i) = \left(\sum_{j=1}^{q} j a_j^{i-1} \right) w_2(i), \tag{3.52b}$$

respectively, where

$$h_1(i) := \bar{x}_{i+1} - \bar{x}_i, \tag{3.53a}$$

$$w_1(i) := \bar{y}_{i+1} - \bar{y}_i, \tag{3.53b}$$

$$h_2(i) := C_1(\mathbf{q}_d(i))h_1(i-1) + C_2(\mathbf{q}_d(i))w_1(i-1), \tag{3.53c}$$

$$w_2(i) := C_2(\mathbf{q}_d(i))h_1(i-1) - C_1(\mathbf{q}_d(i))w_1(i-1). \tag{3.53d}$$

Substituting (3.48) into (3.52) yields

$$\underbrace{(tr(\mathbf{Q}_i^1\mathbf{H}_0) + tr(\mathbf{R}_i^1(\mathbf{H}_1 - \mathbf{H}_0)))}_{a_1^i}h_1(i) =$$

$$= \left(q(\underbrace{tr(\mathbf{Q}_{i-1}^1\mathbf{H}_{q-1}) + tr(\mathbf{R}_{i-1}^1(\mathbf{H}_q - \mathbf{H}_{q-1}))}_{a_q^{i-1}}) + \right.$$

$$+ (q-1)(\underbrace{tr(\mathbf{Q}_{i-1}^1\mathbf{H}_{q-2}) + tr(\mathbf{R}_{i-1}^1(\mathbf{H}_{q-1} - \mathbf{H}_{q-2}))}_{a_{q-1}^{i-1}}) + \cdots$$

$$\left. \cdots + \underbrace{tr(\mathbf{Q}_{i-1}^1\mathbf{H}_0) + tr(\mathbf{R}_{i-1}^1(\mathbf{H}_1 - \mathbf{H}_0))}_{a_1^{i-1}} \right) h_2(i),$$

and

$$
\underbrace{(tr(\mathbf{Q}_i^1\mathbf{H}_0) + tr(\mathbf{R}_i^1(\mathbf{H}_1 - \mathbf{H}_0)))}_{a_1^i}w_1(i) =
$$

$$
= \Big(q(\underbrace{tr(\mathbf{Q}_{i-1}^1\mathbf{H}_{q-1}) + tr(\mathbf{R}_{i-1}^1(\mathbf{H}_q - \mathbf{H}_{q-1}))}_{a_q^{i-1}}) +
$$

$$
+ (q-1)(\underbrace{tr(\mathbf{Q}_{i-1}^1\mathbf{H}_{q-2}) + tr(\mathbf{R}_{i-1}^1(\mathbf{H}_{q-1} - \mathbf{H}_{q-2}))}_{a_{q-1}^{i-1}}) + \cdots
$$

$$
\cdots + \underbrace{tr(\mathbf{Q}_{i-1}^1\mathbf{H}_0) + tr(\mathbf{R}_{i-1}^1(\mathbf{H}_1 - \mathbf{H}_0))}_{a_1^{i-1}} \Big) w_2(i).
$$

3.3.3 A Motion planning result

In view of the results obtained in Section 3.3.1 and 3.3.2, a solution of Problem 2 is given by the following result, which permits to find velocity profiles for the reference paths under the imposed constraints.

Theorem 7. *A family of polynomials $l_i(t - i)$, $i \in \{0, 1, \ldots, N - 1\}$ of degree $q \geq 1$ is a solution of Problem 2 with resulting trajectory in the form (3.33), if and only if there exist symmetric and positive semidefinite matrices $\mathbf{Q}_i^1, \mathbf{R}_i^1, \mathbf{Q}_i^2$ and $\mathbf{R}_i^2$ such that the LMI problem (3.54) is feasible. In this case, the coefficients of $l_i(t - i)$ can be computed using (3.48) or (3.49).*

The LMI problem in the $4N$ symmetric and positive semidefinite matrices $\mathbf{Q}_i^1, \mathbf{R}_i^1, \mathbf{Q}_i^2$ and $\mathbf{R}_i^2$ for $i = 0, 1, \ldots, N - 1$ referred in Theorem 7, which can be obtained by collecting the results previously obtained, is reported in the

following.

$$
\begin{cases}
N \text{ equalities:} \begin{cases} a_0^0 = 0, \\ \vdots \\ a_0^{N-1} = 0, \end{cases} \\[2em]
N \text{ equalities:} \begin{cases} a_q^0 + a_{q-1}^0 + \cdots + a_1^0 + a_0^0 = 1, \\ \vdots \\ a_q^{N-1} + a_{q-1}^{N-1} + \cdots + a_1^{N-1} + a_0^{N-1} = 1, \end{cases} \\[2em]
2N \text{ equalities:} \begin{cases} a_1^0 h_1(0) = (qa_q^{N-1} + (q-1)a_{q-1}^{N-1} + \cdots + a_1^{N-1})h_2(0), \\ a_1^0 w_1(0) = (qa_q^{N-1} + (q-1)a_{q-1}^{N-1} + \cdots + a_1^{N-1})w_2(0), \\ \vdots \\ a_1^{N-1} h_1(N-1) = (qa_q^{N-2} + (q-1)a_{q-1}^{N-2} + \cdots + a_1^{N-2})h_2(N-1), \\ a_1^{N-1} w_1(N-1) = (qa_q^{N-2} + (q-1)a_{q-1}^{N-2} + \cdots + a_1^{N-2})w_2(N-1), \end{cases} \\[2em]
(q+1)N \text{ equalities:} \begin{cases} a_0^0 = \hat{a}_0^0, \\ \vdots \\ a_q^0 = \hat{a}_q^0, \\ \vdots \\ a_0^{N-1} = \hat{a}_0^{N-1}, \\ \vdots \\ a_q^{N-1} = \hat{a}_q^{N-1}, \end{cases} \\[2em]
4N \text{ inequalities:} \begin{cases} \mathbf{Q}_1^1 \succeq 0, \mathbf{R}_1^1 \succeq 0, \mathbf{Q}_1^2 \succeq 0, \mathbf{R}_1^2 \succeq 0, \\ \vdots \\ \mathbf{Q}_N^1 \succeq 0, \mathbf{R}_N^1 \succeq 0, \mathbf{Q}_N^2 \succeq 0, \mathbf{R}_N^2 \succeq 0, \end{cases}
\end{cases}
\tag{3.54}
$$

where in (3.49) coefficients a_j^i have been renamed as $\hat{a}_j^i$.

A pseudo-algorithm implementing such a result is reported below.

1. Let $q = 1$;

2. Let $l_i(t - i) = \displaystyle\sum_{j=0}^{q} a_j^i (t - i)^j, \quad i = 0, 1, \ldots, N - 1;$

3. If the LMIs problem (3.54) is feasible, then

    Compute $a_j^i, \quad j \in \{0, 1, \ldots, q\}$ by using (3.48),

    Go to Step 5);

4. Else

    $q = q + 1,$

    Go to Step 2);

5. End.

3.4   Examples

In this section, examples of desired trajectories (rotational and librational) are depicted. The procedure described in Section 3.2.1 is followed for finding periodic paths inside the elliptical billiards, whereas velocity profiles satisfying Problem 2 are computed by means of the pseudo-algorithm given in Section 3.2.2, which implements Theorem 7.[4]

For the sake of simplicity, the same elliptical billiard table is considered for the examples reported below. In the cartesian coordinates, this is an ellipse centered at the origin with $a = 4$ and $b = 2$ the semi-major and semi-minor axis, respectively.

Rotational motion: $(N = 4, R = 1)$

Consider the case of rotational motion with the following parameters

$$\begin{aligned} &\textbf{winding number:} \quad (N = 4, R = 1), \\ &\textbf{starting vertex:} \quad \bar{\mathbf{q}}_0 = \begin{bmatrix} 4 & 0 \end{bmatrix}^T, \end{aligned} \qquad (3.55)$$

---

[4]The LMI problem is solved by SeDuMi 1.1 (an open source LMIs solver for Matlab®) with Yalmip 3 as interface.

where N and R are defined in Theorem 4. In order to find the nominal path relevant to these parameters, procedure described in Section 3.2.1 is followed. At Step 3), the caustic curve is computed. Since the motion is rotational, it is an inner, confocal ellipse, whose semi-major axis a_c and semi-minor axis b_c are computed by solving condition (2.33) so as to obtain

$$\textbf{caustic curve:}\quad a_c = 3.57771,\ b_c = 0.89443.$$

At this point, applying Step 5) and Step 6) for the case of rotational motion, the whole reference path can be obtained. In particular, the vertices of the closed Poncelet polygon of parameters (3.55) are

$$\bar{\mathbf{q}}_0 = \begin{bmatrix} 4 \\ 0 \end{bmatrix},\ \bar{\mathbf{q}}_1 = \begin{bmatrix} 0 \\ 2 \end{bmatrix},\ \bar{\mathbf{q}}_2 = \begin{bmatrix} -4 \\ 0 \end{bmatrix},\ \bar{\mathbf{q}}_3 = \begin{bmatrix} 0 \\ -2 \end{bmatrix}.$$

In order to find velocity profiles solving Problem 2, the pseudo-algorithm in
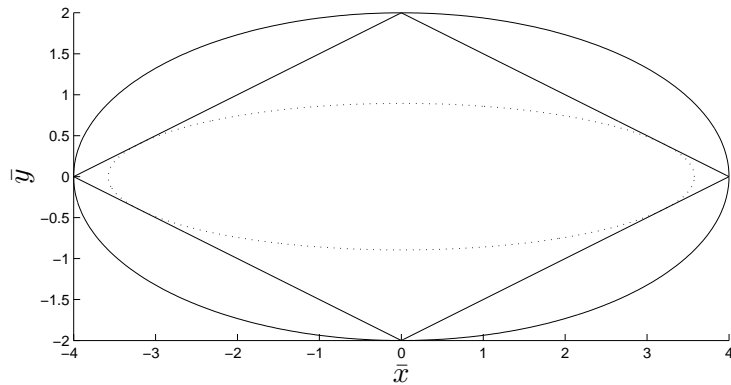
Figure 3.6: Rotational motion ($N = 4, R = 1$): nominal path with winding number: ($N = 4, R = 1$) and starting vertex: ($\bar{x}_0 = 4,\ \bar{y}_0 = 0$) (solid line) and the confocal caustic curve (dotted line).

Section 3.2.2 is carried out. Solving the LMI problem given by (3.54) yields

$q = 1$ and the following interpolating polynomials

$$l_0(t) = t,$$
$$l_1(t - 1) = t - 1,$$
$$l_2(t - 2) = t - 2,$$
$$l_3(t - 3) = t - 3,$$

which are depicted in Fig. 3.7 with their derivatives in Fig. 3.8. The
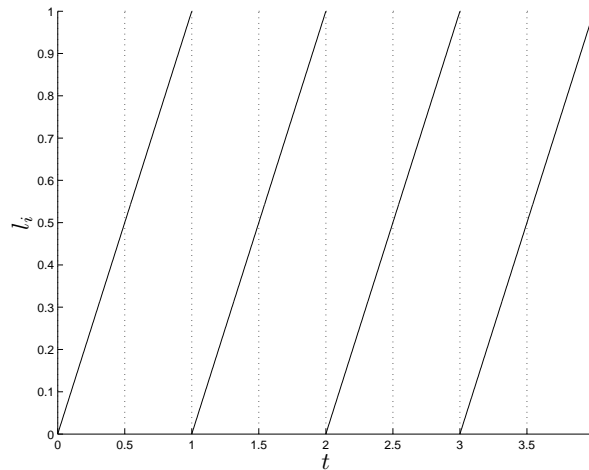
Figure 3.7: Rotational motion $(N = 4, R = 1)$: interpolating polynomials $l_i(\cdot)$.

corresponding velocities $\dot{x}(t)$ and $\dot{y}(t)$ are shown in Fig. 3.9 and 3.10.

Remark 8. For this simple example the nominal path is a regular polygon (a rhombus) inscribed inside the elliptical billiards (see Fig. 3.6). As seen in [56] (see also Remark 7), in this case a velocity profile with constant velocities along the path segments is solution of Problem 2.
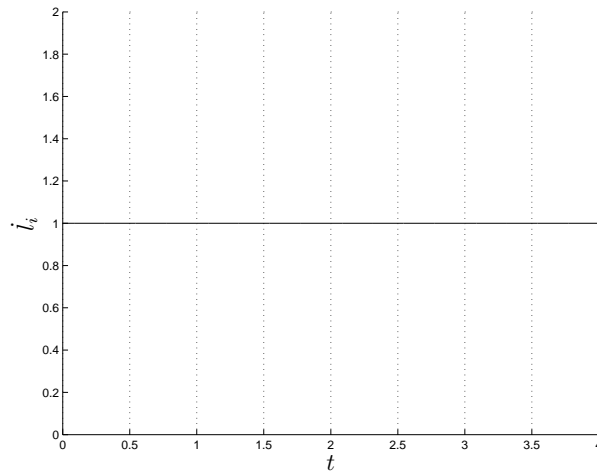
Figure 3.8: Rotational motion ($N = 4, R = 1$): $\dot{l}_i(\cdot)$.
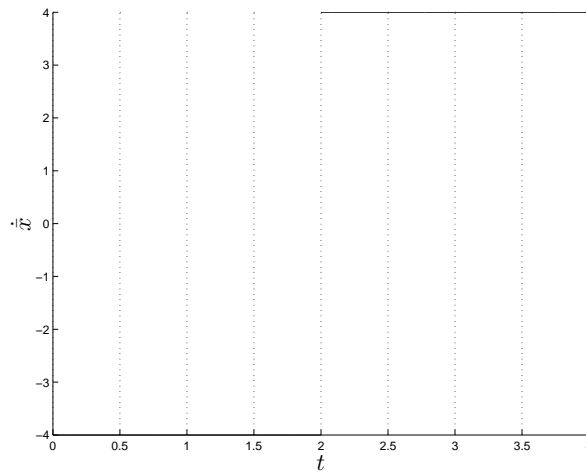
Figure 3.9: Rotational motion ($N = 4, R = 1$): $\dot{\bar{x}}(t)$.
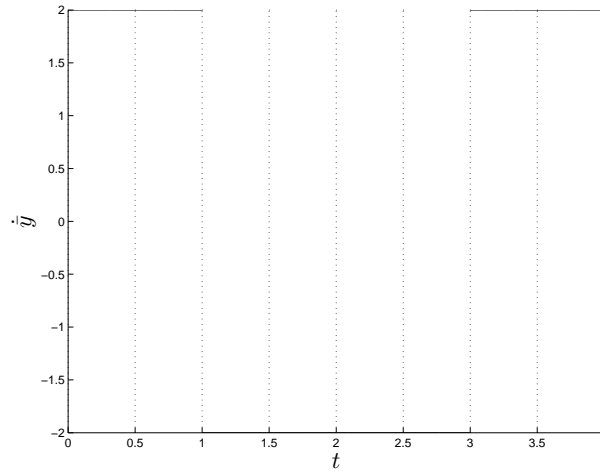
Figure 3.10: Rotational motion ($N = 4, R = 1$): $\dot{\bar{y}}(t)$.

Rotational motion: $(N = 7, R = 2)$

Consider the case of rotational motion with the following parameters

$$
\begin{aligned}
&\textbf{winding number:} \quad (N = 7, R = 2), \\
&\textbf{starting vertex:} \quad \bar{\mathbf{q}}_0 = \begin{bmatrix} 0.3 & 1.99437 \end{bmatrix}^T,
\end{aligned}
\tag{3.56}
$$

where N and R are defined in Theorem 4. In order to find the nominal path relevant to these parameters, procedure described in Section 3.2.1 is followed. At Step 3), the caustic curve is computed. Since the motion is rotational, it is an inner, confocal ellipse, whose semi-major axis a_c and semi-minor axis b_c are computed by solving condition (2.33) so as to obtain

$$
\textbf{caustic curve:} \quad a_c = 3.51678, \ b_c = 0.60644.
$$

At this point, applying Step 5) and Step 6) for the case of rotational motion, the whole reference path can be obtained. In particular, the vertices of the

closed Poncelet polygon of parameters (3.56) are

$$\bar{\mathbf{q}}_0 = \begin{bmatrix} 0.3 \\ 1.99437 \end{bmatrix}, \bar{\mathbf{q}}_1 = \begin{bmatrix} 3.98199 \\ -0.18957 \end{bmatrix},$$

$$\bar{\mathbf{q}}_2 = \begin{bmatrix} -3.01861 \\ -1.31225 \end{bmatrix}, \bar{\mathbf{q}}_3 = \begin{bmatrix} -3.77791 \\ 0.65715 \end{bmatrix},$$

$$\bar{\mathbf{q}}_4 = \begin{bmatrix} 3.84097 \\ 0.55833 \end{bmatrix}, \bar{\mathbf{q}}_5 = \begin{bmatrix} 2.72405 \\ -1.46455 \end{bmatrix}, \bar{\mathbf{q}}_6 = \begin{bmatrix} -3.99119 \\ -0.13268 \end{bmatrix}.$$

In order to find velocity profiles solving Problem 2, the pseudo-algorithm in
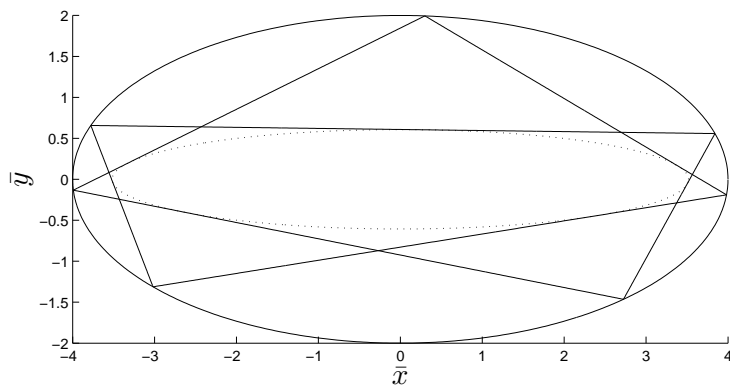
Figure 3.11: Rotational motion ($N = 7, R = 2$): nominal path with winding number: ($N = 7, R = 2$) and starting vertex: ($\bar{x}_0 = 0.3$, $\bar{y}_0 = 1.99437$) (solid line) and the confocal caustic curve (dotted line).

Section 3.2.2 is carried out. Solving the LMI problem given by (3.54) yields

$q = 3$ and the following interpolating polynomials

$$l_0(t) = 0.47295t^3 - 1.2063t^2 + 1.7333t,$$
$$l_1(t-1) = 0.6883(t-1)^3 - 0.51579(t-1)^2 + 0.82749(t-1),$$
$$l_2(t-2) = -0.48932(t-2)^3 + 0.36576(t-2)^2 + 1.1236(t-2),$$
$$l_3(t-3) = 1.1215(t-3)^3 - 1.4219(t-3)^2 + 1.3004(t-3),$$
$$l_4(t-4) = -1.0448(t-4)^3 + 1.5403(t-4)^2 + 0.50448(t-4),$$
$$l_5(t-5) = 1.0357(t-5)^3 - 1.5219(t-5)^2 + 1.4862(t-5),$$
$$l_6(t-6) = -0.26438(t-6)^3 + 0.74136(t-6)^2 + 0.52302(t-6),$$

which are depicted in Fig. 3.12 with their derivatives in Fig. 3.13. The
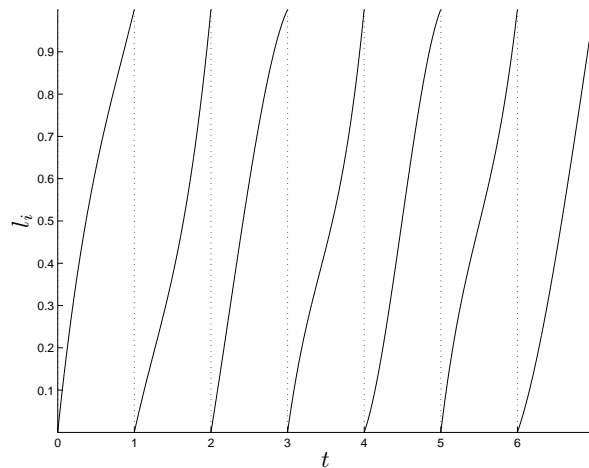
Figure 3.12: Rotational motion $(N = 7, R = 2)$: interpolating polynomials $l_i(\cdot)$.

corresponding velocities $\dot{\bar{x}}(t)$ and $\dot{\bar{y}}(t)$ are shown in Fig. 3.14 and 3.15.
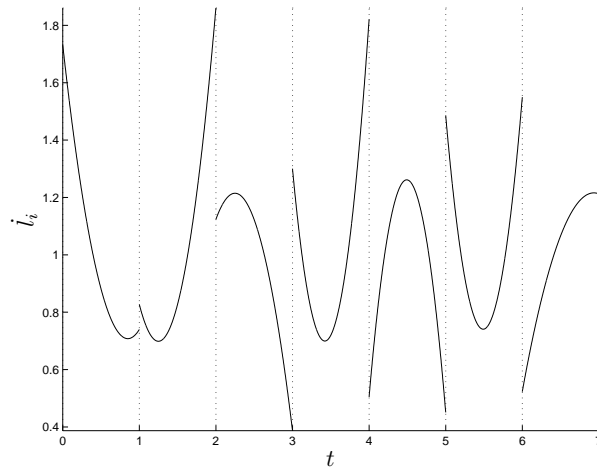
Figure 3.13: Rotational motion ($N = 7, R = 2$): $\dot{l}_i(\cdot)$.
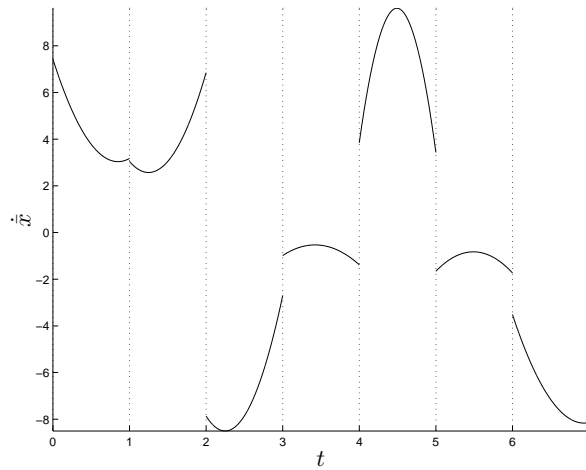
Figure 3.14: Rotational motion ($N = 7, R = 2$): $\ddot{x}(t)$.
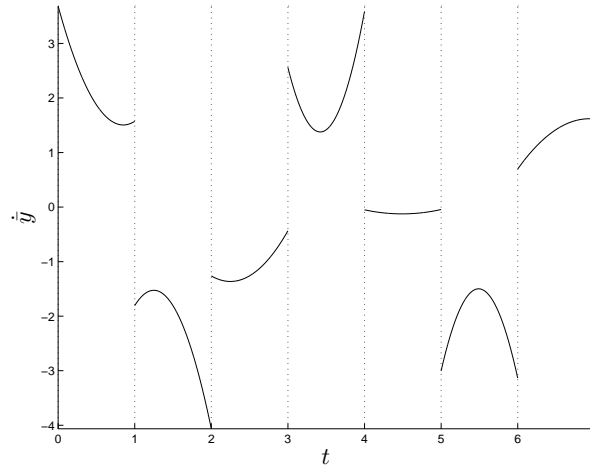
Figure 3.15: Rotational motion $(N = 7, R = 2)$: $\dot{\bar{y}}(t)$.

Librational motion: $(N = 4, R = 1)$

Consider the case of librational motion with the following parameters

$$
\begin{aligned}
\textbf{winding number:} \quad & (N = 4, R = 1), \\
\textbf{starting vertex:} \quad & \bar{\mathbf{q}}_0 = \begin{bmatrix} 1.3 & 1.89143 \end{bmatrix}^T,
\end{aligned}
\tag{3.57}
$$

where N and R are defined in Theorem 5. In order to find the nominal path relevant to these parameters, procedure described in Section 3.2.1 is followed. At Step 3), the caustic curve is computed. Since the motion is librational, it is a confocal hyperbola, whose semi-transversal axis a_c and semi-conjugate axis b_c are computed by solving condition (2.34) so as to obtain

$$
\textbf{caustic curve:} \quad a_c = 3.26599, \; b_c = 1.15470.
$$

At this point, applying Step 5) and Step 6) for the case of librational motion, the whole reference path can be obtained. In particular, the vertices of the

closed Poncelet polygon of parameters (3.57) are

$$\bar{\mathbf{q}}_0 = \begin{bmatrix} 1.3 \\ 1.89143 \end{bmatrix}, \bar{\mathbf{q}}_1 = \begin{bmatrix} -3.74330 \\ -0.70493 \end{bmatrix}, \bar{\mathbf{q}}_2 = \begin{bmatrix} -1.3 \\ 1.89143 \end{bmatrix}, \bar{\mathbf{q}}_3 = \begin{bmatrix} 3.74330 \\ -0.70493 \end{bmatrix}.$$

In order to find velocity profiles solving Problem 2, the pseudo-algorithm in
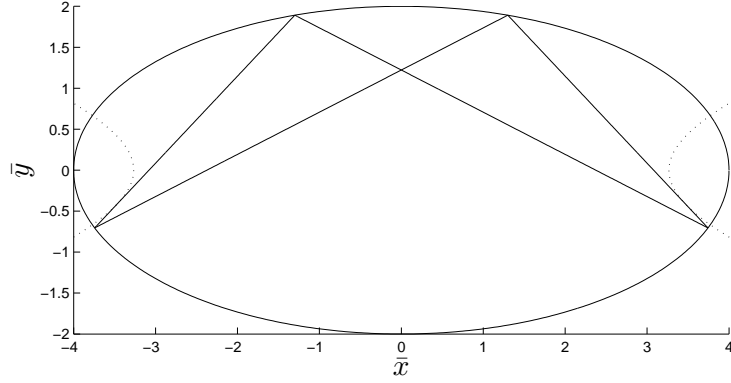
Figure 3.16: Librational motion $(N = 4, R = 1)$: nominal path with winding number: $(N = 4, R = 1)$ and starting vertex: $(\bar{x}_0 = 1.3, \bar{y}_0 = 1.89143)$ (solid line) and the confocal caustic curve (dotted line).

Section 3.2.2 is carried out. Solving the LMI problem given by (3.54) yields $q = 3$ and the following interpolating polynomials

$$l_0(t) = 1.0331t^3 - 1.4569t^2 + 1.4237t,$$
$$l_1(t-1) = -0.093702(t-1)^3 + 0.082157(t-1)^2 + 1.0115(t-1),$$
$$l_2(t-2) = 1.0337(t-2)^3 - 1.4572(t-2)^2 + 1.4236(t-2),$$
$$l_3(t-3) = -0.093182(t-3)^3 + 0.081211(t-3)^2 + 1.012(t-3),$$

which are depicted in Fig. 3.17 with their derivatives in Fig. 3.18.   The corresponding velocities $\dot{\bar{x}}(t)$ and $\dot{\bar{y}}(t)$ are shown in Fig. 3.19 and 3.20.
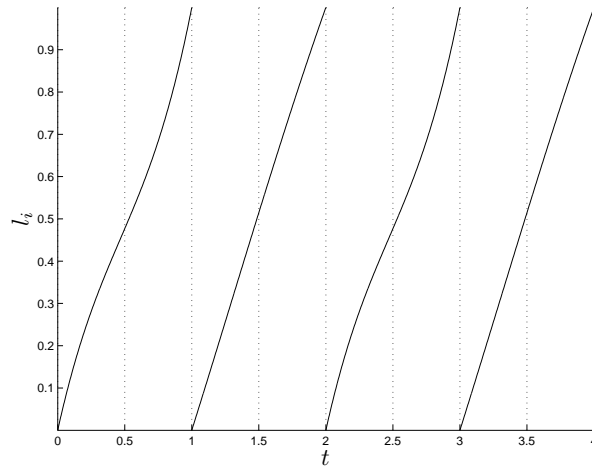
Figure 3.17: Librational motion ($N = 4, R = 1$): interpolating polynomials $l_i(\cdot)$.
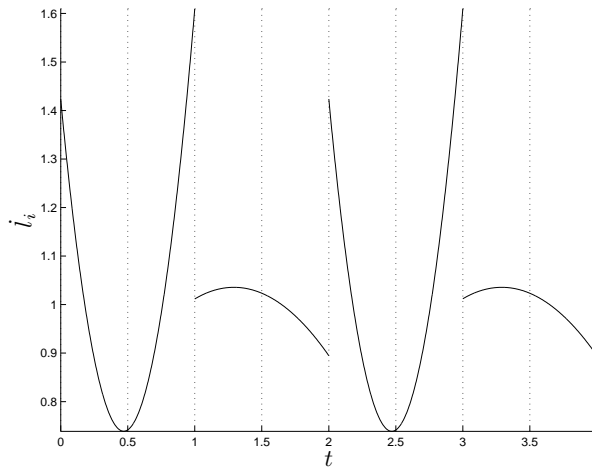
Figure 3.18: Librational motion ($N = 4, R = 1$): $\dot{l}_i(\cdot)$.
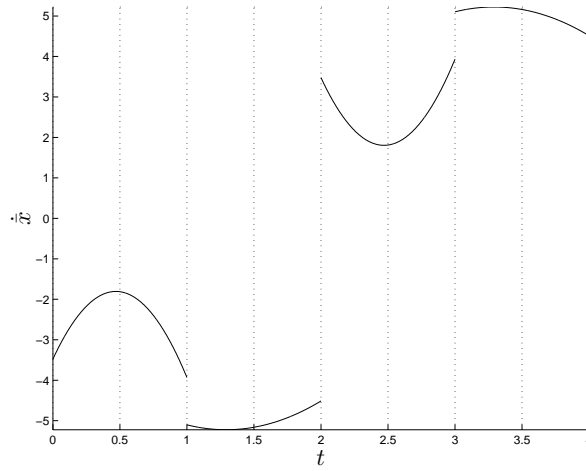
Figure 3.19: Librational motion ($N = 4, R = 1$): $\dot{x}(t)$.
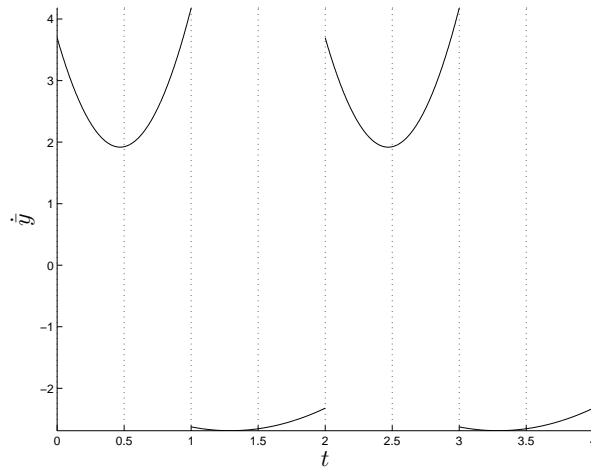
Figure 3.20: Librational motion ($N = 4, R = 1$): $\dot{y}(t)$.

Chapter 4

Trajectory tracking in the elliptical billiard system

In this chapter, a tracking control problem is defined so as to asymptotically track periodic trajectories belong to the class of desired trajectories defined in Chapter 3. Since the vector state of the considered dynamical system is intrinsically subject to *jumps*, the classical stability and attractivity properties cannot be obtained (as shown in [56]) so that suitable modifications are required. Hence, the tracking control problem dealt with in this work is quite similar to the one in [56], where notions similar to the *quasi stability* concept proposed in [50] for impulsive differential systems are used. In order to solve the proposed control problem a controller based on the internal model principle has been designed. It is to be stressed that, similarly to the system to be controlled, the state of the precompensator used to guarantee the presence of the internal model of the reference trajectory presents discontinuities (*nonsmooth* internal model principle).

4.1   The problem of trajectory tracking in presence of nonsmooth impacts

In this section, a tracking control problem taking into account the presence of impulsive effects (due to nonsmooth impacts between the particle and the elliptical boundary) is defined for the elliptical billiard system.

The class of desired trajectories (i.e., paths together with velocity profiles) considered hereafter have been defined in Chapter 3. Let $\mathbf{q}(t) = \begin{bmatrix} x(t) & y(t) \end{bmatrix}^T \in \mathbb{R}^2$ and $\bar{\mathbf{q}}(t) = \begin{bmatrix} \bar{x}(t) & \bar{y}(t) \end{bmatrix}^T \in \mathbb{R}^2$ be the position at time t of a particle moving on the actual trajectory and on the desired trajectory, respectively. The (position) tracking error at time t can be defined as

$$\mathbf{e_q}(t) := \mathbf{q}(t) - \bar{\mathbf{q}}(t).$$

By means of a suitable piecewise continuous control law (impulsive control inputs are not considered in this work), stability properties that one would like to guarantee for the closed-loop system are:

(i) for each $\varepsilon > 0$ and for each $t_0 \in \mathbb{R}$, there exists $\delta_\varepsilon > 0$ such that if $\|\mathbf{e_q}(t_0)\| \leq \delta_\varepsilon$ and $\|\dot{\mathbf{e}}_\mathbf{q}(t_0^-)\| \leq \delta_\varepsilon$, then

$$\|\mathbf{e_q}(t)\| \leq \varepsilon, \quad \forall t \geq t_0, \tag{4.1a}$$

and

$$\|\dot{\mathbf{e}}_\mathbf{q}(t^-)\| \leq \varepsilon, \quad \forall t \geq t_0, \tag{4.1b}$$

$$\|\dot{\mathbf{e}}_\mathbf{q}(t^+)\| \leq \varepsilon, \quad \forall t \geq t_0; \tag{4.1c}$$

(ii) for each $t_0 \in \mathbb{R}$, there exists a neighborhood $\mathbf{\Theta}_{t_0}$ of $\begin{bmatrix} \bar{\mathbf{q}}^T(t_0) & \dot{\bar{\mathbf{q}}}^T(t_0^-) \end{bmatrix}^T$ such that the following relationships hold for each $\begin{bmatrix} \mathbf{q}^T(t_0) & \dot{\mathbf{q}}^T(t_0^-) \end{bmatrix}^T \in$

$\mathbf{\Theta}_{t_0} \cap \left(\mathcal{A} \times \mathbb{R}^2 \right)$:

$$\lim_{t \to +\infty} \|\mathbf{e_q}(t)\| = 0, \tag{4.2a}$$

and

$$\lim_{t \to +\infty} \|\dot{\mathbf{e}}_{\mathbf{q}}(t^-)\| = 0, \tag{4.2b}$$

$$\lim_{t \to +\infty} \|\dot{\mathbf{e}}_{\mathbf{q}}(t^+)\| = 0, \tag{4.2c}$$

where the limits in (4.2) are taken with t being real and $\mathcal{A}$ denotes the admissible region defined in (3.1).

However, the presence of the Erdmann-Weierstrass corner conditions (3.7) and of the constraints (3.6c) and (3.6d) complicates the trajectory tracking problem for the considered system as compared with the case of unconstrained mechanical systems and, in general, it is too difficult (if not impossible) to guarantee both properties (i) and (ii), as shown in the following remark [56].

Remark 9. Consider statement (i). Let $0 < \varepsilon < 1$. Let the initial time t_0 be negative and very close to 0 (so that there is no impact in the interval $(t_0, 0)$), with the initial conditions $\bar{\mathbf{q}}(t_0)$, $\dot{\bar{\mathbf{q}}}(t_0^+)$, $\dot{\mathbf{q}}(t_0^+)$ and $\mathbf{q}(t_0)$ chosen so that $\bar{\mathbf{q}}(0) = \begin{bmatrix} 1 & 0 \end{bmatrix}^T$, $\dot{\bar{\mathbf{q}}}(0^-) = \begin{bmatrix} 2 & 0 \end{bmatrix}^T$, $\dot{\mathbf{q}}(0^-) = \dot{\bar{\mathbf{q}}}(0^-)$ and $\mathbf{q}(0) = (1 - \varepsilon)\,\bar{\mathbf{q}}(0)$ (due to these choices, as $\mathbf{q}(0)$ is an interior point of $\mathcal{A}$, $t = 0$ is not an impact time for the controlled body). On the other hand, $t = 0$ is an impact time for the *fictitious* body moving on the reference trajectory, whence $\dot{\bar{\mathbf{q}}}(0^+) = \begin{bmatrix} -2 & 0 \end{bmatrix}^T$. As t_0 is negative and very close to 0, $\|\dot{\mathbf{e}}_{\mathbf{q}}(t_0^+)\| \simeq \|\dot{\mathbf{e}}_{\mathbf{q}}(0^-)\| = 0$ and $\|\mathbf{e_q}(t_0^+)\| \simeq \|\mathbf{e_q}(0)\| = \varepsilon$. Taking into account the expression of $\dot{\bar{\mathbf{q}}}(0^+)$, one has $\dot{\mathbf{e}}_{\mathbf{q}}(0^+) = \begin{bmatrix} 4 & 0 \end{bmatrix}^T$, and $\|\dot{\mathbf{e}}_{\mathbf{q}}(0^+)\| = 4$; this implies that $\|\dot{\mathbf{e}}_{\mathbf{q}}(t^-)\|$ and $\|\dot{\mathbf{e}}_{\mathbf{q}}(t^+)\|$ are greater than ε for all $t \neq 0$ belonging to a short interval starting from 0, and property (i) is violated. Notice that as the control inputs are not impulsive, they do not influence the previous reasoning, which therefore shows that property (i) cannot be satisfied for any piecewise continuous and

bounded control law.

As far as property (ii) is concerned, for each arbitrarily high real T, if $\|\mathbf{e_q}(T)\|+\|\dot{\mathbf{e}}_\mathbf{q}(T^-)\| \neq 0$ (this is not the case when either $\|\mathbf{e_q}(t_0)\|+\|\dot{\mathbf{e}}_\mathbf{q}(t_0^-)\| = 0$ or when the considered control law has a dead-beat property; this second case can happen only in the nominal case, and, therefore, can be neglected in real applications), then it is generically true that there exists an integer $k > T$ that is not an impact time for the controlled body; for such a k, even if $\|\dot{\mathbf{e}}_\mathbf{q}(k^-)\|$ is almost zero, one has $\dot{\mathbf{e}}_\mathbf{q}(k^+) = \dot{\mathbf{e}}_\mathbf{q}(k^-) + \begin{bmatrix} 4 & 0 \end{bmatrix}^T$ if k is even, and $\dot{\mathbf{e}}_\mathbf{q}(k^+) = \dot{\mathbf{e}}_\mathbf{q}(k^-) - \begin{bmatrix} 4 & 0 \end{bmatrix}$ if k is odd, whence $\|\dot{\mathbf{e}}_\mathbf{q}(k^+)\|$ is almost equal to 4, which (by the arbitrariness of T) means that property (ii) does not hold. Therefore, it seems that, by requiring property (ii), one actually requires that for sufficiently high times, the impact times of the controlled body coincide exactly with the impact times $k \in \mathbb{Z}$ of the desired trajectory, which seems to be difficult (if not impossible) to be guaranteed in practice for a significant set of initial conditions.

In order to overcome the difficulties previously discussed about properties (i) and (ii) (i.e., the classical asymptotic stability properties), the tracking control problem solved here is stated as follows.

Problem 3. *Find, if any, a piecewise continuous control law such that the following properties hold for the closed-loop system:*

(a) *for each $t_0 \in \mathbb{R}$, $(\mathbf{q}(t), \dot{\mathbf{q}}(t)) = (\bar{\mathbf{q}}(t), \dot{\bar{\mathbf{q}}}(t))$ is a piecewise differentiable solution of the closed-loop system for $t \geq t_0$;*

(b) *for each initial conditions $\begin{bmatrix} \mathbf{q}^T(t_0) & \dot{\mathbf{q}}^T(t_0^+) \end{bmatrix}^T \in \hat{\mathcal{A}}$ and for each initial time $t_0 \in \mathbb{R}$, there exists a unique piecewise differentiable solution $\mathbf{q}(t)$ along the interval $(t_0, +\infty)$;*

(c) *for each $\varepsilon > 0$, for each $t_0 \in \mathbb{R}$ and for each $\gamma \in (0, \frac{1}{2})$, there exists $\delta_{\varepsilon,\gamma} > 0$ such that if $\begin{bmatrix} \mathbf{q}^T(t_0) & \dot{\mathbf{q}}^T(t_0^+) \end{bmatrix}^T \in \hat{\mathcal{A}}$, $\|\mathbf{e_q}(t_0)\| < \delta_{\varepsilon,\gamma}$ and*

$\|\dot{\mathbf{e}}_{\mathbf{q}}(t_0^+)\| < \delta_{\varepsilon,\gamma}$, *then*

$$\|\mathbf{e}_{\mathbf{q}}(t)\| \quad < \quad \varepsilon, \quad \forall t \in \mathbb{R}, \ t \geq t_0, \tag{4.3a}$$

$$\|\dot{\mathbf{e}}_{\mathbf{q}}(t^-)\| \quad < \quad \varepsilon, \quad \forall t \in \mathbb{R}, \ t > t_0, \ |t - \langle t \rangle| > \gamma, \tag{4.3b}$$

$$\|\dot{\mathbf{e}}_{\mathbf{q}}(t^+)\| \quad < \quad \varepsilon, \quad \forall t \in \mathbb{R}, \ t > t_0, \ |t - \langle t \rangle| > \gamma, \tag{4.3c}$$

where $\langle t \rangle$ *denotes the integer nearest to* t. *In the case in which* t *is a half-integer,* $\langle t \rangle$ *denotes the smallest integer larger than* t;

(d) for each $t_0 \in \mathbb{R}$, *there exists a neighborhood* Θ_{t_0} *of* $\begin{bmatrix} \bar{\mathbf{q}}^T(t_0) & \bar{\dot{\mathbf{q}}}^T(t_0^+) \end{bmatrix}^T$ *such that the following relationships hold for each* $\begin{bmatrix} \mathbf{q}^T(t_0) & \dot{\mathbf{q}}^T(t_0^+) \end{bmatrix}^T \in \Theta_{t_0} \cap \hat{\mathcal{A}}$:

$$\lim_{t \to +\infty} \|\mathbf{e}_{\mathbf{q}}(t)\| \quad = \quad 0, \tag{4.4a}$$

$$\lim_{k \to +\infty} \|\dot{\mathbf{e}}_{\mathbf{q}}((k+\tau)^-)\| \quad = \quad 0, \quad \forall \tau \in (0, 1), \tag{4.4b}$$

$$\lim_{k \to +\infty} \|\dot{\mathbf{e}}_{\mathbf{q}}((k+\tau)^+)\| \quad = \quad 0, \quad \forall \tau \in (0, 1), \tag{4.4c}$$

where the limits in equations (4.4b) and (4.4c) are taken with k *being integer, whereas the limit in equation (4.4a) is taken with* t *being real.*

Remark 10. In the following, some comments on the definition of Problem 3 are reported.

Comments on property (a): in [56], it has been shown that if the initial position and velocity of the plant are properly chosen, then each reference trajectory is an "admissible" trajectory of the circular billiard system when no control is exerted on the moving mass (i.e., $u_x(t) = u_y(t) = 0$) and it involves an impact at each integer time. In the present case, since the velocity along the nominal path is in general non-constant, the plant cannot contain the whole *internal model* of the reference trajectory to track. The presence of such an internal model is guaranteed here through a dynamic precompensator so that property (a) can be obtained. Moreover, by property (a), condition

(4.4b) implies condition (4.4c), which has been reported in the statement of property (d) for the sake of clarity.

Comments on requirement (b): this requirement is very important in the case of impacting systems. As a matter of fact, it is possible to construct examples of impacting systems having unique solution in each interval of time that does not contain any impact time, but with a finite accumulation point of impact times t_I, $I \geq 1$, (*i.e.*, $\lim_{I \to +\infty} t_I = t^*$, with t^* being a finite real), whose solution cannot be continued after t^* as $\lim_{I \to +\infty} \dot{\mathbf{q}}(t_I^-) \neq \lim_{I \to +\infty} \dot{\mathbf{q}}(t_I^+)$ (in such a case the solution of the system does not exist over all $(t_0, +\infty)$, but only on (t_0, t^*)). There are two simple ways to ensure that requirement (b) holds (both of them give rise to sufficient conditions for the existence of the solution). The first one consists in guaranteeing that, for any considered initial condition, there is only a finite number of impact times in $(t_0, +\infty)$; the second one, which will be pursued here, is that of guaranteeing the following two properties:

(e) for each initial time $\hat{t}_0 \in \mathbb{R}$ and for each $\begin{bmatrix} \mathbf{q}^T(\hat{t}_0) & \dot{\mathbf{q}}^T(\hat{t}_0^+) \end{bmatrix}^T \in \hat{\mathcal{A}}$, there exists a unique differentiable solution $\mathbf{q}(t)$ along the interval $(\hat{t}_0, \hat{t}_1)$, where $\hat{t}_1$ is the first impact time after $\hat{t}_0$;

(f) for each initial time $t_0 \in \mathbb{R}$ and for each $\begin{bmatrix} \mathbf{q}^T(\hat{t}_0) & \dot{\mathbf{q}}^T(\hat{t}_0^+) \end{bmatrix}^T \in \hat{\mathcal{A}}$, there exists a sequence of impact times $\{t_I\}_{I \in \mathbb{Z}^+}$, such that $t_{I+1} > t_I$ and $\lim_{I \to +\infty} t_I = +\infty$.

Properties (e) and (f) imply that, for each admissible initial condition, the solution of the closed-loop system exists and is unique not only up to the first impact time but up to infinity, as the solution can be uniquely continued over each impact time (remember that the Erdmann-Weierstrass corner conditions can be uniquely solved at the impact times), and the impact times have $+\infty$ as accumulation point.

Comments on property (c): considering $t \geq t_0$ such that $|t - k| > \gamma$, $k \in \mathbb{Z}$, for what concerns the error in the velocities, allows one to avoid in

the stability analysis the times in the intervals $[k - \gamma, \, k + \gamma]$, $k \in \mathbb{Z}$, in which one has jumps in the desired velocities. In order to reduce the size of these intervals, it is sufficient to properly choose the initial conditions according to the statement of property (c). Notice that γ is an arbitrarily small positive number and cannot be taken equal to zero, as discussed in Remark 9.

Comments on property (d): for each $\tau \in (0, \, 1)$, $k + \tau$ is not integer for all $k \in \mathbb{Z}$; for $\tau \in (0, \, 1)$ sufficiently close to 0, $k + \tau$ is close to k^+, whereas for $\tau \in (0, \, 1)$ sufficiently close to 1, $k + \tau$ is close to $(k+1)^-$. Finally, notice that the limits in equations (4.4b) and (4.4c) are weaker than the following limits (they have sense, as $+\infty$ is adherent to $\mathbb{R} - \mathbb{Z}$) $\lim_{t \to +\infty, \, t \in \mathbb{R} - \mathbb{Z}} \quad \|\dot{\mathbf{e}}_\mathbf{q}(t^-)\| = 0$, $\lim_{t \to +\infty, \, t \in \mathbb{R} - \mathbb{Z}} \quad \|\dot{\mathbf{e}}_\mathbf{q}(t^+)\| = 0$, which are too difficult to be satisfied, as one can see with a reasoning similar to the one adopted in Remark 9 for a real t.

4.2 A first control scheme based on the internal model principle

By assuming that the whole plant state is measured, a control scheme based on a nonsmooth version of the internal model principle is depicted in Fig. 4.1, whose component blocks will be described in the following.
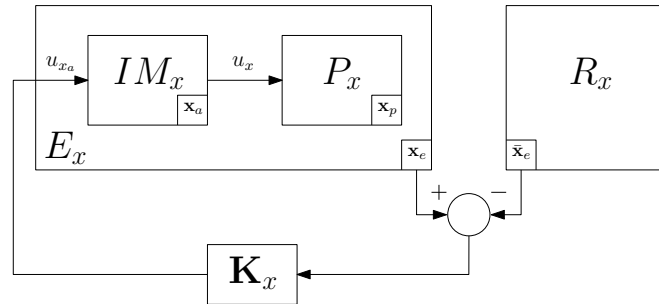
Figure 4.1: A control scheme based on the internal model principle. The whole plant state is assumed to be measured.

Remark 11. In Fig. 4.1, only the scheme relevant to x-coordinate is shown, the

other one being completely analogous. In fact, in absence of impacts equations (3.6a) and (3.6b) are decoupled (the coupling between the two degrees of freedom of the mass is due to the impact of the mass with the elliptical surface delimiting the admissible region, see (3.15)).

The exosystem: R_x, R_y

As for the reference signals given in (3.33), they are polynomials in $t - \lfloor t \rfloor$ of degree q. Hence, for some $\boldsymbol{\Omega}_x, \boldsymbol{\Omega}_y, \mathbf{v}_x, \mathbf{v}_y$, they can be written in the following form

$$\bar{x}(t) = \boldsymbol{\Omega}_x e^{\mathbf{M}(t-\lfloor t \rfloor)} \mathbf{v}_x, \tag{4.5a}$$

$$\bar{y}(t) = \boldsymbol{\Omega}_y e^{\mathbf{M}(t-\lfloor t \rfloor)} \mathbf{v}_y, \tag{4.5b}$$

where

$$\mathbf{M} := \begin{bmatrix} 0 & 1 & 0 & \cdots & 0 \\ 0 & 0 & 1 & \cdots & 0 \\ \vdots & & \ddots & & \vdots \\ \vdots & & & 0 & 1 \\ 0 & \cdots & \cdots & 0 & 0 \end{bmatrix} \in \mathbb{R}^{(q+1)\times(q+1)}.$$

In particular, by defining

$$\boldsymbol{\Omega}_x = \begin{bmatrix} 1 & 0 & \cdots & 0 \end{bmatrix},$$
$$\boldsymbol{\Omega}_y = \begin{bmatrix} 1 & 0 & \cdots & 0 \end{bmatrix},$$

one has

$$\boldsymbol{\Omega}_x e^{\mathbf{M}(t-\lfloor t \rfloor)} = \boldsymbol{\Omega}_y e^{\mathbf{M}(t-\lfloor t \rfloor)} =$$
$$= \begin{bmatrix} 1, & t-\lfloor t \rfloor, & \frac{1}{2!}(t-\lfloor t \rfloor)^2, & \frac{1}{3!}(t-\lfloor t \rfloor)^3, & \cdots, & \frac{1}{q!}(t-\lfloor t \rfloor)^q \end{bmatrix},$$

so that $\bar{x}(t)$ and $\bar{y}(t)$ can be obtained in the form (3.33) by taking

$$
\mathbf{v}_x(t) = \begin{bmatrix} \bar{x}_{\lfloor t \rfloor} \\ a_1^{\lfloor t \rfloor}(\bar{x}_{\lfloor t \rfloor+1} - \bar{x}_{\lfloor t \rfloor}) \\ 2a_2^{\lfloor t \rfloor}(\bar{x}_{\lfloor t \rfloor+1} - \bar{x}_{\lfloor t \rfloor}) \\ \vdots \\ q!a_q^{\lfloor t \rfloor}(\bar{x}_{\lfloor t \rfloor+1} - \bar{x}_{\lfloor t \rfloor}) \end{bmatrix} \in \mathbb{R}^{q+1}, \tag{4.6a}
$$

$$
\mathbf{v}_y(t) = \begin{bmatrix} \bar{y}_{\lfloor t \rfloor} \\ a_1^{\lfloor t \rfloor}(\bar{y}_{\lfloor t \rfloor+1} - \bar{y}_{\lfloor t \rfloor}) \\ 2a_2^{\lfloor t \rfloor}(\bar{y}_{\lfloor t \rfloor+1} - \bar{y}_{\lfloor t \rfloor}) \\ \vdots \\ q!a_q^{\lfloor t \rfloor}(\bar{y}_{\lfloor t \rfloor+1} - \bar{y}_{\lfloor t \rfloor}) \end{bmatrix} \in \mathbb{R}^{q+1}, \tag{4.6b}
$$

with a_j^i being the polynomial coefficients in (3.45) (see Section 3.2.2).

A state-space representation of the exosystem during the unconstrained motion is thus given by

Free-motion:

$$
R_x : \begin{cases} \dot{\bar{\mathbf{x}}}_e(t) = \mathbf{M}\bar{\mathbf{x}}_e(t) \\ \bar{x}(t) = \mathbf{\Omega}_x \bar{\mathbf{x}}_e(t) \end{cases}, \quad \forall t \in (\bar{t}_i, \bar{t}_{i+1}), i \in \mathbb{Z}^+, \tag{4.7a}
$$

$$
R_y : \begin{cases} \dot{\bar{\mathbf{y}}}_e(t) = \mathbf{M}\bar{\mathbf{y}}_e(t) \\ \bar{y}(t) = \mathbf{\Omega}_y \bar{\mathbf{y}}_e(t) \end{cases}, \quad \forall t \in (\bar{t}_i, \bar{t}_{i+1}), i \in \mathbb{Z}^+, \tag{4.7b}
$$

whereas, at the desired impact times, the following reset rules hold

Reset-values:

$$
\bar{\mathbf{x}}_e(\bar{t}_i^+) = \mathbf{v}_x(\bar{t}_i), \quad i \in \mathbb{N}, \tag{4.8a}
$$

$$
\bar{\mathbf{y}}_e(\bar{t}_i^+) = \mathbf{v}_y(\bar{t}_i), \quad i \in \mathbb{N}. \tag{4.8b}
$$

The plant model: P_x, P_y

The equations of motion of a particle moving in an elliptical billiards under the action of control forces have been obtained in Section 3.1. By letting

$$\mathbf{x}_p(t) := \begin{bmatrix} x(t) \\ \dot{x}(t) \end{bmatrix}, \quad \mathbf{y}_p(t) := \begin{bmatrix} y(t) \\ \dot{y}(t) \end{bmatrix},$$

in absence of impacts (*free-motion phases*) the equations (3.6a) and (3.6b) can be rewritten as:

Free-motion:

$$P_x : \begin{cases} \dot{\mathbf{x}}_p(t) = \mathbf{A}_p\mathbf{x}_p(t) + \mathbf{B}_p u_x(t) \\ y_{x_p}(t) = \mathbf{C}_p\mathbf{x}_p(t) \end{cases}, \quad \forall t \in (t_i, t_{i+1}), i \in \mathbb{Z}^+, \qquad (4.9a)$$

$$P_y : \begin{cases} \dot{\mathbf{y}}_p(t) = \mathbf{A}_p\mathbf{y}_p(t) + \mathbf{B}_p u_y(t) \\ y_{y_p}(t) = \mathbf{C}_p\mathbf{y}_p(t) \end{cases}, \quad \forall t \in (t_i, t_{i+1}), i \in \mathbb{Z}^+, \qquad (4.9b)$$

where

$$\mathbf{A}_p := \begin{bmatrix} 0 & 1 \\ 0 & 0 \end{bmatrix}, \quad \mathbf{B}_p := \begin{bmatrix} 0 \\ 1 \end{bmatrix}, \quad \mathbf{C}_p := \begin{bmatrix} 1 & 0 \end{bmatrix}.$$

On the other hand, at the impact times the corner conditions (3.7) become

Constrained-motion:

$$\mathbf{x}_p(t_i^+) = \mathbf{C}_1^p(\mathbf{q}(t_i))\mathbf{x}_p(t_i^-) + \mathbf{C}_2^p(\mathbf{q}(t_i))\mathbf{y}_p(t_i^-), \ i \in \mathbb{N}, \qquad (4.10a)$$

$$\mathbf{y}_p(t_i^+) = \mathbf{C}_2^p(\mathbf{q}(t_i))\mathbf{x}_p(t_i^-) + \mathbf{C}_3^p(\mathbf{q}(t_i))\mathbf{y}_p(t_i^-), \ i \in \mathbb{N}, \qquad (4.10b)$$

where $\mathbf{C}_1^p(\cdot) \in \mathbb{R}^{2\times2}, \mathbf{C}_2^p(\cdot) \in \mathbb{R}^{2\times2}$ and $\mathbf{C}_3^p(\cdot) \in \mathbb{R}^{2\times2}$ are given by

$$\mathbf{C}_1^p(\mathbf{q}(t_i)) := \begin{bmatrix} 1 & 0 \\ 0 & C_1(\mathbf{q}(t_i)) \end{bmatrix}, \mathbf{C}_2^p(\mathbf{q}(t_i)) := \begin{bmatrix} 0 & 0 \\ 0 & C_2(\mathbf{q}(t_i)) \end{bmatrix},$$

$$\mathbf{C}_3^p(\mathbf{q}(t_i)) := \begin{bmatrix} 1 & 0 \\ 0 & -C_1(\mathbf{q}(t_i)) \end{bmatrix},$$

with $C_1(\mathbf{q}(t_i))$ and $C_2(\mathbf{q}(t_i))$ being defined in (3.15).[1]

The precompensator: IM_x, IM_y

In order to solve the tracking problem, the internal model principle is considered, which possibly involves the design of a precompensator in the form:

Free-motion:

$$IM_x : \begin{cases} \dot{\mathbf{x}}_a(t) = \mathbf{A}_a\mathbf{x}_a(t) + \mathbf{B}_a u_{x_a}(t) \\ u_x(t) = \mathbf{C}_a\mathbf{x}_a(t) \end{cases} , \quad \forall t \in (t_i, t_{i+1}), i \in \mathbb{Z}^+, \quad (4.11a)$$

$$IM_y : \begin{cases} \dot{\mathbf{y}}_a(t) = \mathbf{A}_a\mathbf{y}_a(t) + \mathbf{B}_a u_{y_a}(t) \\ u_y(t) = \mathbf{C}_a\mathbf{y}_a(t) \end{cases} , \quad \forall t \in (t_i, t_{i+1}), i \in \mathbb{Z}^+, \quad (4.11b)$$

where $\mathbf{x}_a(t) \in \mathbb{R}^{q-1}$ and $\mathbf{y}_a(t) \in \mathbb{R}^{q-1}$ are the state vectors of the precompensator, $u_{x_a}(t) \in \mathbb{R}$ and $u_{y_a}(t) \in \mathbb{R}$ are the control inputs for the cascade precompensator–plant and the matrix $\mathbf{A}_a$ is chosen such that the dynamic matrix $\mathbf{A}$ in (4.14) for the cascade precompensator–plant has the same Jordan structure as $\mathbf{M}$. So, since the minimum polynomial of $\mathbf{M}$ is $p(\lambda) = \lambda^{q+1}$, a realization $(\mathbf{A}_a, \mathbf{B}_a, \mathbf{C}_a)$ of the precompensator, with $\mathbf{A}_a \in \mathbb{R}^{(q-1)\times(q-1)}, \mathbf{B}_a \in \mathbb{R}^{q-1}$ and $\mathbf{C}_a^T \in \mathbb{R}^{q-1}$ is

$$\mathbf{A}_a = \begin{bmatrix} 0 & 1 & 0 & \cdots & 0 \\ 0 & 0 & 1 & \cdots & 0 \\ \vdots & & \ddots & & \vdots \\ \vdots & & & 0 & 1 \\ 0 & \cdots & \cdots & 0 & 0 \end{bmatrix}, \mathbf{B}_a = \begin{bmatrix} 0 \\ \vdots \\ 0 \\ 1 \end{bmatrix}, \mathbf{C}_a = \begin{bmatrix} 1 & 0 & \cdots & 0 \end{bmatrix}.$$

Moreover, at each impact time t_i, let the right-side values of the state vector of the precompensator be given by

---

[1] Alternatively, the polar representation can be used in order to consider $\mathbf{C}_1^p(\cdot), \mathbf{C}_2^p(\cdot)$ and $\mathbf{C}_3^p(\cdot)$ as functions of the polar angle θ_i.

Reset-values:

$$\mathbf{x}_a(t_i^+) = \boldsymbol{\Lambda}_{ax}(\langle t_i \rangle), \tag{4.12a}$$

$$\mathbf{y}_a(t_i^+) = \boldsymbol{\Lambda}_{ay}(\langle t_i \rangle), \tag{4.12b}$$

where, in view of (4.6), one has

$$\boldsymbol{\Lambda}_{ax}(i) := \begin{bmatrix} \mathbf{0}_{q-1,2} & \mathbf{I}_{q-1} \end{bmatrix} \mathbf{v}_x(i) = \begin{bmatrix} 2a_2^i h_1(i) & \cdots & q! a_q^i h_1(i) \end{bmatrix}^T \in \mathbb{R}^{q-1},$$

$$\boldsymbol{\Lambda}_{ay}(i) := \begin{bmatrix} \mathbf{0}_{q-1,2} & \mathbf{I}_{q-1} \end{bmatrix} \mathbf{v}_y(i) = \begin{bmatrix} 2a_2^i w_1(i) & \cdots & q! a_q^i w_1(i) \end{bmatrix}^T \in \mathbb{R}^{q-1},$$

with $h_1(i) := \bar{x}_{i+1} - \bar{x}_i$, $w_1(i) := \bar{y}_{i+1} - \bar{y}_i$, and $a_j^i, j = 2, \ldots, q$ being the coefficients of polynomials $l_i(\cdot)$ in (3.33).

Notice that in (4.12) a discontinuity is imposed at each time t_i to the vector state of the precompensator, which is part of the proposed controller. In other words, at each impact time t_i system (4.11) is "stopped" and its state is reinitialized according to (4.12).

The augmented system (precompensator–plant): E_x, E_y

By (4.9) and (4.11) and by defining the augmented state vectors $\mathbf{x}_e$, $\mathbf{y}_e \in \mathbb{R}^{q+1}$ as

$$\mathbf{x}_e(t) := \begin{bmatrix} \mathbf{x}_p(t) \\ \mathbf{x}_a(t) \end{bmatrix}, \quad \mathbf{y}_e(t) := \begin{bmatrix} \mathbf{y}_p(t) \\ \mathbf{y}_a(t) \end{bmatrix},$$

one has

Free-motion:

$$E_x : \begin{cases} \dot{\mathbf{x}}_e(t) = \mathbf{A}\mathbf{x}_e(t) + \mathbf{B}u_{x_a}(t) \\ y_{x_e}(t) = \mathbf{C}\mathbf{x}_e(t) \end{cases}, \quad \forall t \in (t_i, t_{i+1}), i \in \mathbb{Z}^+, \tag{4.13a}$$

$$E_y : \begin{cases} \dot{\mathbf{y}}_e(t) = \mathbf{A}\mathbf{y}_e(t) + \mathbf{B}u_{y_a}(t) \\ y_{y_e}(t) = \mathbf{C}\mathbf{y}_e(t) \end{cases}, \quad \forall t \in (t_i, t_{i+1}), i \in \mathbb{Z}^+, \tag{4.13b}$$

where the matrices $\mathbf{A} \in \mathbb{R}^{(q+1)\times(q+1)}, \mathbf{B} \in \mathbb{R}^{q+1}$ and $\mathbf{C}^T \in \mathbb{R}^{q+1}$ are given by

$$\mathbf{A} := \begin{bmatrix} \mathbf{A}_p & \mathbf{B}_p\mathbf{C}_a \\ \mathbf{0} & \mathbf{A}_a \end{bmatrix}, \quad \mathbf{B} := \begin{bmatrix} \mathbf{0} \\ \mathbf{B}_a \end{bmatrix}, \quad \mathbf{C} := \begin{bmatrix} \mathbf{C}_p & \mathbf{0} \end{bmatrix}. \tag{4.14}$$

Remark 12. By (4.9) and (4.11), it follows that $\mathbf{A} = \mathbf{M}$. Moreover, controllability and observability of the plant implies that the pairs $(\mathbf{A}, \mathbf{B})$ and $(\mathbf{A}, \mathbf{C})$ are controllable and observable, respectively.

At each impact time it holds that

Constrained-motion

$$\mathbf{x}_e(t_i^+) = \mathbf{C}_1^e(\mathbf{q}(t_i))\mathbf{x}_e(t_i^-) + \mathbf{C}_2^e(\mathbf{q}(t_i))\mathbf{y}_e(t_i^-) + \mathbf{\Lambda}_{ax}^e(\bar{t}_i), \ i \in \mathbb{N}, \tag{4.15a}$$

$$\mathbf{y}_e(t_i^+) = \mathbf{C}_2^e(\mathbf{q}(t_i))\mathbf{x}_e(t_i^-) + \mathbf{C}_3^e(\mathbf{q}(t_i))\mathbf{y}_e(t_i^-) + \mathbf{\Lambda}_{ay}^e(\bar{t}_i), \ i \in \mathbb{N}, \tag{4.15b}$$

where $\mathbf{C}_1^e(\cdot), \mathbf{C}_2^e(\cdot), \mathbf{C}_3^e(\cdot) \in \mathbb{R}^{(q+1)\times(q+1)}$ are given by

$$\mathbf{C}_k^e(\mathbf{q}(t_i)) := \begin{bmatrix} \mathbf{C}_k^p(\mathbf{q}(t_i)) & \mathbf{0} \\ \mathbf{0} & \mathbf{0} \end{bmatrix}, \quad k \in \{1, 2, 3\},$$

with $\mathbf{C}_1^p(\cdot), \mathbf{C}_2^p(\cdot)$ and $\mathbf{C}_3^p(\cdot)$ being defined in (4.10), and $\mathbf{\Lambda}_x^e(\cdot), \mathbf{\Lambda}_y^e(\cdot) \in \mathbb{R}^{q+1}$ are defined as

$$\mathbf{\Lambda}_{ax}^e(i) := \begin{bmatrix} \mathbf{0} \\ \mathbf{\Lambda}_{ax}(i) \end{bmatrix}, \quad \mathbf{\Lambda}_{ay}^e(i) := \begin{bmatrix} \mathbf{0} \\ \mathbf{\Lambda}_{ay}(i) \end{bmatrix}.$$

By using the notation so far introduced, the dynamics relevant to the x and y coordinates can be merged by defining (see also Remark 11)

$$\mathbf{z}(t) := \begin{bmatrix} \mathbf{x}_e(t) \\ \mathbf{y}_e(t) \end{bmatrix} \in \mathbb{R}^{2(q+1)}, \quad \bar{\mathbf{z}}(t) := \begin{bmatrix} \bar{\mathbf{x}}_e(t) \\ \bar{\mathbf{y}}_e(t) \end{bmatrix} \in \mathbb{R}^{2(q+1)}, \tag{4.16}$$

so that the overall dynamics are

Free-motion:

$$\textbf{Actual:}\quad \dot{\textbf{z}}(t) = \bar{\textbf{A}}\textbf{z}(t) + \bar{\textbf{B}}\textbf{u}_a(t), \tag{4.17}$$

$$\textbf{Desired:}\quad \dot{\bar{\textbf{z}}}(t) = \bar{\textbf{A}}\bar{\textbf{z}}(t), \tag{4.18}$$

where $\bar{\textbf{A}} := \begin{bmatrix} \textbf{A} & \textbf{0} \\ \textbf{0} & \textbf{A} \end{bmatrix}$, $\bar{\textbf{B}} := \begin{bmatrix} \textbf{B} & \textbf{0} \\ \textbf{0} & \textbf{B} \end{bmatrix}$ and $\textbf{u}_a(t) := \begin{bmatrix} u_{xa}(t) \\ u_{ya}(t) \end{bmatrix}$.

Constrained-motion:

$$\textbf{Actual:}\quad \textbf{z}(t_i^+) = \textbf{C}(\textbf{q}(t_i))\textbf{z}(t_i^-) + \boldsymbol{\Lambda}_a(\langle t_i \rangle), \quad i \in \mathbb{N}, \tag{4.19a}$$

$$\textbf{Desired:}\quad \bar{\textbf{z}}(\bar{t}_i^+) = \textbf{C}(\bar{\textbf{q}}(t_i))\bar{\textbf{z}}(\bar{t}_i^-) + \boldsymbol{\Lambda}_a(\bar{t}_i), \quad i \in \mathbb{N}, \tag{4.19b}$$

where $\boldsymbol{\Lambda}_a(i) := \begin{bmatrix} \boldsymbol{\Lambda}_{ax}^e(i) \\ \boldsymbol{\Lambda}_{ay}^e(i) \end{bmatrix}$ and $\textbf{C}(\textbf{q}) := \begin{bmatrix} \textbf{C}_1^e(\textbf{q}) & \textbf{C}_2^e(\textbf{q}) \\ \textbf{C}_2^e(\textbf{q}) & \textbf{C}_3^e(\textbf{q}) \end{bmatrix} \in \mathbb{R}^{2(q+1)\times 2(q+1)}$,

with $\textbf{C}_1^e(\cdot)$, $\textbf{C}_2^e(\cdot)$, $\textbf{C}_3^e(\cdot)$ and $\boldsymbol{\Lambda}_{ax}^e(\cdot)$, $\boldsymbol{\Lambda}_{ay}^e(\cdot)$ being defined in (4.15).

4.3 A switched control algorithm

In the ideal case that the actual trajectory coincides with the desired one, both trajectories impact at the same times. It is thus reasonable to expect that actual trajectories which are close enough to the desired ones will have impact times very close to the desired impact times. Hence, in the overall control algorithm three possible events, which can occur at time $t > t_0$, are taken into account:

1) the desired trajectory hits the boundary;

2) the actual trajectory hits the boundary;

3) too much time is elapsed since the last impact of one of the two trajectories without further impacts.

The algorithm implementing the proposed control strategy is described by means of both a Finite State Automata (FSA) [44] (Fig. 4.2) and by pseudo-code (Fig. 4.3) more suitable for simulation purposes. The output of the (Moore) FSA represents the control status: **ON** means that the control action is applied; **OFF** means that the control is turned off. The states of the FSA are characterized by the flags *DES* and *ACT*, which are set to 1 when the desired trajectory impacts whereas the actual one is still in unconstrained motion and viceversa, respectively. The labels on the arcs denote the events that cause the transition from a state to another. Essentially, those are the events listed above with the threshold σ defined as the maximum allowed time interval with the control switched off. This small positive number σ guarantees to avoid to keep down the control for too much time, that is bad for the tracking purpose. By assuming that the plant state $\mathbf{z}(t)$ in (4.17) is available, during the interval of time with the control active, the control law is

$$u_{x_a} = \mathbf{K}_x(\mathbf{x}_e - \bar{\mathbf{x}}_e), \tag{4.20a}$$

$$u_{y_a} = \mathbf{K}_y(\mathbf{y}_e - \bar{\mathbf{y}}_e), \tag{4.20b}$$

where $u_{x_a} \in \mathbb{R}$ and $u_{y_a} \in \mathbb{R}$ are the control inputs to the cascade precompensator plus plant (see (4.11)) and $\mathbf{K}_x^T \in \mathbb{R}^{2(q+1)}$ and $\mathbf{K}_y^T \in \mathbb{R}^{2(q+1)}$ are chosen such that all eigenvalues of $\mathbf{A} + \mathbf{B}\mathbf{K}_x$ and $\mathbf{A} + \mathbf{B}\mathbf{K}_y$ have real part less than or equal to $-\eta$, with η being a positive real constant and $\mathbf{A}, \mathbf{B}$ are defined in (4.14). During the intervals of time with the control off, one has $u_{x_a} = 0$ and $u_{y_a} = 0$.

Remark 13. The aim to switch off of the control is to improve the behavior of the considered system. Some reasons and possible scenarios can be considered in order to justify such a choice. As a matter of fact, assume that the control is always active and that the nominal trajectory impacts before the corresponding impact of the controlled trajectory, the latter starts to "change" in order to track the new reference, that is bouncing away from the boundary;

```
Initialize the system;
des_impacted=0;
act_impacted=0;
switch-on the control;
while ("system is running")
  % Events 1) AND 2)
  if ("desired AND actual trajectories impact")
    des_impacted=0; act_impacted=0;
    switch-on or keep-on the control;
  % Event 1)
  else if ("desired trajectory impacts")
    if (act_impacted==0)
      des_impacted=1;
      switch-off the control;
    else
      act_impacted=0;
      switch-on the control;
    end
  % Event 2)
  else if ("actual trajectory impacts")
    if (des_impacted==0)
      act_impacted=1;
      switch-off the control;
    else
      des_impacted=0;
      switch-on the control;
    end
  % Event 3)
  else if ("the maximum time is elapsed")
    des_impacted=0; act_impacted=0;
    switch-on the control;
  % No Event has occurred
  else
    keep the present status of the control;
  end
end
```

Figure 4.2: Pseudo-code of the algorithm implementing the control strategy.
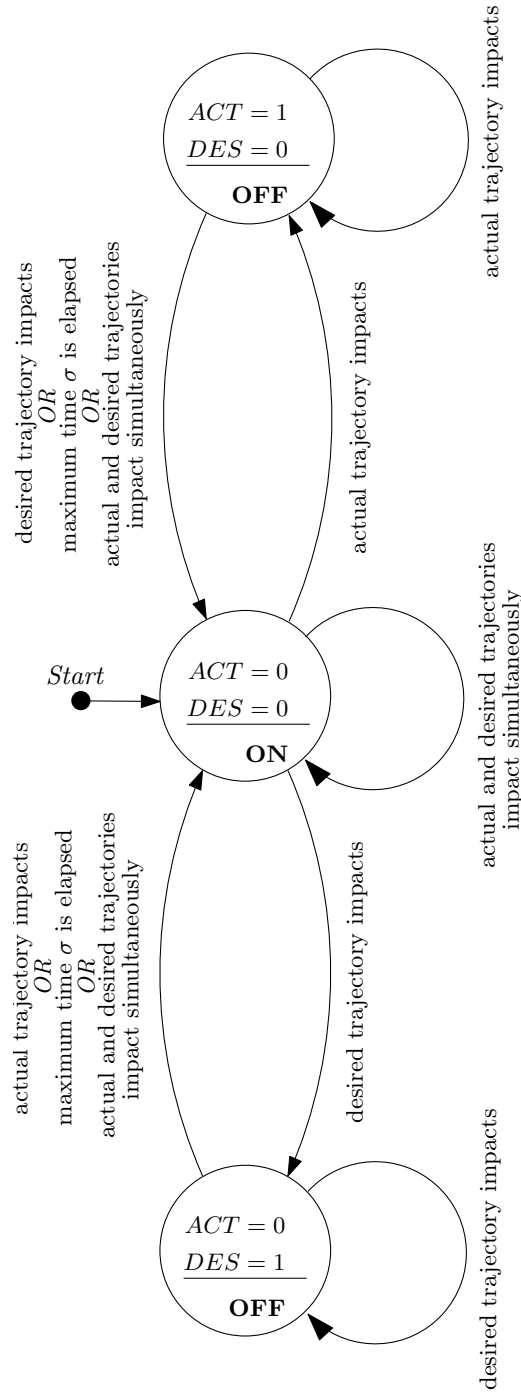
Figure 4.3: Finite State Automata describing the proposed control strategy.

hence, even if the actual trajectory hits the boundary, such an impact can be very far from its nominal value (see Fig. 4.4); in such conditions it is quite easy that the actual trajectory does not impact at all (see Fig. 4.6(a)). Still
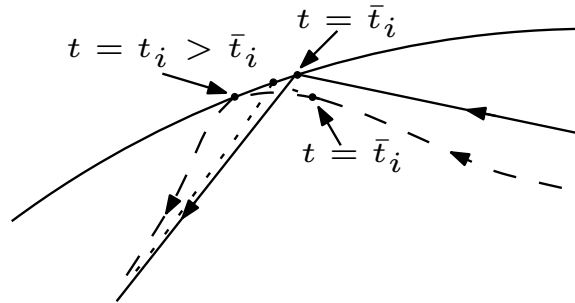
Figure 4.4: The nominal trajectory (solid) impacts before the actual one (dashed: when the control is always active; dotted: if the switching strategy is used).

with the control always active, if the controlled trajectory impacts before the nominal one, one can easily have an accumulation point of the impact times of the actual trajectory close to the impact of the desired trajectory (see Fig. 4.5); although this fact is not necessarily bad for the tracking objective, it seems better to avoid as much as possible such a possibility. Through many
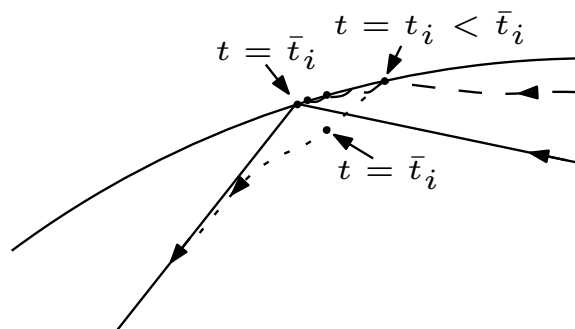
Figure 4.5: The nominal trajectory (solid) impacts after the actual one (dashed: when the control is always active; dotted: if the switching strategy is used).

simulations, it has been shown that the proposed algorithm permits to obtain the tracking purpose also when the initial conditions are quite far from the desired ones (see Fig. 4.6).

Note that, sometimes in the present chapter and in Chapter 5, the desired variables are also denoted by means of the subscript "$_d$" (e.g., $\bar{x}(t) \equiv x_d(t)$).

4.4   Main result

Assumption 1. If the initial time t_0 is an impact time for the desired trajectory (i.e., $t_0 \in \mathbb{Z}$), then $\bar{\mathbf{z}}(t_0) = \bar{\mathbf{z}}(t_0^+)$, i.e., $\bar{\mathbf{z}}(t_0) = \begin{bmatrix} \mathbf{v}_x^T(t_0) & \mathbf{v}_y^T(t_0) \end{bmatrix}^T$ with $\mathbf{v}_x(\cdot)$ and $\mathbf{v}_y(\cdot)$ being defined in (4.6).

By choosing the initial conditions sufficiently close to the desired ones (as allowed by the stability-like requirements in Problem 3) and under the Assumption 1[2], for all integer $i > \lfloor t_0 \rfloor$ the impact time $t_i \in \mathbb{R}$ of the actual trajectory can be forced to be close to the impact time i of the desired trajectory (see proof of the subsequent Theorem 8), so that the proposed control algorithm coincides with

$$u_{x_a}(t) = \begin{cases} \mathbf{K}_x(\mathbf{x}_e(t) - \bar{\mathbf{x}}_e(t)), & \forall t \in (t_i^M, t_{i+1}^m), i \in \mathbb{Z}, i \geq \lfloor t_0 \rfloor, \\ 0, & \text{otherwise,} \end{cases} \tag{4.21a}$$

$$u_{y_a}(t) = \begin{cases} \mathbf{K}_y(\mathbf{y}_e(t) - \bar{\mathbf{y}}_e(t)), & \forall t \in (t_i^M, t_{i+1}^m), i \in \mathbb{Z}, i \geq \lfloor t_0 \rfloor, \\ 0, & \text{otherwise,} \end{cases} \tag{4.21b}$$

where $t_{\lfloor t_0 \rfloor}^M := t_0$ and, for each $\bar{t}_i := i \in \mathbb{Z}, i \geq \lfloor t_0 \rfloor + 1$, one defines

$$t_i^m := \min\{t_i, \bar{t}_i\}, \quad t_i^M := \max\{t_i, \bar{t}_i\}.$$

Theorem 8. *Under the Assumption 1, there exists $\eta^* \in \mathbb{R}^+$ such that the controller characterized by (4.11),(4.12) and (4.21) solves Problem 3, for all*

---

[2]Assumption 1 with the hypothesis of the Problem 3 permits to avoid that the actual trajectory hits the boundary just after t_0.
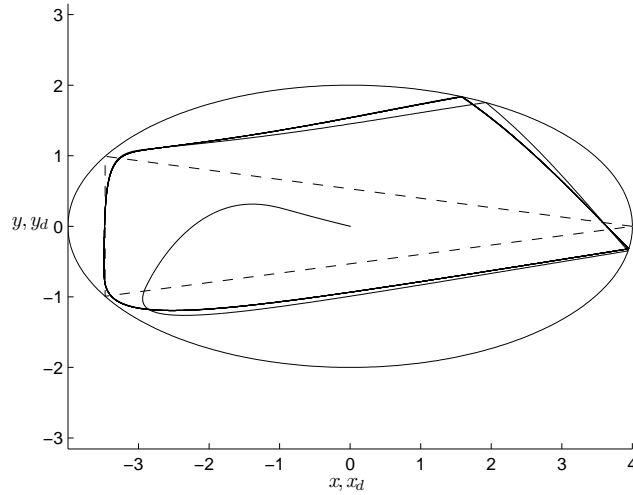
(a) The control is never switched off.
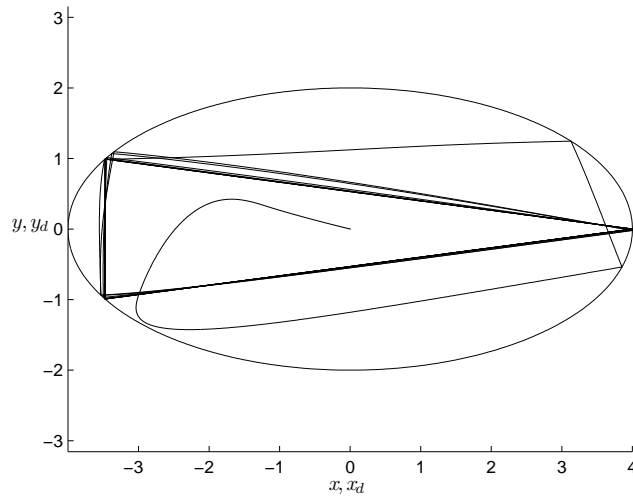
(b) The switching control with a threshold $\sigma = 0.15$ is used.

Figure 4.6: The desired (dashed) and actual (solid) trajectories obtained using a control strategy with or without switching. The case of rotational motion with winding number $(N = 3, R = 1)$ is considered with all the closed loop eigenvalues placed at -3 (in (b) the desired trajectory is not visible being overlapped with the actual one).

$\eta \geq \eta^*$.

Proof. In the following, in view of Remark 10 and by considering the extended tracking error vector defined as

$$\mathbf{e}(t) := \mathbf{z}(t) - \bar{\mathbf{z}}(t), \qquad (4.22)$$

it is shown how the properties (c) and (d) of Problem 3, which are close to the classical stability and attractivity properties, respectively, can be guaranteed also when $\mathbf{e_q}(t)$ is replaced by $\mathbf{e}(t)$, thus satisfying a stronger requirement. The proof can be carried out by means of the steps described below, based on the following facts whose proofs, for the sake of readability, are given at the end of this chapter in Section 6.5.

$$\exists \delta_0, M_1 \in \mathbb{R}^+ : \|\mathbf{e}(t_i^{m-})\| < \delta_0 \Rightarrow \left\| \begin{bmatrix} \Delta t_i \\ \Delta \theta_i \end{bmatrix} \right\| \leq M_1 \|\mathbf{e}(t_i^{m-})\|, \quad (4.23)$$

$$\exists \delta_1, M_2, M_3 \in \mathbb{R}^+ : \|\mathbf{e}(t_i^{m-})\| < \delta_1, \left\| \begin{bmatrix} \Delta t_i \\ \Delta \theta_i \end{bmatrix} \right\| < \delta_1 \Rightarrow$$

$$\Rightarrow \|\mathbf{e}(t_i^{M+})\| \leq M_2 \|\mathbf{e}(t_i^{m-})\| + M_3 \left\| \begin{bmatrix} \Delta t_i \\ \Delta \theta_i \end{bmatrix} \right\|, \qquad (4.24)$$

$$\forall \eta \in \mathbb{R}^+, \|\mathbf{e}(t)\| \leq L(\eta) e^{-\eta(t - t_i^M)} \|\mathbf{e}(t_i^{M+})\|, \quad \forall t \in (t_i^M, t_{i+1}^m), \quad (4.25)$$

$$\forall \varepsilon^* > 0, \forall T > 0, \exists \eta^* > 0 : \eta > \eta^* \Rightarrow L(\eta) e^{-\eta T} < \varepsilon^*, \qquad (4.26)$$

where $\Delta t_i := t_i - \bar{t}_i, \Delta \theta_i := \theta_i - \bar{\theta}_i$ and, in view of the periodicity of the desired trajectory, (6.17) and (6.18) hold for all $i \in \mathbb{Z}, i \geq \lfloor t_0 \rfloor + 1$ whereas (6.19) and (6.20) hold for all $i \in \mathbb{Z}, i \geq \lfloor t_0 \rfloor$.

Remark 14. Roughly speaking, (6.17) and (6.18) show that the *minimal* amount of continuity needed to obtain the stability properties is still present despite the jumps affecting the system. The fact that such properties can be proved is essential as this represents one technical difficulty that is intrinsic to nonsmooth systems.

Step (i): in view of (6.17) and (6.18) and in order to guarantee that for any $i \in \mathbb{Z}, i \geq \lfloor t_0 \rfloor + 1$ the actual impact time t_i belongs to the interval $(\bar{t}_i - \gamma, \bar{t}_i + \gamma)$ for a fixed $\gamma \in (0, 1/2)$, one can take $\|\mathbf{e}(t_i^{m-})\| < \bar{\delta}_0$ where $\bar{\delta}_0 := \min\{\delta_0, \delta_1, \delta_1/M_1, \gamma/M_1\}$.

Step (ii): by putting together (6.17) and (6.18), the following inequality is obtained

$$\|\mathbf{e}(t_i^{M+})\| \leq (M_2 + M_3 M_1)\|\mathbf{e}(t_i^{m-})\| =: \beta\|\mathbf{e}(t_i^{m-})\|, \qquad (4.27)$$

where $\beta := M_2 + M_3 M_1$.

Step (iii): by using (6.19) and (6.22), for each $i \in \mathbb{Z}, i \geq \lfloor t_0 \rfloor + 1$ one has[3]

$$\|\mathbf{e}(t_{i+1}^{m-})\| \leq L(\eta)e^{-\eta(t_{i+1}^m - t_i^M)}\|\mathbf{e}(t_i^{M+})\| \leq L(\eta)e^{-\eta(1-2\gamma)}\beta\|\mathbf{e}(t_i^{m-})\|.$$

At this point, by taking in (6.20) $\varepsilon^* \leq \xi/\beta$ with $0 < \xi < 1$, there exists η^* such that, for all $\eta > \eta^*$, it follows that $Le^{-\eta(1-2\gamma)}\beta \leq \xi$, which implies[4]

$$\|\mathbf{e}(t_{i+1}^{m-})\| \leq \xi\|\mathbf{e}(t_i^{m-})\|, \quad \xi \in (0,1), \qquad (4.28)$$

for $i \in \mathbb{Z}, i \geq \lfloor t_0 \rfloor + 1$.

Step (iv): for a generic time interval $(t_i^M, t_{i+1}^m), i \in \mathbb{Z}, i \geq \lfloor t_0 \rfloor + 1$, from (6.19) one has

$$\|\mathbf{e}(t)\| \leq Le^{-\eta(t-t_i^M)}\|\mathbf{e}(t_i^{M+})\| \leq L\beta\|\mathbf{e}(t_i^{m-})\|,$$

and taking $\|\mathbf{e}(t_i^{m-})\| < \bar{\bar{\delta}}_0$ with $\bar{\bar{\delta}}_0 := \min\{\bar{\delta}_0, \varepsilon/(L\beta)\}$ for a generic $\varepsilon > 0$ follows that $\|\mathbf{e}(t)\| < \varepsilon$ for all $t \in (t_i^M, t_{i+1}^m), i \in \mathbb{Z}, i \geq \lfloor t_0 \rfloor + 1$. By (6.23), if $\|\mathbf{e}(t_i^{m-})\| < \bar{\bar{\delta}}_0$, then $\|\mathbf{e}(t_{i+1}^{m-})\| < \bar{\bar{\delta}}_0$, in fact

$$\|\mathbf{e}(t_{i+1}^{m-})\| \leq \xi\|\mathbf{e}(t_i^{m-})\| < \xi\bar{\bar{\delta}}_0 < \bar{\bar{\delta}}_0.$$

---

[3]By **Step (i)**, the minimum flight-time in free motion is $1 - 2\gamma$.

[4]From now on, η is fixed so that L is a real positive constant (dependence on η is omitted).

Now, in order to guarantee that $\|\mathbf{e}(t_i^{m-})\| < \bar{\bar{\delta}}_0$ for any $i \in \mathbb{Z}, i \geq \lfloor t_0 \rfloor + 1$ and $\|\mathbf{e}(t)\| < \varepsilon$ for all $t \in (t_0, t_{\lfloor t_0 \rfloor + 1}^m)$, it is sufficient to take $\delta_{\varepsilon,\gamma} := \min\{\bar{\bar{\delta}}_0/L, \varepsilon/L\}$. In summary, for all $i \in \mathbb{Z}, i \geq \lfloor t_0 \rfloor$ the following result has been obtained

$$\|\mathbf{e}(t_0^+)\| < \delta_{\varepsilon,\gamma} \Rightarrow \|\mathbf{e}(t)\| < \varepsilon, \quad \forall t \in (t_i^M, t_{i+1}^m), \tag{4.29}$$

and since $|\Delta t_i| < \gamma, i \in \mathbb{Z}, i \geq \lfloor t_0 \rfloor + 1$ (see **Step (i)**), then (4.29) implies property (c) in Problem 3.

To complete the proof it remains to prove property (d) in Problem 3.

Step (v): since $\xi \in (0, 1)$, if $\|\mathbf{e}(t_0^+)\| < \delta_{\varepsilon,\gamma}$, then applying iteratively (6.23) yields

$$\|\mathbf{e}(t_i^{m-})\| < \xi\|\mathbf{e}(t_{i-1}^{m-})\| < \xi^{i+(\lfloor t_0 \rfloor - 1)}L\|\mathbf{e}(t_0^+)\| < \xi^{i+(\lfloor t_0 \rfloor - 1)}L\delta_{\varepsilon,\gamma} \overset{i \to +\infty}{\to} 0. \tag{4.30}$$

By (4.30) and (6.17), it follows that

$$\left\| \begin{bmatrix} \Delta t_i \\ \Delta \theta_i \end{bmatrix} \right\| \leq M_1\|\mathbf{e}(t_i^{m-})\| \to 0 \Rightarrow \begin{cases} t_i \to \bar{t}_i \\ \theta_i \to \bar{\theta}_i \end{cases} \text{ as } i \to +\infty, \tag{4.31}$$

and by using similar reasonings, it is shown that in each interval (t_i^M, t_{i+1}^m)

$$\|\mathbf{e}(t)\| \to 0 \text{ as } i \to \infty,$$

and by this result and (6.30) it follows that

$$\forall \tau \in (0, 1), \exists i^* : i > i^* \Rightarrow \bar{t}_i + \tau \in \underbrace{(t_i^M, t_{i+1}^m)}_{\to (\bar{t}_i, \bar{t}_{i+1})} \text{ and}$$

$$\|\mathbf{e}(\bar{t}_i + \tau)\| \to 0 \text{ as } i \to +\infty.$$

Since $t_i \to \bar{t}_i$ as $i \to +\infty$, time $\bar{t}_i + \tau, \forall \tau \in (0, 1)$ is an impact time neither for the actual trajectory nor for the desired one. Therefore, $\lim\limits_{i \to +\infty} \|\mathbf{e}((\bar{t}_i + \tau)^-)\| =$

$\lim\limits_{i\to+\infty} \|\mathbf{e}((\bar{t}_i + \tau)^+)\| = \lim\limits_{i\to+\infty} \|\mathbf{e}(\bar{t}_i + \tau))\| = 0$. This last fact, together with the definition of $\mathbf{e}(t)$ given in (4.22), proves property (d) of Problem 3.   □

4.5   Examples

Concerning the problem of generating reference signals in an elliptical billiard system, examples of rotational and librational motion have been presented in Section 3.4. In particular, the following cases:

Rotational motion: $(N = 7, R = 2)$,
Librational motion: $(N = 4, R = 1)$,

are reconsidered here in order to show the effectiveness of the proposed control law.

In both cases, the static gains $\mathbf{K}_x$ and $\mathbf{K}_y$ in (4.20) are chosen such that all the eigenvalues of the closed-loop dynamic matrix are moved at $-\eta = -7$ and the value of the threshold σ is set to 0.15. The behavior of the controlled trajectories during the first 9.5 seconds of motion, starting from zero initial conditions at the initial time $t_0 = 0.5$, can be observed in Fig. 4.7 and Fig. 4.8 for the rotational case and in Fig. 4.9 and Fig. 4.10 for the librational case.   Though the switching algorithm with the threshold σ has been used, due to the fact that the desired trajectory is periodic and the system to be controlled is time-invariant, in order to obtain simulation examples of the situation considered in Theorem 8 (when it is assumed that the initial error is sufficiently small so that the threshold σ is never active) one can consider the same examples proposed here starting from a time $t_0^* \geq t_0$, such that the controlled trajectory at time t_0^* is close to the nominal one (e.g., for both examples depicted here one can take (roughly) $t_0^* = 3$). The simulation was performed in Matlab® using the *event* option of the ODE solvers for impact detection and handling.

Remark 15. In the present work all the results are obtained under the assumption that the coefficient of restitution e is equal to 1. If $e < 1$, different desired

(a) $\mathbf{q}(t), \bar{\mathbf{q}}(t)$

(b) $x(t), \bar{x}(t)$ and $y(t), \bar{y}(t)$

(c) $\dot{x}(t), \dot{\bar{x}}(t)$ and $\dot{y}(t), \dot{\bar{y}}(t)$
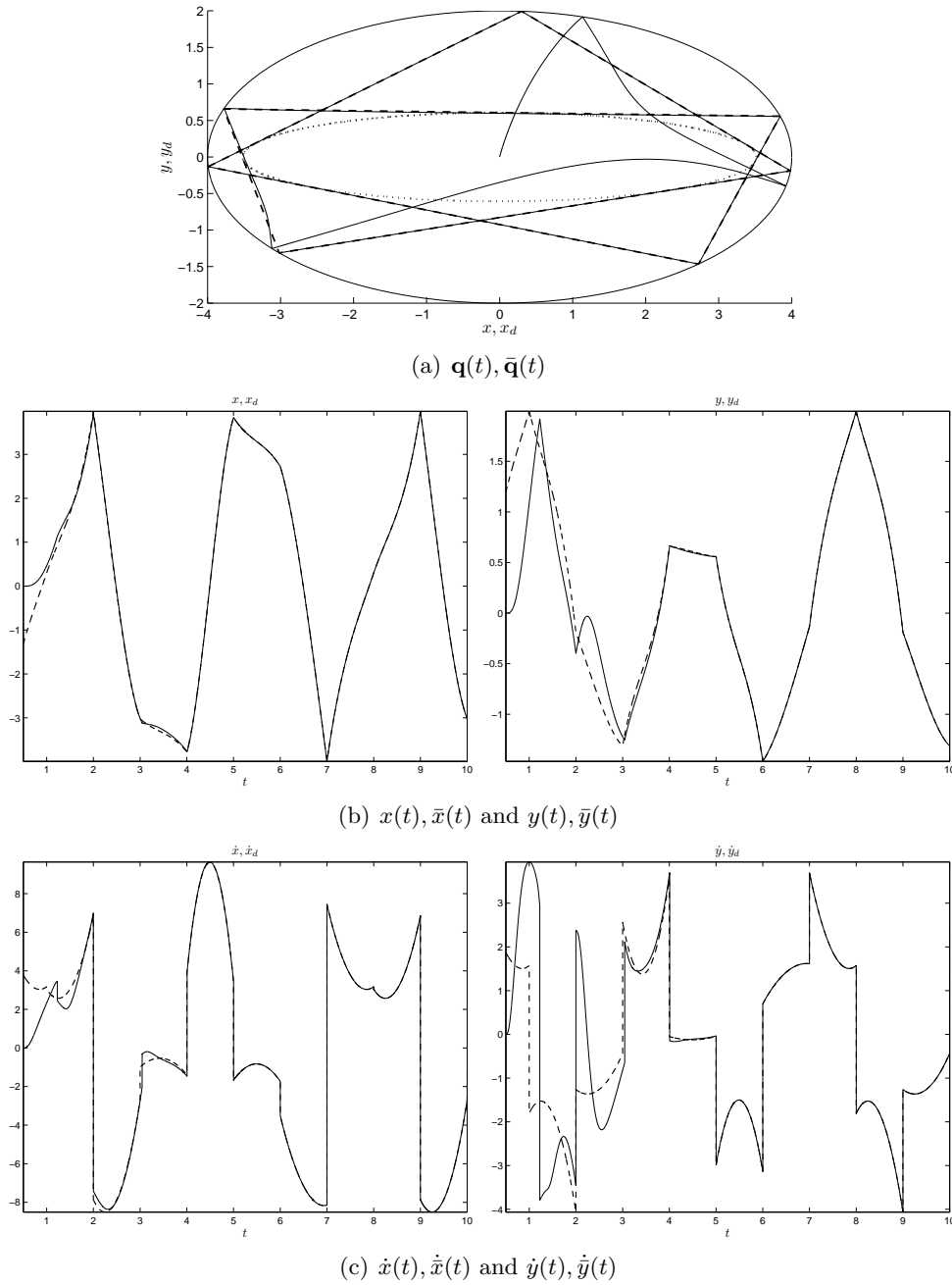
Figure 4.7: *Rotational motion* $(N = 7, R = 2)$: the inner caustic curve (dotted) with the desired (dashed) trajectory, which is completely overlapped with the actual (solid) one, in the xy-plane (a) and time behavior of the desired (dashed) and actual (solid) positions (b) and velocities (c).
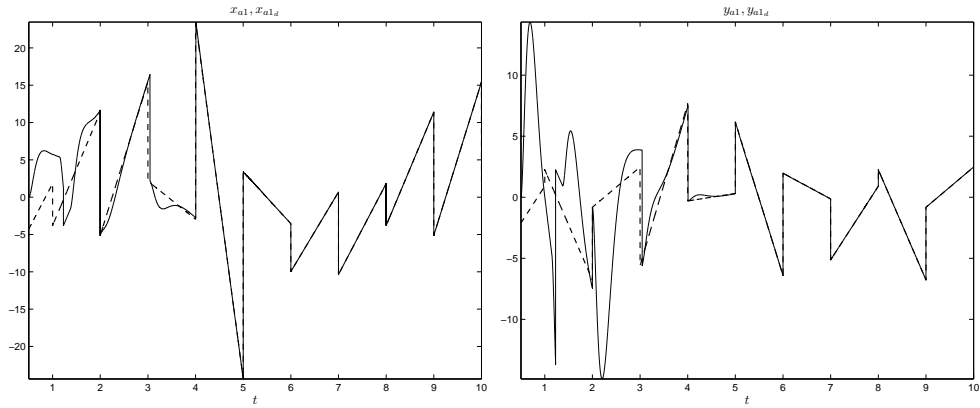
(a) $x_{a1}(t), \bar{x}_{a1}(t)$ and $y_{a1}(t), \bar{y}_{a1}(t)$
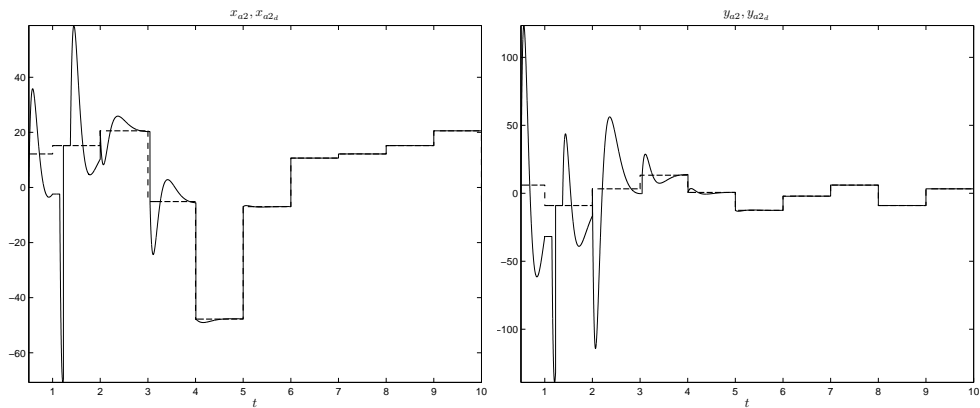
(b) $x_{a2}(t), \bar{x}_{a2}(t)$ and $y_{a2}(t), \bar{y}_{a2}(t)$

Figure 4.8: *Rotational motion* $(N = 7, R = 2)$: time behavior of the desired (dashed) and actual (solid) first (a) and second (b) precompensator state variables.

(a) $\mathbf{q}(t), \bar{\mathbf{q}}(t)$

(b) $x(t), \bar{x}(t)$ and $y(t), \bar{y}(t)$

(c) $\dot{x}(t), \dot{\bar{x}}(t)$ and $\dot{y}(t), \dot{\bar{y}}(t)$
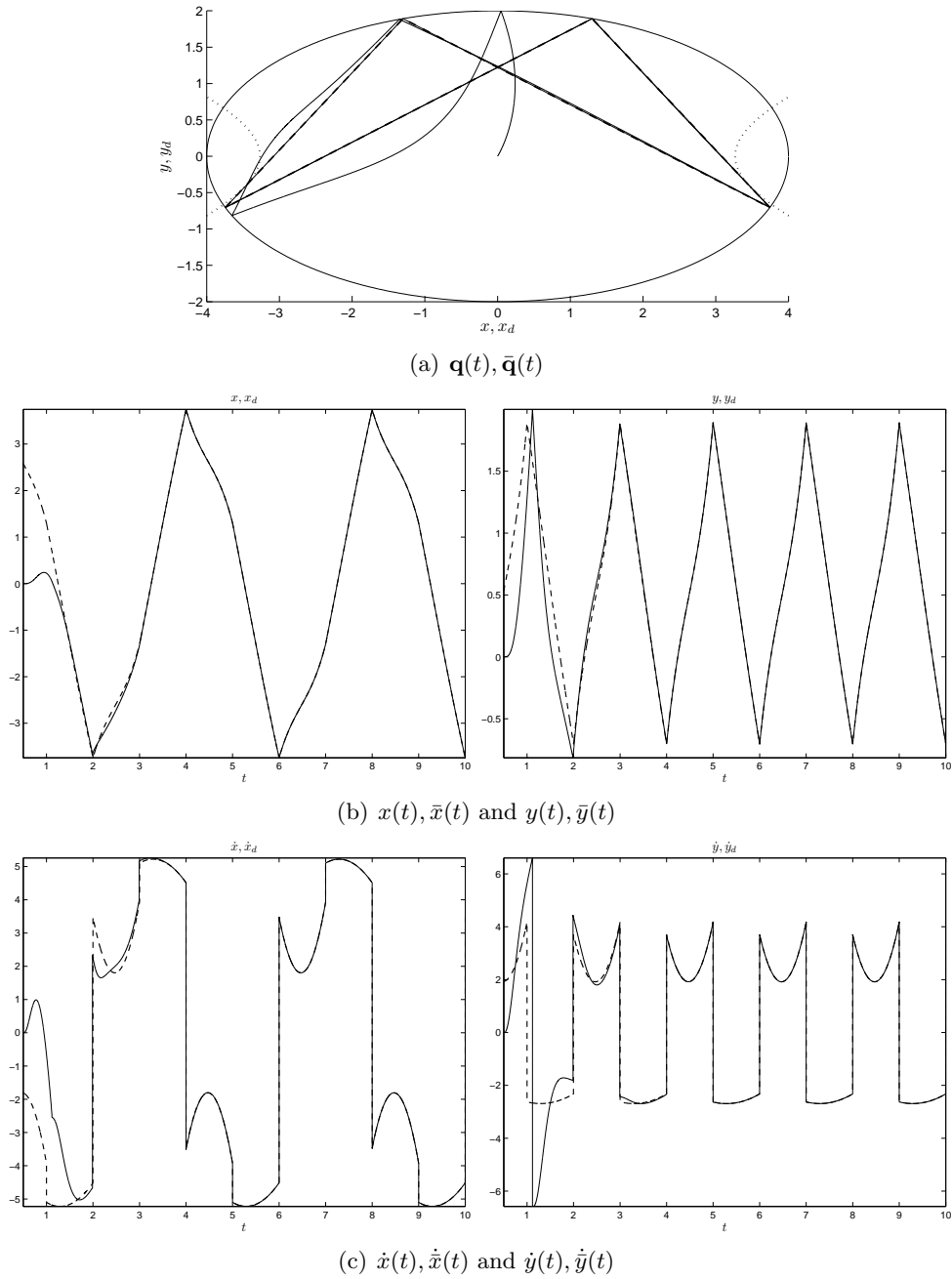
Figure 4.9: *Librational motion* ($N = 4, R = 1$): the inner caustic curve (dotted) with the desired (dashed) trajectory, which is completely overlapped with the actual (solid) one, in the *xy*-plane (a) and time behavior of the desired (dashed) and actual (solid) positions (b) and velocities (c).
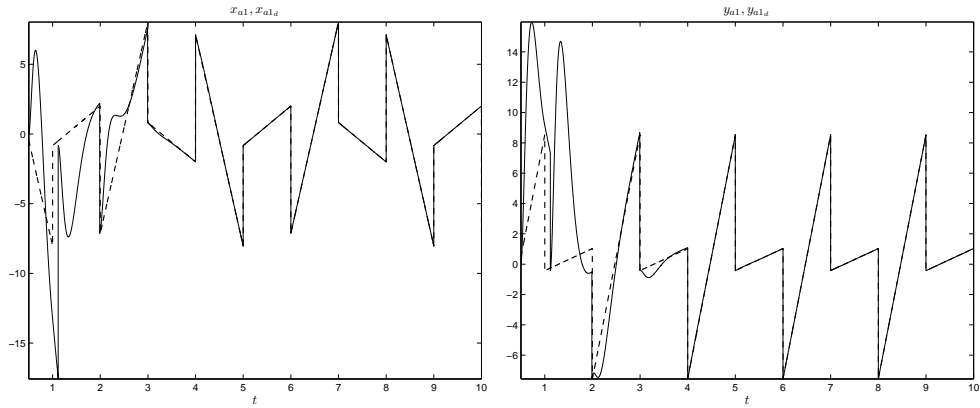
(a) $x_{a1}(t), \bar{x}_{a1}(t)$ and $y_{a1}(t), \bar{y}_{a1}(t)$
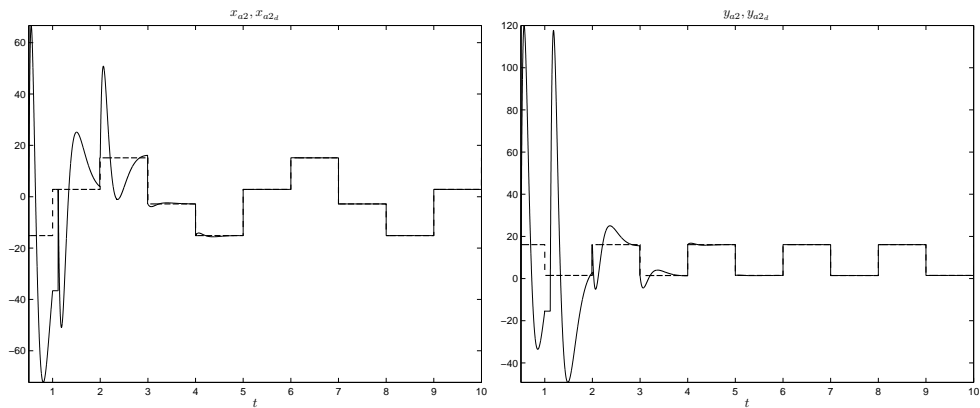
(b) $x_{a2}(t), \bar{x}_{a2}(t)$ and $y_{a2}(t), \bar{y}_{a2}(t)$

Figure 4.10: *Librational motion* ($N = 4, R = 1$): time behavior of the desired (dashed) and actual (solid) first (a) and second (b) precompensator state variables.

paths should be computed in order to take into account that, at each impact, the angle of incidence is different from the angle of reflection. In such a case one first possibility, for sufficiently large e, still requiring that the path between two consecutive impacts is a straight line, would be to compute a closed desired path numerically by guessing an initial segment and adjusting it in order to obtain a closed orbit. Otherwise, and such a second possibility would be feasible for all values of e, one should accept that the path between two consecutive impacts is not a straight line. On the other hand, by keeping the desired trajectories proposed here, if $e < 1$, then only impulsive control can be a solution of Problem 3: as a matter of fact, in order for $(\mathbf{q}(t), \dot{\mathbf{q}}(t)) = (\bar{\mathbf{q}}(t), \dot{\bar{\mathbf{q}}}(t))$ to be a piecewise solution of the closed-loop system for $t \geq t_0$ (as required by property (a) of Problem 3), it is necessary that the kinetic energy lost at each impact time due to the coefficient of restitution less than one is restored so that the kinetic energy immediately after the impact takes its value immediately before the impact, through the action of the control: this is impossible as the control forces are not impulsive.

Moreover, although here it has been assumed that the impacts can be detected in real time, a slightly modified control problem involving a relaxed tracking requirement can be solved even without such an assumption.

4.6 Details of the proof of main result

This appendix contains details about the proofs of the facts (6.17),(6.18), (6.19) and (6.20).

Details of the proof of fact (6.17)

Regarding the presence of impacts, for all $i \in \mathbb{Z}, i \geq \lfloor t_0 \rfloor + 1$, there are two possible cases (see Fig. 4.11):

$$\textbf{Case a)}: \quad t_i < \bar{t}_i \;\Rightarrow\; t_i^m = t_i,\, t_i^M = \bar{t}_i;$$
$$\textbf{Case b)}: \quad t_i > \bar{t}_i \;\Rightarrow\; t_i^m = \bar{t}_i,\, t_i^M = t_i.$$
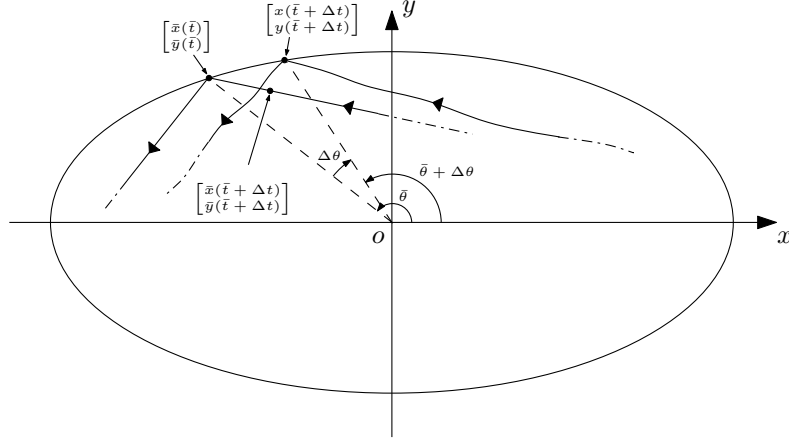
Figure 4.11: **Case a)**: the actual trajectory impacts before the desired trajectory ($t_i < \bar{t}_i, \Delta t_i < 0$).

Remark 16. Since the desired trajectory is periodic, all the results obtained in the following considering $i \in \{\lfloor t_0 \rfloor + 1, \ldots, N + \lfloor t_0 \rfloor\} =: \mathcal{I}_N$, remain proved for $i \in \mathbb{Z}, i \geq \lfloor t_0 \rfloor + 1$.

Define, for each $i \in \mathcal{I}_N$,

$$\mathbf{g}_i(x_1, y_1, \Delta\theta) := \begin{bmatrix} g_1(x_1, y_1) \\ g_{2,i}(x_1, y_1, \Delta\theta) \end{bmatrix} : \mathbb{R}^3 \to \mathbb{R}^2,$$

where $g_1 : \mathbb{R}^2 \to \mathbb{R}$ and $g_{2,i} : \mathbb{R}^3 \to \mathbb{R}$ are given by[5]

$$g_1(x_1, y_1) := \frac{x_1^2}{a^2} + \frac{y_1^2}{b^2} - 1, \tag{4.32a}$$

$$g_{2,i}(x_1, y_1, \Delta\theta) := \sin(\bar{\theta}_i + \Delta\theta)x_1 - \cos(\bar{\theta}_i + \Delta\theta)y_1. \tag{4.32b}$$

---

[5]The dependence of $g_{2,i}$ on i is due to the fact that the straight-line defined by such an implicit function changes with $\bar{\theta}_i$, whereas for all the vertices of the actual trajectory the implicit function g_1 remains unchanged.

Therefore, by (4.32a) and (4.32b) it follows that $\mathbf{g}_i(x_1, y_1, \Delta\theta) = \mathbf{0}$, for $i \in \mathcal{I}_N$, at the intersection between the elliptical boundary and a straight-line starting from the origin with direction normal to the vector $\begin{bmatrix} \sin(\bar{\theta}_i + \Delta\theta) & -\cos(\bar{\theta}_i + \Delta\theta) \end{bmatrix}^T$.

If x_1 and y_1 are defined as the position coordinates for the actual trajectory at the impact time $t_i, i \in \mathcal{I}_N$, i.e., $x_1 := x(t_i)$ and $y_1 := y(t_i)$, then they can be written as

$$\begin{bmatrix} x_1 \\ y_1 \end{bmatrix} = \begin{bmatrix} h_{1,i}(\Delta t_i, \mathbf{e}(t_i^{m-})) \\ h_{2,i}(\Delta t_i, \mathbf{e}(t_i^{m-})) \end{bmatrix}, \tag{4.33}$$

where $h_{1,i}, h_{2,i} : \mathbb{R}^{2(q+1)+1} \to \mathbb{R}$ and $\Delta t_i := t_i - \bar{t}_i$. In particular, in order to show that x_1 and y_1 can be expressed as functions of Δt_i and $\mathbf{e}(t_i^{m-})$ for $i \in \mathcal{I}_N$, the two possible cases are considered separately.

Case a) $t_i^m = t_i$, $t_i^M = \bar{t}_i$, so that $\Delta t_i < 0$ and $\mathbf{z}(t_i^-) = \mathbf{z}(t_i^{m-})$, where $\mathbf{z}(t)$ is defined in (4.16). In this case, one has

$$\mathbf{z}(t_i^-) = \mathbf{z}(t_i^{m-}) = \mathbf{e}(t_i^{m-}) + \bar{\mathbf{z}}(t_i^{m-}) = \mathbf{e}(t_i^{m-}) + e^{-\bar{\mathbf{A}}(t_i^M - t_i^m)}\bar{\mathbf{z}}(t_i^{M-}) =$$
$$= \mathbf{e}(t_i^{m-}) + e^{\bar{\mathbf{A}}\Delta t_i}\bar{\mathbf{z}}(t_i^{d-}); \tag{4.34}$$

Case b) $t_i^m = \bar{t}_i$, $t_i^M = t_i$, so that $\Delta t_i > 0$ and $\mathbf{z}(t_i^-) = \mathbf{z}(t_i^{M-})$, where $\mathbf{z}(t)$ is defined in (4.16). In this case, one has

$$\mathbf{z}(t_i^-) = \mathbf{z}(t_i^{M-}) = e^{\bar{\mathbf{A}}(t_i^M - t_i^m)}\mathbf{z}(t_i^{m+}) = e^{\bar{\mathbf{A}}(t_i^M - t_i^m)}\mathbf{z}(t_i^{m-}) =$$
$$= e^{\bar{\mathbf{A}}\Delta t_i}\mathbf{e}(t_i^{m-}) + e^{\bar{\mathbf{A}}\Delta t_i}\bar{\mathbf{z}}(t_i^{d-}). \tag{4.35}$$

By (4.34) and (4.35), for $i \in \mathcal{I}_N$, it is shown that $\mathbf{z}(t_i^-)$ is a function of Δt_i and $\mathbf{e}(t_i^{m-})$ and given that $x(t_i^-) = x(t_i)$ and $y(t_i^-) = y(t_i)$ are the first and the $((q+1)+1)$-th component of $\mathbf{z}(t_i^-)$, respectively, there exist two functions $h_{1,i}$ and $h_{2,i}$ of Δt_i and $\mathbf{e}(t_i^{m-})$ such that (4.33) holds.

Moreover, $\mathbf{z}(t_i^-)$ is an analytic function of Δt_i and $\mathbf{e}(t_i^{m-})$ for $\Delta t_i < 0$ and $\Delta t_i > 0$, for $i \in \mathcal{I}_N$. In the hyperplane characterized by $\Delta t_i = 0$, $\mathbf{z}(t_i^-)$ is a continuous function with respect to its variables. As a matter of fact, one can

observe that in a whole period (i.e., for $i \in \mathcal{I}_N$)

Case a)

$$\mathbf{z}(t_i^-)|_{\Delta t_i = 0} = \mathbf{e}(t_i^{m-}) + \mathbf{I}\bar{\mathbf{z}}(t_i^{d-}) = \mathbf{e}(t_i^{d-}) + \bar{\mathbf{z}}(t_i^{d-});$$

Case b)

$$\mathbf{z}(t_i^-)|_{\Delta t_i = 0} = \mathbf{I}\mathbf{e}(t_i^{m-}) + \mathbf{I}\bar{\mathbf{z}}(t_i^{d-}) = \mathbf{e}(t_i^{d-}) + \bar{\mathbf{z}}(t_i^{d-}),$$

and the continuity of $\mathbf{z}(t_i^-)$ in $\Delta t_i = 0$ implies the continuity also for $x(t_i), y(t_i), \dot{x}(t_i^-)$ and $\dot{y}(t_i^-)$ with respect to Δt_i, since they are just four components of $\mathbf{z}(t_i^-)$. In other words, by defining $\mathbf{V}_1^T \in \mathbb{R}^{2(q+1)}, \mathbf{V}_2^T \in \mathbb{R}^{2(q+1)}, \mathbf{V}_3^T \in \mathbb{R}^{2(q+1)}$ and $\mathbf{V}_4^T \in \mathbb{R}^{2(q+1)}$ as

$$\mathbf{V}_1 := \begin{bmatrix} 1 & 0 & 0 & \cdots & 0 \end{bmatrix}, \quad \mathbf{V}_2 := \begin{bmatrix} \mathbf{0}_{1\times(q+1)} & 1 & 0 & \cdots & 0 \end{bmatrix},$$
$$\mathbf{V}_3 := \begin{bmatrix} 0 & 1 & 0 & \cdots & 0 \end{bmatrix}, \quad \mathbf{V}_4 := \begin{bmatrix} \mathbf{0}_{1\times(q+2)} & 1 & 0 & \cdots & 0 \end{bmatrix},$$

where $\mathbf{0}_{i\times j}$ denotes the zero matrix of size $i \times j$, and since

$$\mathbf{e}(t_i^{d-}) + \bar{\mathbf{z}}(t_i^{d-}) = \mathbf{z}(t_i^{d-}),$$

in both cases **a)** and **b)** one has[6]

$$x(t_i)|_{\Delta t_i = 0} = \mathbf{V}_1 \mathbf{z}(t_i^{d-}),$$
$$y(t_i)|_{\Delta t_i = 0} = \mathbf{V}_2 \mathbf{z}(t_i^{d-}),$$
$$\dot{x}(t_i^-)|_{\Delta t_i = 0} = \mathbf{V}_3 \mathbf{z}(t_i^{d-}),$$
$$\dot{y}(t_i^-)|_{\Delta t_i = 0} = \mathbf{V}_4 \mathbf{z}(t_i^{d-}).$$

---

[6]Take the derivative with respect to Δt or t is equivalent, that is $\frac{\partial x(\cdot)}{\partial \Delta t} = \dot{x}(\cdot)$, since $\Delta t := t - i, i \in \mathbb{Z}$.

Moreover, as for the partial derivatives, after some computations, in both cases
a) and **b)** the following results hold

$$
\left.\frac{\partial \mathbf{z}(t_i^-)}{\partial \mathbf{e}(t_i^{m-})}\right|_{\Delta t_i=0} = \mathbf{I} \Rightarrow
\begin{cases}
\left.\dfrac{\partial \mathbf{V}_1 \mathbf{z}(t_i^-)}{\partial \mathbf{e}(t_i^{m-})}\right|_{\Delta t_i=0} = \left.\dfrac{\partial x(t_i)}{\partial \mathbf{e}(t_i^{m-})}\right|_{\Delta t_i=0} = \mathbf{V}_1 \\[2mm]
\left.\dfrac{\partial \mathbf{V}_2 \mathbf{z}(t_i^-)}{\partial \mathbf{e}(t_i^{m-})}\right|_{\Delta t_i=0} = \left.\dfrac{\partial y(t_i)}{\partial \mathbf{e}(t_i^{m-})}\right|_{\Delta t_i=0} = \mathbf{V}_2
\end{cases},
$$

and

$$
\left.\frac{\partial \mathbf{z}(t_i^-)}{\partial \Delta \theta_i}\right|_{\Delta t_i=0} = \mathbf{0} \Rightarrow
\begin{cases}
\left.\dfrac{\partial \mathbf{V}_1 \mathbf{z}(t_i^-)}{\partial \Delta \theta_i}\right|_{\Delta t_i=0} = \left.\dfrac{\partial x(t_i)}{\partial \Delta \theta_i}\right|_{\Delta t_i=0} = \mathbf{0} \\[2mm]
\left.\dfrac{\partial \mathbf{V}_2 \mathbf{z}(t_i^-)}{\partial \Delta \theta_i}\right|_{\Delta t_i=0} = \left.\dfrac{\partial y(t_i)}{\partial \Delta \theta_i}\right|_{\Delta t_i=0} = \mathbf{0}
\end{cases}.
$$

Therefore, for all $i \in \mathcal{I}_N$, the functions $\mathbf{g}_i$ are continuously differentiable also
on the hyperplane $\Delta t_i = 0$, in fact by the results so far obtained it follows that
the partial derivatives of g_1 and $g_{2,i}$ with respect to $\Delta t_i, \Delta \theta_i$ and $\mathbf{e}(t_i^{m-})$ are
in both cases exactly the same when $\Delta t_i = 0$. At this point, by using (4.33),
the functions $\tilde{\mathbf{g}}_i : \mathbb{R}^{2(q+1)+2} \to \mathbb{R}^2$ can be defined, for $i \in \mathcal{I}_N$, as

$$
\tilde{\mathbf{g}}_i(\underbrace{\Delta t_i, \Delta \theta_i}_{=:\boldsymbol{\chi}}, \underbrace{\mathbf{e}(t_i^{m-})}_{=:\boldsymbol{\psi}}) := \mathbf{g}_i(h_{1,i}(\Delta t_i, \mathbf{e}(t_i^{m-})), h_{2,i}(\Delta t_i, \mathbf{e}(t_i^{m-})), \Delta \theta_i), \quad (4.36)
$$

where

$$
h_{1,i}(\Delta t_i, \mathbf{e}(t_i^{m-})) :=
\begin{cases}
\mathbf{V}_1(\mathbf{e}(t_i^{m-}) + e^{\bar{\mathbf{A}} \Delta t_i} \bar{\mathbf{z}}(t_i^{d-})), & \Delta t_i \leq 0 \\[2mm]
\mathbf{V}_1 e^{\bar{\mathbf{A}} \Delta t_i}(\mathbf{e}(t_i^{m-}) + \bar{\mathbf{z}}(t_i^{d-})), & \Delta t_i \geq 0
\end{cases},
$$

and

$$
h_{2,i}(\Delta t_i, \mathbf{e}(t_i^{m-})) :=
\begin{cases}
\mathbf{V}_2(\mathbf{e}(t_i^{m-}) + e^{\bar{\mathbf{A}} \Delta t_i} \bar{\mathbf{z}}(t_i^{d-})), & \Delta t_i \leq 0 \\[2mm]
\mathbf{V}_2 e^{\bar{\mathbf{A}} \Delta t_i}(\mathbf{e}(t_i^{m-}) + \bar{\mathbf{z}}(t_i^{d-})), & \Delta t_i \geq 0
\end{cases}.
$$

Remark 17. In view of the results above, there exists a neighborhood $\boldsymbol{\Omega}$ of

$\Delta t_i = 0, \Delta \theta_i = 0$ and $\mathbf{e}(t_i^{m-}) = 0$ such that (4.36) are continuously differentiable on that neighborhood for all $i \in \mathcal{I}_N$.

Lemma 3 (*(implicit function theorem, see, e.g., [3])*)**.** *Let $\tilde{\mathbf{g}}_i(\boldsymbol{\chi}, \boldsymbol{\psi}) : \mathbb{R}^{2+2(q+1)} \supseteq \boldsymbol{\Omega} \to \mathbb{R}^2$ be continuously differentiable on the open set $\boldsymbol{\Omega}$. Let $(\boldsymbol{\chi}^0, \boldsymbol{\psi}^0)$ be a point in $\boldsymbol{\Omega}$ for which $\tilde{\mathbf{g}}_i(\boldsymbol{\chi}^0, \boldsymbol{\psi}^0) = \mathbf{0}$ and for which $\det\left(\nabla_{\boldsymbol{\chi}}\tilde{\mathbf{g}}_i(\boldsymbol{\chi}^0, \boldsymbol{\psi}^0)\right) \neq 0$. Then, there exists a neighborhood $\boldsymbol{\Psi}$ of $\boldsymbol{\psi}^0$ and a unique function $\boldsymbol{\phi}_i(\cdot) : \boldsymbol{\chi} = \boldsymbol{\phi}_i(\boldsymbol{\psi})$ with $\boldsymbol{\phi}_i : \boldsymbol{\Psi} \to \mathbb{R}^2$ being continuously differentiable on $\boldsymbol{\Psi}$, such that $\boldsymbol{\chi}^0 = \boldsymbol{\phi}_i(\boldsymbol{\psi}^0)$ and $\tilde{\mathbf{g}}_i(\boldsymbol{\phi}_i(\boldsymbol{\psi}), \boldsymbol{\psi}) = \mathbf{0}, \forall \boldsymbol{\psi} \in \boldsymbol{\Psi}$. In addition, the following result holds*

$$\nabla_{\boldsymbol{\psi}}\boldsymbol{\phi}_i = -(\nabla_{\boldsymbol{\chi}}\tilde{\mathbf{g}}_i)^{-1}\nabla_{\boldsymbol{\psi}}\tilde{\mathbf{g}}_i.$$

By using Lemma 3 for the implicit functions defined in (4.36), it is possible to prove that for all $i \in \mathcal{I}_N$

$$\exists \delta_0 \in \mathbb{R}^+, M_1 \in \mathbb{R}^+ : \|\mathbf{e}(t_i^{m-})\| < \delta_0 \Rightarrow \left\|\begin{bmatrix} \Delta t_i \\ \Delta \theta_i \end{bmatrix}\right\| \leq M_1 \|\mathbf{e}(t_i^{m-})\|. \quad (6.17)$$

First of all, in order to apply the implicit function theorem, all its hypothesis have to be verified. Taking $\boldsymbol{\chi}^0 = \mathbf{0}$ and $\boldsymbol{\psi}^0 = \mathbf{0}$, i.e., $\Delta t_i = 0, \Delta \theta_i = 0$ and $\mathbf{e}(t_i^{m-}) = \mathbf{0}$, one has $\tilde{\mathbf{g}}_i(\boldsymbol{\chi}^0, \boldsymbol{\psi}^0) = \mathbf{0}$, for $i \in \mathcal{I}_N$. In fact, such a choice yields in both cases the following results.

  Case a) by setting $\Delta t_i = 0, \Delta \theta_i = 0$ and $\mathbf{e}(t_i^{m-}) = \mathbf{0}$ in (4.34) one
  obtains

$$\mathbf{z}(t_i^{m-})|_{(\boldsymbol{\chi}^0, \boldsymbol{\psi}^0)} = \mathbf{0} + \mathbf{I}\bar{\mathbf{z}}(t_i^{d-}) \Rightarrow \begin{cases} x_1^0 = \bar{x}(\bar{t}_i) \\ y_1^0 = \bar{y}(\bar{t}_i) \end{cases} ;$$

  Case b) by setting $\Delta t_i = 0, \Delta \theta_i = 0$ and $\mathbf{e}(t_i^{m-}) = \mathbf{0}$ in (4.35) one
  obtains

$$\mathbf{z}(t_i^{M-})|_{(\boldsymbol{\chi}^0, \boldsymbol{\psi}^0)} = \mathbf{I}\mathbf{0} + \mathbf{I}\bar{\mathbf{z}}(t_i^{d-}) = \bar{\mathbf{z}}(t_i^{d-}) \Rightarrow \begin{cases} x_1^0 = \bar{x}(\bar{t}_i) \\ y_1^0 = \bar{y}(\bar{t}_i) \end{cases} .$$

Hence, by (4.36) and (4.32), it follows that

$$
\begin{cases}
\tilde{g}_1(0,0,\mathbf{0}) = g_1(x_1^0, y_1^0, 0) = \bar{x}(\bar{t}_i)/a^2 + \bar{y}(\bar{t}_i)/b^2 - 1, \\
\tilde{g}_{2,i}(0,0,\mathbf{0}) = g_{2,i}(x_1^0, y_1^0, 0) = \sin(\bar{\theta}_i)\bar{x}(\bar{t}_i) - \cos(\bar{\theta}_i)\bar{y}(\bar{t}_i),
\end{cases}
$$

and since $\bar{t}_i = i, i \in \mathbb{Z}$ are impact times for the desired trajectory, then $\tilde{g}_1(0,0,\mathbf{0}) = 0$ and $\tilde{g}_{2,i}(0,0,\mathbf{0}) = 0$ for $i \in \mathcal{I}_N$, i.e., $\tilde{\mathbf{g}}_i(0,0,\mathbf{0}) = \mathbf{0}$. The Jacobian of $\tilde{\mathbf{g}}_i$ with respect to $\boldsymbol{\chi} := \begin{bmatrix} \Delta t_i & \Delta \theta_i \end{bmatrix}^T$ at the point $(\boldsymbol{\chi}^0, \boldsymbol{\psi}^0)$ can be computed as:

$$
\nabla_{\boldsymbol{\chi}} \tilde{\mathbf{g}}_i(\boldsymbol{\chi}^0, \boldsymbol{\psi}^0) = \begin{bmatrix} \dfrac{\partial \tilde{g}_1}{\partial \Delta t_i} & \dfrac{\partial \tilde{g}_1}{\partial \Delta \theta_i} \\[2mm] \dfrac{\partial \tilde{g}_{2,i}}{\partial \Delta t_i} & \dfrac{\partial \tilde{g}_{2,i}}{\partial \Delta \theta_i} \end{bmatrix} \Bigg|_{(\boldsymbol{\chi}, \boldsymbol{\psi}) = (\boldsymbol{\chi}^0, \boldsymbol{\psi}^0)},
$$

where by considering that $\bar{t}_i = i, i \in \mathcal{I}_N$ are impact times for the desired trajectory, the following results hold

$$
\frac{\partial \tilde{g}_1}{\partial \Delta t_i}\bigg|_{(\boldsymbol{\chi}^0, \boldsymbol{\psi}^0)} = \frac{2}{a^2}\bar{x}(\bar{t}_i)\dot{\bar{x}}(\bar{t}_i) + \frac{2}{b^2}\bar{y}(\bar{t}_i)\dot{\bar{y}}(\bar{t}_i) \neq 0,
$$

$$
\frac{\partial \tilde{g}_1}{\partial \Delta \theta_i}\bigg|_{(\boldsymbol{\chi}^0, \boldsymbol{\psi}^0)} = 0,
$$

$$
\frac{\partial \tilde{g}_{2,i}}{\partial \Delta \theta_i}\bigg|_{(\boldsymbol{\chi}^0, \boldsymbol{\psi}^0)} = \cos(\bar{\theta}_i)\bar{x}(\bar{t}_i) + \sin(\bar{\theta}_i)\bar{y}(\bar{t}_i) \neq 0,
$$

and this implies that $\det(\nabla_{\boldsymbol{\chi}} \tilde{\mathbf{g}}_i(\boldsymbol{\chi}^0, \boldsymbol{\psi}^0)) \neq 0$.

By Lemma 3, it follows that, for each $i \in \mathcal{I}_N$, the functions $\tilde{\mathbf{g}}_i(\Delta t_i, \Delta \theta_i, \mathbf{e}(t_i^{m-}))$ implicitly define $\boldsymbol{\chi} = \boldsymbol{\phi}_i(\boldsymbol{\psi})$ in a neighborhood of $\boldsymbol{\psi} = \mathbf{0}$. In other words, there exists a neighborhood $\boldsymbol{\Psi}$ of $\mathbf{e}(t_i^{m-}) = \mathbf{0}$ such that on that neighborhood one can write

$$
\begin{bmatrix} \Delta t_i \\ \Delta \theta_i \end{bmatrix} = \boldsymbol{\phi}_i(\mathbf{e}(t_i^{m-})), \quad \text{for any } \mathbf{e}(t_i^{m-}) \in \boldsymbol{\Psi},
$$

and the functions $\boldsymbol{\phi}_i(\cdot)$ are continuously differentiable. Hence, by the well

known Weierstrass theorem (see, e.g., [3]) there exist N constants $M_{1,i} \in \mathbb{R}^+$ such that $\|\nabla_{\boldsymbol{\psi}}\boldsymbol{\phi}_i(\boldsymbol{\psi}^0)\| \leq M_{1,i}$ on the closure of $\boldsymbol{\Psi}$, and hence also on $\boldsymbol{\Psi}$, for $i \in \mathcal{I}_N$. By using this fact, a first order approximation for the functions $\boldsymbol{\phi}_i(\cdot)$ can be considered on a neighborhood of $\boldsymbol{\psi}^0 = \mathbf{0}$ as

$$
\begin{bmatrix} \Delta t_i \\ \Delta \theta_i \end{bmatrix} = \boldsymbol{\phi}_i(\boldsymbol{\psi}^0) + \nabla_{\boldsymbol{\psi}}\boldsymbol{\phi}_i(\boldsymbol{\psi}^0)(\boldsymbol{\psi} - \boldsymbol{\psi}^0) + o(\|\boldsymbol{\psi}\|) = \nabla_{\boldsymbol{\psi}}\boldsymbol{\phi}_i(\boldsymbol{\psi}^0)\boldsymbol{\psi} + o(\|\boldsymbol{\psi}\|),
$$

where $\boldsymbol{\psi} := \mathbf{e}(t_i^{m-})$. At this point, (6.17) is proved for each $i \in \mathcal{I}_N$, just by defining $M_1 := \max_{i \in \mathcal{I}_N}\{M_{1,i}\}$ and by considering a sufficiently small neighborhood of $\mathbf{e}(t_i^{m-}) = 0$ of radius $\delta_0 \in \mathbb{R}^+$.

Details of the proof of fact (6.18)

For all $i \in \mathcal{I}_N$, one has to prove that

$$
\exists \delta_1 \in \mathbb{R}^+, M_2 \in \mathbb{R}^+, M_3 \in \mathbb{R}^+ : \|\mathbf{e}(t_i^{m-})\| < \delta_1, \left\| \begin{bmatrix} \Delta t_i \\ \Delta \theta_i \end{bmatrix} \right\| < \delta_1 \Rightarrow
$$

$$
\Rightarrow \|\mathbf{e}(t_i^{M+})\| \leq M_2\|\mathbf{e}(t_i^{m-})\| + M_3 \left\| \begin{bmatrix} \Delta t_i \\ \Delta \theta_i \end{bmatrix} \right\|. \tag{6.18}
$$

The two possible cases are considered separately.

Case a) $t_i^m = t_i$, $t_i^M = \bar{t}_i$, so that $\Delta t_i < 0$, and the error at time t_i^{M+}, that is after the i-th couple of impacts, is given by $\mathbf{e}(t_i^{M+}) := \mathbf{z}(t_i^{M+}) - \bar{\mathbf{z}}(t_i^{M+})$, where

$$
\mathbf{z}(t_i^{M+}) = e^{\bar{\mathbf{A}}(t_i^M - t_i^m)}\mathbf{z}(t_i^{m+}) = e^{\bar{\mathbf{A}}(t_i^M - t_i^m)}(\mathbf{C}(\theta_i)\mathbf{z}(t_i^{m-}) + \boldsymbol{\Lambda}_a(t_i^M)) =
$$
$$
= e^{\bar{\mathbf{A}}(t_i^M - t_i^m)}\mathbf{C}(\theta_i)(\mathbf{e}(t_i^{m-}) + \bar{\mathbf{z}}(t_i^{m-})) + e^{\bar{\mathbf{A}}(t_i^M - t_i^m)}\boldsymbol{\Lambda}_a(t_i^M),
$$
$$
\bar{\mathbf{z}}(t_i^{M+}) = \mathbf{C}(\bar{\theta}_i)\bar{\mathbf{z}}(t_i^{M-}) + \boldsymbol{\Lambda}_a(t_i^M).
$$

Hence, it follows that

$$
\begin{aligned}
\mathbf{e}(t_i^{M+}) &= e^{\bar{\mathbf{A}}(t_i^M - t_i^m)}\mathbf{C}(\theta_i)(\mathbf{e}(t_i^{m-})+ \\
&\quad + \bar{\mathbf{z}}(t_i^{m-})) + e^{\bar{\mathbf{A}}(t_i^M - t_i^m)}\mathbf{\Lambda}_a(t_i^M) - \mathbf{C}(\bar{\theta}_i)\bar{\mathbf{z}}(t_i^{M-}) - \mathbf{\Lambda}_a(t_i^M) = \\
&= (e^{\bar{\mathbf{A}}(t_i^M - t_i^m)} - \mathbf{I})\mathbf{\Lambda}_a(t_i^M)+ \\
&\quad + (e^{\bar{\mathbf{A}}(t_i^M - t_i^m)}\mathbf{C}(\theta_i) - \mathbf{C}(\bar{\theta}_i)e^{\bar{\mathbf{A}}(t_i^M - t_i^m)})\bar{\mathbf{z}}(t_i^{m-})+ \\
&\quad + e^{\bar{\mathbf{A}}(t_i^M - t_i^m)}\mathbf{C}(\theta_i)\mathbf{e}(t_i^{m-}) = \\
&= (e^{-\bar{\mathbf{A}}\Delta t_i} - \mathbf{I})\mathbf{\Lambda}_a(\bar{t}_i)+ \\
&\quad + (e^{-\bar{\mathbf{A}}\Delta t_i}\mathbf{C}(\bar{\theta}_i + \Delta\theta_i) - \mathbf{C}(\bar{\theta}_i)e^{-\bar{\mathbf{A}}\Delta t_i})e^{\bar{\mathbf{A}}\Delta t_i}\bar{\mathbf{z}}(t_i^{d-})+ \\
&\quad + e^{-\bar{\mathbf{A}}\Delta t_i}\mathbf{C}(\bar{\theta}_i + \Delta\theta_i)\mathbf{e}(t_i^{m-}),
\end{aligned}
$$

where $\Delta\theta_i := \theta_i - \bar{\theta}_i$;

Case b) $t_i^m = \bar{t}_i$, $t_i^M = t_i$, so that $\Delta t_i > 0$, and the error at time t_i^{M+}, that is after the i-th couple of impacts, is given by $\mathbf{e}(t_i^{M+}) := \mathbf{z}(t_i^{M+}) - \bar{\mathbf{z}}(t_i^{M+})$, where

$$
\begin{aligned}
\mathbf{z}(t_i^{M+}) &= \mathbf{C}(\theta_i)\mathbf{z}(t_i^{M-}) + \mathbf{\Lambda}_a(t_i^m), \\
\bar{\mathbf{z}}(t_i^{M+}) &= e^{\bar{\mathbf{A}}(t_i^M - t_i^m)}\bar{\mathbf{z}}(t_i^{m+}) = e^{\bar{\mathbf{A}}(t_i^M - t_i^m)}(\mathbf{C}(\bar{\theta}_i)\bar{\mathbf{z}}(t_i^{m-}) + \mathbf{\Lambda}_a(t_i^m)) = \\
&= e^{\bar{\mathbf{A}}(t_i^M - t_i^m)}\mathbf{C}(\bar{\theta}_i)\bar{\mathbf{z}}(t_i^{m-}) + e^{\bar{\mathbf{A}}(t_i^M - t_i^m)}\mathbf{\Lambda}_a(t_i^m).
\end{aligned}
$$

Hence, it follows that

$$
\begin{aligned}
\mathbf{e}(t_i^{M+}) &= \mathbf{C}(\theta_i)\mathbf{z}(t_i^{M-})+ \\
&\quad + \boldsymbol{\Lambda}_a(t_i^m) - e^{\bar{\mathbf{A}}(t_i^M - t_i^m)}\mathbf{C}(\bar{\theta}_i)\bar{\mathbf{z}}(t_i^{m-}) - e^{\bar{\mathbf{A}}(t_i^M - t_i^m)}\boldsymbol{\Lambda}_a(t_i^m) = \\
&= (\mathbf{I} - e^{\bar{\mathbf{A}}(t_i^M - t_i^m)})\boldsymbol{\Lambda}_a(t_i^m)+ \\
&\quad + (\mathbf{C}(\theta_i)e^{\bar{\mathbf{A}}(t_i^M - t_i^m)} - e^{\bar{\mathbf{A}}(t_i^M - t_i^m)}\mathbf{C}(\bar{\theta}_i))\bar{\mathbf{z}}(t_i^{m-})+ \\
&\quad + \mathbf{C}(\theta_i)e^{\bar{\mathbf{A}}(t_i^M - t_i^m)}\mathbf{e}(t_i^{m-}) = \\
&= (\mathbf{I} - e^{\bar{\mathbf{A}}\Delta t_i})\boldsymbol{\Lambda}_a(t_i^d) + (\mathbf{C}(\bar{\theta}_i + \Delta\theta_i)e^{\bar{\mathbf{A}}\Delta t_i} - e^{\bar{\mathbf{A}}\Delta t_i}\mathbf{C}(\bar{\theta}_i))\bar{\mathbf{z}}(t_i^{d-})+ \\
&\quad + \mathbf{C}(\bar{\theta}_i + \Delta\theta_i)e^{\bar{\mathbf{A}}\Delta t_i}\mathbf{e}(t_i^{m-}),
\end{aligned}
$$

where $\Delta\theta_i := \theta_i - \bar{\theta}_i$.

For each $i \in \mathcal{I}_N$, in both cases **a)** and **b)**, i.e., for $\Delta t_i < 0$ and $\Delta t_i > 0$, respectively, the functions $\mathbf{e}(t_i^{M+})$ are equal to $\mathbf{0}$ when $\Delta t_i = 0, \Delta\theta_i = 0$ and $\mathbf{e}(t_i^{m-}) = 0$ and they are analytic functions with respect to their variables. In view of this fact, the following results hold

Case a)

$$
\exists \delta_1 \in \mathbb{R}^+, M_{2,a,i} \in \mathbb{R}^+, M_{3,a,i} \in \mathbb{R}^+ :
$$

$$
\|\mathbf{e}(t_i^{m-})\| < \delta_1, -\delta_1 < \Delta t_i < 0, |\Delta\theta_i| < \delta_1 \Rightarrow
$$

$$
\Rightarrow \|\mathbf{e}(t_i^{M+})\| \le M_{2,a,i}\|\mathbf{e}(t_i^{m-})\| + M_{3,a,i}\left\|\begin{bmatrix} \Delta t_i \\ \Delta\theta_i \end{bmatrix}\right\|;
$$

Case b)

$$
\exists \delta_1 \in \mathbb{R}^+, M_{2,b,i} \in \mathbb{R}^+, M_{3,b,i} \in \mathbb{R}^+ :
$$

$$
\|\mathbf{e}(t_i^{m-})\| < \delta_1, 0 < \Delta t_i < \delta_1, |\Delta\theta_i| < \delta_1 \Rightarrow
$$

$$
\Rightarrow \|\mathbf{e}(t_i^{M+})\| \le M_{2,b,i}\|\mathbf{e}(t_i^{m-})\| + M_{3,b,i}\left\|\begin{bmatrix} \Delta t_i \\ \Delta\theta_i \end{bmatrix}\right\|.
$$

Moreover, for all $i \in \mathcal{I}_N$, the functions $\mathbf{e}(t_i^{M+})$ are continuous on the hyperplane characterized by $\Delta t_i = 0$.[7] In particular, in both cases **a)** and **b)**, one has

$$\mathbf{e}(t_i^{M+})|_{\Delta t_i = 0} = (\mathbf{C}(\bar{\theta}_i + \Delta\theta_i) - \mathbf{C}(\bar{\theta}_i))\bar{\mathbf{z}}(t_i^{d-}) + \mathbf{C}(\bar{\theta}_i + \Delta\theta_i)\mathbf{e}(t_i^{m-}).$$

Therefore, (6.18) are proved, for all $i \in \mathcal{I}_N$, by choosing $M_2 := \max\limits_{\substack{i \in \mathcal{I}_N \\ j \in \{a,b\}}} \{M_{2,j,i}\}$

and $M_3 := \max\limits_{\substack{i \in \mathcal{I}_N \\ j \in \{a,b\}}} \{M_{3,j,i}\}$.

Details of the proof of facts (6.19) and (6.20)

The closed-loop dynamics during the unconstrained motion are given by (5.24a). By using the control law given in (4.21) and by defining $\bar{\mathbf{K}} := blockdiag\{\mathbf{K}_x, \mathbf{K}_y\} \in \mathbb{R}^{2 \times 2(q+1)}$ the error dynamics of the closed-loop system are

$$\dot{\mathbf{e}}(t) = (\bar{\mathbf{A}} + \bar{\mathbf{B}}\bar{\mathbf{K}})\mathbf{e}(t) =: \tilde{\mathbf{A}}\mathbf{e}(t), \quad \forall t \in (t_i^M, t_{i+1}^m), i \in \mathbb{Z}, i \geq \lfloor t_0 \rfloor, \qquad (4.37)$$

where all eigenvalues of $\tilde{\mathbf{A}}$ have real part less than or equal to $-\eta$. Hence, in each interval of time without impacts one has

$$\exists L \in \mathbb{R}^+ : \|\mathbf{e}(t)\| \leq Le^{-\eta(t - t_i^M)}\|\mathbf{e}(t_i^{M+})\|, \quad \forall t \in (t_i^M, t_{i+1}^m), i \in \mathbb{Z}, i \geq \lfloor t_0 \rfloor.$$

In order to prove

$$\forall \eta \in \mathbb{R}^+ : \|\mathbf{e}(t)\| \leq L(\eta)e^{-\eta(t - t_i^M)}\|\mathbf{e}(t_i^{M+})\|, \quad \forall t \in (t_i^M, t_{i+1}^m), i \in \mathbb{Z}, i \geq \lfloor t_0 \rfloor,$$
$$\text{with } \lim_{\eta \to +\infty} L(\eta)e^{-\eta T} = 0, \forall T > 0, \qquad (6.19\text{–}6.20)$$

---

[7]Functions $\mathbf{e}(t_i^{M+})$ are differentiable at $(\Delta t_i = 0, \Delta\theta_i = 0, \mathbf{e}(t_i^{M+}) = 0)$.

the error dynamics given in (4.37) can be rewritten in terms of $\mathbf{e}_{\mathbf{x}_e} := \mathbf{x}_e - \bar{\mathbf{x}}_e$ and $\mathbf{e}_{\mathbf{y}_e} := \mathbf{y}_e - \bar{\mathbf{y}}_e$ as

$$\begin{cases} \dot{\mathbf{e}}_{\mathbf{x}_e} = (\mathbf{A} + \mathbf{B}\mathbf{K}_x)\mathbf{e}_{\mathbf{x}_e} =: \tilde{\mathbf{A}}_x\mathbf{e}_{\mathbf{x}_e}, \\ \dot{\mathbf{e}}_{\mathbf{y}_e} = (\mathbf{A} + \mathbf{B}\mathbf{K}_y)\mathbf{e}_{\mathbf{y}_e} =: \tilde{\mathbf{A}}_y\mathbf{e}_{\mathbf{y}_e}, \end{cases}$$

where the matrix $\tilde{\mathbf{A}}_x$ is in companion form[8]

$$\tilde{\mathbf{A}}_x = \begin{bmatrix} 0 & 1 & 0 & \cdots & 0 \\ 0 & 0 & 1 & \cdots & 0 \\ \vdots & & \ddots & & \vdots \\ \vdots & & & 0 & 1 \\ K_1^x & \cdots & \cdots & K_q^x & K_{q+1}^x \end{bmatrix},$$

and $\mathbf{K}_x := \begin{bmatrix} K_1^x & \cdots & K_q^x & K_{q+1}^x \end{bmatrix}$, $K_i^x \in \mathbb{R}$, $i \in \{1, \ldots, q+1\}$.

If the eigenvalues of $\tilde{\mathbf{A}}_x$ denoted as $(\lambda_1, \lambda_2, \ldots, \lambda_{q+1})$, are all real and distinct[9], then the eigenvectors relative to such eigenvalues are given by [23]

$$\begin{bmatrix} 1 \\ \lambda_1 \\ \lambda_1^2 \\ \vdots \\ \lambda_1^q \end{bmatrix} \quad \cdots \quad \begin{bmatrix} 1 \\ \lambda_{q+1} \\ \lambda_{q+1}^2 \\ \vdots \\ \lambda_{q+1}^q \end{bmatrix}.$$

Without loss of generality, the i-th eigenvalue can be written as

$$\lambda_i = -\mu_i\eta, \tag{4.38}$$

where $\eta, \mu_i \in \mathbb{R}$ and $\eta > 0$, $\mu_i \geq 1$ with $\mu_i \neq \mu_j$ for any $i \neq j$, so that $\lambda_i \leq -\eta$

---

[8]For the sake of brevity, the case $\mathbf{e}_{\mathbf{y}_e}$ is not considered being analogous to $\mathbf{e}_{\mathbf{x}_e}$.

[9]The case of complex eigenvalues is not considered here for the sake of brevity. It can be carried out with similar reasonings, by considering $\lambda_i = -\mu_i\eta + j\omega_i$ in place of (4.38), where $\mu_i, \eta, \omega_i \in \mathbb{R}$ and $\mu_i \geq 1, \eta > 0$.

for any $i \in \{1, \ldots, q+1\}$. The matrix of eigenvectors is thus given by

$$\mathbf{Q}_x := \begin{bmatrix} 1 & 1 & & 1 \\ (-\mu_1\eta) & (-\mu_2\eta) & & (-\mu_{q+1}\eta) \\ (-\mu_1\eta)^2 & (-\mu_2\eta)^2 & \cdots & (-\mu_{q+1}\eta)^2 \\ \vdots & \vdots & & \vdots \\ (-\mu_1\eta)^q & (-\mu_2\eta)^q & & (-\mu_{q+1}\eta)^q \end{bmatrix},$$

and since the eigenvalues are all distinct, then $\det(\mathbf{Q}_x) \neq 0$. By considering the infinity norm defined as $\|\mathbf{Q}_x\|_\infty := \max\limits_{i \in \{1,\ldots,q+1\}} \left(\sum\limits_{j=1}^{q+1} |\mathbf{Q}_x(i,j)| \right)$, where $\mathbf{Q}_x(i,j)$ denotes the ij-th element of $\mathbf{Q}_x$, and by the equivalence norms (see, e.g., [38]), it follows that

$$\exists C_1 \in \mathbb{R}^+ : \|\mathbf{Q}_x\| \leq C_1 p_1(\eta),$$

where $p_1(\eta) := \sum_{\forall (i,j)} |\mathbf{Q}_x(i,j)|$ is a polynomial in η of degree q. The inverse matrix of $\mathbf{Q}_x$ can be computed as

$$\mathbf{Q}_x^{-1} = \frac{1}{\det(\mathbf{Q}_x)} Adj(\mathbf{Q}_x).$$

In view of the particular structure of the matrix $\mathbf{Q}_x$, it holds that $\det(\mathbf{Q}_x) = L_1 \eta^{\frac{q(q+1)}{2}}, L_1 \in \mathbb{R}$ and the generic element of $Adj(\mathbf{Q}_x)$ is given by $Adj(\mathbf{Q}_x)(i,j) = L_2^{(i,j)} \eta^{\frac{q(q+1)}{2}-(j-1)}, L_2^{(i,j)} \in \mathbb{R}$ where $i, j \in \{1, \ldots, q+1\}$. Therefore, the ij-th element of $\mathbf{Q}_x^{-1}$ can be written as $\mathbf{Q}_x^{-1}(i,j) = L_3^{(i,j)} \eta^{1-j}, L_3^{(i,j)} \in \mathbb{R}$ with $i, j \in \{1, \ldots, q+1\}$, so that

$$\|\mathbf{Q}_x^{-1}\| \leq C_1 p_2(\eta^{-1}),$$

where $p_2(\eta^{-1}) := \sum_{\forall (i,j)} |\mathbf{Q}_x^{-1}(i,j)|$ is a polynomial in η^{-1} of degree q. Finally, the following upper bound for the condition number of $\mathbf{Q}_x$ holds

$$\|\mathbf{Q}_x\|\|\mathbf{Q}_x^{-1}\| \leq C_1^2 p_1(\eta) p_2(\eta^{-1}) =: L(\eta),$$

where $L(\eta)$ is a polynomial in η of degree q. This result implies that

$$\|e^{(\mathbf{A}+\mathbf{B}\mathbf{K}_x)T}\| \leq \|\mathbf{Q}_x\|\|\mathbf{diag}(e^{-\mu_1\eta T}, e^{-\mu_2\eta T}, \ldots, e^{-\mu_{q+1}\eta T})\|\|\mathbf{Q}_x^{-1}\| \leq$$
$$\leq e^{-\eta T}L(\eta) \to 0 \text{ as } \eta \to +\infty, \text{ for any fixed } T > 0, \quad (4.39)$$

and this complete the proof of (6.19–6.20) when all the eigenvalues of $\tilde{\mathbf{A}}_x$ are real and distinct. In a similar way, the bound (4.39) can be proved in the case of repeated real eigenvalues, taking into account that if λ_i is an eigenvalue of the matrix $\tilde{\mathbf{A}}_x$ with multiplicity m_i, then there exist m_i generalized eigenvectors of $\tilde{\mathbf{A}}_x$ associated with λ_i: $\mathbf{e}_1^{\lambda_i}, \ldots, \mathbf{e}_{m_i}^{\lambda_i}$, such that the k-th element of the j-th of such eigenvectors is given by

$$\mathbf{e}_j^{\lambda_i}(k) = \begin{pmatrix} k-1 \\ j-1 \end{pmatrix} \lambda_i^{k-j},$$

where $k = 1, \ldots, q+1$, $j = 1, \ldots, m_i$ and

$$\begin{pmatrix} k \\ j \end{pmatrix} := \begin{cases} 0, & \text{if } k < j; \\ 1, & \text{if } k = j; \\ \frac{k(k-1)\cdots(k+1-j)}{1\,2\,3\cdots j}, & \text{otherwise.} \end{cases}$$

Chapter 5

Robust trajectory tracking in the elliptical billiard system

In the previous chapters, it is assumed for the the elliptical billiard system that there is no friction, no uncertainty on the plant (i.e., the mass of the actuated particle is known and equal to one) and the full state vector of the plant is measured. The goal of the present chapter is to guarantee a wholly similar tracking control result as detailed in Problem 3, both when the full plant state is accessible, and when only the position error is available for the feedback, also in the case in which the body is subject to friction and the system parameters (i.e., mass and damping factor) are not known exactly. Such an extension is complicated by the need to estimate suitable jumps for the state of the internal model, which depend on the unknown parameters.

5.1   Problem preliminaries and equations of motion

In the following, a dimensionless body having mass $M \in \mathbb{R}^+$ is taken into account and a linear internal damping term is considered, with $D \in \mathbb{R}^+$ being the damping factor. In this case, the system is completely characterized by the total Lagrangian function $L_t = (1/2)M(\dot{x}^2(t)+\dot{y}^2(t))+u_x(t)x(t)+u_y(t)y(t)$, by

the Rayleigh dissipation function $R = (1/2)D(\dot{x}^2(t) + \dot{y}^2(t))$, by the inequality $x^2(t)/a^2 + y^2(t)/b^2 \leq 1$ and by the assumption that the impacts are nonsmooth, perfectly elastic and without friction. As seen in Section 3.1, the method of *the Valentine variables* can be used for modeling the considered mechanical system as in [77].

The motion satisfies (in each open interval of time without impacts) the following *Euler-Lagrange equations*, where the dissipative term has been considered:

$$M\ddot{x}(t) + D\dot{x}(t) + \frac{2}{a^2}\dot{\lambda}(t)x(t) = u_x(t), \tag{5.1a}$$

$$M\ddot{y}(t) + D\dot{y}(t) + \frac{2}{b^2}\dot{\lambda}(t)y(t) = u_y(t), \tag{5.1b}$$

$$2\gamma(t)\dot{\lambda}(t) = 0, \tag{5.1c}$$

$$\frac{2}{a^2}x(t)\dot{x}(t) + \frac{2}{b^2}y(t)\dot{y}(t) + 2\gamma(t)\dot{\gamma}(t) = 0, \tag{5.1d}$$

where $\gamma(t)$ is the Valentine variable and $\dot{\lambda}(t)$ is the derivative (in the distributional sense) of the Lagrange multiplier used to account for the constraint. The impacts can occur only at the times $t_i \in \mathbb{R}$ with $t_{i+1} > t_i, i \in \mathbb{N}$, where the following *Erdmann-Weierstrass corner conditions*, which are necessarily at corner points where $\mathbf{q}(t)$ is not differentiable, are satisfied

$$\dot{x}^2(t_i^-) + \dot{y}^2(t_i^-) = \dot{x}^2(t_i^+) + \dot{y}^2(t_i^+), \tag{5.2a}$$

$$M\dot{x}(t_i^-) + \frac{2}{a^2}\lambda(t_i^-)x(t_i) = M\dot{x}(t_i^+) + \frac{2}{a^2}\lambda(t_i^+)x(t_i), \tag{5.2b}$$

$$M\dot{y}(t_i^-) + \frac{2}{b^2}\lambda(t_i^-)y(t_i) = M\dot{y}(t_i^+) + \frac{2}{b^2}\lambda(t_i^+)y(t_i). \tag{5.2c}$$

Remark 18. In the following, if $i \in \mathbb{Z}^+$, then t_i is either the initial time t_0 or the i-th impact time, else if $i \in \mathbb{N}$, then t_i is the i-th impact time.

As seen in Section 3.1, the initial conditions at the initial time t_0 are

$$x(t_0) = x_0, \ y(t_0) = y_0, \ \dot{x}(t_0^+) = v_{x,0}, \ \dot{y}(t_0^+) = v_{y,0},$$
$$\gamma(t_0) = \sqrt{-f(\mathbf{q}(t_0))}, \ \lambda(t_0^+) = 0,$$

and

$$\hat{\mathcal{A}} := \{(\mathbf{q}, \dot{\mathbf{q}}) \in \mathcal{A} \times \mathbb{R}^2 \ : \ \mathbf{J}(\mathbf{q})\dot{\mathbf{q}} \leq 0 \text{ if } f(\mathbf{q}) = 0\},$$

where $\mathbf{J}(\mathbf{q}) = \begin{bmatrix} (2/a^2)x & (2/b^2)y \end{bmatrix}$. For the initial time t_0, it is required that $(\mathbf{q}(t_0), \dot{\mathbf{q}}(t_0^+)) \in \hat{\mathcal{A}}$ so that, if $\mathbf{q}(t_0)$ is on the boundary, the velocity vector $\dot{\mathbf{q}}(t_0^+)$ points toward the interior of the admissible region.

An impact for the controlled body occurs if, at a given time $t_i > t_0$, one has

$$f(\mathbf{q}(t_i)) = 0 \quad \text{and} \quad \mathbf{J}(\mathbf{q}(t_i))\dot{\mathbf{q}}(t_i^-) > 0.$$

By requiring that $\mathbf{J}(\mathbf{q}(t_i))\dot{\mathbf{q}}(t_i^+) \leq 0$, the Erdmann-Weierstrass corner conditions (5.2) can be solved uniquely in the unknowns $\dot{x}(t_i^+)$ and $\dot{y}(t_i^+)$ at the impact time t_i as

$$\dot{x}(t_i^+) = C_1(\mathbf{q}(t_i))\dot{x}(t_i^-) + C_2(\mathbf{q}(t_i))\dot{y}(t_i^-), \tag{5.3a}$$

$$\dot{y}(t_i^+) = C_2(\mathbf{q}(t_i))\dot{x}(t_i^-) - C_1(\mathbf{q}(t_i))\dot{y}(t_i^-), \tag{5.3b}$$

where $C_1(\mathbf{q}(t_i)) := (a^4 y^2(t_i) - b^4 x^2(t_i))/(a^4 y^2(t_i) + b^4 x^2(t_i))$ and $C_2(\mathbf{q}(t_i)) := (-2a^2 b^2 x(t_i) y(t_i))/(a^4 y^2(t_i) + b^4 x^2(t_i))$.

Remark 19. Although the corner conditions (5.2) are different with respect to (3.7), once they are solved in the unknowns $\dot{x}(t_i^+)$ and $\dot{y}(t_i^+)$ the same post-impact rules are obtained.

In Section 3.2, closed polygons inscribed in an ellipse (centered at the origin with a and b being the semi-major and the semi-minor axis, respectively) and having winding number (N, R) in both the cases of rotational and librational motion are considered as reference paths. Moreover, in order to find velocity profiles that yield the resulting periodic trajectories admissible for the

billiard system with the impact times being equally spaced, a motion planning problem is properly stated and solved. In particular, it is shown that when the velocity profiles are generic polynomials of degree q, such a problem can be addressed through LMIs by using some results from the theory of non-negative polynomials (see, e.g., [64],[42]). An easy algorithm is also given for finding such a class of polynomials when the problem parameters are fixed. Here, the same class of desired trajectories will be considered for the tracking control problem, which will be defined in the following.

Remark 20. The choice to impose impact times at arbitrarily fixed times permits to consider target periodic trajectories which are not admissible for the billiard system when no control is exerted on the moving mass. In this way, a more general problem is taken into account and the controller has to be designed such that an internal model of such a class of trajectories is contained in the closed-loop system, so that the control forces steer the tracking error to zero in the sense specified in the subsequent Problem 4. For simplicity of exposition, in this chapter, as in Chapters 3 and 4, equally spaced impact times occurring at integer times have been considered; however the proposed control laws can be easily adapted to deal with any choice of impact times for periodic trajectories as it will be shown in Chapter 6.

5.2   The robust trajectory tracking problem: statement and solution

The goal of this section is the design of a control law such that the actual trajectory asymptotically tracks the desired one also in presence of uncertainties on the system parameters. More specifically the classical servomechanism problem (see, e.g., [25],[23]) is taken into account and, in the following, it will be properly amended in order to deal with the considered class of mechanical systems subject to nonsmooth impacts. In Section 4.1, it is shown for a similar case that the error on the velocity immediately after the impact times has in

general absolute value greater than a given positive quantity. For this reason the classical stability and attractivity properties are difficult (if not impossible) to be obtained and Problem 3 has been defined in order to neglect in the analysis the times belonging to infinitesimal intervals about the impact times, thus ensuring a sort of asymptotic stability for the error dynamics, similarly to what is proposed in [50] for impulsive differential systems. For the sake of clarity, some definitions already seen in Chapter 4 are recalled in the following. Letting

$$\mathbf{q}(t) := \begin{bmatrix} x(t) \\ y(t) \end{bmatrix} \in \mathbb{R}^2 \quad \text{and} \quad \bar{\mathbf{q}}(t) := \begin{bmatrix} \bar{x}(t) \\ \bar{y}(t) \end{bmatrix} \in \mathbb{R}^2,$$

so that $\mathbf{q}(t)$ and $\bar{\mathbf{q}}(t)$ denote the controlled and the desired trajectories, respectively (see Section 3.2), the tracking error at time t is defined as

$$\mathbf{e_q}(t) := \mathbf{q}(t) - \bar{\mathbf{q}}(t) = \begin{bmatrix} x(t) - \bar{x}(t) \\ y(t) - \bar{y}(t) \end{bmatrix} \in \mathbb{R}^2.$$

By following the approach introduced in Chapter 4, a controller based on a nonsmooth-version of the classical internal model principle will be considered. In particular, in order to obtain *asymptotic tracking* (in the sense specified in the subsequent Problem 4), in absence of impacts a continuous-time internal model of the desired trajectory is needed in the forward path of the feedback control system. The presence of such an internal model is guaranteed through a dynamic precompensator, whose state vector will be subject to jumps. Let $\mathbf{e}_a(t)$ be the error between the actual state vector of the precompensator and its nominal value and $\tilde{\mathbf{\Lambda}}_a(i)$ be the error at time $i \in \mathbb{Z}$ between the correct jump in the precompensator and the estimated one.[1] Moreover, by defining $\boldsymbol{\beta} := \begin{bmatrix} M & D \end{bmatrix}^T \in \mathbf{\Omega} \subseteq \mathbb{R}^2$ as the vector of parameters which are subject to variations and/or uncertainties and assuming the nominal value $\boldsymbol{\beta}_0 := \begin{bmatrix} M_0 & D_0 \end{bmatrix}^T$ of $\boldsymbol{\beta}$ be an interior point of the bounded set $\mathbf{\Omega}$, the control problem solved here can be stated as follows.

---

[1] The meaning of $\mathbf{e}_a$ and $\tilde{\mathbf{\Lambda}}_a$ will be clarified in the following.

Problem 4. *Find, if any, a piecewise continuous control law such that for each* $\varepsilon > 0$, $t_0 \in \mathbb{R}$ *and* $\gamma \in (0, 1/2)$, *there exists* $\delta_{\varepsilon,\gamma} > 0$ *and a neighborhood* $\mathbf{\Psi} \subseteq \mathbf{\Omega}$ *of* $\boldsymbol{\beta}_0$ *such that if* $[\mathbf{q}^T(t_0), \dot{\mathbf{q}}^T(t_0^+)]^T \in \hat{\mathcal{A}}$, $\|[\mathbf{e}_q^T(t_0), \dot{\mathbf{e}}_q^T(t_0^+), \mathbf{e}_a^T(t_0^+)]^T\| < \delta_{\varepsilon,\gamma}$ *and* $\|\tilde{\mathbf{\Lambda}}_a(\bar{t}_1)\| < \delta_{\varepsilon,\gamma}, \cdots, \|\tilde{\mathbf{\Lambda}}_a(\bar{t}_{N-1})\| < \delta_{\varepsilon,\gamma}$, *then the following properties hold for the closed-loop system and for all* $\boldsymbol{\beta} \in \mathbf{\Psi}$:

$$\textbf{1)} \quad \begin{cases} \|\mathbf{e_q}(t)\| < \varepsilon, & \forall t \in \mathbb{R},\ t > t_0, \\ \|\dot{\mathbf{e}}_{\mathbf{q}}(t)\| < \varepsilon, & \forall t \in \mathbb{R},\ t > t_0,\ |t - \langle t \rangle| > \gamma, \end{cases}$$

where $\langle t \rangle$ *denotes the integer nearest to* t. *In the case in which* t *is a half-integer,* $\langle t \rangle$ *denotes the smallest integer larger than* t;

$$\textbf{2)} \quad \begin{cases} \lim\limits_{t \to +\infty} \|\mathbf{e_q}(t)\| = 0, \\ \lim\limits_{i \to +\infty} \|\dot{\mathbf{e}}_{\mathbf{q}}((i + \tau)^+)\| = 0, & \forall \tau \in (0, 1), \end{cases}$$

where the limits for $\|\mathbf{e_q}(\cdot)\|$ *and* $\|\dot{\mathbf{e}}_{\mathbf{q}}(\cdot)\|$ *are taken with* t *and* i *being real and integer, respectively.*

In the following, first the assumption of measuring the whole state vector of the plant will be made (*Full-Information problem*), and then such an assumption will be removed in order to deal with the more realistic case in which only the position-error is available for the feedback (*Error-Feedback problem*).

5.2.1   Full-Information problem

In order to solve Problem 4 when both $\mathbf{q}(t)$ and $\dot{\mathbf{q}}(t)$ are measured, the control scheme depicted in Fig. 5.1 is considered, where the dashed-arrows denote the jump times for the blocks they point to (for the sake of brevity, only the scheme relative to x-coordinate is shown (see Remark 11)). In the following, the blocks in Fig. 5.1 will be characterized during the unconstrained and constrained motion so as to solve the tracking control Problem 4.
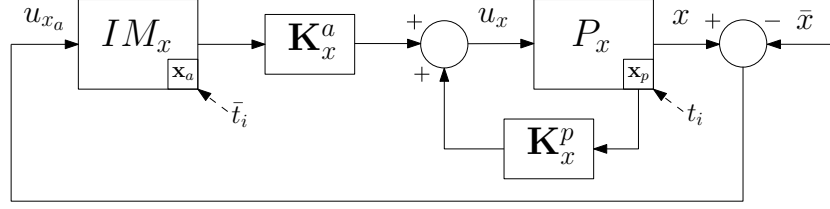
Figure 5.1: **Full-Information:** structure of the control scheme based on the internal model principle (only x-coordinate).

The plant model: P_x, P_y

The equations of motion of a body having mass $M \in \mathbb{R}^+$ and moving in an elliptical billiards under the action of control forces and subject to friction with damping factor $D \in \mathbb{R}^+$ have been obtained in Section 5.1. By defining $\mathbf{x}_p(t) := \begin{bmatrix} x(t) & \dot{x}(t) \end{bmatrix}^T \in \mathbb{R}^2$, equations (5.1) can be rewritten as:

$$P_x : \begin{cases} \dot{\mathbf{x}}_p(t) = \mathbf{A}_p(\boldsymbol{\beta})\mathbf{x}_p(t) + \mathbf{B}_p(\boldsymbol{\beta})u_x(t) \\ y_{x_p}(t) = \mathbf{C}_p\mathbf{x}_p(t) \end{cases} , \forall t \in \mathcal{F}_i, i \in \mathbb{Z}^+, \quad (5.4a)$$

$$P_y : \begin{cases} \dot{\mathbf{y}}_p(t) = \mathbf{A}_p(\boldsymbol{\beta})\mathbf{y}_p(t) + \mathbf{B}_p(\boldsymbol{\beta})u_y(t) \\ y_{y_p}(t) = \mathbf{C}_p\mathbf{y}_p(t) \end{cases} , \forall t \in \mathcal{F}_i, i \in \mathbb{Z}^+, \quad (5.4b)$$

where $\mathcal{F}_i := (t_i, t_{i+1})$ (i.e., $\mathcal{F}_i$ denotes a time interval without impacts for the controlled body) and $\mathbf{A}_p(\boldsymbol{\beta}) \in \mathbb{R}^{2\times2}, \mathbf{B}_p(\boldsymbol{\beta}) \in \mathbb{R}^2, \mathbf{C}_p^T \in \mathbb{R}^2$ are given by

$$\mathbf{A}_p(\boldsymbol{\beta}) := \begin{bmatrix} 0 & 1 \\ 0 & -D/M \end{bmatrix} , \quad \mathbf{B}_p(\boldsymbol{\beta}) := \begin{bmatrix} 0 \\ 1/M \end{bmatrix} , \quad \mathbf{C}_p := \begin{bmatrix} 1 & 0 \end{bmatrix} .$$

Remark 21. All the entries of $(\mathbf{A}_p(\boldsymbol{\beta}), \mathbf{B}_p(\boldsymbol{\beta}), \mathbf{C}_p)$ are continuous functions of $\boldsymbol{\beta}$, whenever $M > 0$.

The coupling between the two degrees of freedom of the mass is due to the impact of the mass with the barrier. The jumps in the state vectors $\mathbf{x}_p(t)$ and $\mathbf{y}_p(t)$ at the generic impact time $t_i \in \mathbb{R}$ are then given in terms of $\mathbf{x}_p(t_i^-)$ and

$\mathbf{y}_p(t_i^-)$ as

$$\mathbf{x}_p(t_i^+) = \mathbf{C}_1^p(\mathbf{q}(t_i))\mathbf{x}_p(t_i^-) + \mathbf{C}_2^p(\mathbf{q}(t_i))\mathbf{y}_p(t_i^-),\ i \in \mathbb{N}, \tag{5.5a}$$

$$\mathbf{y}_p(t_i^+) = \mathbf{C}_2^p(\mathbf{q}(t_i))\mathbf{x}_p(t_i^-) + \mathbf{C}_3^p(\mathbf{q}(t_i))\mathbf{y}_p(t_i^-),\ i \in \mathbb{N}, \tag{5.5b}$$

where $\mathbf{C}_1^p(\cdot) \in \mathbb{R}^{2\times 2}, \mathbf{C}_2^p(\cdot) \in \mathbb{R}^{2\times 2}$ and $\mathbf{C}_3^p(\cdot) \in \mathbb{R}^{2\times 2}$ are

$$\mathbf{C}_1^p(\mathbf{q}(t_i)) := \begin{bmatrix} 1 & 0 \\ 0 & C_1(\mathbf{q}(t_i)) \end{bmatrix},\ \mathbf{C}_2^p(\mathbf{q}(t_i)) := \begin{bmatrix} 0 & 0 \\ 0 & C_2(\mathbf{q}(t_i)) \end{bmatrix},$$

$$\mathbf{C}_3^p(\mathbf{q}(t_i)) := \begin{bmatrix} 1 & 0 \\ 0 & -C_1(\mathbf{q}(t_i)) \end{bmatrix},$$

with $C_1(\mathbf{q}(t_i))$ and $C_2(\mathbf{q}(t_i))$ being defined in (5.3).

The precompensator: $IM_x,\ IM_y$

In Section 4.2, it has been shown that, for some $\boldsymbol{\Omega}_x, \boldsymbol{\Omega}_y$ and $\mathbf{v}_x, \mathbf{v}_y$, the reference signals can be written as

$$\bar{x}(t) = \boldsymbol{\Omega}_x e^{\mathbf{M}(t-\lfloor t \rfloor)}\mathbf{v}_x,$$

$$\bar{y}(t) = \boldsymbol{\Omega}_y e^{\mathbf{M}(t-\lfloor t \rfloor)}\mathbf{v}_y,$$

where

$$\mathbf{M} = \begin{bmatrix} 0 & 1 & 0 & \cdots & 0 \\ 0 & 0 & 1 & \cdots & 0 \\ \vdots & & \ddots & & \vdots \\ \vdots & & & 0 & 1 \\ 0 & \cdots & \cdots & 0 & 0 \end{bmatrix} \in \mathbb{R}^{(q+1)\times(q+1)}, \tag{5.6}$$

and each impact time for the desired trajectory occurs at an integer time. By following the guidelines of the internal model principle (see, e.g., [23]), the block IM_x in Fig. 5.1 has to be designed so that a complete internal model of the class of trajectories to be tracked is contained in it. Its dynamics are

given by

$$IM_x : \begin{cases} \dot{\mathbf{x}}_a(t) = \mathbf{A}_a \mathbf{x}_a(t) + \mathbf{B}_a u_{x_a}(t) \\ \mathbf{y}_{x_a}(t) = \mathbf{x}_a(t) \end{cases}, \ \forall t \in \bar{\mathcal{F}}_i, i \in \mathbb{Z}^+, \quad (5.7a)$$

$$IM_y : \begin{cases} \dot{\mathbf{y}}_a(t) = \mathbf{A}_a \mathbf{y}_a(t) + \mathbf{B}_a u_{y_a}(t) \\ \mathbf{y}_{y_a}(t) = \mathbf{y}_a(t) \end{cases}, \ \forall t \in \bar{\mathcal{F}}_i, i \in \mathbb{Z}^+, \quad (5.7b)$$

with $\bar{\mathcal{F}}_i := (\bar{t}_i, \bar{t}_{i+1})$ and pair $(\mathbf{A}_a \in \mathbb{R}^{(q+1)\times(q+1)}, \mathbf{B}_a \in \mathbb{R}^{q+1})$ being in the Brunowsky canonical form, that is

$$\mathbf{A}_a(= \mathbf{M}) = \begin{bmatrix} 0 & 1 & 0 & \cdots & 0 \\ 0 & 0 & 1 & \cdots & 0 \\ \vdots & & \ddots & & \vdots \\ \vdots & & & 0 & 1 \\ 0 & \cdots & \cdots & 0 & 0 \end{bmatrix}, \quad \mathbf{B}_a = \begin{bmatrix} 0 \\ \vdots \\ 0 \\ 1 \end{bmatrix}.$$

In the following, in order to find the correct reset values for the precompensator state vectors $\mathbf{x}_a(t) \in \mathbb{R}^{q+1}$ and $\mathbf{y}_a(t) \in \mathbb{R}^{q+1}$ at the generic impact time $\bar{t}_i \in \mathbb{Z}$, first such values will be computed in the nominal parameters (i.e., $M = M_0$ and $D = D_0$), and then an algorithm to estimate them will be given in order to deal with possible uncertainties (i.e., $M = M_0 + \delta M$ and $D = D_0 + \delta D$, with $\delta M, \delta D \in \mathbb{R}$).

Controller reset values in the nominal parameters

Remark 22. In the following, only the computations relative to x-coordinate will be detailed, the results relative to y-coordinate being obtainable in a wholly similar way.

By assuming perfect tracking, i.e., the particle moves along the desired

trajectory and impacts at the desired impact times, it follows that

$$
\begin{cases}
t_i = \bar{t}_i, & i \in \mathbb{N}, \\
x(t) = \bar{x}(t) =: \bar{x}(t), & \forall t \in (\bar{t}_i, \bar{t}_{i+1}), i \in \mathbb{Z}^+,
\end{cases}
\tag{5.8}
$$

where the *bar*-notation denotes the desired values. By substituting (5.8) into (5.7a), one obtains

$$
\dot{\bar{\mathbf{x}}}_a(t) = \mathbf{A}_a \bar{\mathbf{x}}_a(t) \Rightarrow \bar{\mathbf{x}}_a(t) = e^{\mathbf{A}_a(t-\bar{t}_i)} \bar{\mathbf{x}}_a(\bar{t}_i^+), \ \forall t \in (\bar{t}_i, \bar{t}_{i+1}), i \in \mathbb{Z}^+. \tag{5.9}
$$

By (5.9) and (5.8), it follows that

$$
\bar{\mathbf{x}}_a(\bar{t}_{i+1}^-) = e^{\mathbf{A}_a(\bar{t}_{i+1}-\bar{t}_i)} \bar{\mathbf{x}}_a(\bar{t}_i^+) = e^{\mathbf{A}_a} \bar{\mathbf{x}}_a(\bar{t}_i^+),
$$

which implies that

$$
\bar{\mathbf{x}}_a(\bar{t}_i^+) = e^{-\mathbf{A}_a} \bar{\mathbf{x}}_a(\bar{t}_{i+1}^-).
$$

Moreover, by considering the control input (see Fig. 5.1):

$$
u_x(t) = \mathbf{K}_x^a \bar{\mathbf{x}}_a(t) + \mathbf{K}_x^p \bar{\mathbf{x}}_p(t),
$$

the state equation (5.4a) becomes

$$
\dot{\bar{\mathbf{x}}}_p(t) = (\mathbf{A}_p + \mathbf{B}_p \mathbf{K}_x^p) \bar{\mathbf{x}}_p(t) + \mathbf{B}_p \mathbf{K}_x^a \bar{\mathbf{x}}_a(t). \tag{5.10}
$$

By using (5.8), the closed loop plant dynamics (5.10) can be rewritten as:

$$
\begin{bmatrix} \dot{\bar{x}}(t) \\ \ddot{\bar{x}}(t) \end{bmatrix} = (\mathbf{A}_p + \mathbf{B}_p \mathbf{K}_x^p) \begin{bmatrix} \bar{x}(t) \\ \dot{\bar{x}}(t) \end{bmatrix} + \mathbf{B}_p \mathbf{K}_x^a \bar{\mathbf{x}}_a(t).
$$

This vector equation provides two scalar equalities, which have to be satisfied for each free-motion interval (i.e., $\forall t \in (\bar{t}_i, \bar{t}_{i+1}), i \in \mathbb{Z}^+$). In particular, the first of them is just the identity $\dot{\bar{x}}(t) = \dot{\bar{x}}(t)$, which is trivially satisfied, whereas

the second one is given by

$$M\ddot{\bar{x}}(t) + D\dot{\bar{x}}(t) - (K^p_{x,1}\bar{x}(t) + K^p_{x,2}\dot{\bar{x}}(t)) =$$
$$= K^a_{x,1}x_{a,1}(t) + \cdots + K^a_{x,q+1}x_{a,q+1}(t), \tag{5.11}$$

where $\mathbf{K}^p_x, \mathbf{K}^a_x$ are partitioned as

$$\mathbf{K}^p_x = \begin{bmatrix} K^p_{x,1} & K^p_{x,2} \end{bmatrix},$$
$$\mathbf{K}^a_x = \begin{bmatrix} K^a_{x,1} & \cdots & K^a_{x,q+1} \end{bmatrix},$$

and $\bar{\mathbf{x}}_a(t) = \begin{bmatrix} \bar{x}_{a,1}(t) & \cdots & \bar{x}_{a,q+1}(t) \end{bmatrix}^T$. Since the desired trajectory $\bar{x}(t)$ is a polynomial of degree q in $t - \lfloor t \rfloor$, it is clear that its $(q+1)$-th derivative with respect to t will be equal to zero, that is

$$\frac{d^{q+1}\bar{x}(t)}{dt^{q+1}} = 0. \tag{5.12}$$

Moreover, given that the precompensator IM_x is realized in the Brunowsky canonical form, the following relations hold between the components of its state vector $\mathbf{x}_a(t)$

$$\begin{cases} \dot{\bar{x}}_{a,1}(t) = \bar{x}_{a,2}(t), \\ \dot{\bar{x}}_{a,2}(t) = \bar{x}_{a,3}(t), \\ \vdots \\ \dot{\bar{x}}_{a,q+1}(t) = 0. \end{cases} \tag{5.13}$$

Hence, by considering (5.12) and (5.13), the successive time derivatives (from the 0-th to the q-th) of (5.11) can be computed in order to obtain $q + 1$ equations to solve in the $q + 1$ unknowns: $\bar{x}_{a,1}, \cdots, \bar{x}_{a,q+1}, \forall t \in (\bar{t}_i, \bar{t}_{i+1}), i \in \{0, 1, \cdots, N - 1\})$, where the periodicity of the desired trajectory has been

considered, so as to obtain

$$
\begin{cases}
M\ddot{\bar{x}}(t) + D\dot{\bar{x}}(t) - (K^p_{x,1}\bar{x}(t) + K^p_{x,2}\dot{\bar{x}}(t)) = \\
\qquad = K^a_{x,1}\bar{x}_{a,1}(t) + \cdots + K^a_{x,q+1}\bar{x}_{a,q+1}(t), \\
\\
M\bar{x}^{(3)}(t) + D\ddot{\bar{x}}(t) - (K^p_{x,1}\dot{\bar{x}}(t) + K^p_{x,2}\ddot{\bar{x}}(t)) = \\
\qquad = K^a_{x,1}\bar{x}_{a,2}(t) + \cdots + K^a_{x,q}\bar{x}_{a,q+1}(t), \\
\vdots \\
D\bar{x}^{(q)}(t) - (K^p_{x,1}\bar{x}^{(q-1)}(t) + K^p_{x,2}\bar{x}^{(q)}(t)) = \\
\qquad = K^a_{x,1}\bar{x}_{a,q}(t) + K^a_{x,2}\bar{x}_{a,q+1}(t), \\
\\
-K^p_{x,1}\bar{x}^{(q)}(t) = K^a_{x,1}\bar{x}_{a,q+1}(t),
\end{cases}
\tag{5.14}
$$

where $\bar{x}^{(j)}(t)$ denotes the j-th time derivative of $\bar{x}(t)$, i.e., $\bar{x}^{(j)}(t) := d^j\bar{x}(t)/dt^j$. By assuming $K^a_{x,1} \neq 0$, the system (5.14) can be solved by backward substitution starting from the last equation, which provides the $(q+1)$-th element of $\bar{\mathbf{x}}_a$. Hence, the *jump* of the precompensator state vector at the instant $\bar{t}_i$ is given by

$$
\bar{\mathbf{x}}_a(\bar{t}_i^+) =
\begin{bmatrix}
\bar{x}_{a,1}(\bar{t}_i^+) \\
\vdots \\
\bar{x}_{a,q}(\bar{t}_i^+) \\
\bar{x}_{a,q+1}(\bar{t}_i^+)
\end{bmatrix}
=: \bar{\mathbf{\Lambda}}_{x_a}(\bar{t}_i) \in \mathbb{R}^{q+1},
\tag{5.15}
$$

where

$$\bar{x}_{a,q+1}(\bar{t}_i^+) = -\frac{K_{x,1}^p}{K_{x,1}^a}\bar{x}^{(q)}(\bar{t}_i^+),$$

$$\bar{x}_{a,q}(\bar{t}_i^+) = \frac{1}{K_{x,1}^a}\left(D\bar{x}^{(q)}(\bar{t}_i^+) - \left(K_{x,1}^p\bar{x}^{(q-1)}(\bar{t}_i^+)+\right.\right.$$
$$\left.\left. + K_{x,2}^p\bar{x}^{(q)}(\bar{t}_i^+)\right) - K_{x,2}^a\bar{x}_{a,q+1}(t_i^+)\right),$$

$$\bar{x}_{a,q-1}(\bar{t}_i^+) = \frac{1}{K_{x,1}^a}\left(M\bar{x}^{(q)}(\bar{t}_i^+) + D\bar{x}^{(q-1)}(\bar{t}_i^+)+\right.$$
$$\left. - \left(K_{x,1}^p\bar{x}^{(q-2)}(\bar{t}_i^+) + K_{x,2}^p\bar{x}^{(q-1)}(\bar{t}_i^+)\right)+\right.$$
$$\left. - \left(K_{x,2}^a\bar{x}_{a,q}(t_i^+) - K_{x,3}^a\bar{x}_{a,q+1}(t_i^+)\right)\right),$$

$$\vdots$$

Finally, the reset values in the actual state vectors $\mathbf{x}_a$ and $\mathbf{y}_a$ when the system parameters are exactly known can be computed as:

$$\mathbf{x}_a(\bar{t}_i^+) = \bar{\mathbf{\Lambda}}_{x_a}(\bar{t}_i), \quad i \in \mathbb{N}, \tag{5.16a}$$

$$\mathbf{y}_a(\bar{t}_i^+) = \bar{\mathbf{\Lambda}}_{y_a}(\bar{t}_i), \quad i \in \mathbb{N}, \tag{5.16b}$$

where $\bar{\mathbf{\Lambda}}_{y_a}(i)$ is obtainable from $\bar{\mathbf{\Lambda}}_{x_a}(i)$ defined in (5.15) substituting wherever x with y. By the results above, it is clear that $\mathbf{x}_a(\bar{t}_i^+)$ and $\mathbf{y}_a(\bar{t}_i^+)$ depend upon the plant parameters M and D. In order to deal with possible uncertainties on these parameters, the following algorithm is considered to estimate the correct jumps.

Controller reset values in presence of uncertainties

In (5.16) the jumps in $\bar{\mathbf{x}}_a$ and $\bar{\mathbf{y}}_a$ at the instant $\bar{t}_i$ depend upon the system parameters M and D. It is clear that if such parameters are not exactly known the results above will yield wrong reset values. In this case the correct jumps for the state vectors of the precompensator at the instant $\bar{t}_i$ can be estimated

in real time (see proof of Theorem 9) by applying the following rules

$$\mathbf{x}_a(\bar{t}^+_{i+N}) = e^{-\mathbf{A}_a}\mathbf{x}_a(\bar{t}^-_{i+1}), \quad i \in \mathbb{Z}^+, \tag{5.17a}$$

$$\mathbf{y}_a(\bar{t}^+_{i+N}) = e^{-\mathbf{A}_a}\mathbf{y}_a(\bar{t}^-_{i+1}), \quad i \in \mathbb{Z}^+. \tag{5.17b}$$

A code-like algorithm implementing such rules is described below.

- <u>Initialize</u> $\mathbf{U}_{x_a}, \mathbf{U}_{y_a} \in \mathbb{R}^{N \times (q+1)}$ as

$$\mathbf{U}_{x_a} = \mathbf{U}^0_{x_a} := \begin{bmatrix} \bar{\mathbf{\Lambda}}^T_{x_a}(0) \\ \bar{\mathbf{\Lambda}}^T_{x_a}(1) \\ \vdots \\ \bar{\mathbf{\Lambda}}^T_{x_a}(N-1) \end{bmatrix}, \quad \mathbf{U}_{y_a} = \mathbf{U}^0_{y_a} := \begin{bmatrix} \bar{\mathbf{\Lambda}}^T_{y_a}(0) \\ \bar{\mathbf{\Lambda}}^T_{y_a}(1) \\ \vdots \\ \bar{\mathbf{\Lambda}}^T_{y_a}(N-1) \end{bmatrix}.$$

- At any instant of impact $\bar{t}_i \in \mathbb{Z}$, the jumps of $\mathbf{x}_a$ and $\mathbf{y}_a$ are

$$\mathbf{x}_a(\bar{t}^+_i) = \mathbf{U}^T_{x_a}\left((\bar{t}_i \bmod N) + 1, :\right),$$

$$\mathbf{y}_a(\bar{t}^+_i) = \mathbf{U}^T_{y_a}\left((\bar{t}_i \bmod N) + 1, :\right),$$

- and the update rules of $\mathbf{U}_{x_a}$ and $\mathbf{U}_{y_a}$ are

$$\mathbf{U}^T_{x_a}\left(((\bar{t}_i - 1) \bmod N) + 1, :\right) = e^{-\mathbf{A}_a}\mathbf{x}_a(\bar{t}^-_i),$$

$$\mathbf{U}^T_{y_a}\left(((\bar{t}_i - 1) \bmod N) + 1, :\right) = e^{-\mathbf{A}_a}\mathbf{y}_a(\bar{t}^-_i),$$

where $\mathbf{U}_{x_a}(i, :)$ and $\mathbf{U}_{y_a}(i, :)$ denote the i-th row of the matrices $\mathbf{U}_{x_a}$ and $\mathbf{U}_{y_a}$, respectively.

Remark 23. The proposed algorithm permits to estimate the correct jumps for the precompensator even when the plant parameters are not exactly known. Moreover, if the uncertainties on the parameters are expressed as $M = M_0 + \delta M$ and $D = D_0 + \delta D$, with $\delta M, \delta D \in \mathbb{R}$ and M_0, D_0 being the actual mass

and the actual damping factor, respectively, then in the computation of $\bar{\mathbf{x}}_a(\bar{t}_i^+)$ in (5.15) the errors due to the unknowns δM and δD are always divided by the scalar factor $K_{x,1}^a$. Hence, in order to reduce the effect of such errors on the jump estimate it is enough to choose $K_{x,1}^a >> 1$, which can be carried out by a shrewd choice of the eigenvalues for the closed-loop dynamic matrix (5.23).

The augmented system (plant–precompensator)

In order to compute the static gains $\mathbf{K}_x^p$, $\mathbf{K}_x^a$ and $\mathbf{K}_y^p$, $\mathbf{K}_y^a$, the state-space representation of the augmented system (plant–precompensator) is here reported. Since the control input to the plant is given by (see Fig. 5.1)

$$u_x(t) = \mathbf{K}_x^a \mathbf{x}_a(t) + \mathbf{K}_x^p \mathbf{x}_p(t),$$

in any time interval without impacts the free-motion dynamics for the augmented state vector $\mathbf{x}_e(t) := \begin{bmatrix} \mathbf{x}_p^T(t) & \mathbf{x}_a^T(t) \end{bmatrix}^T \in \mathbb{R}^{q+3}$ can be written as

$$\begin{cases} \dot{\mathbf{x}}_e(t) = \mathbf{A}_e^x \mathbf{x}_e(t) + \mathbf{B}_e^x \bar{x}(t) \\ y_{x_e}(t) = \mathbf{C}_e^x \mathbf{x}_e(t) \end{cases}, \tag{5.18}$$

where $\mathbf{A}_e^x \in \mathbb{R}^{(q+3)\times(q+3)}, \mathbf{B}_e^x \in \mathbb{R}^{q+3}$ and $\mathbf{C}_e^{xT} \in \mathbb{R}^{q+3}$ are

$$\mathbf{A}_e^x := \begin{bmatrix} \mathbf{A}_p + \mathbf{B}_p \mathbf{K}_x^p & \mathbf{B}_p \mathbf{K}_x^a \\ -\mathbf{B}_a \mathbf{C}_p & \mathbf{A}_a \end{bmatrix}, \quad \mathbf{B}_e^x := \begin{bmatrix} \mathbf{0} \\ \mathbf{B}_a \end{bmatrix}, \quad \mathbf{C}_e^x := \begin{bmatrix} \mathbf{C}_p & \mathbf{0} \end{bmatrix}.$$

At this point, the augmented state vector $\mathbf{x}_e$ can be rewritten as

$$\mathbf{x}_e(t) = \bar{\mathbf{x}}_e(t) + \tilde{\mathbf{x}}_e(t), \tag{5.19}$$

where $\bar{\mathbf{x}}_e$ is the *nominal* part of $\mathbf{x}_e$, i.e., $\bar{\mathbf{x}}_e = \begin{bmatrix} \bar{x} & \dot{\bar{x}} & \bar{\mathbf{x}}_a^T \end{bmatrix}^T$ with $\bar{\mathbf{x}}_a(t)$ being defined in (5.9) and it has jumps at the instants $\bar{t}_i$ (see (5.15) and (5.45a)).[2] From (5.10),(5.7a) and (5.8) the dynamics of $\bar{\mathbf{x}}_e$ during the free-motion can be easily obtained as

$$\dot{\bar{\mathbf{x}}}_e(t) = \begin{bmatrix} \mathbf{A}_p + \mathbf{B}_p \mathbf{K}_x^p & \mathbf{B}_p \mathbf{K}_x^a \\ \mathbf{0} & \mathbf{A}_a \end{bmatrix} \bar{\mathbf{x}}_e(t) =: \bar{\mathbf{A}}_e^x \bar{\mathbf{x}}_e(t), \tag{5.20}$$

and by using the definition of $\bar{\mathbf{A}}_e^x$, the state equation given by (5.18) for the actual system becomes

$$\dot{\mathbf{x}}_e(t) = \bar{\mathbf{A}}_e^x \mathbf{x}_e(t) + \bar{\mathbf{B}}_e^x u_{x_a}(t), \tag{5.21}$$

where $\bar{\mathbf{B}}_e^x := \mathbf{B}_e^x$. On the other hand, $\tilde{\mathbf{x}}_e(t)$ is nothing else the difference between the actual value of $\mathbf{x}_e$ and the nominal one, so that, since $u_{x_a}(t) = \begin{bmatrix} -\mathbf{C}_p & \mathbf{0} \end{bmatrix} \tilde{\mathbf{x}}_e(t)$, its dynamics are obtained as

$$\dot{\tilde{\mathbf{x}}}_e(t) = \mathbf{A}_e^x \tilde{\mathbf{x}}_e(t), \tag{5.22}$$

where $\mathbf{A}_e^x$ is the closed-loop dynamic matrix and it can be rewritten as:

$$\mathbf{A}_e^x = \underbrace{\begin{bmatrix} \mathbf{A}_p & \mathbf{0} \\ -\mathbf{B}_a \mathbf{C}_p & \mathbf{A}_a \end{bmatrix}}_{=:\underline{\mathbf{A}}_e^x} + \underbrace{\begin{bmatrix} \mathbf{B}_p \\ \mathbf{0} \end{bmatrix}}_{=:\underline{\mathbf{B}}_e^x} \underbrace{\begin{bmatrix} \mathbf{K}_x^p & \mathbf{K}_x^a \end{bmatrix}}_{=:\mathbf{K}_x}, \tag{5.23}$$

with the row-vector $\mathbf{K}_x^T := \begin{bmatrix} \mathbf{K}_x^p & \mathbf{K}_x^a \end{bmatrix}^T \in \mathbb{R}^{q+3}$ being the only unknown. Since $(\underline{\mathbf{A}}_e^x, \underline{\mathbf{B}}_e^x)$ is controllable, $\mathbf{K}_x$ can be chosen such that all eigenvalues of $\mathbf{A}_e^x$ have real part less than or equal to $-\eta_x$, with $\eta_x \in \mathbb{R}^+$. After that, $\mathbf{K}_x^a$

---

[2] Since $\bar{\mathbf{x}}_e$ incorporates $\bar{\mathbf{x}}_a$, which depends upon the actual system parameters at the instants of impact, it is in general unknown.

and $\mathbf{K}_x^p$ will be given by

$$\mathbf{K}_x^p = \mathbf{K}_x \begin{bmatrix} \mathbf{I}_2 \\ \mathbf{0}_{(q+1)\times 2} \end{bmatrix}, \quad \mathbf{K}_x^a = \mathbf{K}_x \begin{bmatrix} \mathbf{0}_{2\times(q+1)} \\ \mathbf{I}_{q+1} \end{bmatrix}.$$

Obviously, wholly similar results can be obtained for the y-coordinate. In particular, by defining $\mathbf{z}(t) := \begin{bmatrix} \mathbf{x}_e^T & \mathbf{y}_e^T \end{bmatrix}^T \in \mathbb{R}^{2(q+3)}$ and by using (5.21), (5.20) and (5.22), respectively, in absence of impacts one obtains

$$\textbf{Actual:} \quad \dot{\mathbf{z}}(t) = \bar{\mathbf{A}}\mathbf{z}(t) + \bar{\mathbf{B}}\mathbf{u}_a(t), \tag{5.24a}$$

$$\textbf{Desired:} \quad \dot{\bar{\mathbf{z}}}(t) = \bar{\mathbf{A}}\bar{\mathbf{z}}(t), \tag{5.24b}$$

$$\textbf{Error:} \quad \dot{\tilde{\mathbf{z}}}(t) = \tilde{\mathbf{A}}\tilde{\mathbf{z}}(t), \tag{5.24c}$$

where $\bar{\mathbf{A}} := blockdiag\{\bar{\mathbf{A}}_e^x, \bar{\mathbf{A}}_e^y\} \in \mathbb{R}^{2(q+3)\times 2(q+3)}$, $\bar{\mathbf{B}} := blockdiag\{\bar{\mathbf{B}}_e^x, \bar{\mathbf{B}}_e^y\} \in \mathbb{R}^{2(q+3)\times 2}$ and $\mathbf{u}_a(t) := \begin{bmatrix} u_{x_a} & u_{y_a} \end{bmatrix}^T \in \mathbb{R}^2$. Moreover, it is clear that all the eigenvalues of $\tilde{\mathbf{A}}$ have real part less than or equal to $-\eta$, with $\eta := \min\{\eta_x, \eta_y\} \in \mathbb{R}^+$.

Main result (*Full-Information*)

By choosing the initial conditions sufficiently close to the desired ones, for all $i \in \mathbb{N}$, the impact times $t_i > t_0$, $t_i \in \mathbb{R}$ of the actual trajectory can be forced to be close to the impact times $\bar{t}_i$ of the desired trajectory (see proof of Theorem 9) so that, following the control strategy detailed in Chapter 4, the precompensator input u_{x_a} can be expressed by

$$u_{x_a}(t) = \begin{cases} e_x(t), & \forall t \in \mathcal{F}_i^b, i \in \mathbb{Z}^+, \\ 0, & \text{otherwise}, \end{cases} \tag{5.25a}$$

$$u_{y_a}(t) = \begin{cases} e_y(t), & \forall t \in \mathcal{F}_i^b, i \in \mathbb{Z}^+, \\ 0, & \text{otherwise}, \end{cases} \tag{5.25b}$$

where $t_0^M := t_0$ and, for any $\bar{t}_i \in \mathbb{Z}, i \in \mathbb{N}$, one defines $t_i^m := \min\{t_i, \bar{t}_i\}$, $t_i^M := \max\{t_i, \bar{t}_i\}$ and $\mathcal{F}_i^b := (t_i^M, t_{i+1}^m)$.

Remark 24. As in Chapter 4, the precompensator input is switched off between the impact times t_i^m and t_i^M (see Fig. 5.2) in order to improve the behavior of the considered system when it is initialized with initial conditions quite far from the desired trajectory. Moreover, also when the actual and the nominal trajectories are very close, it is observed that switching off the control between the impacts improves the tracking (see Remark 13).
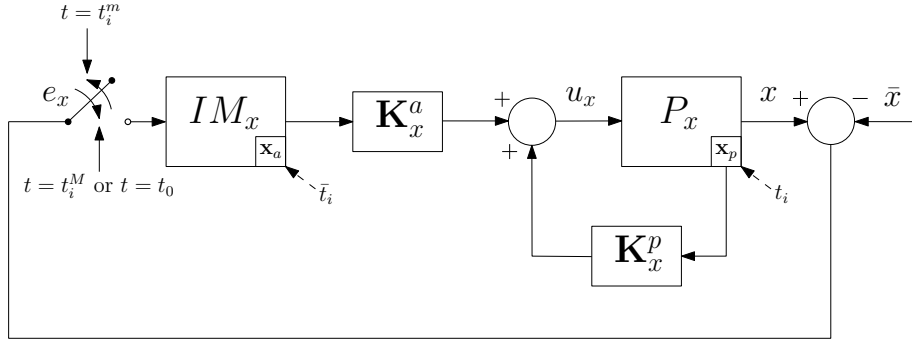
Figure 5.2: **Full-Information:** structure of the *switching* control scheme based on the internal model principle (only x-coordinate).

At this point the following result can be stated and proved.

Theorem 9. *There exists $\eta^* \in \mathbb{R}^+$ such that the control scheme in Fig. 5.1 solves Problem 4, for all $\eta \geq \eta^*$.*

Proof. The proof can be carried out by means of the steps described below, based on the following facts whose proofs, for the sake of readability, are given at the end of this chapter in Section 5.4.

There exist constants $M_1, M_2, M_3, M_4, M_5 \in \mathbb{R}^+$ and $\delta_0, \delta_1 \in \mathbb{R}^+$ such that

$$\|\tilde{\mathbf{z}}(t_i^{m-})\| < \delta_0 \Rightarrow \left\| \begin{bmatrix} \Delta t_i \\ \Delta \theta_i \end{bmatrix} \right\| \leq M_1 \|\tilde{\mathbf{z}}(t_i^{m-})\|, \tag{5.26}$$

$$\|\tilde{\mathbf{z}}(t_i^{m-})\| < \delta_1, \left\|\begin{bmatrix} \Delta t_i \\ \Delta \theta_i \end{bmatrix}\right\| < \delta_1, \|\tilde{\boldsymbol{\Lambda}}_a(\bar{t}_i)\| < \delta_1$$
$$\Downarrow \tag{5.27}$$
$$\|\tilde{\mathbf{z}}(t_i^{M+})\| \leq M_2 \|\tilde{\mathbf{z}}(t_i^{m-})\| + M_3 \left\|\begin{bmatrix} \Delta t_i \\ \Delta \theta_i \end{bmatrix}\right\| + M_4 \|\tilde{\boldsymbol{\Lambda}}_a(\bar{t}_i)\|,$$

$$\forall \eta \in \mathbb{R}^+ : \|\tilde{\mathbf{z}}(t)\| \leq L(\eta) e^{-\eta(t - t_i^M)} \|\tilde{\mathbf{z}}(t_i^{M+})\|, \ \forall t \in \mathcal{F}_i^b, \tag{5.28a}$$

$$\forall \varepsilon^* > 0, \forall T > 0, \exists \eta^* > 0 : \eta > \eta^* \Rightarrow L(\eta) e^{-\eta T} < \varepsilon^*, \tag{5.28b}$$

$$\|\tilde{\boldsymbol{\Lambda}}_a(\bar{t}_{i+N})\| \leq M_5 \|\tilde{\mathbf{z}}(t_{i+1}^{m-})\|, \tag{5.29}$$

where $\Delta t_i := t_i - \bar{t}_i$, $\Delta \theta_i := \theta_i - \bar{\theta}_i$ and, in view of the periodicity of the desired trajectory, (6.17) and (6.18) hold for all $i \in \mathbb{N}$ whereas (5.28) and (6.21) hold for all $i \in \mathbb{Z}^+$.

Step 1: In view of (6.17) and (6.18) and in order to guarantee that for each $i \in \mathbb{N}$ the actual impact time t_i belongs to the interval $(\bar{t}_i - \gamma, \bar{t}_i + \gamma)$ for a fixed $\gamma \in (0, 1/2)$, one can take $\|\tilde{\boldsymbol{\Lambda}}_a(\bar{t}_i)\| < \bar{\delta}_0$ and $\|\tilde{\mathbf{z}}(t_i^{m-})\| < \bar{\delta}_0$ where $\bar{\delta}_0 := \min\{\delta_0, \delta_1, \delta_1/M_1, \gamma/M_1\}$.

Step 2: By putting together (6.17) and (6.18), the following inequality is obtained

$$\|\tilde{\mathbf{z}}(t_i^{M+})\| \leq \mu \|\tilde{\mathbf{z}}(t_i^{m-})\| + M_4 \|\tilde{\boldsymbol{\Lambda}}_a(\bar{t}_i)\|, \tag{5.30}$$

where $\mu := M_2 + M_3 M_1$.

Step 3: By using (6.19) and (6.22), for all $i \in \mathbb{N}$ one has[3]

$$\|\tilde{\mathbf{z}}(t_{i+1}^{m-})\| \leq L(\eta) e^{-\eta(t_{i+1}^m - t_i^M)} \|\tilde{\mathbf{z}}(t_i^{M+})\| \leq$$
$$\leq L(\eta) e^{-\eta(1-2\gamma)} \mu \|\tilde{\mathbf{z}}(t_i^{m-})\| + L(\eta) e^{-\eta(1-2\gamma)} M_4 \|\tilde{\boldsymbol{\Lambda}}_a(\bar{t}_i)\|.$$

At this point, by taking in (6.20) $\varepsilon^* \leq \min\{\xi/\mu, \xi/M_4\}$, there exists η^* such

---

[3]By *Step 1*, the minimum flight-time in free motion is $1 - 2\gamma$.

that, for all $\eta > \eta^*$, it follows that[4]

$$\|\tilde{\mathbf{z}}(t_{i+1}^{m-})\| \leq \xi\|\tilde{\mathbf{z}}(t_i^{m-})\| + \xi\|\tilde{\mathbf{\Lambda}}_a(\bar{t}_i)\|, \tag{5.31}$$

for all $i \in \mathbb{N}$ with $\xi \in \mathbb{R}^+$ being a free parameter.

Step 4: By using iteratively (6.23), one obtains

$$\|\tilde{\mathbf{z}}(t_{i+N}^{m-})\| \leq \xi^N\|\tilde{\mathbf{z}}(t_i^{m-})\| + \xi^N\|\tilde{\mathbf{\Lambda}}_a(\bar{t}_i)\| + \xi^{N-1}\|\tilde{\mathbf{\Lambda}}_a(\bar{t}_{i+1})\| +$$
$$+ \cdots + \xi^2\|\tilde{\mathbf{\Lambda}}_a(\bar{t}_{i+N-2})\| + \xi\|\tilde{\mathbf{\Lambda}}_a(\bar{t}_{i+N-1})\|,$$

whereas by (6.21) and (6.23) it follows that

$$\|\tilde{\mathbf{\Lambda}}_a(\bar{t}_{i+N+j})\| \leq \xi^{j+1}M_5\|\tilde{\mathbf{z}}(t_i^{m-})\| + \xi^{j+1}M_5\|\tilde{\mathbf{\Lambda}}_a(\bar{t}_i)\| +$$
$$+ \xi^j M_5\|\tilde{\mathbf{\Lambda}}_a(\bar{t}_{i+1})\| + \cdots + \xi M_5\|\tilde{\mathbf{\Lambda}}_a(\bar{t}_{i+j})\|,$$

for each $j = \{0, \ldots, N-1\}$. Now, choosing $\xi := \min\{\bar{\xi}, \bar{\xi}/M_5\}$ with $0 < \bar{\xi} < 1$ and defining

$$\mathbf{\Gamma}(i) := \begin{bmatrix} \tilde{\mathbf{z}}^T(t_i^{m-}) & \tilde{\mathbf{\Lambda}}_a^T(\bar{t}_i) & \cdots & \tilde{\mathbf{\Lambda}}_a^T(\bar{t}_{i+N-1}) \end{bmatrix}^T \in \mathbb{R}^{2(N+1)(q+3)},$$

yield the following inequalities

$$\|\tilde{\mathbf{z}}(t_{i+N}^{m-})\| \leq \bar{\xi}\|\mathbf{\Gamma}(i)\|, \quad \|\tilde{\mathbf{\Lambda}}_a(\bar{t}_{i+j})\| \leq \bar{\xi}\|\mathbf{\Gamma}(i)\|,$$

for each $j = \{N, \ldots, 2N-1\}$, which imply that

$$\|\mathbf{\Gamma}(i+N)\| \leq \bar{\xi}\|\mathbf{\Gamma}(i)\|, \quad 0 < \bar{\xi} < 1. \tag{5.32}$$

By applying iteratively (6.24), with $k \in \mathbb{N}$ and $\bar{\xi} \in (0, 1)$, one obtains

$$\|\mathbf{\Gamma}(i)\| \leq \bar{\xi}\|\mathbf{\Gamma}(i-N)\| \leq \cdots \leq \bar{\xi}^k\|\mathbf{\Gamma}(i-kN)\|. \tag{5.33}$$

---

[4]From now on, η is fixed so that L is a real positive constant (dependence on η is omitted).

If the initial errors are sufficiently *small*, that is

$$\|\tilde{\mathbf{z}}(t_0^+)\| < \delta_{\varepsilon,\gamma}, \|\tilde{\mathbf{\Lambda}}_a(\bar{t}_1)\| < \delta_{\varepsilon,\gamma}, \cdots, \|\tilde{\mathbf{\Lambda}}_a(\bar{t}_{N-1})\| < \delta_{\varepsilon,\gamma}, \tag{5.34}$$

with $\delta_{\varepsilon,\gamma} \in \mathbb{R}^+$, by using (6.19),(6.22) and (6.21) it is possible to show that $\|\mathbf{\Gamma}(j)\| \le M_{\Gamma,j}\delta_{\varepsilon,\gamma}$ with $M_{\Gamma,j} \in \mathbb{R}^+$, $j = \{1,\ldots,N\}$ and, by defining $M_\Gamma := \max_{j\in\{1,\ldots,N\}}\{M_{\Gamma,j}\}$, inequality (5.33) yields

$$\|\mathbf{\Gamma}(i)\| \le \bar{\xi}^{\lfloor \frac{i-N}{N} \rfloor} M_\Gamma \delta_{\varepsilon,\gamma} \stackrel{i\to+\infty}{\to} 0 \text{ since } \bar{\xi} \in (0,1), \tag{5.35}$$

which implies that each component of $\|\mathbf{\Gamma}(i)\|$ goes to zero as i goes to infinity, that is

$$\|\tilde{\mathbf{z}}(t_i^{m-})\| \to 0, \|\tilde{\mathbf{\Lambda}}_a(\bar{t}_i)\| \to 0, \cdots, \|\tilde{\mathbf{\Lambda}}_a(\bar{t}_{i+N-1})\| \to 0. \tag{5.36}$$

By (6.29) and (6.17), it follows that

$$\left\| \begin{bmatrix} \Delta t_i \\ \Delta \theta_i \end{bmatrix} \right\| \le M_1 \|\tilde{\mathbf{z}}(t_i^{m-})\| \to 0 \stackrel{i\to\pm\infty}{\Rightarrow} \begin{cases} t_i \to \bar{t}_i \\ \theta_i \to \bar{\theta}_i \end{cases}. \tag{5.37}$$

Moreover, in any free-motion interval, i.e., $t \in \mathcal{F}_i^b$, the following result holds

$$\|\tilde{\mathbf{z}}(t)\| \le L(\mu \underbrace{\|\tilde{\mathbf{z}}(t_i^{m-})\|}_{\to 0} + M_4 \underbrace{\|\tilde{\mathbf{\Lambda}}_a(\bar{t}_i)\|}_{\to 0}) \to 0 \text{ as } i \to +\infty,$$

where (6.29) is used. By this result and (6.30), it follows that $\forall \tau \in (0,1), \exists i^* : i > i^* \Rightarrow \bar{t}_i + \tau \in \mathcal{F}_i^b \to (\bar{t}_i, \bar{t}_{i+1})$ and

$$\|\tilde{\mathbf{z}}(\bar{t}_i + \tau)\| \to 0 \text{ as } i \to +\infty.$$

Since $t_i \to \bar{t}_i$ as $i \to +\infty$, then $\bar{t}_i + \tau, \forall \tau \in (0,1)$ is an impact time neither for the actual trajectory nor for the desired one. Therefore, $\lim_{i\to+\infty} \|\tilde{\mathbf{z}}((\bar{t}_i+\tau)^-)\| = \lim_{i\to+\infty} \|\tilde{\mathbf{z}}((\bar{t}_i+\tau)^+)\| = \lim_{i\to+\infty} \|\tilde{\mathbf{z}}(\bar{t}_i+\tau))\| = 0$. This last fact and the definition

of $\tilde{\mathbf{z}}(t)$ prove property **2)** of Problem 4.

   Step 5: In order to complete the proof, it remains to prove property **1)** of Problem 4. By (6.19) and (6.22), for all t in a generic time interval $\mathcal{F}_i^b, i \in \mathbb{Z}^+$, one has

$$\|\tilde{\mathbf{z}}(t)\| \leq L\|\tilde{\mathbf{z}}(t_i^{M+})\| \leq L\mu\|\tilde{\mathbf{z}}(t_i^{m-})\| + LM_4\|\tilde{\boldsymbol{\Lambda}}_a(\bar{t}_i)\|.$$

Now, by using the inequality in (6.28) and by considering the definition of $\boldsymbol{\Gamma}(i)$, one obtains $\|\tilde{\mathbf{z}}(t)\| \leq (L\mu + LM_4)M_\Gamma\delta_{\varepsilon,\gamma}$. In addition, if $\delta_{\varepsilon,\gamma} < \bar{\delta}_0/M_\Gamma$, $\|\tilde{\mathbf{z}}(t_i^{m-})\| < \bar{\delta}_0$ and $\|\tilde{\boldsymbol{\Lambda}}_a(\bar{t}_i)\| < \bar{\delta}_0$ then

$$\|\tilde{\mathbf{z}}(t_{i+1}^{m-})\| \leq \bar{\xi}^{\left\lfloor \frac{i+1-N}{N} \right\rfloor} M_\Gamma\delta_{\varepsilon,\gamma} < M_\Gamma\delta_{\varepsilon,\gamma} < M_\Gamma\frac{\bar{\delta}_0}{M_\Gamma} = \bar{\delta}_0,$$

$$\|\tilde{\boldsymbol{\Lambda}}_a(\bar{t}_{i+1})\| \leq \bar{\xi}^{\left\lfloor \frac{i+1-N}{N} \right\rfloor} M_\Gamma\delta_{\varepsilon,\gamma} < M_\Gamma\delta_{\varepsilon,\gamma} < M_\Gamma\frac{\bar{\delta}_0}{M_\Gamma} = \bar{\delta}_0,$$

so that by choosing $\delta_{\varepsilon,\gamma} := \min\{\frac{\bar{\delta}_0}{M_\Gamma}, \frac{\varepsilon}{(L\mu+LM_4)M_\Gamma}\}$ the following result is obtained

$$(6.26) \quad \Rightarrow \quad \|\tilde{\mathbf{z}}(t)\| \leq \varepsilon, \quad \forall t \in \mathcal{F}_i^b, i \in \mathbb{Z}^+,$$

and since $|\Delta t_i| < \gamma$ (see *Step 1*), property **1)** in Problem 4 is proved.   □

5.2.2   Error-Feedback problem

In this section, the assumption of full state knowledge is removed. More precisely, by considering the control scheme in Fig. 5.3, with the tracking error being the only available measurement for feedback, it will be shown how the tracking control problem stated in Problem 4 can still be solved. The block P_x in Fig. 5.3 denotes the plant model whose dynamics have just been described in the paragraph **Plant model** for the *Full-Information* case.

The precompensator

For the sake of brevity, only the results needed for the design of the controller will be given, since they are obtained with computations wholly similar to the
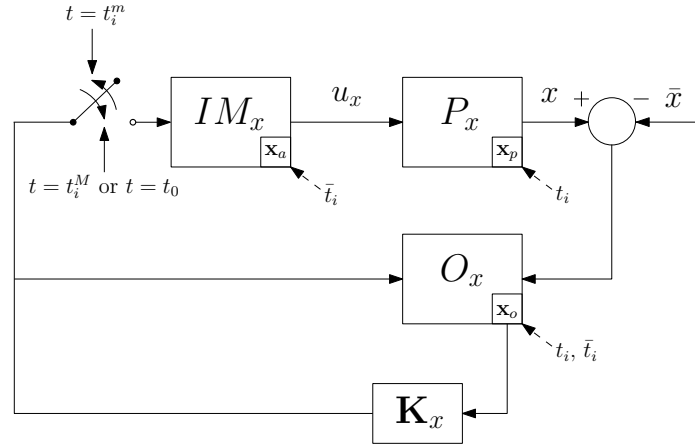
Figure 5.3: **Error-Feedback**: structure of the *switching* control scheme based on the internal model principle when only the position-error is measured (only x-coordinate).

ones detailed in Section 5.2.1.

Remark 25. As for the *Full-Information* case, the block IM_x in Fig. 5.2 has been designed so that a complete internal model of the class of trajectories to be tracked is contained in it. Actually, if the plant contains part of such an internal model, then the precompensator can also be designed with just a partial internal model of the desired trajectories in such a way to ensure that the cascade connection of IM and P contains a complete internal model. As a matter of fact, the plant matrix $\mathbf{A}_p(\boldsymbol{\beta})$ considered here has an eigenvalue at zero, so that a smaller matrix $\mathbf{A}_a$ would be chosen provided that the minimal polynomial of $\mathbf{M}$ in (5.6) is a divisor of the minimal polynomial of the cascade of the precompensator and the plant.

By Remark 25, during each free-motion interval, the precompensator can

be designed as follows:

$$IM_x : \begin{cases} \dot{\mathbf{x}}_a(t) = \mathbf{A}_a\mathbf{x}_a(t) + \mathbf{B}_a u_{x_a}(t) \\ \mathbf{y}_{x_a}(t) = \mathbf{C}_a\mathbf{x}_a(t) \end{cases} , \ \forall t \in \bar{\mathcal{F}}_i, i \in \mathbb{Z}^+, \qquad (5.38)$$

$$IM_y : \begin{cases} \dot{\mathbf{y}}_a(t) = \mathbf{A}_a\mathbf{y}_a(t) + \mathbf{B}_a u_{y_a}(t) \\ \mathbf{y}_{y_a}(t) = \mathbf{C}_a\mathbf{y}_a(t) \end{cases} , \ \forall t \in \bar{\mathcal{F}}_i, i \in \mathbb{Z}^+, \qquad (5.39)$$

with triple $(\mathbf{A}_a \in \mathbb{R}^{q \times q}, \mathbf{B}_a \in \mathbb{R}^q, \mathbf{C}_a^T \in \mathbb{R}^q)$ being in the Brunowsky canonical form, i.e.,

$$\mathbf{A}_a = \begin{bmatrix} 0 & 1 & 0 & \cdots & 0 \\ 0 & 0 & 1 & \cdots & 0 \\ \vdots & & \ddots & & \vdots \\ \vdots & & & 0 & 1 \\ 0 & \cdots & \cdots & 0 & 0 \end{bmatrix}, \ \mathbf{B}_a = \begin{bmatrix} 0 \\ \vdots \\ 0 \\ 1 \end{bmatrix}, \ \mathbf{C}_a = \begin{bmatrix} 1 & 0 & \ldots & 0 \end{bmatrix}.$$

Concerning the constrained motion, in the nominal parameters (i.e., $M = M_0$ and $D = D_0$), the jump of the precompensator state vector at time $\bar{t}_i$ is given by

$$\bar{\mathbf{x}}_a(\bar{t}_i^+) = \begin{bmatrix} \bar{x}_{a,1}(\bar{t}_i^+) & \cdots & \bar{x}_{a,q}(\bar{t}_i^+) & \bar{x}_{a,q+1}(\bar{t}_i^+) \end{bmatrix}^T,$$

where, for each $j \in \{1, \ldots, q\}$, one has

$$\bar{x}_{a,j}(\bar{t}_i^+) = M\bar{x}^{(j+1)}(t) + D\bar{x}^{(j)}(t).$$

In order to deal with possible uncertainties, exactly the same algorithm proposed for the *Full-Information* case will be used. More specifically, the correct jumps for the state vectors of the precompensator at time $\bar{t}_i$ can be estimated in real time by applying the rules defined in (5.17).

The (error) observer

During each free-motion interval (i.e., in absence of impacts for both the controlled trajectory and the nominal one), the blocks O_x and O_y are described by

$$O_x : \begin{cases} \dot{\mathbf{x}}_o(t) = \mathbf{A}(\boldsymbol{\beta})\mathbf{x}_o(t) + \mathbf{B}u_{x_a}(t) + \mathbf{L}_x u_{x_o}(t) \\ \mathbf{y}_{x_o}(t) = \mathbf{x}_o(t) \end{cases} , \qquad (5.40)$$

$$O_y : \begin{cases} \dot{\mathbf{y}}_o(t) = \mathbf{A}(\boldsymbol{\beta})\mathbf{y}_o(t) + \mathbf{B}u_{y_a}(t) + \mathbf{L}_y u_{y_o}(t) \\ \mathbf{y}_{y_o}(t) = \mathbf{y}_o(t) \end{cases} , \qquad (5.41)$$

where $\mathbf{A}(\boldsymbol{\beta}) \in \mathbb{R}^{(q+2)\times(q+2)}, \mathbf{B} \in \mathbb{R}^{q+2}, \mathbf{C}^T \in \mathbb{R}^{q+2}$ are

$$\mathbf{A}(\boldsymbol{\beta}) := \begin{bmatrix} \mathbf{A}_p(\boldsymbol{\beta}) & \mathbf{B}_p(\boldsymbol{\beta})\mathbf{C}_p \\ \mathbf{0} & \mathbf{A}_a \end{bmatrix}, \ \mathbf{B} := \begin{bmatrix} \mathbf{0} \\ \mathbf{B}_a \end{bmatrix}, \ \mathbf{C} := \begin{bmatrix} \mathbf{C}_p & \mathbf{0} \end{bmatrix}.$$

the precompensator inputs are

$$u_{x_a}(t) = \begin{cases} \mathbf{K}_x \mathbf{x}_o(t), & \forall t \in \mathcal{F}_i^b, i \in \mathbb{Z}^+, \\ 0, & \text{otherwise,} \end{cases} \qquad (5.42)$$

$$u_{y_a}(t) = \begin{cases} \mathbf{K}_y \mathbf{y}_o(t), & \forall t \in \mathcal{F}_i^b, i \in \mathbb{Z}^+, \\ 0, & \text{otherwise,} \end{cases} \qquad (5.43)$$

whereas the observer inputs are

$$u_{x_o}(t) = \begin{cases} e_x(t) - \mathbf{C}\mathbf{x}_o(t), & \forall t \in \mathcal{F}_i^b, i \in \mathbb{Z}^+, \\ 0, & \text{otherwise.} \end{cases}$$

$$u_{y_o}(t) = \begin{cases} e_y(t) - \mathbf{C}\mathbf{y}_o(t), & \forall t \in \mathcal{F}_i^b, i \in \mathbb{Z}^+, \\ 0, & \text{otherwise.} \end{cases}$$

Moreover, regarding the constrained motion, at each impact time t_i and $\bar{t}_i$, the jump in the state vector $\mathbf{x}_o$ is just a reset to zero, that is

$$\mathbf{x}_o(t^+) = \mathbf{0}, \quad t = \{t_i, \bar{t}_i\}, i \in \mathbb{Z}^+.$$

At this point, by recalling the meaning of the error vector $\tilde{\mathbf{x}}_e$ (see (5.19)) and by defining $\tilde{\tilde{\mathbf{x}}}_e := [\tilde{\mathbf{x}}_e^T, (\tilde{\mathbf{x}}_e - \mathbf{x}_o)^T]^T$, it follows that

$$\dot{\tilde{\tilde{\mathbf{x}}}}_e = \left[\begin{array}{cc} \mathbf{A}(\boldsymbol{\beta}) + \mathbf{B}\mathbf{K}_x & -\mathbf{B}\mathbf{K}_x \\ \mathbf{0} & \mathbf{A}(\boldsymbol{\beta}) - \mathbf{L}_x\mathbf{C} \end{array} \right] \tilde{\tilde{\mathbf{x}}}_e.$$

Since triple $(\mathbf{A}(\boldsymbol{\beta}), \mathbf{B}, \mathbf{C})$ is controllable and observable, $\mathbf{K}_x$ and $\mathbf{L}_x$ can be chosen such that all eigenvalues of $\mathbf{A}(\boldsymbol{\beta}_0) + \mathbf{B}\mathbf{K}_x$ and $\mathbf{A}(\boldsymbol{\beta}_0) - \mathbf{L}_x\mathbf{C}$ have real part less than or equal to $-\eta_x$ and $-\rho_x$, respectively, with $\eta_x, \rho_x \in \mathbb{R}^+$. In view of Remark 21, there exists a neighborhood $\boldsymbol{\Psi}$ of $\boldsymbol{\beta}_0$ such that, for all $\boldsymbol{\beta} \in \boldsymbol{\Psi}$, also the eigenvalues of $\mathbf{A}(\boldsymbol{\beta}) + \mathbf{B}\mathbf{K}_x$ and $\mathbf{A}(\boldsymbol{\beta}) - \mathbf{L}_x\mathbf{C}$ have real part less than or equal to $-\eta_x$ and $-\rho_x$.

Finally, the following result holds, whose proof is wholly similar to the previous one and thus omitted for the sake of brevity.

Theorem 10. *There exists $\eta^* \in \mathbb{R}^+$ and $\rho^* \in \mathbb{R}^+$ such that the control scheme in Fig. 5.3 solves Problem 4, for all $\eta \geq \eta^*$ and $\rho \geq \rho^*$.*

5.3 Examples

In this last section an example is considered in order to show the effectiveness of the proposed control strategy. The parameters describing the elliptical billiard table, which is assumed to be centered at the origin, are $a = 4$ and $b = 2$. The case of rotational motion with winding number $(N = 3, R = 1)$ and starting vertex at $\bar{q}_0 = \left[\begin{array}{cc} 4 & 0 \end{array} \right]^T$ is taken into account.

Solving the LMI problem defined in Chapter 3 yields $q = 2$ as minimum degree of the interpolating polynomials defining the velocity profiles on the

target path (a triangle inscribed into the elliptical billiards with one revolution around the origin), which are given by

$$l_0(t) = -0.737t^2 + 1.737t,$$
$$l_1(t-1) = t-1,$$
$$l_2(t-2) = 0.737(t-2)^2 + 0.263(t-2).$$

Moreover, the vertices of the desired path are

$$\bar{\mathbf{q}}_0 = \begin{bmatrix} 4 \\ 0 \end{bmatrix}, \quad \bar{\mathbf{q}}_1 = \begin{bmatrix} -3.4741 \\ 0.9913 \end{bmatrix}, \quad \bar{\mathbf{q}}_2 = \begin{bmatrix} -3.4741 \\ -0.9913 \end{bmatrix}.$$

Full-information

Concerning the controller design, the precompensator free-dynamics are characterized by

$$\mathbf{A}_a = \begin{bmatrix} 0 & 1 & 0 \\ 0 & 0 & 1 \\ 0 & 0 & 0 \end{bmatrix}, \quad \mathbf{B}_a = \begin{bmatrix} 0 \\ 0 \\ 1 \end{bmatrix},$$

and by (5.23) one has

$$\underline{\mathbf{A}}_e^x = \underline{\mathbf{A}}_e^y =: \underline{\mathbf{A}}_e = \begin{bmatrix} 0 & 1 & 0 & 0 & 0 \\ 0 & -\frac{12}{30} & 0 & 0 & 0 \\ 0 & 0 & 0 & 1 & 0 \\ 0 & 0 & 0 & 0 & 1 \\ -1 & 0 & 0 & 0 & 0 \end{bmatrix}, \quad \underline{\mathbf{B}}_e^x = \underline{\mathbf{B}}_e^y =: \underline{\mathbf{B}}_e = \begin{bmatrix} 0 \\ \frac{1}{30} \\ 0 \\ 0 \\ 0 \end{bmatrix},$$

where, for simplicity, it is assumed that $\mathbf{K}_x = \mathbf{K}_y =: \mathbf{K}$. Now, by defining $\bar{\mathbf{p}}^K = \begin{bmatrix} -19 & -18 & -17 & -16 & -15 \end{bmatrix}$ as the vector of the desired eigenvalues of the matrix $\mathbf{A}_e^x = \mathbf{A}_e^y$, the acker function provided by Matlab® returns the

following result

$$\mathbf{K} = -\texttt{acker}(\underline{\mathbf{A}}_e, \underline{\mathbf{B}}_e, \bar{\mathbf{p}}^K) =$$

$$= \left[\begin{array}{ccccc} -86550 & -2538 & 41860800 & 12398220 & 1466250 \end{array} \right],$$

so that

$$\mathbf{K}_x^p = \mathbf{K}_y^p = \left[\begin{array}{cc} -86550 & -2538 \end{array} \right],$$

$$\mathbf{K}_x^a = \mathbf{K}_y^a = \left[\begin{array}{ccc} 41860800 & 12398220 & 1466250 \end{array} \right].$$

On the other hand, by solving the system (5.14) and by using the notation introduced in the previous section, one obtains

$$\mathbf{U}_{x_a}^0 = \left[\begin{array}{ccc} 0.0164388758 & -0.0329174399 & 0.0227780182 \\ -0.0071829338 & 0 & 0 \\ -0.0072575135 & -0.0020110380 & 0.0227780182 \end{array} \right], \quad (5.44\text{a})$$

$$\mathbf{U}_{y_a}^0 = \left[\begin{array}{ccc} -0.0010834136 & 0.0043658846 & -0.0030210794 \\ 0.0031428842 & -0.0040991579 & 0 \\ -0.0020594706 & -0.0002667267 & 0.0030210794 \end{array} \right]. \quad (5.44\text{b})$$

At this point, by starting from zero initial conditions at the initial time $t_0 = 0.5$ and by setting the threshold $\sigma = 0.15$ in the extended-algorithm proposed in Chapter 4, the behavior of the controlled trajectory during the first 12.5 seconds of motion can be observed in the subsequent figures, where first the case in which all the plant parameters are exactly known is considered, i.e., $M = M_0$ and $D = D_0$ (see Fig. 5.4,5.9), and then the possible presence of uncertainties is considered in order to show the robustness of the proposed control strategy (see Fig. 5.6,5.7). In the latter case, the algorithm previously proposed is used in order to estimate the correct jumps for the precompensator,

in particular the Remark 23 is validated by the following simulation results

$$\|\mathbf{U}_{x_a} - \mathbf{U}^0_{x_a}\|_\infty = 8.7 \cdot 10^{-6},$$
$$\|\mathbf{U}_{y_a} - \mathbf{U}^0_{y_a}\|_\infty = 1.2 \cdot 10^{-6},$$

where $\mathbf{U}^0_{x_a}$ and $\mathbf{U}^0_{y_a}$ are computed in the nominal parameter (see (5.44)), whereas $\mathbf{U}_{x_a}$ and $\mathbf{U}_{y_a}$ are the estimated one, with $\|\cdot\|_\infty$ denotes the infinity norm (i.e., the largest row sum) of the matrix at argument. It is interesting to note that in both cases when the position tracking errors, i.e., $e_x := \bar{x} - x$ and $e_y := \bar{y} - y$, tend to zero the augmented system evolve as an unforced system, i.e., $u_{x_a} = u_{y_a} = 0$, which is according to the spirit of the internal model principle (sometimes in the figures below the desired variables are also denoted by means of the subscript "$_d$" (e.g., $\bar{x}(t) \equiv x_d(t)$)).

Error-feedback

By choosing $\mathbf{K}_x = \mathbf{K}_y =: \mathbf{K}$ and $\mathbf{L}_x = \mathbf{L}_y =: \mathbf{L}$ such that all the eigenvalues of $\mathbf{A}(\boldsymbol{\beta}) + \mathbf{BK}$ and $\mathbf{A}(\boldsymbol{\beta}) - \mathbf{LC}$ have real part less than or equal to $-\eta$ and $-\rho$, respectively, with $\eta = 6$ and $\rho = 11$, by following the guidelines given in Section 5.2.2, the control scheme in Fig. 5.3 can be implemented. At this point, by starting from initial conditions sufficiently close to the desired one (as it is required in Problem 4) at the initial time $t_0 = 0.1$ and by considering an actual body of mass $M = 23$ and damping factor $D = 14$, the behavior of the controlled trajectory can be observed in Fig. 5.10. The simulation was performed in Matlab where the *event* option for impact detection and handling has been used. It is interesting to note that in both cases when the position tracking errors tend to zero the augmented system (i.e., the cascade connection precompensator-plant) evolves as an unforced system (see Fig. 5.10(d)), which is according to the spirit of the internal model principle. As for the observer variables, their time behaviour is depicted in Fig. 5.11.

(a) $\mathbf{q}(t), \bar{\mathbf{q}}(t)$

(b) $x(t), \bar{x}(t)$ and $y(t), \bar{y}(t)$

(c) $\dot{x}(t), \dot{\bar{x}}(t)$ and $\dot{y}(t), \dot{\bar{y}}(t)$
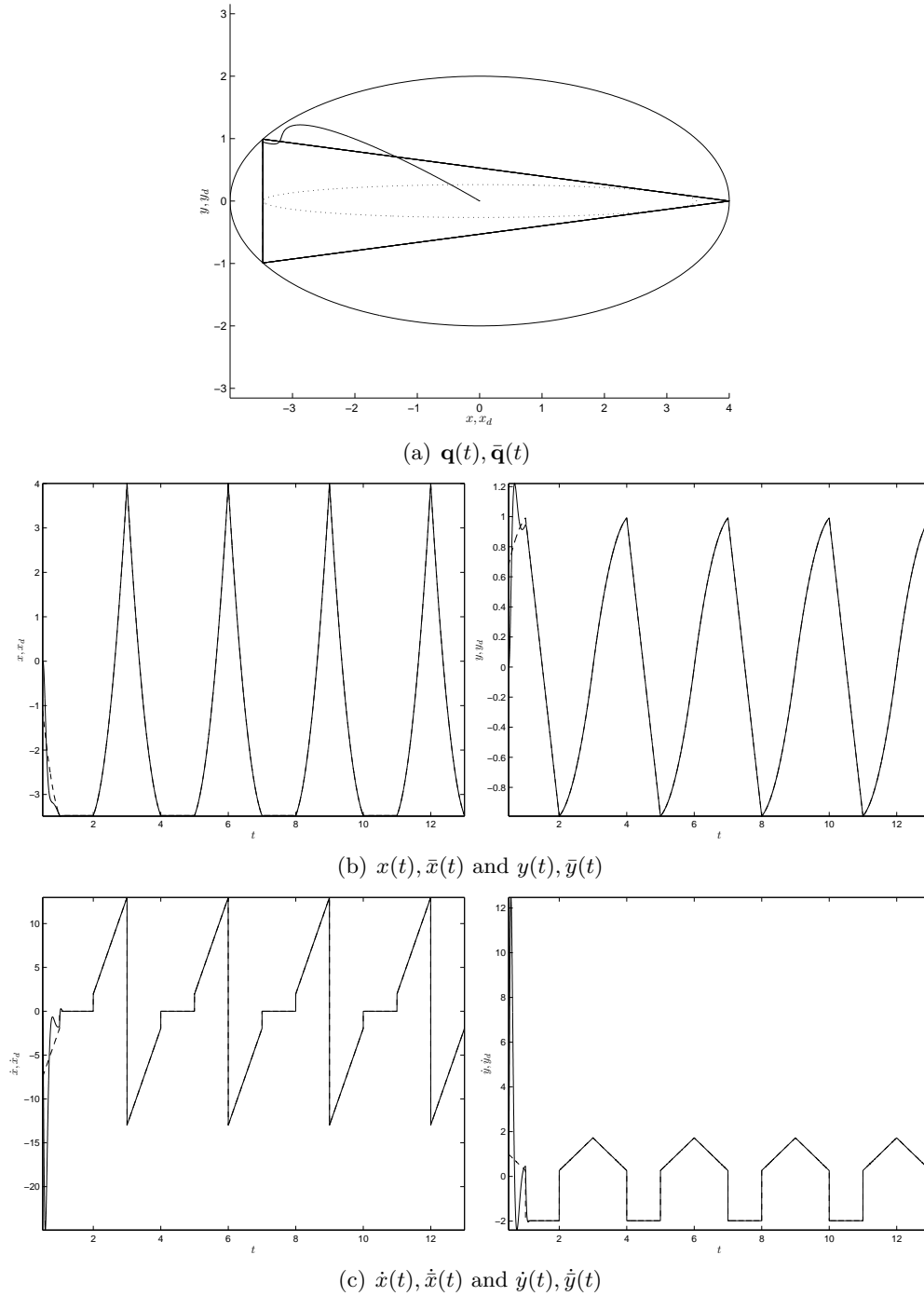
Figure 5.4: The inner caustic curve (dotted) with the desired (dashed) trajectory, which is completely overlapped with the actual (solid) one, in the xy-plane (a); time behavior of the desired (dashed) and actual (solid) positions and velocities, (b) and (c), respectively.
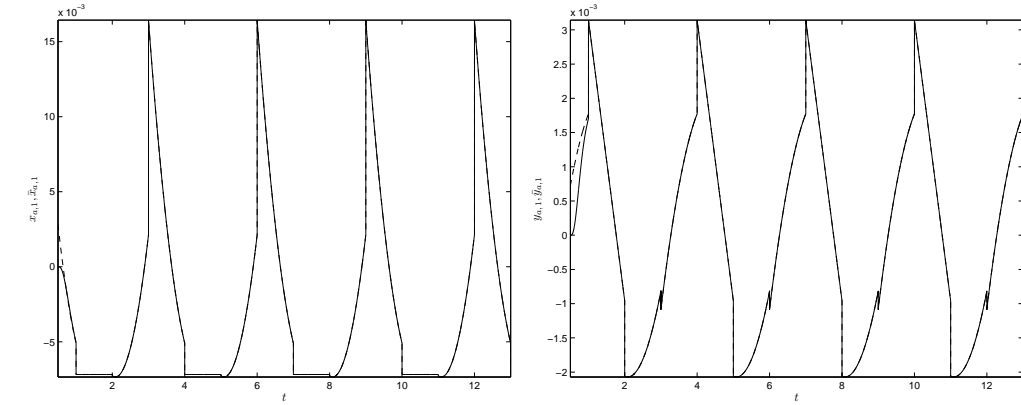
(a) $x_{a,1}(t), \bar{x}_{a,1}(t)$ and $y_{a,1}(t), \bar{y}_{a,1}(t)$
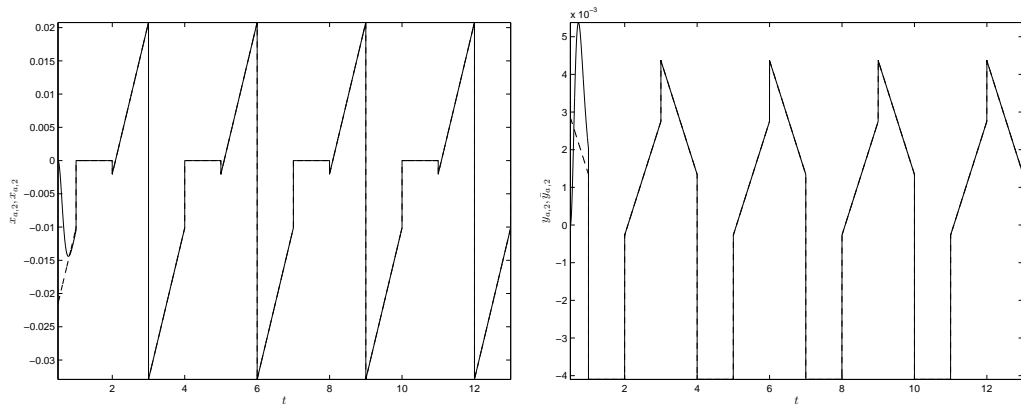
(b) $x_{a,2}(t), \bar{x}_{a,2}(t)$ and $y_{a,2}(t), \bar{y}_{a,2}(t)$
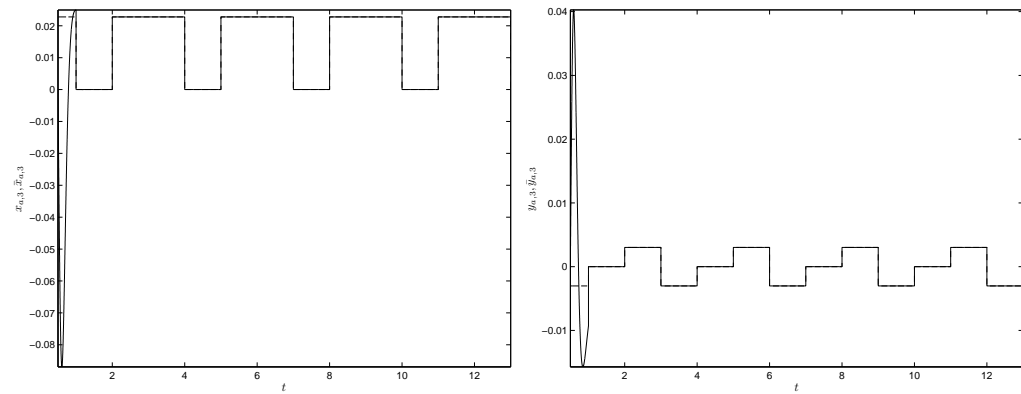
(c) $x_{a,3}(t), \bar{x}_{a,3}(t)$ and $y_{a,3}(t), \bar{y}_{a,3}(t)$

Figure 5.5: Time behavior of the desired (dashed) and actual (solid) state variables of the precompensator (a),(b) and (c).

(a) $\mathbf{q}(t), \bar{\mathbf{q}}(t)$

(b) $x(t), \bar{x}(t)$ and $y(t), \bar{y}(t)$

(c) $\dot{x}(t), \dot{\bar{x}}(t)$ and $\dot{y}(t), \dot{\bar{y}}(t)$
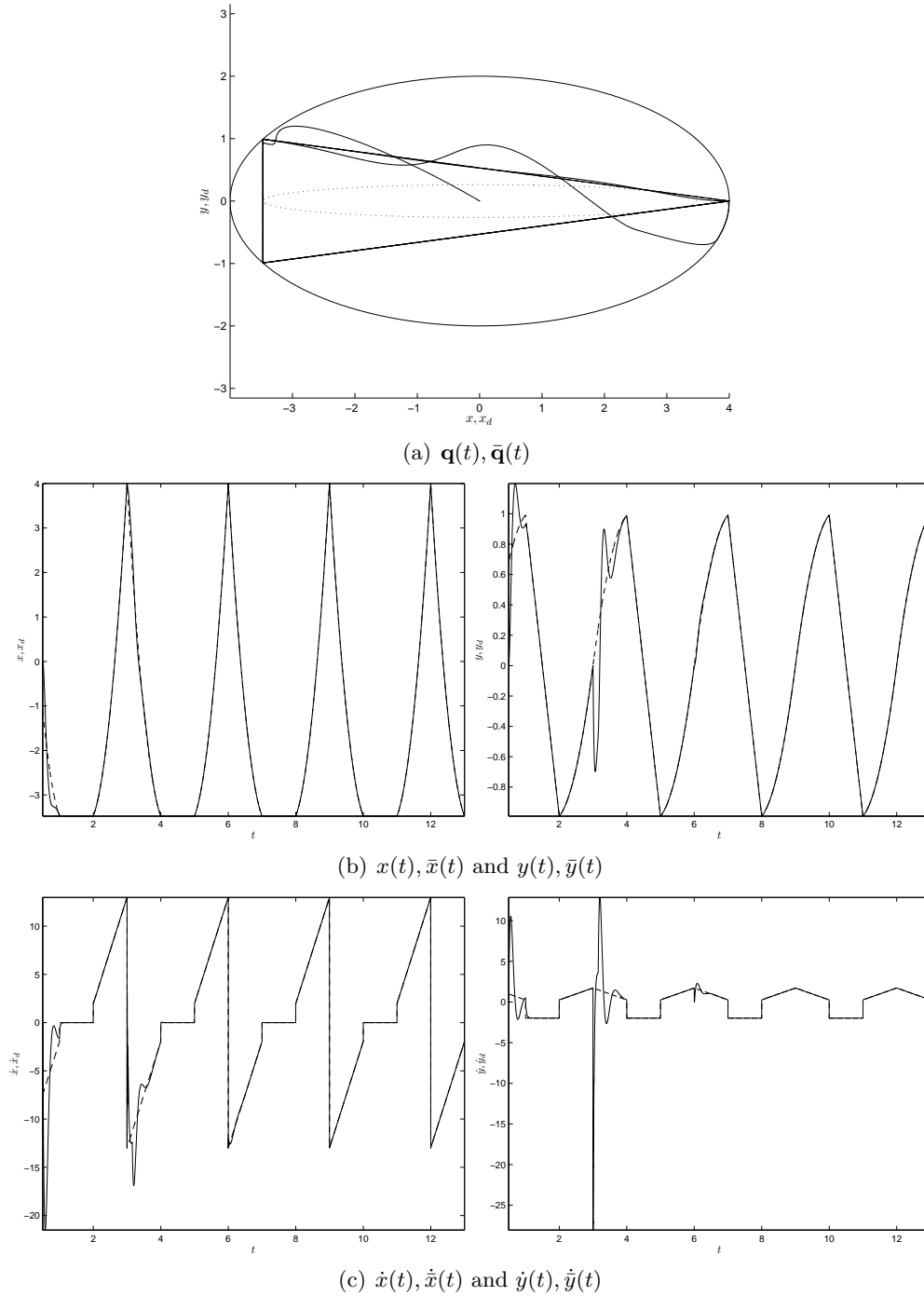
Figure 5.6: The inner caustic curve (dotted) with the desired (dashed) tra-
jectory, which is completely overlapped with the actual (solid) one, in the
xy-plane (a); time behavior of the desired (dashed) and actual (solid) posi-
tions and velocities, (b) and (c), respectively.
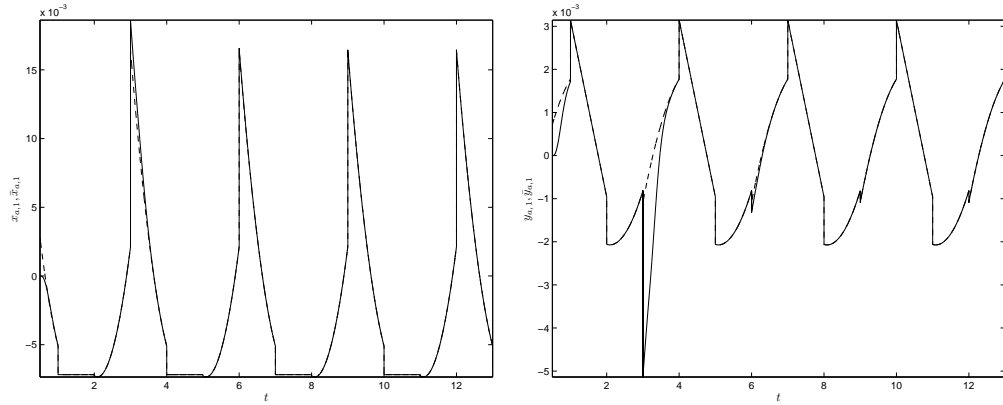
(a) $x_{a,1}(t), \bar{x}_{a,1}(t)$ and $y_{a,1}(t), \bar{y}_{a,1}(t)$
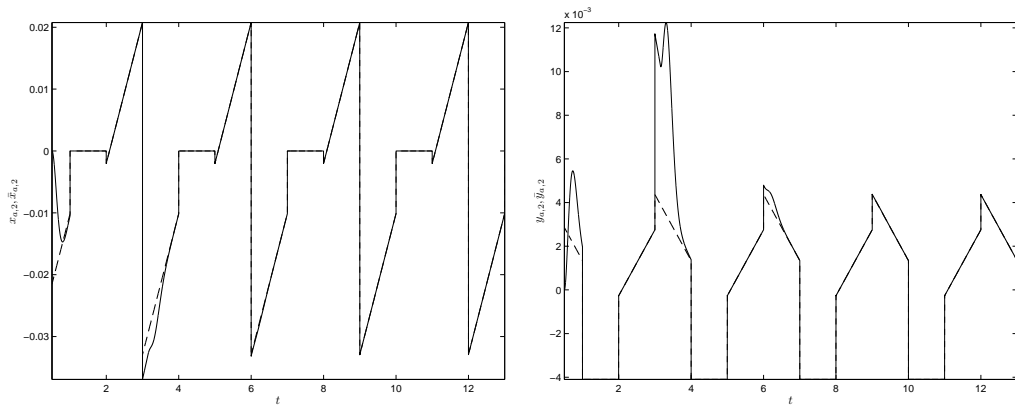
(b) $x_{a,2}(t), \bar{x}_{a,2}(t)$ and $y_{a,2}(t), \bar{y}_{a,2}(t)$
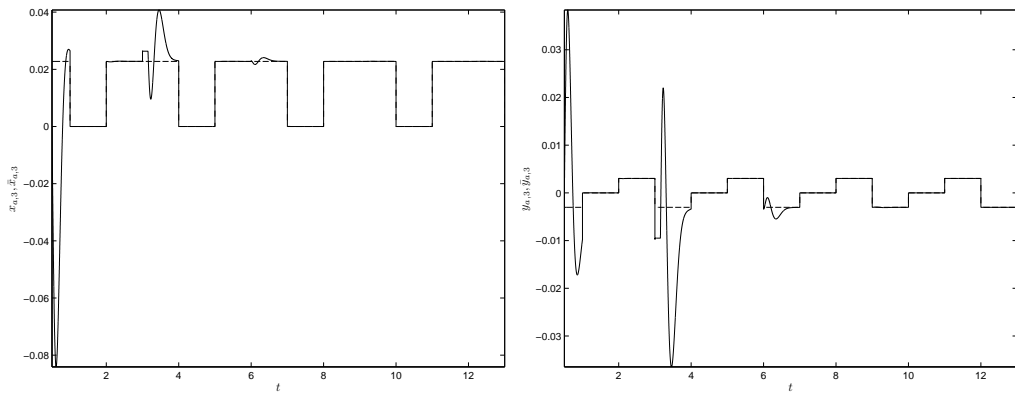
(c) $x_{a,3}(t), \bar{x}_{a,3}(t)$ and $y_{a,3}(t), \bar{y}_{a,3}(t)$

Figure 5.7: Time behavior of the desired (dashed) and actual (solid) state variables of the precompensator (a),(b) and (c).

(a) $\mathbf{q}(t), \bar{\mathbf{q}}(t)$

(b) $x(t), \bar{x}(t)$ and $y(t), \bar{y}(t)$

(c) $\dot{x}(t), \dot{\bar{x}}(t)$ and $\dot{y}(t), \dot{\bar{y}}(t)$
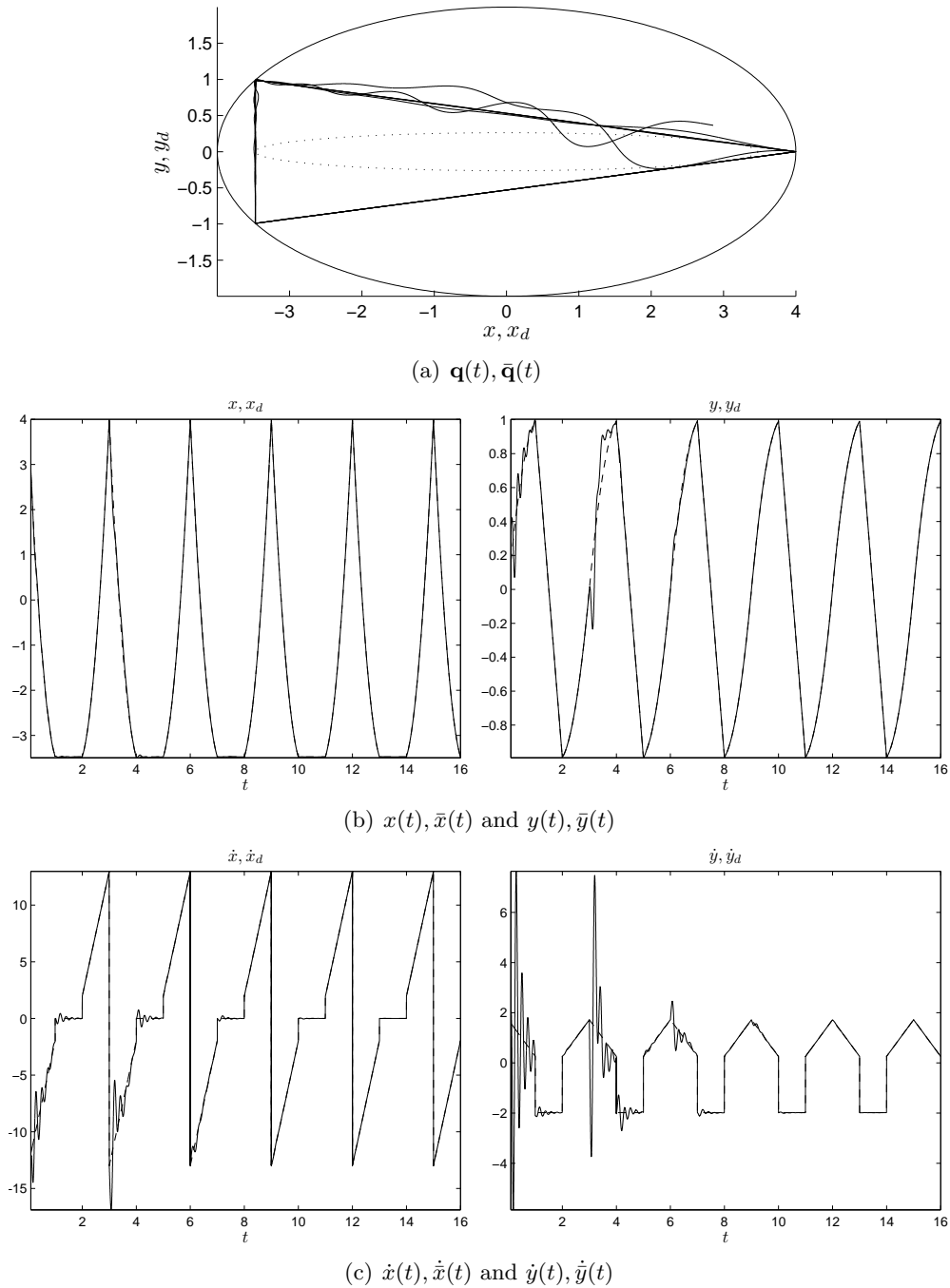
Figure 5.8: The inner caustic curve (dotted) with the desired (dashed) trajectory, which is completely overlapped with the actual (solid) one, in the xy-plane (a); time behavior of the desired (dashed) and actual (solid) positions (b) and velocities (c).
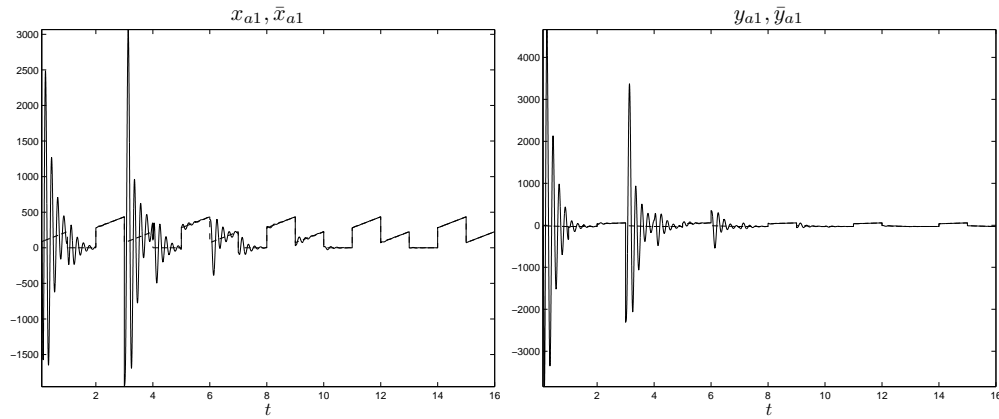
(a) $x_{a,1}(t), \bar{x}_{a,1}(t)$ and $y_{a,1}(t), \bar{y}_{a,1}(t)$
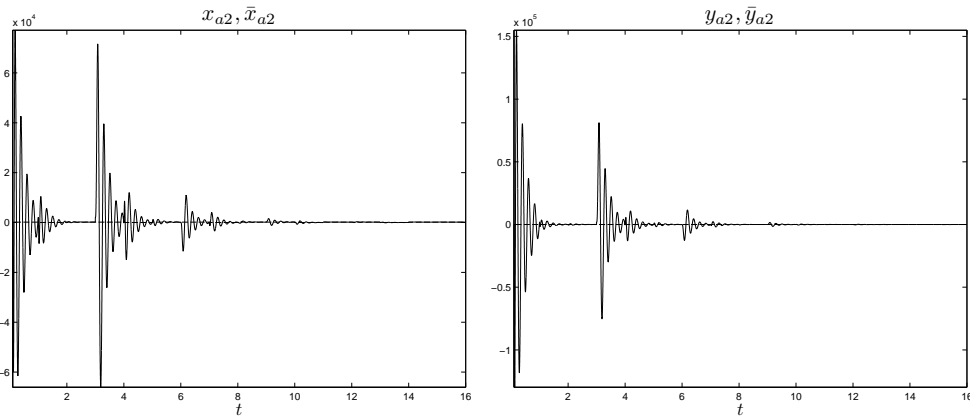
(b) $x_{a,2}(t), \bar{x}_{a,2}(t)$ and $y_{a,2}(t), \bar{y}_{a,2}(t)$

Figure 5.9: Time behavior of the desired (dashed) and actual (solid) state variables of the precompensator (a) and (b).
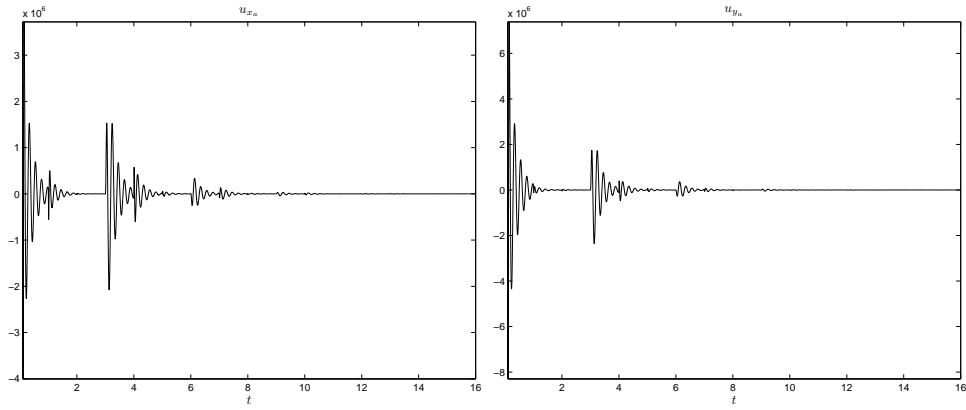
(a) $u_{x_a}(t)$ and $u_{y_a}(t)$

Figure 5.10: Time behavior of the control inputs u_{x_a} and u_{y_a} (d).
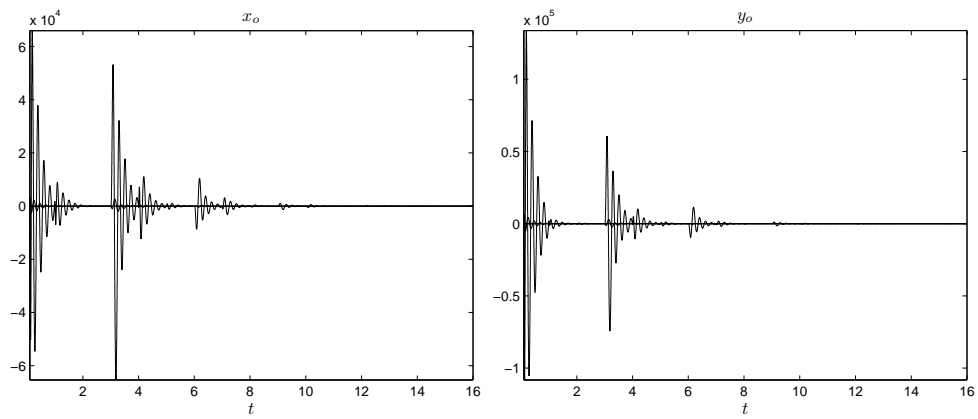
(a) $x_o(t)$ and $y_o(t)$

Figure 5.11: Time behavior of the observer state variables $\mathbf{x}_o$ and $\mathbf{y}_o$ (a).

5.4 Details of the proof of main result (Full-Information)

Remark 26. Since the desired trajectory is periodic, all the results obtained in the following for $i \in \{1, \dots, N\} =: \mathcal{I}_N$, remain proved for $i \in \mathbb{N}$.

For all $i \in \mathcal{I}_N$, the following fact can be proved

$$\exists \delta_0 \in \mathbb{R}^+, M_1 \in \mathbb{R}^+ : \|\tilde{\mathbf{z}}(t_i^{m-})\| < \delta_0 \Rightarrow \left\| \begin{bmatrix} \Delta t_i \\ \Delta \theta_i \end{bmatrix} \right\| \le M_1 \|\tilde{\mathbf{z}}(t_i^{m-})\|, \quad (6.17)$$

where $\Delta t_i := t_i - \bar{t}_i$ and $\Delta \theta_i := \theta_i - \bar{\theta}_i$.

The proof of (6.17) follows immediately from the proof of fact (26) in Section 6.5 just by considering in it the present error vector $\tilde{\mathbf{z}}(\cdot)$ in place of $\mathbf{e}(\cdot)$.

Details of the proof of the fact (6.18)

The dynamics during the free-motion intervals (i.e., in absence of impacts for both the actual and the nominal trajectories) are completely characterized by the equations (5.24). On the other hand, the state vector $\bar{\mathbf{z}}(\cdot)$ is subject to jump at the integer instants $\bar{t}_i$, whereas the vectors $\mathbf{z}(\cdot)$ and $\tilde{\mathbf{z}}(\cdot)$ have jumps at the impact times both of the controlled body and of the desired trajectory. In particular, such jumps can be given in terms of $\bar{\mathbf{z}}$ and $\mathbf{z}$ as

$$\bar{\mathbf{z}}(\bar{t}_i^+) = \mathbf{\Lambda}_p(\bar{\theta}_i)\bar{\mathbf{z}}(\bar{t}_i^-) + \bar{\mathbf{\Lambda}}_a(\bar{t}_i), \quad i \in \mathbb{N}, \quad (5.45a)$$

and

$$\mathbf{z}(t^+) = \begin{cases} \mathbf{\Lambda}_{p,1}(\theta_i)\mathbf{z}(t^-), & t = t_i, i \in \mathbb{N}, \\ \mathbf{\Lambda}_{p,2}\mathbf{z}(t^-) + \mathbf{\Lambda}_a(t), & t = \bar{t}_i, i \in \mathbb{N}, \end{cases} \quad (5.45b)$$

where $\mathbf{\Lambda}_p(\theta), \mathbf{\Lambda}_{p,1}(\theta), \mathbf{\Lambda}_{p,2}(\theta) \in \mathbb{R}^{2(q+3) \times 2(q+3)}$ and $\bar{\mathbf{\Lambda}}_a(i) \in \mathbb{R}^{2(q+3)}$ are given by

$$\mathbf{\Lambda}_p(\theta) := \begin{bmatrix} \mathbf{C}_1^p(\theta) & \mathbf{0} & \mathbf{C}_2^p(\theta) & \mathbf{0} \\ \mathbf{0} & \mathbf{0} & \mathbf{0} & \mathbf{0} \\ \mathbf{C}_2^p(\theta) & \mathbf{0} & \mathbf{C}_3^p(\theta) & \mathbf{0} \\ \mathbf{0} & \mathbf{0} & \mathbf{0} & \mathbf{0} \end{bmatrix}, \quad \bar{\mathbf{\Lambda}}_a(i) := \begin{bmatrix} \mathbf{0} \\ \bar{\mathbf{\Lambda}}_{x_a}(i) \\ \mathbf{0} \\ \bar{\mathbf{\Lambda}}_{y_a}(i) \end{bmatrix},$$

and

$$\mathbf{\Lambda}_{p,1}(\theta) := \begin{bmatrix} \mathbf{C}_1^p(\theta) & \mathbf{0} & \mathbf{C}_2^p(\theta) & \mathbf{0} \\ \mathbf{0} & \mathbf{I}_{q+1} & \mathbf{0} & \mathbf{0} \\ \mathbf{C}_2^p(\theta) & \mathbf{0} & \mathbf{C}_3^p(\theta) & \mathbf{0} \\ \mathbf{0} & \mathbf{0} & \mathbf{0} & \mathbf{I}_{q+1} \end{bmatrix}, \quad \mathbf{\Lambda}_{p,2} := \begin{bmatrix} \mathbf{I}_2 & \mathbf{0} & \mathbf{0} & \mathbf{0} \\ \mathbf{0} & \mathbf{0} & \mathbf{0} & \mathbf{0} \\ \mathbf{0} & \mathbf{0} & \mathbf{I}_2 & \mathbf{0} \\ \mathbf{0} & \mathbf{0} & \mathbf{0} & \mathbf{0} \end{bmatrix},$$

with $\mathbf{C}_1^p(\theta), \mathbf{C}_2^p(\theta)$ and $\mathbf{C}_3^p(\theta)$ being defined in (5.5) and $\bar{\mathbf{\Lambda}}_{x_a}(i)$ being defined in (5.15)[5]. Regarding the vector $\mathbf{\Lambda}_a(i)$, it can be expressed as

$$\mathbf{\Lambda}_a(i) = \bar{\mathbf{\Lambda}}_a(i) + \tilde{\mathbf{\Lambda}}_a(i),$$

where $\tilde{\mathbf{\Lambda}}_a(i)$ denotes the error between the actual value of the jump in the precompensator state vector at the instant $i \in \mathbb{Z}$ and the estimated one. As seen before, such an error is due to the possible presence of uncertainties upon the system parameters.

---

[5]The vector $\bar{\mathbf{\Lambda}}_{y_a}(i)$ is defined in an analogous way as $\bar{\mathbf{\Lambda}}_{x_a}(i)$ substituting wherever x with y.

By using the notation so far introduced, for all $i \in \mathcal{I}_N$, one can prove that

$$\exists \delta_1 \in \mathbb{R}^+, M_2 \in \mathbb{R}^+, M_3 \in \mathbb{R}^+, M_4 \in \mathbb{R}^+ :$$

$$\|\tilde{\mathbf{z}}(t_i^{m-})\| < \delta_1, \left\| \begin{bmatrix} \Delta t_i \\ \Delta \theta_i \end{bmatrix} \right\| < \delta_1, \|\tilde{\mathbf{\Lambda}}_a(\bar{t}_i)\| < \delta_1 \Rightarrow$$

$$\Rightarrow \|\tilde{\mathbf{z}}(t_i^{M+})\| \leq M_2 \|\tilde{\mathbf{z}}(t_i^{m-})\| + M_3 \left\| \begin{bmatrix} \Delta t_i \\ \Delta \theta_i \end{bmatrix} \right\| + M_4 \|\tilde{\mathbf{\Lambda}}_a(\bar{t}_i)\|. \quad (5.46)$$

The two possible cases are considered separately.

Case a) $t_i^m = t_i$, $t_i^M = \bar{t}_i$, so that $\Delta t_i := t_i - \bar{t}_i < 0$, and the error at time t_i^{M+}, that is after the i-th couple of impacts, is given by $\tilde{\mathbf{z}}(t_i^{M+}) := \mathbf{z}(t_i^{M+}) - \bar{\mathbf{z}}(t_i^{M+})$, where

$$\begin{aligned} \mathbf{z}(t_i^{M+}) = \mathbf{z}(\bar{t}_i^+) &= \mathbf{\Lambda}_{p,2}\mathbf{z}(\bar{t}_i^-) + \mathbf{\Lambda}_a(\bar{t}_i) = \\ &= \mathbf{\Lambda}_{p,2}e^{\bar{\mathbf{A}}(\bar{t}_i - t_i)}\mathbf{z}(t_i^+) + \bar{\mathbf{\Lambda}}_a(\bar{t}_i) + \tilde{\mathbf{\Lambda}}_a(\bar{t}_i) = \\ &= \mathbf{\Lambda}_{p,2}e^{-\bar{\mathbf{A}}\Delta t_i}\mathbf{\Lambda}_{p,1}(\theta_i)\mathbf{z}(t_i^-) + \bar{\mathbf{\Lambda}}_a(\bar{t}_i) + \tilde{\mathbf{\Lambda}}_a(\bar{t}_i) = \\ &= \mathbf{\Lambda}_{p,2}e^{-\bar{\mathbf{A}}\Delta t_i}\mathbf{\Lambda}_{p,1}(\bar{\theta}_i + \Delta \theta_i)(\tilde{\mathbf{z}}(t_i^-) + \bar{\mathbf{z}}(t_i^-)) + \bar{\mathbf{\Lambda}}_a(\bar{t}_i) + \tilde{\mathbf{\Lambda}}_a(\bar{t}_i) = \\ &= \mathbf{\Lambda}_{p,2}e^{-\bar{\mathbf{A}}\Delta t_i}\mathbf{\Lambda}_{p,1}(\bar{\theta}_i + \Delta \theta_i)\tilde{\mathbf{z}}(t_i^-) + \\ &\quad + \mathbf{\Lambda}_{p,2}e^{-\bar{\mathbf{A}}\Delta t_i}\mathbf{\Lambda}_{p,1}(\bar{\theta}_i + \Delta \theta_i)e^{\bar{\mathbf{A}}\Delta t_i}\bar{\mathbf{z}}(\bar{t}_i^-) + \bar{\mathbf{\Lambda}}_a(\bar{t}_i) + \tilde{\mathbf{\Lambda}}_a(\bar{t}_i), \\ \bar{\mathbf{z}}(t_i^{M+}) = \bar{\mathbf{z}}(\bar{t}_i^+) &= \mathbf{\Lambda}_p(\bar{\theta}_i)\bar{\mathbf{z}}(\bar{t}_i^-) + \bar{\mathbf{\Lambda}}_a(\bar{t}_i). \end{aligned}$$

Hence, it follows that

$$\begin{aligned} \tilde{\mathbf{z}}(t_i^{M+}) &= \mathbf{\Lambda}_{p,2}e^{-\bar{\mathbf{A}}\Delta t_i}\mathbf{\Lambda}_{p,1}(\bar{\theta}_i + \Delta \theta_i)\tilde{\mathbf{z}}(t_i^{m-}) + \\ &\quad + (\mathbf{\Lambda}_{p,2}e^{-\bar{\mathbf{A}}\Delta t_i}\mathbf{\Lambda}_{p,1}(\bar{\theta}_i + \Delta \theta_i)e^{\bar{\mathbf{A}}\Delta t_i} - \mathbf{\Lambda}_p(\bar{\theta}_i))\bar{\mathbf{z}}(\bar{t}_i^-) + \\ &\quad + \tilde{\mathbf{\Lambda}}_a(\bar{t}_i), \end{aligned}$$

where $\Delta \theta_i := \theta_i - \bar{\theta}_i$;

Case b) $t_i^m = \bar{t}_i$, $t_i^M = t_i$, so that $\Delta t_i := t_i - \bar{t}_i > 0$, and the error at time t_i^{M+}, that is after the i-th couple of impacts, is given by $\tilde{\mathbf{z}}(t_i^{M+}) :=$

$\mathbf{z}(t_i^{M+}) - \bar{\mathbf{z}}(t_i^{M+})$, where

$$
\begin{aligned}
\mathbf{z}(t_i^{M+}) &= \mathbf{z}(t_i^+) = \mathbf{\Lambda}_{p,1}(\theta_i)\mathbf{z}(t_i^-) = \mathbf{\Lambda}_{p,1}(\bar{\theta}_i + \Delta\theta_i)e^{\mathbf{A}(t_i - \bar{t}_i)}\mathbf{z}(\bar{t}_i^+) = \\
&= \mathbf{\Lambda}_{p,1}(\bar{\theta}_i + \Delta\theta_i)e^{\bar{\mathbf{A}}\Delta t_i}(\mathbf{\Lambda}_{p,2}\mathbf{z}(\bar{t}_i^-) + \mathbf{\Lambda}_a(\bar{t}_i)) = \\
&= \mathbf{\Lambda}_{p,1}(\bar{\theta}_i + \Delta\theta_i)e^{\bar{\mathbf{A}}\Delta t_i}\mathbf{\Lambda}_{p,2}\tilde{\mathbf{z}}(t_i^{m-}) + \mathbf{\Lambda}_{p,1}(\bar{\theta}_i + \Delta\theta_i)e^{\bar{\mathbf{A}}\Delta t_i}\mathbf{\Lambda}_{p,2}\bar{\mathbf{z}}(\bar{t}_i^-) + \\
&\quad + \mathbf{\Lambda}_{p,1}(\bar{\theta}_i + \Delta\theta_i)e^{\bar{\mathbf{A}}\Delta t_i}\bar{\mathbf{\Lambda}}_a(\bar{t}_i) + \mathbf{\Lambda}_{p,1}(\bar{\theta}_i + \Delta\theta_i)e^{\bar{\mathbf{A}}\Delta t_i}\tilde{\mathbf{\Lambda}}_a(\bar{t}_i), \\
\bar{\mathbf{z}}(t_i^{M+}) &= \bar{\mathbf{z}}(t_i^+) = e^{\bar{\mathbf{A}}(t_i - \bar{t}_i)}\bar{\mathbf{z}}(\bar{t}_i^+) = e^{\bar{\mathbf{A}}\Delta t_i}(\mathbf{\Lambda}_p(\bar{\theta}_i)\bar{\mathbf{z}}(\bar{t}_i^-) + \bar{\mathbf{\Lambda}}_a(\bar{t}_i)) = \\
&= e^{\bar{\mathbf{A}}\Delta t_i}\mathbf{\Lambda}_p(\bar{\theta}_i)\bar{\mathbf{z}}(\bar{t}_i^-) + e^{\bar{\mathbf{A}}\Delta t_i}\bar{\mathbf{\Lambda}}_a(\bar{t}_i).
\end{aligned}
$$

Hence, it follows that

$$
\begin{aligned}
\tilde{\mathbf{z}}(t_i^{M+}) &= \mathbf{\Lambda}_{p,1}(\bar{\theta}_i + \Delta\theta_i)e^{\bar{\mathbf{A}}\Delta t_i}\mathbf{\Lambda}_{p,2}\tilde{\mathbf{z}}(t_i^{m-}) + \\
&\quad + (\mathbf{\Lambda}_{p,1}(\bar{\theta}_i + \Delta\theta_i)e^{\bar{\mathbf{A}}\Delta t_i}\mathbf{\Lambda}_{p,2} - e^{\bar{\mathbf{A}}\Delta t_i}\mathbf{\Lambda}_p(\bar{\theta}_i))\bar{\mathbf{z}}(\bar{t}_i^-) + \\
&\quad + (\mathbf{\Lambda}_{p,1}(\bar{\theta}_i + \Delta\theta_i)e^{\bar{\mathbf{A}}\Delta t_i} - e^{\bar{\mathbf{A}}\Delta t_i})\bar{\mathbf{\Lambda}}_a(\bar{t}_i) + \\
&\quad + \mathbf{\Lambda}_{p,1}(\bar{\theta}_i + \Delta\theta_i)e^{\bar{\mathbf{A}}\Delta t_i}\tilde{\mathbf{\Lambda}}_a(\bar{t}_i),
\end{aligned}
$$

where $\Delta\theta_i := \theta_i - \bar{\theta}_i$.

By using the following facts

$$
\begin{aligned}
\mathbf{\Lambda}_{p,2}\mathbf{\Lambda}_{p,1}(\bar{\theta}_i) &= \mathbf{\Lambda}_{p,1}(\bar{\theta}_i)\mathbf{\Lambda}_{p,2} = \mathbf{\Lambda}_p(\bar{\theta}_i), \\
\mathbf{\Lambda}_{p,1}(\bar{\theta}_i)\bar{\mathbf{\Lambda}}_a(\bar{t}_i) &= \bar{\mathbf{\Lambda}}_a(\bar{t}_i),
\end{aligned}
$$

it is easy to see that, for any $i \in \mathcal{I}_N$, in both cases **a)** and **b)**, that is for $\Delta t_i < 0$ and $\Delta t_i > 0$, respectively, the functions $\tilde{\mathbf{z}}(t_i^{M+})$ are equal to $\mathbf{0}$ when $\Delta t_i = 0, \Delta\theta_i = 0, \tilde{\mathbf{\Lambda}}_a(\bar{t}_i) = \mathbf{0}$ and $\tilde{\mathbf{z}}(t_i^{m-}) = 0$ and they are analytic functions with respect to their variables. In view of this fact, for each case separately the following results hold

Case a)

$$\exists \delta_1, M_{2,a,i}, M_{3,a,i}, M_{4,a,i} \in \mathbb{R}^+ :$$

$$\|\tilde{\mathbf{z}}(t_i^{m-})\| < \delta_1, -\delta_1 < \Delta t_i < 0, |\Delta\theta_i| < \delta_i, \|\tilde{\mathbf{\Lambda}}_a(\bar{t}_i)\| < \delta_i \Rightarrow$$

$$\Rightarrow \|\tilde{\mathbf{z}}(t_i^{M+})\| \le M_{2,a,i}\|\tilde{\mathbf{z}}(t_i^{m-})\| + M_{3,a,i} \left\| \begin{bmatrix} \Delta t_i \\ \Delta\theta_i \end{bmatrix} \right\| + M_{4,a,i}\|\tilde{\mathbf{\Lambda}}_a(\bar{t}_i)\|;$$

Case b)

$$\exists \delta_1, M_{2,b,i}, M_{3,b,i}, M_{4,b,i} \in \mathbb{R}^+ :$$

$$\|\tilde{\mathbf{z}}(t_i^{m-})\| < \delta_1, 0 < \Delta t_i < \delta_i, |\Delta\theta_i| < \delta_i, \|\tilde{\mathbf{\Lambda}}_a(\bar{t}_i)\| < \delta_i \Rightarrow$$

$$\Rightarrow \|\tilde{\mathbf{z}}(t_i^{M+})\| \le M_{2,b,i}\|\tilde{\mathbf{z}}(t_i^{m-})\| + M_{3,b,i} \left\| \begin{bmatrix} \Delta t_i \\ \Delta\theta_i \end{bmatrix} \right\| + M_{4,b,i}\|\tilde{\mathbf{\Lambda}}_a(\bar{t}_i)\|.$$

Moreover, it is easy to see that, for all $i \in \mathcal{I}_N$, the functions $\tilde{\mathbf{z}}(t_i^{M+})$ are continuous on the hyperplane characterized by $\Delta t_i = 0$. In particular, in both cases **a)** and **b)**, one has

$$\tilde{\mathbf{z}}(t_i^{M+})|_{\Delta t_i=0} = (\mathbf{\Lambda}_p(\bar{\theta}_i + \Delta\theta_i) - \mathbf{\Lambda}_p(\bar{\theta}_i))\bar{\mathbf{z}}(\bar{t}_i^-) + \mathbf{\Lambda}_p(\bar{\theta}_i + \Delta\theta_i)\tilde{\mathbf{z}}(t_i^{m-}) + \tilde{\mathbf{\Lambda}}_a(\bar{t}_i).$$

Therefore, (6.18) are proved, for all $i \in \mathcal{I}_N$, by choosing $M_2 := \max\limits_{\substack{i \in \mathcal{I}_N \\ j \in \{a,b\}}} \{M_{2,j,i}\}$, $M_3 :=$

$\max\limits_{\substack{i \in \mathcal{I}_N \\ j \in \{a,b\}}} \{M_{3,j,i}\}$ and $M_4 := \max\limits_{\substack{i \in \mathcal{I}_N \\ j \in \{a,b\}}} \{M_{4,j,i}\}$.

Details of the proof of the fact (5.28)

Since all the eigenvalues of $\tilde{\mathbf{A}}$ have real part less than or equal to $-\eta$, with $\eta := \min\{\eta_x, \eta_y\} \in \mathbb{R}^+$ and by the linearity of (5.24c), it follows that in each interval of time without impacts one has

$$\exists L(\eta) \in \mathbb{R}^+ : \|\tilde{\mathbf{z}}(t)\| \le L(\eta)e^{-\eta(t-t_i^M)}\|\tilde{\mathbf{z}}(t_i^{M+})\|, \quad \forall t \in (t_i^M, t_{i+1}^m), i \in \mathbb{Z}^+.$$

Remark 27. In the following, the vector $\tilde{\mathbf{z}}(t)$ plays the role of the error vector $\mathbf{e}(t)$, which has been used in Section 4.2.

Moreover, the following result can be proved

$$\forall \eta \in \mathbb{R}^+, \exists L(\eta) \in \mathbb{R}^+ :$$

$$\|\tilde{\mathbf{z}}(t)\| \leq L(\eta) e^{-\eta(t - t_i^M)} \|\tilde{\mathbf{z}}(t_i^{M+})\|, \ \forall t \in (t_i^M, t_{i+1}^m), i \in \mathbb{Z}^+, \tag{5.28}$$

$$\text{with} \ \lim_{\eta \to +\infty} L(\eta) e^{-\eta T} = 0, \ \text{for any } T > 0.$$

In order to prove (5.28), the following change of coordinates can be carried out

$$\tilde{\mathbf{x}}_{e,H}(t) := \underbrace{\begin{bmatrix} \mathbf{0} & -\mathbf{I}_{q+1} \\ \mathbf{I}_2 & \mathbf{0} \end{bmatrix}}_{=:\mathbf{H}} \tilde{\mathbf{x}}_e(t) \quad \Rightarrow \quad \tilde{\mathbf{x}}_e(t) = \underbrace{\begin{bmatrix} \mathbf{0} & \mathbf{I}_2 \\ -\mathbf{I}_{q+1} & \mathbf{0} \end{bmatrix}}_{=\mathbf{H}^{-1}} \tilde{\mathbf{x}}_{e,H}(t),$$

so that

$$\dot{\tilde{\mathbf{x}}}_{e,H}(t) = \mathbf{H}\mathbf{A}_e^x \mathbf{H}^{-1} \tilde{\mathbf{x}}_{e,H}(t) =: \mathbf{A}_{e,H}^x \tilde{\mathbf{x}}_{e,H}(t),$$

where $\|\mathbf{H}\| = \|\mathbf{H}^{-1}\| = 1$ and the matrix $\mathbf{A}_{e,H}^x$ is in companion form with the same eigenvalues of $\mathbf{A}_e^x$. From now on, (5.28) can be proved as it is shown in Section 6.5.

Remark 28. If uncertainties are present on the system parameters, then the eigenvalues of the actual matrix $\tilde{\mathbf{A}}$ are in general different from the desired one assigned by the choice of $\mathbf{K}_x$ and $\mathbf{K}_y$ (see (5.23)). In this case, it is sufficient to require that the eigenvalues of the closed-loop dynamic matrix $\tilde{\mathbf{A}}$ still have real part less than or equal to $-\eta$ even if $M \neq M_0$ and $D \neq D_0$.

Details of the proof of the fact (6.21)

By the definition of $\mathbf{\Lambda}_a$, the periodicity of $\bar{\mathbf{\Lambda}}_a$ (see (5.15)) and by using the update rule given in (5.17a), the following result can be obtained

$$\tilde{\mathbf{\Lambda}}_a(\bar{t}_{i+N}) = \mathbf{\Lambda}_a(\bar{t}_{i+N}) - \bar{\mathbf{\Lambda}}_a(\bar{t}_{i+N}) =$$
$$= e^{-\mathbf{A}_a}\mathbf{x}_a(\bar{t}_{i+1}^-) - e^{-\mathbf{A}_a}\bar{\mathbf{x}}_a(\bar{t}_{i+1}^-) = e^{-\mathbf{A}_a}\tilde{\mathbf{x}}_a(\bar{t}_{i+1}^-),$$

which implies

$$\|\tilde{\mathbf{\Lambda}}_a(\bar{t}_{i+N})\| \leq M_a\|\tilde{\mathbf{x}}_a(\bar{t}_{i+1}^-)\|, \tag{5.47}$$

where $M_a := \|e^{-\mathbf{A}_a}\| \in \mathbb{R}^+$. For all $i \in \mathcal{I}_N$, one has to prove that

$$\exists M_5 \in \mathbb{R}^+ : \|\tilde{\mathbf{\Lambda}}_a(\bar{t}_{i+N})\| \leq M_5\|\tilde{\mathbf{z}}(t_{i+1}^{m-})\|. \tag{6.21}$$

The two possible cases are considered separately.

Case a) $t_{i+1}^m = t_{i+1}$ and $t_{i+1}^M = \bar{t}_{i+1}$. From (6.46), one has

$$\|\tilde{\mathbf{\Lambda}}_a(\bar{t}_{i+N})\| = M_a\|\mathbf{x}_a(\bar{t}_{i+1}^-) - \bar{\mathbf{x}}_a(\bar{t}_{i+1}^-)\| = M_a\|e^{\mathbf{A}_a(t_{i+1}^M - t_{i+1}^m)}\tilde{\mathbf{x}}_a(t_{i+1}^+)\| \leq$$
$$\leq M_a M_{a,1}\|\tilde{\mathbf{x}}_a(t_{i+1}^-)\| \leq M_a M_{a,1}\|\tilde{\mathbf{z}}(t_{i+1}^-)\| =: M_{5,1}\|\tilde{\mathbf{z}}(t_{i+1}^{m-})\|,$$

where $M_{a,1} := \max\limits_{T \in (0,\gamma)} \|e^{\mathbf{A}_a T}\|$.

Case b) $t_{i+1}^m = \bar{t}_{i+1}$ and $t_{i+1}^M = t_{i+1}$. From (6.46), one has

$$\|\tilde{\mathbf{\Lambda}}_a(\bar{t}_{i+N})\| \leq M_a\|\tilde{\mathbf{x}}_a(\bar{t}_{i+1}^-)\| \leq M_a\|\tilde{\mathbf{z}}(t_{i+1}^{m-})\|.$$

Therefore, (6.21) follows just by choosing $M_5 := \max\{M_{5,1}, M_a\}$.

Chapter 6

Trajectory tracking in switched systems

In the previous chapters, the elliptical billiard system has been used as a benchmark for studying and developing a nonsmooth version of the internal model principle to asymptotically track some reference trajectories. This chapter attempts to generalize such results for a class of switched systems with linear dynamics during the unconstrained motion, linear reset maps at the switching times and with possible nonuniform state space among the different modes of the system.

6.1 The class of considered systems

In most cases, the uniformity of continuous state space (i.e., continuous state space is unique and limited to n-dimensional real-valued space) is assumed. Branicky proposed the model of general hybrid dynamical systems [12] as a unified framework which captures various aspects within hybrid dynamics. It was mentioned in his work that failure situations can be modeled as hybrid dynamics by relaxing the common assumption about the dimension of continuous state space. Provided that the re-initialization of continuous states is

properly defined, the relaxation is quite natural because each continuous dynamics can be defined separately from others [81]. In [81], well-posedness for a class of bimodal modular hybrid dynamical systems is studied. The notion of modularity (i.e., the system dynamics change according to each alteration of structure (state space) in the form of component/module attachment or detachment) enables to model several interesting phenomena, e.g., component breakdown and hot-swap of modules, which are forbidden in the conventional framework of system theory. In [12], it is remarked that the state space may change in modeling component failures or changes in dynamical description based on autonomous or controlled events which change it. Examples include the collision of two inelastic particles, an aircraft mode transition that changes variables to be controlled [57], the problem to take into account overlapping local coordinate systems on a manifold [4] and so on. In [83], switched dynamical systems with state-space dilation and contraction formed by concatenating the states of a set of local dynamical systems or semi-flows on state spaces with different dimensions at specified time-instants are considered. Such systems arise naturally in many aerospace applications such as multi-body dynamic systems involving changes in the degrees of freedom, and systems composed of multiple spacecraft with docking and undocking capabilities flying in formation. Other examples of hybrid systems with possibly non-uniform state space representations are considered in [26]–[34], where Bond-Graphs are used in order to model physical hybrid systems.

In this work, switched systems characterized by

- (possible) non-uniform continuous state space among system modes;

- state-dependent switching;

- autonomous switching,

are considered. In the following, in order to characterize such dynamical systems, the switching surfaces, the continuous-time subsystems and the reset maps are formally defined (see Section 2.2.1).

Index set: the (finite) *index set* is defined as follows:

$$\mathcal{P} := \{1, \ldots, M\}. \tag{6.1}$$

Switching surfaces: the switching surface $\mathcal{C}_{ij}$ characterizes the *boundary* between the operating region relevant to the mode j and the one associated to the mode i when the system is *switching* from mode j to mode i. It is defined as follows:

$$\mathcal{C}_{ij} := \{\mathbf{x} \in \mathbb{R}^{n_j} : \mathbf{J}_{ij}\mathbf{x} = b_{ij}, \}, \quad i, j \in \mathcal{P}, \tag{6.2}$$

where $\mathbf{J}_{ij}^T \in \mathbb{R}^{n_j}$, $b_{ij} \in \mathbb{R}$ and $n_j \in \mathbb{N}$, so that the j-th operating region can be expressed as

$$\mathcal{X}_j := \left\{ \mathbf{x} \in \mathbb{R}^{n_j} : \bigcap_{i \in \mathcal{P}} \left(\mathbf{J}_{ij}\mathbf{x} - b_{ij} \leq 0 \right) \right\} \subseteq \mathbb{R}^{n_j}. \tag{6.3}$$

Remark 29. In (6.2) and (6.3), it is assumed that $\mathbf{J}_{ij} = \mathbf{0}$ and $b_{ij} = 1$ for all $i \in \mathcal{P}$ such that the transition from mode j to mode i is not defined.

Remark 30. Notation so far introduced permits to model a wide class of switched systems. In the following, two particular cases are taken into account.

Transition from a mode to itself: in order to model the transition from one mode to itself it is sufficient to consider equal indices, i.e., $i = j$, in (6.2), (6.3) and (6.6). This situation is shown in Fig. 6.1.
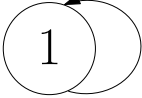
$$\mathbf{J}_{11}\mathbf{x}_1 - b_{11} = 0$$

Figure 6.1: Example in which the arrival mode coincides with the departure mode.

More than one switching surfaces between two modes: in Fig. 6.2(a), it is

shown an example of a system with two different modes. The transition from mode 1 to mode 2 is characterized by the switching surface with $(\mathbf{J}_{21}, b_{21})$, whereas the transition from 2 to 1 can occur across two different switching surfaces with $(\mathbf{J}_{12}^a, b_{12}^a)$ and $(\mathbf{J}_{12}^b, b_{12}^b)$, respectively. In order to model this case by using the notation introduced before, the following *trick* can be considered (see Fig. 6.2(b)). In fact, if the mode 1 is replicated so as to obtain the mode $1'$, then parameters $(\mathbf{J}_{12}^a, b_{12}^a)$ and $(\mathbf{J}_{12}^b, b_{12}^b)$ can be replaced by $(\mathbf{J}_{12}, b_{12})$ and $(\mathbf{J}_{1'2}, b_{1'2})$, respectively, where $\mathbf{J}_{12} = \mathbf{J}_{12}^a$, $\mathbf{J}_{1'2} = \mathbf{J}_{12}^b$ and $b_{12} = b_{12}^a$, $b_{1'2} = b_{12}^b$. Finally, a further switching surface $(\mathbf{J}_{21'}, b_{21'})$ with $\mathbf{J}_{21'} = \mathbf{J}_{21}$ and $b_{21'} = b_{21}$ has to be added.

(a) Original system with 2 modes.

(b) Transformed system with 3 modes.
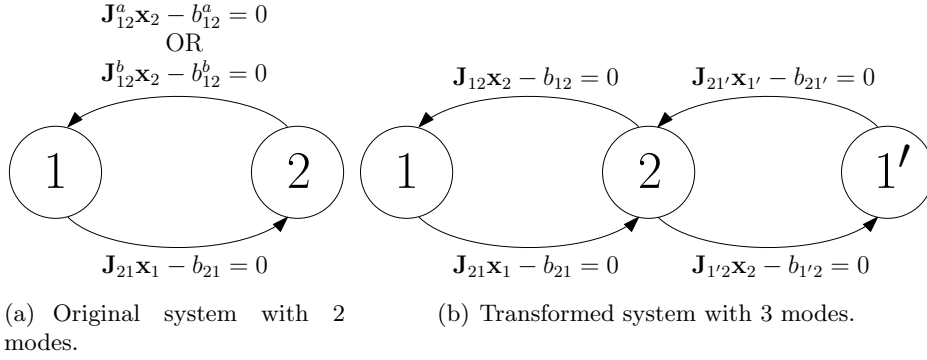
Figure 6.2: Example of a system with more than one switching surface between two modes.

System modes: for each operating region (or *mode*), continuous-time, linear, time-invariant dynamical subsystems are considered. In particular, in the generic i-th mode, the system evolves according to the following dynamics

$$\mathrm{P}_i : \begin{cases} \dot{\mathbf{x}}_i(t) = \mathbf{A}_i(\boldsymbol{\beta})\mathbf{x}_i(t) + \mathbf{B}_i(\boldsymbol{\beta})\mathbf{u}(t) \\ \mathbf{y}(t) = \mathbf{C}_i(\boldsymbol{\beta})\mathbf{x}_i(t) + \mathbf{D}_i(\boldsymbol{\beta})\mathbf{u}(t) \end{cases} , \quad i \in \mathcal{P}, \tag{6.4}$$

where $\mathbf{A}_i(\boldsymbol{\beta}) \in \mathbb{R}^{n_i \times n_i}, \mathbf{B}_i(\boldsymbol{\beta}) \in \mathbb{R}^{n_i \times q}, \mathbf{C}_i(\boldsymbol{\beta}) \in \mathbb{R}^{q \times n_i}$ and $\mathbf{D}_i(\boldsymbol{\beta}) \in \mathbb{R}^{q \times q}$ are matrices with real entries depending on a vector $\boldsymbol{\beta} \in \boldsymbol{\Theta}$ of parameters which are subject to variations and/or uncertainties and play the role of the

physical parameters of the plant. The nominal value $\bar{\boldsymbol{\beta}}$ of $\boldsymbol{\beta}$ is assumed to be an interior point of the bounded set $\boldsymbol{\Theta}$. Note that, for the sake of simplicity each subsystem P_i is assumed to be square, i.e., having the same number of inputs and outputs. However, all the results obtained in this work can be easily extended to the case in which such an assumption is removed.

In this chapter, the following technical assumptions are considered.

Assumption 2. There exists a closed neighborhood $\boldsymbol{\Phi}_a \subseteq \boldsymbol{\Theta}$ of $\bar{\boldsymbol{\beta}} \in \boldsymbol{\Theta}$ such that all the entries of $\mathbf{A}_i(\boldsymbol{\beta}), \mathbf{B}_i(\boldsymbol{\beta}), \mathbf{C}_i(\boldsymbol{\beta})$ and $\mathbf{D}_i(\boldsymbol{\beta})$ are continuous functions of $\boldsymbol{\beta}$ in $\boldsymbol{\Phi}_a$, for all $i \in \mathcal{P}$.

Proposition 1 ([37])**.** *If there exists a neighborhood* $\bar{\bar{\boldsymbol{\Phi}}}_a \subseteq \boldsymbol{\Theta}$ *of some* $\bar{\bar{\boldsymbol{\beta}}} \in \boldsymbol{\Theta}$ *such that all the entries of* $\mathbf{A}_i(\boldsymbol{\beta}), \mathbf{B}_i(\boldsymbol{\beta}), \mathbf{C}_i(\boldsymbol{\beta})$ *and* $\mathbf{D}_i(\boldsymbol{\beta})$ *are continuous functions of* $\boldsymbol{\beta}$ *in* $\bar{\bar{\boldsymbol{\Phi}}}_a$*, then there exists an interior point* $\bar{\boldsymbol{\beta}}$ *of* $\bar{\bar{\boldsymbol{\Phi}}}_a$*, such that Assumption 2 holds, for all* $i \in \mathcal{P}$*.*

Hence, Assumption 2 also can be satisfied by a proper choice of some $\bar{\boldsymbol{\beta}}$ near the initial choice $\bar{\bar{\boldsymbol{\beta}}}$ of it, provided that the matrices involved are continuous in some neighborhood $\bar{\bar{\boldsymbol{\Phi}}}_a$ of $\bar{\bar{\boldsymbol{\beta}}}$.

Assumption 3. There exists a neighborhood $\boldsymbol{\Phi}_b \subseteq \boldsymbol{\Theta}$ of $\bar{\boldsymbol{\beta}}$, such that for all $\boldsymbol{\beta} \in \boldsymbol{\Phi}_b$ the triples $(\mathbf{A}_i(\boldsymbol{\beta}), \mathbf{B}_i(\boldsymbol{\beta}), \mathbf{C}_i(\boldsymbol{\beta}))$ are reachable and observable, for all $i \in \mathcal{P}$.

Remark 31. In view of Assumption 2, there exists a neighborhood $\boldsymbol{\Phi}_{ab} \subseteq (\boldsymbol{\Phi}_a \cap \boldsymbol{\Phi}_b) \subseteq \boldsymbol{\Theta}$ of $\bar{\boldsymbol{\beta}}$ such that if Assumptions 3 is satisfied for $\boldsymbol{\beta} = \bar{\boldsymbol{\beta}}$, then it is automatically satisfied for all $\boldsymbol{\beta} \in \boldsymbol{\Phi}_{ab}$.

Switching events and reset maps: concerning the transition between modes, a time t_k is a *switching time*, if

$$\mathbf{J}_{\sigma(t_k^+)\sigma(t_k^-)}\mathbf{x}_{\sigma(t_k^-)}(t_k^-) - b_{\sigma(t_k^+)\sigma(t_k^-)} = 0, \tag{6.5a}$$

$$\mathbf{J}_{\sigma(t_k^+)\sigma(t_k^-)}\dot{\mathbf{x}}_{\sigma(t_k^-)}(t_k^-) > 0, \tag{6.5b}$$

where the piecewise constant function $\sigma : \mathbb{R} \to \mathcal{P}$ is the *switching signal*, which is defined by Definition 3 in Chapter 2.

Remark 32. The manifold of $\mathcal{X}_j$ identified by (6.5a) represents the condition of *contact* among the dynamical system with the constraint surface $\mathcal{C}_{ij}$. On the other hand, (6.5b) represents the *transversality* condition which guarantees that, at the intersection, the flow of (6.4) is not tangent to the constraint (6.2) [84].

At switching time t_k, the transition from the *departure mode* d_k to the *arrival mode* a_k is given by $\sigma(t_k^-) = d_k$ and $\sigma(t_k^+) = \sigma(t_k) = a_k$, where $d_k, a_k \in \mathcal{P}$. As for the jump in the plant state vector, the following (linear) reset map is considered

$$\mathbf{x}_{\sigma(t_k^+)}(t_k^+) = \boldsymbol{\Gamma}_{\sigma(t_k^+)\sigma(t_k^-)}\mathbf{x}_{\sigma(t_k^-)}(t_k^-), \tag{6.6}$$

where, letting j and i be the indexes relevant to the departure and the arrival modes, respectively, then $\boldsymbol{\Gamma}_{ij} \in \mathbb{R}^{n_i \times n_j}$.

6.2   The class of admissible reference trajectories

The reference trajectories considered in this chapter for the class of hybrid systems defined above are assumed to be periodic with period $T \in \mathbb{R}^+$ and $N \in \mathbb{Z}^+$ switching events per period. In summary, in a whole period the nominal trajectory can be represented as follows (the *bar*-notation denotes the nominal values):

$$\bar{\mathbf{y}}(t) = \begin{cases} \bar{\mathbf{y}}_1(t), & t \in [\bar{t}_1, \bar{t}_2), \\ \quad\vdots \\ \bar{\mathbf{y}}_N(t), & t \in [\bar{t}_N, \bar{t}_{N+1}), \end{cases} \tag{6.7}$$

where $\bar{t}_k$, $k \in \mathbb{Z}^+$ denotes the k-th desired switching time and, in view of the periodicity one has that: $\bar{\mathbf{y}}_{(k \bmod N)}(t+T) = \bar{\mathbf{y}}_k(t)$ and $\bar{t}_{k+N} = \bar{t}_k + T$. For each

$i \in \{1, \ldots, N\} =: \mathcal{I}_N$, the reference signal $\bar{\mathbf{y}}_i(t)$ is assumed to be generated by an autonomous linear system (*exosystem*)

$$
\begin{cases}
\dot{\mathbf{x}}_i^r(t) = \mathbf{A}_i^r \mathbf{x}_i^r(t) \\
\bar{\mathbf{y}}_i(t) = \mathbf{C}_i^r \mathbf{x}_i^r(t)
\end{cases}, \quad \forall t \in [\bar{t}_k, \bar{t}_{k+1}),
$$

with some initial state $\mathbf{x}_i^r(\bar{t}_k^+)$ and $k \in \mathcal{I}_N$. Now, let $\bar{\phi}_i(s)$ be the minimal polynomial of $\mathbf{A}_i^r$, and let

$$
\bar{\phi}(s) = s^m + \alpha_1 s^{m-1} + \cdots + \alpha_m, \tag{6.8}
$$

be the least common multiple of the closed right-half s plane roots of $\bar{\phi}_i(s)$ for all $i \in \mathcal{I}_N$ (thus all roots of $\bar{\phi}(s)$ have nonnegative real parts), the following assumption is made.

Assumption 4. There exists a neighborhood $\boldsymbol{\Phi}_c \subseteq \boldsymbol{\Theta}$ of $\boldsymbol{\beta} \in \boldsymbol{\Theta}$ such that for every root λ of $\bar{\phi}(s)$

$$
rank \left(\begin{bmatrix} \lambda \mathbf{I} - \mathbf{A}_i(\boldsymbol{\beta}) & \mathbf{B}_i(\boldsymbol{\beta}) \\ -\mathbf{C}_i(\boldsymbol{\beta}) & \mathbf{D}_i(\boldsymbol{\beta}) \end{bmatrix} \right) = n_i + q, \tag{6.9}
$$

for all $i \in \mathcal{P}$.

Remark 33. As seen in Remark 31, there exists a neighborhood $\boldsymbol{\Phi}_{ac} \subseteq (\boldsymbol{\Phi}_a \cap \boldsymbol{\Phi}_c) \subseteq \boldsymbol{\Theta}$ of $\bar{\boldsymbol{\beta}} \in \boldsymbol{\Theta}$ such that if Assumption 4 is verified for $\boldsymbol{\beta} = \bar{\boldsymbol{\beta}}$, then Assumption 2 implies that it is verified for all $\boldsymbol{\beta} \in \boldsymbol{\Phi}_{ac}$. Therefore, Assumptions 3 and 4 will be satisfied for all $\boldsymbol{\beta} \in \boldsymbol{\Phi}_{abc}$, where $\boldsymbol{\Phi}_{abc} \subseteq (\boldsymbol{\Phi}_a \cap \boldsymbol{\Phi}_b \cap \boldsymbol{\Phi}_c) \subseteq \boldsymbol{\Theta}$.

Finally, by defining the minimum distance between two consecutive desired switching times as (see Fig. 6.5)

$$
\rho := \min_{k \in \mathcal{I}_N} \{ |\bar{t}_k - \bar{t}_{k+1}| \}, \tag{6.10}
$$

the following definition of admissible desired trajectory can be given.

Definition 5. A reference trajectory $\bar{\mathbf{y}}(t)$ in the form (6.7) is said to be *admissible* for a hybrid system characterized by (6.4) and (6.6) if the following properties hold

1. <u>compatibility of the reset values</u>: for all $k \in \mathcal{I}_N$

$$\bar{\mathbf{x}}_{\bar{\sigma}(\bar{t}_k^+)}(\bar{t}_k^+) = \mathbf{\Gamma}_{\bar{\sigma}(\bar{t}_k^+)\bar{\sigma}(\bar{t}_k^-)}\bar{\mathbf{x}}_{\bar{\sigma}(\bar{t}_k^-)}(\bar{t}_k^-);$$

2. <u>no degenerate switching times</u>: for all $k \in \mathcal{I}_N$

$$\mathbf{J}_{\bar{\sigma}(\bar{t}_k^+)\bar{\sigma}(\bar{t}_k^-)}\bar{\mathbf{x}}_{\bar{\sigma}(\bar{t}_k^-)}(\bar{t}_k^-) - b_{\bar{\sigma}(\bar{t}_k^+)\bar{\sigma}(\bar{t}_k^-)} = 0,$$

$$\mathbf{J}_{\bar{\sigma}(\bar{t}_k^+)\bar{\sigma}(\bar{t}_k^-)}\dot{\bar{\mathbf{x}}}_{\bar{\sigma}(\bar{t}_k^-)}(\bar{t}_k^-) > 0;$$

3. <u>no multiple switching events at the same time</u>: for all $k \in \mathcal{I}_N$ there does not exist a pair (i_1, i_2) with $i_1, i_2 \in \mathcal{P}$ and $i_1 \neq i_2$ such that

$$\mathbf{J}_{i_1\bar{\sigma}(\bar{t}_k^-)}\bar{\mathbf{x}}_{\bar{\sigma}(\bar{t}_k^-)}(\bar{t}_k^-) - b_{i_1\bar{\sigma}(\bar{t}_k^-)} = 0,$$

$$\mathbf{J}_{i_2\bar{\sigma}(\bar{t}_k^-)}\bar{\mathbf{x}}_{\bar{\sigma}(\bar{t}_k^-)}(\bar{t}_k^-) - b_{i_2\bar{\sigma}(\bar{t}_k^-)} = 0;$$

4. <u>nonzero dwell-time</u>: there exists a real positive lower bound $\rho^m > 0$ on ρ, i.e.,

$$\rho > \rho^m > 0,$$

where in 1), 2) and 3), $\bar{\sigma}(t)$ and $\bar{\mathbf{x}}_{\bar{\sigma}(t)}(t)$ denote the nominal switching signal and the nominal value of the plant state vector, respectively, when $\mathbf{y}(t) = \bar{\mathbf{y}}(t)$. The existence and uniqueness of $\bar{\mathbf{x}}_{\bar{\sigma}(t)}(t)$ is guaranteed by Assumptions 3, 4, under the hypothesis that the subsystems P_i are square.

Remark 34. In the case of non-square systems, the uniqueness of $\bar{\mathbf{x}}_{\bar{\sigma}(t)}(t)$ is not guaranteed in general. However, by using, for example, squaring-down techniques the approach proposed hereafter can still be used.

Throughout the present chapter, whenever the reference (or nominal, or desired) trajectory is considered, it is implicitly assumed to be admissible according to Definition 5.

In Fig. 6.3 an example of periodic trajectory (with $N = 4$ switching events per period) for a switched system operating in two different modes with subsystems P_1 and P_2 having dimensions $n_1 = 2$ and $n_2 = 3$, respectively, is shown. The switching signal associated to such a trajectory is depicted in Fig. 6.4.
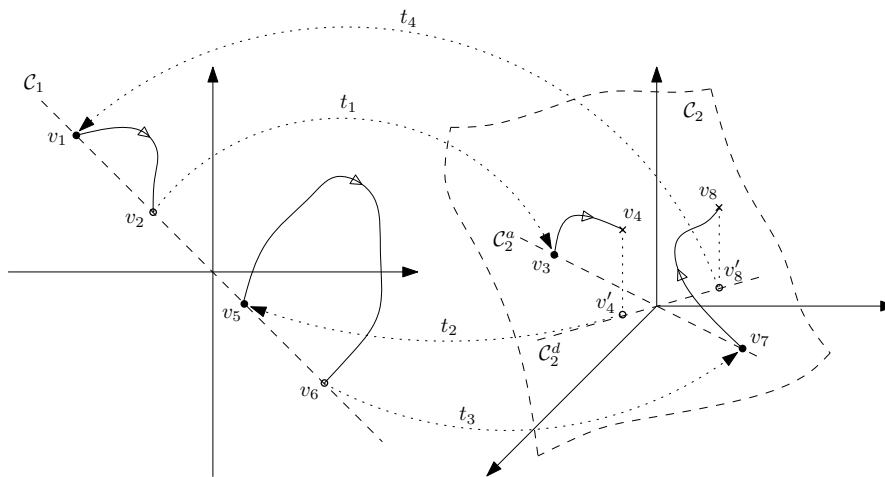
Figure 6.3: Example of (periodic) trajectory for a bi-modal switched system with non-uniform state space.
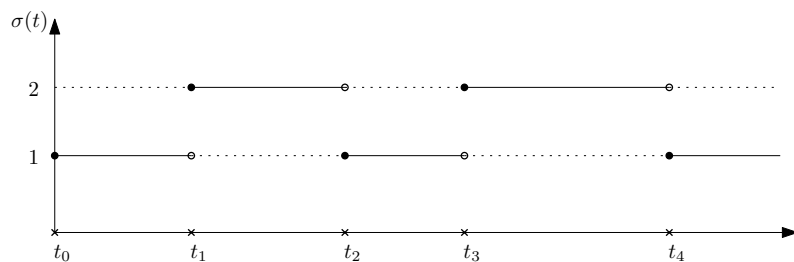
Figure 6.4: The switching signal associated to the trajectory in Fig. 6.3.

6.3   Asymptotic tracking problem: definition and solution

The goal of this section is the design of a control law such that the actual trajectory asymptotically tracks the desired one. More specifically the classical tracking problem (see, e.g., [25]) is taken into account and, in the following, it is properly amended in order to deal with the considered class of hybrid systems. The presence of discontinuities due to the switching events complicates the trajectory tracking problem as compared with the case of unconstrained systems. The problem of trajectory tracking for mechanical systems subject to impacts has been discussed in Chapters 4 and 5. In order to overcome the difficulties relevant to the classical stability and attractivity properties (see Remark 9), the times belonging to infinitesimal intervals about the switching times are neglected in the analysis (see Fig. 6.5), thus ensuring a sort of asymptotic stability for the error dynamics, similarly to what is proposed in [50] for impulsive differential systems. By following the approach introduced
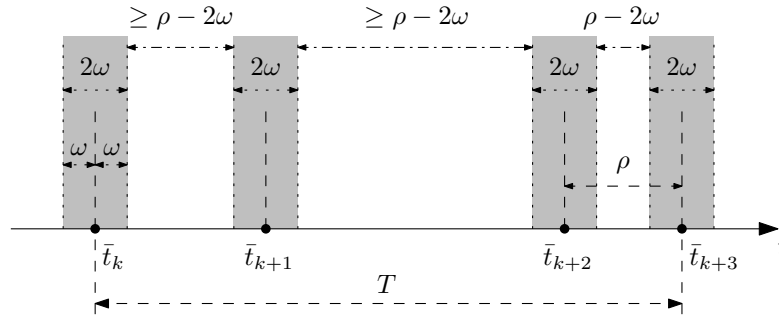
Figure 6.5: Example of possible switching times for a trajectory with period T and $N = 3$ switching events per period. Time intervals identified by the grey blocks are neglected in the stability analysis.

in [33] and [32], a controller based on a discontinuous (nonsmooth) version of the classical internal model principle (see, e.g., [25] and [23]) is considered. It is well known that in absence of discontinuities (i.e., during the free-motion phases) a continuous-time internal model of the desired trajectory is needed

in the forward path of the feedback control system. The presence of such an internal model is guaranteed through a dynamic precompensator, whose state vector is subject to discontinuities at the desired switching times. By defining the error vectors relevant to the plant and the precompensator as follows: $\tilde{\mathbf{x}}_{\sigma(t)}(t) := \mathbf{x}_{\sigma(t)}(t) - \bar{\mathbf{x}}_{\sigma(t)}(t)$, $\tilde{\mathbf{x}}_a(t) := \mathbf{x}_a(t) - \bar{\mathbf{x}}_a(t)$, the output error as $\mathbf{e}(t) := \mathbf{y}(t) - \bar{\mathbf{y}}(t)$, and the error at time $\bar{t}_k$ between the correct jump in the precompensator and the estimated one as $\tilde{\mathbf{\Lambda}}_{\bar{t}_k} := \mathbf{\Lambda}_{\bar{t}_k} - \bar{\mathbf{\Lambda}}_{\bar{t}_k}$, the control problem studied here can be stated as follows.

Problem 5. *Find, if any, a piecewise continuous control law such that for all $\varepsilon > 0$, $t_0 \in \mathbb{R}$ and $\omega \in (0, \rho/2)$, there exists $\delta_{\varepsilon,\omega} > 0$ and a neighborhood $\mathbf{\Phi} \subseteq \mathbf{\Theta}$ of $\bar{\boldsymbol{\beta}}$ such that if $\|\tilde{\mathbf{x}}^e_{\sigma(t_0^+)}(t_0^+)\| < \delta_{\varepsilon,\omega}$, $\|\tilde{\mathbf{x}}_a(t_0^+)\| < \delta_{\varepsilon,\omega}$ and $\|\tilde{\mathbf{\Lambda}}_{\bar{t}_1}\| < \delta_{\varepsilon,\omega}, \cdots, \|\tilde{\mathbf{\Lambda}}_{\bar{t}_{N-1}}\| < \delta_{\varepsilon,\omega}$, then the following properties hold for the closed-loop system and for all $\boldsymbol{\beta} \in \mathbf{\Phi}$:*

$$\textbf{1)} \ \ \|\mathbf{e}(t)\| < \varepsilon, \quad \forall t \in \mathbb{R} \setminus \Omega, \ t > t_0,$$

where $\Omega := \bigcup_{k \in \mathbb{Z}} \Omega_k$ and $\Omega_k := \{\, t : \ |t - \bar{t}_k| \leq \omega \,\}$;

$$\textbf{2)} \ \ \lim_{k \to +\infty} \|\mathbf{e}((\bar{t}_k + \tau)^+)\| = 0, \quad \forall \tau \in (0, \rho),$$

where the limit is taken with k being integer.

In the following, all the steps for the design of the control scheme depicted in Fig. 6.6 are detailed.

Step 1 (*Precompensator design (IM)*): the internal model $\bar{\phi}^{-1}(s)\mathbf{I}_q$ of the class of trajectories to be tracked, with $\bar{\phi}(s)$ defined in (6.8), can be realized
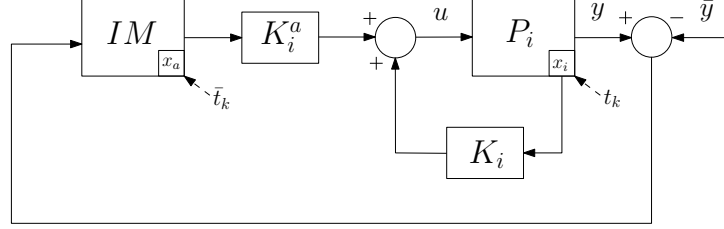
Figure 6.6: Structure of the control scheme based on the internal model principle.

as

$$\begin{cases} \dot{\mathbf{x}}_a(t) = \mathbf{A}_a \mathbf{x}_a(t) + \mathbf{B}_a \mathbf{e}(t) \\ \mathbf{y}_a(t) = \mathbf{x}_a(t) \end{cases} \quad , \quad \forall t \in [\bar{t}_k, \bar{t}_{k+1}),$$

where $\mathbf{A}_a = \mathbf{blockdiag}\{\underbrace{\boldsymbol{\Upsilon}, \cdots, \boldsymbol{\Upsilon}}_{q-\text{tuple}}\} \in \mathbb{R}^{qm \times qm}$ and $\mathbf{B}_a = \mathbf{blockdiag}\{\underbrace{\boldsymbol{v}, \cdots, \boldsymbol{v}}_{q-\text{tuple}}\} \in \mathbb{R}^{qm \times q}$ with

$$\boldsymbol{\Upsilon} := \begin{bmatrix} 0 & 1 & 0 & \cdots & 0 \\ 0 & 0 & 1 & \cdots & 0 \\ \vdots & \vdots & \vdots & & \vdots \\ 0 & 0 & 0 & \cdots & 1 \\ -\alpha_m & -\alpha_{m-1} & -\alpha_{m-2} & \cdots & -\alpha_1 \end{bmatrix}, \; \boldsymbol{v} := \begin{bmatrix} 0 \\ 0 \\ \vdots \\ 0 \\ 1 \end{bmatrix}.$$

Step 2 (*Static gains design* $(\mathbf{K}_i, \mathbf{K}_i^a)$): consider the tandem connection of the plant followed by the precompensator. During the free-motion phases its composite dynamical equation is

$$\underbrace{\begin{bmatrix} \dot{\mathbf{x}}_i \\ \dot{\mathbf{x}}_a \end{bmatrix}}_{\dot{\mathbf{x}}_i^e} = \underbrace{\begin{bmatrix} \mathbf{A}_i(\boldsymbol{\beta}) & \mathbf{0} \\ \mathbf{B}_a \mathbf{C}_i(\boldsymbol{\beta}) & \mathbf{A}_a \end{bmatrix}}_{\mathbf{A}_i^e(\boldsymbol{\beta})} \underbrace{\begin{bmatrix} \mathbf{x}_i \\ \mathbf{x}_a \end{bmatrix}}_{\mathbf{x}_i^e} + \underbrace{\begin{bmatrix} \mathbf{B}_i(\boldsymbol{\beta}) \\ \mathbf{B}_a \mathbf{D}_i(\boldsymbol{\beta}) \end{bmatrix}}_{\mathbf{B}_i^e(\boldsymbol{\beta})} \mathbf{u} =$$

$$= \mathbf{A}_i^e(\boldsymbol{\beta}) \mathbf{x}_i^e + \mathbf{B}_i^e(\boldsymbol{\beta}) \mathbf{u}. \qquad (6.11)$$

This connection is controllable and observable (see, e.g., [23]) if and only if no

root of the polynomial $\bar{\phi}(s)$ is a transmission zero of the plant, or, in other words, (6.11) is controllable if Assumption 4 is satisfied. In particular, if (6.9) is verified for every plant P_i, then the eigenvalues of the closed-loop system can be arbitrarily assigned by the state feedback

$$\mathbf{u}(t) = \underbrace{\left[\begin{array}{cc} \mathbf{K}_i & \mathbf{K}_i^a \end{array}\right]}_{\mathbf{K}_i^e} \left[\begin{array}{c} \mathbf{x}_i(t) \\ \mathbf{x}_a(t) \end{array}\right], \quad \forall t \in [t_k^M, t_{k+1}^m),$$

where $t_k^m := \min\{t_k, \bar{t}_k\}$, $t_k^M := \max\{t_k, \bar{t}_k\}$ and for all $i \in \mathcal{P}$ the gain $\mathbf{K}_i^e \in \mathbb{R}^{q \times (n_i + mq)}$ is chosen such that, for all $\boldsymbol{\beta} \in \boldsymbol{\Phi}_d$ with $\boldsymbol{\Phi}_d \subseteq \boldsymbol{\Theta}$ being a neighborhood of $\bar{\boldsymbol{\beta}}$, all eigenvalues of $(\mathbf{A}_i^e(\boldsymbol{\beta}) + \mathbf{B}_i^e(\boldsymbol{\beta})\mathbf{K}_i^e)$ have real part less than $-\eta$, with $\eta \in \mathbb{R}^+$, i.e.,

$$\mathrm{Re}(\lambda) < -\eta \text{ for all } \lambda \in \Lambda[\mathbf{A}_i^e(\boldsymbol{\beta}) + \mathbf{B}_i^e(\boldsymbol{\beta})\mathbf{K}_i^e], \tag{6.12}$$

with $\mathrm{Re}(\lambda)$ and $\Lambda[\cdot]$ being the real part of λ and the set of the eigenvalues of the matrix at argument, respectively. Note that in view of Assumption 2, if (6.12) is satisfied in the nominal parameters, i.e., for $\boldsymbol{\beta} = \bar{\boldsymbol{\beta}}$, then it is automatically satisfied for all $\boldsymbol{\beta} \in \boldsymbol{\Phi}$, with $\boldsymbol{\Phi} \subseteq (\boldsymbol{\Phi}_d \cap \boldsymbol{\Phi}_{abc}) \subseteq \boldsymbol{\Theta}$ and $\boldsymbol{\Phi}_{abc}$ defined in Remark 31.

Step 3 (*Precompensator reset values* $(\boldsymbol{\Lambda}_{\bar{t}_k})$): at the desired switching time $\bar{t}_k$ the state vector $\mathbf{x}_a$ is reset as follows: $\mathbf{x}_a(\bar{t}_k^+) = \boldsymbol{\Lambda}_{\bar{t}_k}$, where $\boldsymbol{\Lambda}_{\bar{t}_k}$ denotes the reset value for the precompensator state vector at time $\bar{t}_k$.

No uncertainties on the plant parameters: if there are no uncertainties on the plant modeling, i.e., $\boldsymbol{\beta} = \bar{\boldsymbol{\beta}}$, then $\boldsymbol{\Lambda}_{\bar{t}_k} = \bar{\boldsymbol{\Lambda}}_{\bar{t}_k}$, with $\bar{\boldsymbol{\Lambda}}_{\bar{t}_k}$ being the nominal reset value for the precompensator state vector at time $\bar{t}_k$. In order to compute such a vector one can proceed as follows. By assuming perfect tracking, one has

$$\begin{cases} t_k = \bar{t}_k, & \forall k, \\ \mathbf{y}(t) = \bar{\mathbf{y}}(t) \Rightarrow \mathbf{e}(t) = \mathbf{0}, & \forall t \geq t_0, \end{cases}$$

so that, by considering the nominal state vector $\bar{\mathbf{x}}_i^e = \begin{bmatrix} \bar{\mathbf{x}}_i^T & \bar{\mathbf{x}}_a^T \end{bmatrix}^T$, the nominal dynamics can be written as

$$\begin{cases} \dot{\bar{\mathbf{x}}}_i^e(t) = \bar{\mathbf{A}}_i^e(\boldsymbol{\beta})\bar{\mathbf{x}}_i^e(t) \\ \bar{\mathbf{y}}_i(t) = \bar{\mathbf{C}}_i^e(\boldsymbol{\beta})\bar{\mathbf{x}}_i^e(t) \end{cases}, \quad \forall t \in [\bar{t}_k, \bar{t}_{k+1}), \tag{6.13}$$

where

$$\bar{\mathbf{A}}_i^e(\boldsymbol{\beta}) = \begin{bmatrix} \mathbf{A}_i(\boldsymbol{\beta}) + \mathbf{B}_i(\boldsymbol{\beta})\mathbf{K}_i & \mathbf{B}_i(\boldsymbol{\beta})\mathbf{K}_i^a \\ \mathbf{0} & \mathbf{A}_a \end{bmatrix},$$

$$\bar{\mathbf{C}}_i^e(\boldsymbol{\beta}) = \begin{bmatrix} \mathbf{C}_i(\boldsymbol{\beta}) + \mathbf{D}_i(\boldsymbol{\beta})\mathbf{K}_i & \mathbf{D}_i(\boldsymbol{\beta})\mathbf{K}_i^a \end{bmatrix},$$

whereas at the switching time $\bar{t}_k$ the *jump* in the augmented state vector is

$$\bar{\mathbf{x}}_i^e(\bar{t}_k^+) = \underbrace{\begin{bmatrix} \boldsymbol{\Gamma}_{ij} & \mathbf{0} \\ \mathbf{0} & \mathbf{0} \end{bmatrix}}_{\bar{\boldsymbol{\Gamma}}_{ij}^e} \bar{\mathbf{x}}_j^e(\bar{t}_k^-) + \underbrace{\begin{bmatrix} \mathbf{0} \\ \bar{\boldsymbol{\Lambda}}_{\bar{t}_k} \end{bmatrix}}_{\bar{\boldsymbol{\Lambda}}_{\bar{t}_k}^e} =$$

$$= \bar{\boldsymbol{\Gamma}}_{ij}^e \bar{\mathbf{x}}_j^e(\bar{t}_k^-) + \bar{\boldsymbol{\Lambda}}_{\bar{t}_k}^e,$$

where $i = \sigma(\bar{t}_k^+) = \sigma(\bar{t}_k) \in \mathcal{P}$ and $j = \sigma(\bar{t}_k^-) \in \mathcal{P}$.

The problem to compute $\bar{\boldsymbol{\Lambda}}_{\bar{t}_k}$ can be turned into an observability problem. In fact, since it is possible to find stabilizing gains $\mathbf{K}_i^e$ for the closed loop system and all the eigenvalues of IM are in the closed right half plane, then it is clear that the state vector $\bar{\mathbf{x}}_a$ has to be observable from the output. Since observability is in general not preserved under constant state feedback, if necessary, one has to carry out a canonical decomposition in order to separate the observable modes from the others (see, e.g., [23]). More precisely, $\bar{\boldsymbol{\Lambda}}_{\bar{t}_k}$ can be obtained as follows:

1. Define $\bar{\mathbf{A}}_i^e(\boldsymbol{\beta})$ and $\bar{\mathbf{C}}_i^e(\boldsymbol{\beta})$ as in (6.13) where $i = \sigma(\bar{t}_k^+)$;

2. Let $\boldsymbol{\beta} = \bar{\boldsymbol{\beta}}$ (for the sake of readability in the following steps dependence on $\boldsymbol{\beta}$ is omitted);

3. If $rank\left(\begin{bmatrix} \bar{\mathbf{C}}_i^e \\ \bar{\mathbf{C}}_i^e \bar{\mathbf{A}}_i^e \\ \vdots \\ \bar{\mathbf{C}}_i^e (\bar{\mathbf{A}}_i^e)^{n_i+mq-1} \end{bmatrix}\right) = n_i + mq$, then $n_o = n_i + mq$,

$\mathbf{T}_i = \mathbf{I}_{n_o}$, $\bar{\mathbf{A}}_i^o = \bar{\mathbf{A}}_i^e$, $\bar{\mathbf{C}}_i^o = \bar{\mathbf{C}}_i^e$ and go to step 5), else go to step 4);

4. Find a nonsingular matrix $\mathbf{T}_i$ such that $\bar{\mathbf{z}}_i^e = \mathbf{T}_i \bar{\mathbf{x}}_i^e$ and

$$\begin{cases} \dot{\bar{\mathbf{z}}}_i^e(t) = \begin{bmatrix} \bar{\mathbf{A}}_i^o & \mathbf{0} \\ \star & \bar{\mathbf{A}}_i^{no} \end{bmatrix} \bar{\mathbf{z}}_i^e(t), \\ \bar{\mathbf{y}}_i(t) = \begin{bmatrix} \bar{\mathbf{C}}_i^o & \mathbf{0} \end{bmatrix} \bar{\mathbf{z}}_i^e(t), \end{cases}$$

with the pair $(\bar{\mathbf{A}}_i^o \in \mathbb{R}^{n_o \times n_o}, \bar{\mathbf{C}}_i^o \in \mathbb{R}^{q \times n_o})$ being observable;

5. Define[1] $\mathbf{Y}(\bar{t}_k^+) = \begin{bmatrix} \bar{\mathbf{y}}(\bar{t}_k^+) \\ \dot{\bar{\mathbf{y}}}(\bar{t}_k^+) \\ \vdots \\ \bar{\mathbf{y}}^{(n_o-1)}(\bar{t}_k^+) \end{bmatrix}$ and $\mathbf{O}_i = \begin{bmatrix} \bar{\mathbf{C}}_i^o \\ \bar{\mathbf{C}}_i^o \bar{\mathbf{A}}_i^o \\ \vdots \\ \bar{\mathbf{C}}_i^o (\bar{\mathbf{A}}_i^o)^{n_o-1} \end{bmatrix}$ so that

$rank(\mathbf{O}_i) = n_o$;

6. Finally, since $\mathbf{Y}(\bar{t}_k^+) = \mathbf{O}_i \bar{\mathbf{z}}_i^e(\bar{t}_k^+)$, it follows that

$$\bar{\mathbf{z}}_i^e(\bar{t}_k^+) = (\mathbf{O}_i^T \mathbf{O}_i)^{-1} \mathbf{O}_i^T \mathbf{Y}(\bar{t}_k^+),$$

which yields

$$\bar{\mathbf{x}}_a(\bar{t}_k^+) = \begin{bmatrix} \mathbf{0}_{qm \times n_i} & \mathbf{I}_{qm} \end{bmatrix} \mathbf{T}_i^{-1} \bar{\mathbf{z}}_i^e(\bar{t}_k^+) = \bar{\mathbf{\Lambda}}_{\bar{t}_k}. \tag{6.14}$$

Uncertainties on the plant parameters: by (6.14), it is clear that $\bar{\mathbf{\Lambda}}_{\bar{t}_k}$ depends on the plant matrices, so that it can be computed only when such

---

[1] In the following, $\bar{\mathbf{y}}^{(l)}(\bar{t}_k^+) := \left(\frac{d^l}{dt^l}(\bar{\mathbf{y}}_j(t)) \right)\Big|_{t=\bar{t}_k^+}$, where $\bar{\mathbf{y}}(t) = \bar{\mathbf{y}}_j(t)$ for all $t \in [\bar{t}_k, \bar{t}_{k+1})$ (see (6.7)).

matrices are exactly known. In order to deal with possible uncertainties on the plant description, i.e., $\boldsymbol{\beta} \neq \bar{\boldsymbol{\beta}}$, the following rule is used

$$\mathbf{x}_a(\bar{t}_k^+) = e^{-\mathbf{A}_a(\bar{t}_{k-N+1}-\bar{t}_{k-N})}\mathbf{x}_a(\bar{t}_{k-N+1}^-) = \boldsymbol{\Lambda}_{\bar{t}_k}.$$

A code-like algorithm implementing such a rule is described below.

- <u>Initialize</u> $\boldsymbol{\Lambda}_N \in \mathbb{R}^{N \times qm}$ as

$$\boldsymbol{\Lambda}_N = \left[\begin{array}{cccc} \bar{\boldsymbol{\Lambda}}_{\bar{t}_0} & \bar{\boldsymbol{\Lambda}}_{\bar{t}_1} & \cdots & \bar{\boldsymbol{\Lambda}}_{\bar{t}_{N-1}} \end{array} \right]^T.$$

- <u>At the switching time</u> $\bar{t}_k$, the reset value of $\mathbf{x}_a$ is

$$\mathbf{x}_a(\bar{t}_k^+) = \boldsymbol{\Lambda}_N^T\big((k \bmod N) + 1, : \big),$$

- and the update rule of $\boldsymbol{\Lambda}_N$ is

$$\boldsymbol{\Lambda}_N^T\big(((k-1) \bmod N) + 1, : \big) = e^{-\mathbf{A}_a(\bar{t}_k - \bar{t}_{k-1})}\mathbf{x}_a(\bar{t}_k^-),$$

where $\boldsymbol{\Lambda}_N\big(i, : \big)$ denotes the i-th row of the matrix $\boldsymbol{\Lambda}_N$.

Main result

Under the assumption of sufficiently small initial errors, for all $k \in \mathbb{Z}^+$, the switching time t_k of the actual trajectory can be forced to be close to the switching time $\bar{t}_k$ of the desired trajectory so that, by following the guidelines of the control strategy proposed in [33] and [32], the precompensator input $\mathbf{u}_a$ and the control input $\mathbf{u}$ can be expressed by the *switching* laws reported

below (see Fig. 6.7)

$$\mathbf{u}_a(t) = \begin{cases} \mathbf{e}(t), & \forall t \in (t_k^M, t_{k+1}^m), \ k \in \mathbb{Z}^+ \\ \mathbf{0}, & \text{otherwise} \end{cases}, \qquad (6.15)$$

$$\mathbf{u}(t) = \begin{cases} \mathbf{K}_i^e \mathbf{x}_i^e(t), & \forall t \in (t_k^M, t_{k+1}^m), \ k \in \mathbb{Z}^+ \\ \mathbf{0}, & \text{otherwise} \end{cases}, \qquad (6.16)$$

where $t_0^M := t_0$, $i = \sigma(t_k^M)$ and, for all $k \in \mathbb{Z}^+$, one defines $t_k^m := \min\{t_k, \bar{t}_k\}$ and $t_k^M := \max\{t_k, \bar{t}_k\}$.
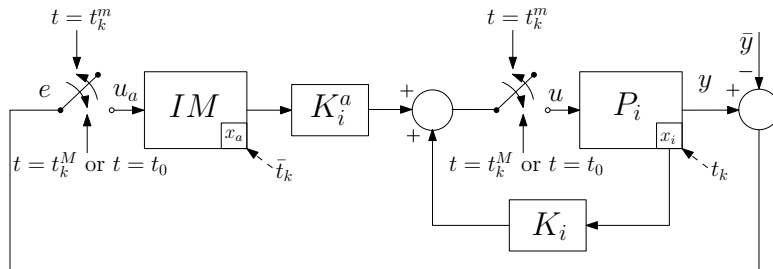
Figure 6.7: Structure of the control scheme based on the internal model principle with switching control laws (6.15) and (6.16).

Remark 35. Through many simulations, it has been observed that the switching control laws given by (6.15) and (6.16) improve the behavior of the controlled system as compared with the case in which the control is never switched off, especially when the initial conditions are not particularly close to the desired ones (see also Remark 13).

At this point, the following result can be stated and proved.

Theorem 11. *Under assumptions (2)–(4), for all $i \in \mathcal{P}$ there exist $\mathbf{K}_i$ and $\mathbf{K}_i^a$ such that the control law depicted in Fig. 6.7 is a solution of Problem 5.*

Proof. The proof can be carried out by means of the steps described below, based on the following facts whose proofs are omitted due to lack of space.

There exist constants M_1, M_2, $M_3 \in \mathbb{R}^+$ and δ_1, $\delta_2 \in \mathbb{R}^+$ and a function

$L(\cdot,\cdot) : \mathbb{R}^+ \times \mathbb{R}^+ \to \mathbb{R}^+$ such that

$$\|\tilde{\mathbf{x}}_j^e(t_k^{m-})\| < \delta_1 \Rightarrow |\Delta t_k| < M_1\|\tilde{\mathbf{x}}_j^e(t_k^{m-})\|, \tag{6.17}$$

$$\|\tilde{\mathbf{x}}_j^e(t_k^{m-})\| < \delta_2, |\Delta t_k| < \delta_2, \|\tilde{\mathbf{\Lambda}}_{\bar{t}_k}\| < \delta_2 \Rightarrow \tag{6.18}$$
$$\Rightarrow \|\tilde{\mathbf{x}}_i^e(t_k^{M+})\| < M_2\|\tilde{\mathbf{x}}_j^e(t_k^{m-})\| + M_2|\Delta t_k| + M_2\|\tilde{\mathbf{\Lambda}}_{\bar{t}_k}\|,$$

$$\|\tilde{\mathbf{x}}_i^e(t)\| < L(\eta, t - t_k^M)e^{-\eta(t-t_k^M)}\|\tilde{\mathbf{x}}_i^e(t_k^{M+})\|, \tag{6.19}$$
$$\forall \varepsilon^* > 0, \zeta > 0, \exists \eta^* > 0 : \eta > \eta^* \Rightarrow \tag{6.20}$$
$$\Rightarrow L(\eta, \zeta)e^{-\eta\zeta} < \varepsilon^*,$$

$$\|\tilde{\mathbf{\Lambda}}_{\bar{t}_{k+N}}\| < M_3\|\tilde{\mathbf{x}}_i^e(t_{k+1}^{m-})\|, \tag{6.21}$$

where $k \in \mathcal{I}_N$, $\Delta t_k := t_k - \bar{t}_k$, $j = \sigma(t_k^{m-})$, $i = \sigma(t_k^{M+}) = \sigma(t_{k+1}^{m-})$ and (6.19) holds for all $t \in (t_k^M, t_{k+1}^m)$.

Remark 36. If no uncertainties are present on the plant description, then the present result still holds just considering $\tilde{\mathbf{\Lambda}}_{\bar{t}_k} = \mathbf{0}$, i.e., $\mathbf{\Lambda}_{\bar{t}_k} = \bar{\mathbf{\Lambda}}_{\bar{t}_k}$ with $\bar{\mathbf{\Lambda}}_{\bar{t}_k}$ given by (6.14), for all $k \in \mathcal{I}_N$.

Step (i): In view of (6.17) and (6.18) and in order to guarantee that the actual switching time t_k belongs to the interval $(\bar{t}_k - \omega, \bar{t}_k + \omega)$ where $\omega \in (0, \rho/2)$ and ρ is defined in (6.10), one can take $\|\tilde{\mathbf{x}}_j^e(t_k^{m-})\| < \bar{\delta}_1$ where $\bar{\delta}_1 := \min\{\delta_1, \delta_2, \delta_1/M_1, \omega/M_1\}$.

Step (ii): By putting together (6.17) and (6.18), the following inequality is obtained

$$\|\tilde{\mathbf{x}}_i^e(t_k^{M+})\| < \mu\|\tilde{\mathbf{x}}_j^e(t_k^{m-})\| + M_2\|\tilde{\mathbf{\Lambda}}_{\bar{t}_k}\|, \tag{6.22}$$

where $\mu := M_2(1 + M_1)$.

Step (iii): By using (6.19) and (6.22), one has

$$\|\tilde{\mathbf{x}}_i^e(t_{k+1}^{m-})\| < L(\eta, \zeta)e^{-\eta\zeta}(\mu\|\tilde{\mathbf{x}}_j^e(t_k^{m-})\| + M_2\|\tilde{\mathbf{\Lambda}}_{\bar{t}_k}\|),$$

with $\zeta := t_{k+1}^m - t_k^M \in \mathbb{R}^+$. At this point, by taking in (6.20) $\varepsilon^* < \min\{\xi/\mu, \xi/M_2\}$, there exists $\eta^* \in \mathbb{R}^+$ such that, for all $\eta > \eta^*$, it follows that (from now on dependence on η and ζ is omitted)

$$\|\tilde{\mathbf{x}}_i^e(t_{k+1}^{m-})\| < \xi\|\tilde{\mathbf{x}}_j^e(t_k^{m-})\| + \xi\|\tilde{\mathbf{\Lambda}}_{\bar{t}_k}\|, \tag{6.23}$$

with $\xi \in \mathbb{R}^+$ being a free parameter.

Step (vi): By using iteratively (6.23) and by the periodicity of the reference trajectory, one obtains

$$\|\tilde{\mathbf{x}}_j^e(t_{k+N}^{m-})\| < \xi^N\|\tilde{\mathbf{x}}_j^e(t_k^{m-})\| + \xi^N\|\tilde{\mathbf{\Lambda}}_{\bar{t}_k}\| + \cdots$$
$$\cdots + \xi^{N-1}\|\tilde{\mathbf{\Lambda}}_{\bar{t}_{k+1}}\| + \xi^2\|\tilde{\mathbf{\Lambda}}_{\bar{t}_{k+N-2}}\| + \xi\|\tilde{\mathbf{\Lambda}}_{\bar{t}_{k+N-1}}\|,$$

Moreover, by (6.21) and (6.23) it follows that

$$\|\tilde{\mathbf{\Lambda}}_{\bar{t}_{k+N}}\| < \xi M_3\|\tilde{\mathbf{x}}_j^e(t_k^{m-})\| + \xi M_3\|\tilde{\mathbf{\Lambda}}_{\bar{t}_k}\|,$$
$$\|\tilde{\mathbf{\Lambda}}_{\bar{t}_{k+N+1}}\| < \xi^2 M_3\|\tilde{\mathbf{x}}_j(t_k^{m-})\| + \xi^2 M_3\|\tilde{\mathbf{\Lambda}}_{\bar{t}_k}\| +$$
$$+ \xi M_3\|\tilde{\mathbf{\Lambda}}_{\bar{t}_{k+1}}\|,$$
$$\vdots$$
$$\|\tilde{\mathbf{\Lambda}}_{\bar{t}_{k+2N-1}})\| < \xi^N M_3\|\tilde{\mathbf{x}}_j^e(t_k^{m-})\| + \xi^N M_3\|\tilde{\mathbf{\Lambda}}_{\bar{t}_k}\| + \cdots$$
$$\cdots + \xi M_3\|\tilde{\mathbf{\Lambda}}_{\bar{t}_{k+N-1}}\|.$$

Now, by defining

$$\mathbf{\Psi}_k := \begin{bmatrix} \tilde{\mathbf{x}}_j^{eT}(t_k^{m-}) & \tilde{\mathbf{\Lambda}}_{\bar{t}_k}^T & \cdots & \tilde{\mathbf{\Lambda}}_{\bar{t}_{k+N-1}}^T \end{bmatrix}^T \in \mathbb{R}^{n_j+(N+1)mq},$$

and by choosing

$$\xi := \min\{\frac{\bar{\xi}}{N+1}, \frac{\bar{\xi}}{M_3(N+1)}\},$$

with

$$0 < \bar{\xi} < \frac{\bar{\bar{\xi}}}{\sqrt{N+1}} \quad \text{and} \quad 0 < \bar{\bar{\xi}} < 1,$$

the following inequalities can be easily proved

$$\|\tilde{\mathbf{x}}_j^e(t_{k+N}^{m-})\| < \bar{\xi}\|\mathbf{\Psi}_k\|,$$

$$\|\tilde{\mathbf{\Lambda}}_{\bar{t}_{k+N}}\| < \bar{\xi}\|\mathbf{\Psi}_k\|,$$

$$\vdots$$

$$\|\tilde{\mathbf{\Lambda}}_{\bar{t}_{k+2N-1}}\| < \bar{\xi}\|\mathbf{\Psi}_k\|,$$

which imply

$$\|\mathbf{\Psi}_{k+N}\| < \bar{\bar{\xi}}\|\mathbf{\Psi}_k\|, \quad 0 < \bar{\bar{\xi}} < 1. \qquad (6.24)$$

For all $k > N$, applying iteratively (6.24), one obtains

$$\|\mathbf{\Psi}_k\| < \bar{\bar{\xi}}\|\mathbf{\Psi}_{k-N}\| < \cdots < \bar{\bar{\xi}}^\nu\|\mathbf{\Psi}_{k-\nu N}\|,$$

where $(k - \nu N) \in \{1, \ldots, N\}$, $\nu \in \mathbb{N}$, so that

$$
\begin{aligned}
k - \nu N = 1 &\quad \Rightarrow \quad \|\mathbf{\Psi}_k\| < \bar{\bar{\xi}}^{\frac{k-1}{N}}\|\mathbf{\Psi}_1\|, \\
k - \nu N = 2 &\quad \Rightarrow \quad \|\mathbf{\Psi}_k\| < \bar{\bar{\xi}}^{\frac{k-2}{N}}\|\mathbf{\Psi}_2\|, \\
&\quad \vdots \\
k - \nu N = N &\quad \Rightarrow \quad \|\mathbf{\Psi}_k\| < \bar{\bar{\xi}}^{\frac{k-N}{N}}\|\mathbf{\Psi}_N\|.
\end{aligned}
\qquad (6.25)
$$

If the initial errors are sufficiently small, that is

$$\|\tilde{\mathbf{x}}_{\sigma(t_0^+)}^e(t_0^+)\| < \delta_{\varepsilon,\omega}, \qquad (6.26a)$$

$$\|\tilde{\mathbf{\Lambda}}_{\bar{t}_1}\| < \delta_{\varepsilon,\omega}, \cdots, \|\tilde{\mathbf{\Lambda}}_{\bar{t}_{N-1}}\| < \delta_{\varepsilon,\omega}, \qquad (6.26b)$$

using (6.19) and (6.22) and defining

$$\bar{L} = \max\{L(\eta, t_1^m - t_0), L(\eta, t_2^m - t_1^M), \ldots, L(\eta, t_N^m - t_{N-1}^M)\},$$

yields after some computations

$$\|\tilde{\mathbf{x}}^e_{\sigma(t_1^{m-})}(t_1^{m-})\| < \bar{L}\delta_{\varepsilon,\omega} =: M_{\tilde{x},1}\delta_{\varepsilon,\omega},$$

$$\|\tilde{\mathbf{x}}^e_{\sigma(t_2^{m-})}(t_2^{m-})\| < (\bar{L}^2\mu + \bar{L}M_2)\delta_{\varepsilon,\omega} =: M_{\tilde{x},2}\delta_{\varepsilon,\omega},$$

$$\vdots$$

$$\|\tilde{\mathbf{x}}^e_{\sigma(t_N^{m-})}(t_N^{m-})\| < (\bar{L}^N\mu^{N-1} + \bar{L}^{N-1}\mu^{N-2}M_2 + \cdots$$

$$\cdots + \bar{L}^2\mu M_2 + \bar{L}M_2)\delta_{\varepsilon,\omega} =: M_{\tilde{x},N}\delta_{\varepsilon,\omega},$$

with $M_{\tilde{x},j} \in \mathbb{R}^+, j = \{1,\ldots,N\}$ and by these results together with (6.21), it follows that

$$\|\tilde{\mathbf{\Lambda}}_{\bar{t}_N}\| < M_3\|\tilde{\mathbf{x}}^e_{\sigma(t_1^{m-})}(t_1^{m-})\| < M_{\tilde{\Lambda},1}\delta_{\varepsilon,\omega},$$

$$\|\tilde{\mathbf{\Lambda}}_{\bar{t}_{N+1}}\| < M_3\|\tilde{\mathbf{x}}^e_{\sigma(t_2^{m-})}(t_2^{m-})\| < M_{\tilde{\Lambda},2}\delta_{\varepsilon,\omega},$$

$$\vdots$$

$$\|\tilde{\mathbf{\Lambda}}_{\bar{t}_{2N-1}}\| < M_3\|\tilde{\mathbf{x}}^e_{\sigma(t_N^{m-})}(t_N^{m-})\| < M_{\tilde{\Lambda},N}\delta_{\varepsilon,\omega},$$

with $M_{\tilde{\Lambda},j} \in \mathbb{R}^+, j = \{1,\ldots,N\}$, so that the following bounds can be proved

$$\|\mathbf{\Psi}_1\| < M_{\Psi,1}\delta_{\varepsilon,\omega}, \tag{6.27a}$$

$$\vdots \tag{6.27b}$$

$$\|\mathbf{\Psi}_N\| < M_{\Psi,N}\delta_{\varepsilon,\omega}, \tag{6.27c}$$

with $M_{\Psi,j} \in \mathbb{R}^+, j = \{1,\ldots,N\}$. Therefore, by defining $M_\Psi := \max\limits_{j\in\{1,\ldots,N\}}\{M_{\Psi,j}\}$ the inequalities in (6.25) give

$$\|\mathbf{\Psi}_k\| < \bar{\bar{\xi}}^{\lfloor\frac{k-N}{N}\rfloor} M_\Psi \delta_{\varepsilon,\omega} \overset{k\to+\infty}{\to} 0 \text{ since } \bar{\bar{\xi}} \in (0,1), \tag{6.28}$$

which implies that any element of $\|\mathbf{\Psi}_k\|$ goes to zero as k goes to infinity, that

is

$$\|\tilde{\mathbf{x}}^e_{\sigma(t^{m-}_k)}(t^{m-}_k)\| \to 0, \tag{6.29a}$$

$$\|\tilde{\mathbf{\Lambda}}_{\bar{t}_k}\| \to 0, \cdots, \|\tilde{\mathbf{\Lambda}}_{\bar{t}_{k+N-1}}\| \to 0. \tag{6.29b}$$

By (6.29a) and (6.17), it follows that

$$|\Delta t_k| < M_1 \|\tilde{\mathbf{x}}^e_{\sigma(t^{m-}_k)}(t^{m-}_k)\| \to 0 \text{ as } k \to +\infty. \tag{6.30}$$

Moreover, in any free-motion interval, for all $t \in (t^M_k, t^m_{k+1})$, the following result holds

$$\|\tilde{\mathbf{x}}^e_{\sigma(t)}(t)\| < L(\eta, t - t^M_k)e^{-\eta(t-t^M_k)}\|\tilde{\mathbf{x}}^e_{\sigma(t^{M+}_k)}(t^{M+}_k)\| <$$

$$< \bar{L}(\mu \underbrace{\|\tilde{\mathbf{x}}^e_{\sigma(t^{m-}_k)}(t^{m-}_k)\|}_{\to 0} + M_2 \underbrace{\|\tilde{\mathbf{\Lambda}}_{\bar{t}_k}\|}_{\to 0}) \to 0 \text{ as } k \to +\infty,$$

where (6.29a) and (6.29b) have been used. By this result and (6.30), it follows that

$$\forall \tau \in (0, \rho), \exists k^* : k > k^* \Rightarrow \bar{t}_k + \tau \in \underbrace{(t^M_k, t^m_{k+1})}_{\to (\bar{t}_k, \bar{t}_{k+1})} \text{ and}$$

$$\|\tilde{\mathbf{x}}^e_{\sigma(\bar{t}_k+\tau)}(\bar{t}_k + \tau)\| \to 0 \text{ as } k \to +\infty.$$

Since $t_k \to \bar{t}_k$ as $k \to +\infty$, time $\bar{t}_k + \tau, \forall \tau \in (0, \rho)$ is a switching time neither for the actual trajectory nor for the desired one. Therefore, $\lim_{k \to +\infty} \|\tilde{\mathbf{x}}^e_{\sigma((\bar{t}_k+\tau)-)}((\bar{t}_k + \tau)^-)\| = \lim_{k \to +\infty} \|\tilde{\mathbf{x}}^e_{\sigma((\bar{t}_k+\tau)+)}((\bar{t}_k + \tau)^+)\| = \lim_{k \to +\infty} \|\tilde{\mathbf{x}}^e_{\sigma(\bar{t}_k+\tau)}(\bar{t}_k + \tau))\| = 0$. This fact and $\mathbf{e}(t) = \mathbf{C}^e_{\sigma(t)}\tilde{\mathbf{x}}^e_{\sigma(t)}(t)$ prove property **2)** of Problem 5.

Step (v): To complete the proof remains to prove property **1)** in Problem 5. As seen before, for all t in a generic time interval $(t^M_k, t^m_{k+1}), k \in \mathbb{Z}^+$, one

has

$$\|\tilde{\mathbf{x}}^e_{\sigma(t)}(t)\| < L(\eta, t - t_k^M)e^{-\eta(t - t_k^M)}\|\tilde{\mathbf{x}}^e_{\sigma(t_k^{M+})}(t_k^{M+})\| <$$
$$< \bar{L}\mu\|\tilde{\mathbf{x}}^e_{\sigma(t_k^{m-})}(t_k^{m-})\| + \bar{L}M_2\|\tilde{\mathbf{\Lambda}}_{\bar{t}_k}\|.$$

Now, by considering the inequality in (6.28) and the definition of $\mathbf{\Psi}_k$, one obtains

$$\|\tilde{\mathbf{x}}^e_{\sigma(t)}(t)\| < (\bar{L}\mu + \bar{L}M_2)M_\Psi \delta_{\varepsilon,\omega},$$

in addition, if $\delta_{\varepsilon,\omega} < \bar{\delta}_1/M_\Psi$, $\|\tilde{\mathbf{x}}^e_{\sigma(t_k^{m-})}(t_k^{m-})\| < \bar{\delta}_1$ and $\|\tilde{\mathbf{\Lambda}}_{\bar{t}_k}\| < \bar{\delta}_1$, then $\|\tilde{\mathbf{x}}^e_{\sigma(t_{k+1}^{m-})}(t_{k+1}^{m-})\| < \bar{\bar{\xi}}^{\lfloor \frac{k+1-N}{N}\rfloor} M_\Psi \delta_{\varepsilon,\omega} < \bar{\delta}_1$ and $\|\tilde{\mathbf{\Lambda}}_{\bar{t}_{k+1}}\| < \bar{\bar{\xi}}^{\lfloor \frac{k+1-N}{N}\rfloor} M_\Psi \delta_{\varepsilon,\omega} < \bar{\delta}_1$, so that choosing $\delta_{\varepsilon,\omega} := \min\{\frac{\bar{\delta}_1}{M_\Psi}, \frac{\varepsilon}{(\bar{L}\mu + \bar{L}M_2)M_\Psi M_e}\}$ with $M_e := \max_{i \in \mathcal{P}}\{\|\bar{\mathbf{C}}^e_i\|\}$ yields

$$(6.26) \quad \Rightarrow \quad \|\tilde{\mathbf{x}}^e_{\sigma(t)}(t)\| < \frac{\varepsilon}{M_e}, \quad \forall t \in (t_k^M, t_{k+1}^m), \ k \in \mathbb{Z}^+,$$

and given that $|\Delta t_k| < \omega$ and $\|\mathbf{e}(t)\| < \|\bar{\mathbf{C}}^e_{\sigma(t)}\|\|\tilde{\mathbf{x}}^e_{\sigma(t)}(t)\| < M_e\|\tilde{\mathbf{x}}^e_{\sigma(t)}(t)\|$ hold, then property **1)** in Problem 5 is proved. $\square$

6.4   A numerical example

In this section, a numerical example is given in order to illustrate the effectiveness of the proposed method; for lake of space only the case with uncertainties and estimate of the precompensator jumps is taken into account.

By using the notation introduced in Section **??** and by defining the number of modes $M = 2$, the switching surfaces parameters

$$
\begin{aligned}
1 \to 2: \quad & \mathbf{J}_{21} = \begin{bmatrix} -1 & 0 \end{bmatrix}, \quad b_{21} = 2, \\
2 \to 1: \quad & \mathbf{J}_{12} = -1, \quad\quad\quad\ b_{12} = 1, \\
1 \to 1: \quad & \mathbf{J}_{11} = \begin{bmatrix} 1 & 0 \end{bmatrix}, \quad\ b_{11} = 4,
\end{aligned}
$$

and the reset maps

$$\mathbf{\Gamma}_{21} = \begin{bmatrix} 1/2 & 0 \end{bmatrix}, \ \mathbf{\Gamma}_{12} = \begin{bmatrix} -1 \\ 2 \end{bmatrix}, \ \mathbf{\Gamma}_{11} = \begin{bmatrix} 0 & 0 \\ 0 & -1/2 \end{bmatrix},$$

the hybrid system considered in this example can be represented as shown in Fig. 6.8.
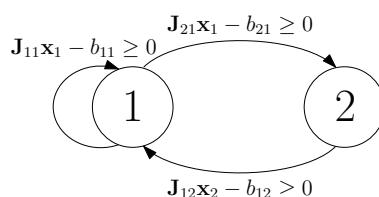
Figure 6.8: Linear hybrid system with 2 modes considered for the example.

On the other hand, the continuous dynamics during the free-motion phases are characterized by

$$\mathbf{A}_1 = \begin{bmatrix} 0 & 1 \\ -1 + \epsilon_1 & -2 + \epsilon_2 \end{bmatrix}, \quad \mathbf{B}_1 = \begin{bmatrix} 0 \\ 1 + \epsilon_3 \end{bmatrix},$$

$$\mathbf{C}_1 = \begin{bmatrix} 1 & 0 \end{bmatrix}, \quad \mathbf{D}_1 = \begin{bmatrix} 0 \\ 0 \end{bmatrix},$$

and

$$\mathbf{A}_2 = 3 + \epsilon_4, \quad \mathbf{B}_2 = 2 + \epsilon_5, \quad \mathbf{C}_2 = 1, \quad \mathbf{D}_2 = 0,$$

where $\epsilon_i \in \mathbb{R}$, $i \in \{1, 2, 3, 4, 5\}$ denote possible uncertainties on the parameters of the plant. In the present example, $\epsilon_1 = \epsilon_2 = \epsilon_3 = \epsilon_4 = \epsilon_5 = 0$ in the nominal parameters, whereas $\epsilon_1 = -0.5$, $\epsilon_2 = 1$, $\epsilon_3 = 0.7$, $\epsilon_4 = -0.8$ and $\epsilon_5 = 0.5$ in the actual parameters.

As for the reference trajectory, it can be given in the form of (6.7) as

follows:

$$\bar{\mathbf{y}}(t) = \begin{cases} 0.5t^2 + t, & t \in [0, 2), \\ -t^2 + 2t + 2, & t \in [2, 3), \\ -2t + 7, & t \in [3, 4.5), \end{cases}$$

with period $T = 4.5$ and $N = 3$ switching events per period.

At this point, by using the control strategy described in Section 6.3 (it is easy to see that all the required assumptions are satisfiable) with static gains $\mathbf{K}_1, \mathbf{K}_1^a$ and $\mathbf{K}_2, \mathbf{K}_2^a$ chosen such that η in (6.12) is at least equal to 3. Starting from the initial time $t_0 = 0.2$ with initial conditions $\mathbf{x}_1(t_0) = \begin{bmatrix} 3 & -2 \end{bmatrix}^T$, $\mathbf{x}_2(t_0) = 0$ and $\mathbf{x}_a(t_0) = \begin{bmatrix} 0.05 & -0.05 & 0.05 \end{bmatrix}^T$, the behavior of the controlled trajectory during the first 19.8 seconds of motion can be observed in Fig. 6.9.

6.5 Details of the proof of main result

This appendix contains details about the proofs of the facts (6.17),(6.18),(5.28) and (6.21). Since the desired trajectory is periodic, all the results obtained in the following considering $k \in \{1, \dots, N\} =: \mathcal{I}_N$, remain proved for $k \in \mathbb{N}$. In the following, for the sake of readability the dependence of dynamics matrices on $\boldsymbol{\beta}$ will be omitted.

Details of the proof of the fact (6.17)

For each $k \in \mathcal{I}_N$, the following fact can be proved

$$\exists \delta_1 \in \mathbb{R}^+, M_1 \in \mathbb{R}^+ : \|\tilde{\mathbf{x}}_j^e(t_k^{m-})\| < \delta_1 \Rightarrow |\Delta t_k| \le M_1 \|\tilde{\mathbf{x}}_j^e(t_k^{m-})\|, \qquad (6.17)$$

where $j = \sigma(t_k^{m-})$, $\tilde{\mathbf{x}}_j^e(t) := \mathbf{x}_j^e(t) - \bar{\mathbf{x}}_j^e(t)$ and $\Delta t_k := t_k - \bar{t}_k$.

Remark 37. Lemma D.1 in [66] states that there exists a neighborhood $\mathcal{U}$ of $\mathbf{x}^*$ such that the function *time to impact* $T_I : \mathcal{U} \to \mathbb{R}^+ \cup \{0\}$ (see, e.g., [84]), which returns the time to impact starting from an initial condition $\mathbf{x} \in \mathcal{U}$, is differentiable.

(a) $\mathbf{y}(t)$ and $\bar{\mathbf{y}}(t)$

(b) Precompensator state vector: $\mathbf{x}_a(t)$

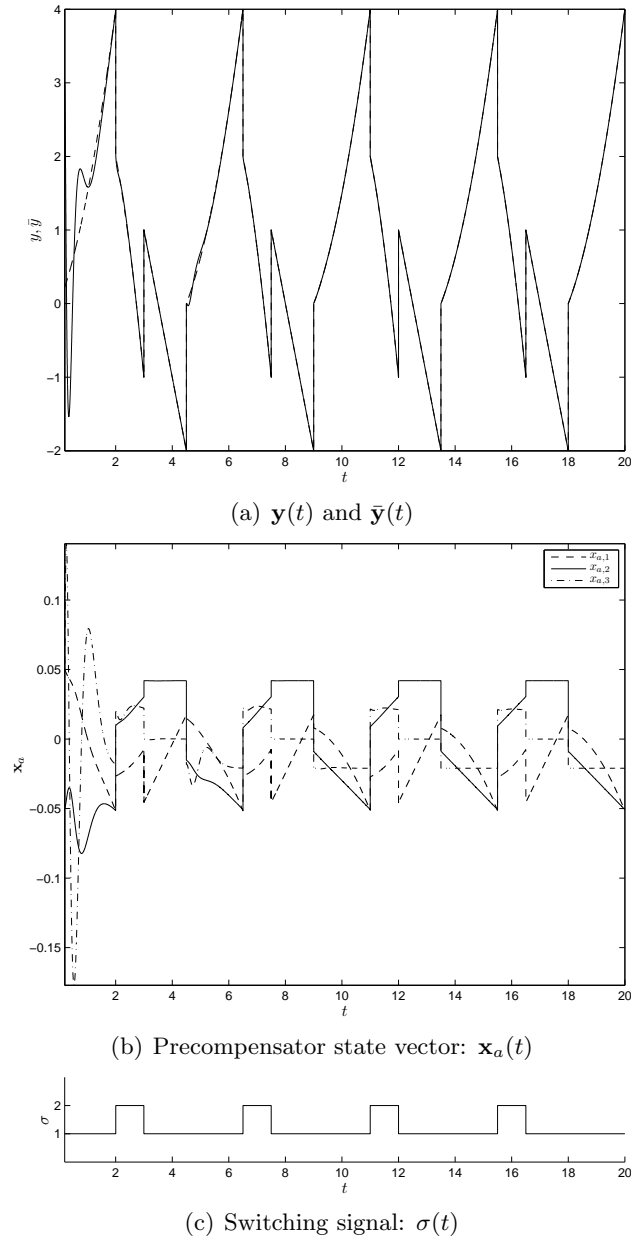

(c) Switching signal: $\sigma(t)$

Figure 6.9: The desired (dashed) trajectory and the actual (solid) one (a); time behavior of the precompensator state variables $\mathbf{x}_a(t)$ (b); switching signal relevant to the controlled trajectory (c).

In the following the assumption $\|\tilde{\mathbf{x}}_j^e(t_k^{m-})\| < \delta_1$ ensures that at time t_k^{m-} the actual trajectory is sufficiently close to the desired one, so that in both the cases **a)** and **b)** described below the neighborhood $\mathcal{U}$ of Lemma D.1 in [66] can be found.

Case a) $t_k^m = t_k$, $t_k^M = \bar{t}_k$, so that $\Delta t_k := t_k - \bar{t}_k < 0$. Since $|\Delta t_k| = |\bar{T}_I(\bar{\mathbf{x}}_j^e(t_k^-))|$ where $\bar{T}_I(\cdot)$ denotes the time to impact function relative to the nominal trajectory, and

$$|\bar{T}_I(\bar{\mathbf{x}}_j^e(t_k^-))| = |\bar{T}_I(\bar{\mathbf{x}}_j^e(t_k^-)) - \bar{T}_I(\Pi_{\mathcal{C}_{ij}}(\bar{\mathbf{x}}_j^e(t_k^-)))| \le$$
$$\le M_{1,a}\|\bar{\mathbf{x}}_j^e(t_k^-) - \Pi_{\mathcal{C}_{ij}}(\bar{\mathbf{x}}_j^e(t_k^-))\| \le$$
$$\le M_{1,a}\|\bar{\mathbf{x}}_j^e(t_k^-) - \mathbf{x}_j^e(t_k^-)\| = M_{1,a}\|\tilde{\mathbf{x}}_j^e(t_k^-)\|,$$

with $\Pi_{\mathcal{C}}(\mathbf{x}^*) \in \mathcal{C}$ being the projection of $\mathbf{x}^*$ on the switching surface $\mathcal{C}$, then

$$\exists M_{1,a} \in \mathbb{R}^+ : |\Delta t_k| \le M_{1,a}\|\tilde{\mathbf{x}}_j^e(t_k^{m-})\|.$$

Case b) $t_k^m = \bar{t}_k$, $t_k^M = t_k$, so that $\Delta t_k := t_k - \bar{t}_k > 0$. Since $|\Delta t_k| = |T_I(\mathbf{x}_j^e(\bar{t}_k^-))|$ where $T_I(\cdot)$ denotes the time to impact function relative to the actual trajectory, and

$$|T_I(\mathbf{x}_j^e(\bar{t}_k^-))| = |T_I(\mathbf{x}_j^e(\bar{t}_k^-)) - T_I(\Pi_{\mathcal{C}_{ij}}(\mathbf{x}_j^e(\bar{t}_k^-)))| \le$$
$$\le M_{1,b}\|\mathbf{x}_j^e(\bar{t}_k^-) - \Pi_{\mathcal{C}_{ij}}(\mathbf{x}_j^e(\bar{t}_k^-))\| \le$$
$$\le M_{1,b}\|\mathbf{x}_j^e(\bar{t}_k^-) - \bar{\mathbf{x}}_j^e(\bar{t}_k^-)\| = M_{1,b}\|\tilde{\mathbf{x}}_j^e(\bar{t}_k^-)\|,$$

with $\Pi_{\mathcal{C}}(\mathbf{x}^*) \in \mathcal{C}$ being the projection of $\mathbf{x}^*$ on the switching surface $\mathcal{C}$, then

$$\exists M_{1,b} \in \mathbb{R}^+ : |\Delta t_k| \le M_{1,b}\|\tilde{\mathbf{x}}_j^e(t_k^{m-})\|.$$

Therefore (6.17) is proved by choosing $M_1 = \max\{M_{1,a}, M_{1,b}\}$.[2]

---

[2]For $\Delta t_k = 0$ inequality (6.17) is trivially satisfied for each $M_1 \in \mathbb{R}^+$.

Details of the proof of the fact (6.18)

The dynamics during the free-motion intervals (i.e., in absence of switches for both the actual and the nominal trajectories) are completely characterized by equations (6.4),(6.3) and (6.13). On the other hand, concerning the constrained motion, the state vector $\bar{\mathbf{x}}_i^e(\cdot)$ is subject to discontinuities at times $\bar{t}_k$, whereas the vectors $\mathbf{x}_i^e(\cdot)$ and $\tilde{\mathbf{x}}_i^e(\cdot)$ have discontinuities at switching times both of the controlled body and of the desired trajectory. For the sake of clarity a summary of such equations is reported below.

$$
\textbf{Actual}:
\begin{cases}
FM:
\begin{cases}
\dot{\mathbf{x}}_i^e(t) = \bar{\mathbf{A}}_i^e \mathbf{x}_i^e(t) + \bar{\mathbf{B}}_i^e \mathbf{u}_a(t), \\
\mathbf{y}(t) = \bar{\mathbf{C}}_i^e \mathbf{x}_i^e(t),
\end{cases} \\[4mm]
CM:
\begin{cases}
\mathbf{x}_i^e(t_k^+) = \mathbf{\Gamma}_{ij}^e \mathbf{x}_j^e(t_k^-), \\
\mathbf{x}_i^e(\bar{t}_k^+) = \mathbf{I}_i^e \mathbf{x}_i^e(\bar{t}_k^-) + \mathbf{\Lambda}_{\bar{t}_k}^e,
\end{cases}
\end{cases}
\tag{6.31a}
$$

$$
\textbf{Nominal}:
\begin{cases}
FM:
\begin{cases}
\dot{\bar{\mathbf{x}}}_i^e(t) = \bar{\mathbf{A}}_i^e \bar{\mathbf{x}}_i^e(t), \\
\bar{\mathbf{y}}(t) = \bar{\mathbf{C}}_i^e \bar{\mathbf{x}}_i^e(t),
\end{cases} \\[4mm]
CM:
\begin{cases}
\bar{\mathbf{x}}_i^e(t_k^+) = \bar{\mathbf{x}}_i^e(t_k^-), \\
\bar{\mathbf{x}}_i^e(\bar{t}_k^+) = \bar{\mathbf{\Gamma}}_{ij}^e \bar{\mathbf{x}}_j^e(\bar{t}_k^-) + \bar{\mathbf{\Lambda}}_{\bar{t}_k}^e,
\end{cases}
\end{cases}
\tag{6.31b}
$$

where $\bar{\mathbf{A}}_i^e = \begin{bmatrix} \mathbf{A}_i + \mathbf{B}_i\mathbf{K}_i & \mathbf{B}_i\mathbf{K}_i^a \\ \mathbf{0} & \mathbf{A}_a \end{bmatrix}$, $\bar{\mathbf{B}}_i^e = \begin{bmatrix} \mathbf{0} \\ \mathbf{B}_a \end{bmatrix}$, $\bar{\mathbf{C}}_i^e = \begin{bmatrix} \mathbf{C}_i + \mathbf{D}_i\mathbf{K}_i & \mathbf{D}_i\mathbf{K}_i^a \end{bmatrix}$

and $\mathbf{\Gamma}_{ij}^e = \begin{bmatrix} \mathbf{\Gamma}_{ij} & \mathbf{0} \\ \mathbf{0} & \mathbf{I}_{n_a} \end{bmatrix}$, $\mathbf{I}_i^e = \begin{bmatrix} \mathbf{I}_{n_i} & \mathbf{0} \\ \mathbf{0} & \mathbf{0} \end{bmatrix}$, $\mathbf{\Lambda}_{\bar{t}_k}^e = \begin{bmatrix} \mathbf{0} \\ \mathbf{\Lambda}_{\bar{t}_k} \end{bmatrix}$, $\bar{\mathbf{\Gamma}}_{ij}^e = \begin{bmatrix} \mathbf{\Gamma}_{ij} & \mathbf{0} \\ \mathbf{0} & \mathbf{0} \end{bmatrix}$, $\bar{\mathbf{\Lambda}}_{\bar{t}_k}^e = \begin{bmatrix} \mathbf{0} \\ \bar{\mathbf{\Lambda}}_{\bar{t}_k} \end{bmatrix}$.

For later use, the following facts are introduced

$$
\mathbf{I}_i^e \mathbf{\Gamma}_{ij}^e = \mathbf{\Gamma}_{ij}^e \mathbf{I}_j^e = \bar{\mathbf{\Gamma}}_{ij}^e,
\tag{6.32a}
$$

$$
(\mathbf{\Gamma}_{ij}^e - \mathbf{I})\bar{\mathbf{\Lambda}}_{\bar{t}_k}^e = \mathbf{0},
\tag{6.32b}
$$

$$
\mathbf{\Gamma}_{ij}^e(\mathbf{\Lambda}_{\bar{t}_k}^e - \bar{\mathbf{\Lambda}}_{\bar{t}_k}^e) = (\mathbf{\Lambda}_{\bar{t}_k}^e - \bar{\mathbf{\Lambda}}_{\bar{t}_k}^e).
\tag{6.32c}
$$

Using the notation so far introduced, for each $k \in \mathcal{I}_N$, one can prove that

$$\exists \delta_2 \in \mathbb{R}^+, M_2 \in \mathbb{R}^+ : \|\tilde{\mathbf{x}}_j^e(t_k^{m-})\| < \delta_2, |\Delta t_k| < \delta_2, \|\tilde{\mathbf{\Lambda}}_{\bar{t}_k}\| < \delta_2 \Rightarrow$$

$$\Rightarrow \|\tilde{\mathbf{x}}_i^e(t_k^{M+})\| \leq M_2\|\tilde{\mathbf{x}}_j^e(t_k^{m-})\| + M_2|\Delta t_k| + M_2\|\tilde{\mathbf{\Lambda}}_{\bar{t}_k}\|. \qquad (6.18)$$

where $j = \sigma(t_k^{m-})$ and $i = \sigma(t_k^{M+})$. The two possible cases are considered separately.

Case a) $t_k^m = t_k$, $t_k^M = \bar{t}_k$, so that $\Delta t_k := t_k - \bar{t}_k < 0$, and the error at time t_k^{M+}, that is after the k-th couple of switches, is given by $\tilde{\mathbf{x}}_i^e(t_k^{M+}) := \mathbf{x}_i^e(t_k^{M+}) - \bar{\mathbf{x}}_i^e(t_k^{M+})$, where

$$\mathbf{x}_i^e(t_k^{M+}) = \mathbf{x}_i^e(\bar{t}_k^+) = \mathbf{I}_i^e \mathbf{x}_i^e(\bar{t}_k^-) + \mathbf{\Lambda}_{\bar{t}_k}^e = \mathbf{I}_i^e e^{-\bar{\mathbf{A}}_i^e \Delta t_k} \mathbf{x}_i^e(t_k^+) + \mathbf{\Lambda}_{\bar{t}_k}^e =$$

$$= \mathbf{I}_i^e e^{-\bar{\mathbf{A}}_i^e \Delta t_k} \mathbf{\Gamma}_{ij}^e \mathbf{x}_j^e(t_k^-) + \mathbf{\Lambda}_{\bar{t}_k}^e =$$

$$= \mathbf{I}_i^e e^{-\bar{\mathbf{A}}_i^e \Delta t_k} \mathbf{\Gamma}_{ij}^e \tilde{\mathbf{x}}_j^e(t_k^-) + \mathbf{I}_i^e e^{-\bar{\mathbf{A}}_i^e \Delta t_k} \mathbf{\Gamma}_{ij}^e e^{\bar{\mathbf{A}}_j^e \Delta t_k} \bar{\mathbf{x}}_j^e(\bar{t}_k^-) + \mathbf{\Lambda}_{\bar{t}_k}^e;$$

$$\bar{\mathbf{x}}_i^e(t_k^{M+}) = \bar{\mathbf{x}}_i^e(\bar{t}_k^+) = \bar{\mathbf{\Gamma}}_{ij}^e \bar{\mathbf{x}}_j^e(\bar{t}_k^-) + \bar{\mathbf{\Lambda}}_{\bar{t}_k}^e.$$

Hence, it follows that

$$\tilde{\mathbf{x}}_i^e(t_k^{M+}) = \mathbf{I}_i^e e^{-\bar{\mathbf{A}}_i^e \Delta t_k} \mathbf{\Gamma}_{ij}^e \tilde{\mathbf{x}}_j^e(t_k^{m-}) + \left(\mathbf{I}_i^e e^{-\bar{\mathbf{A}}_i^e \Delta t_k} \mathbf{\Gamma}_{ij}^e e^{\bar{\mathbf{A}}_j^e \Delta t_k} + \right.$$

$$\left. - \bar{\mathbf{\Gamma}}_{ij}^e \right) \bar{\mathbf{x}}_j^e(\bar{t}_k^-) + \tilde{\mathbf{\Lambda}}_{\bar{t}_k}^e =:$$

$$=: \mathbf{f}_a(\tilde{\mathbf{x}}_j^e(t_k^{m-}), \Delta t_k, \tilde{\mathbf{\Lambda}}_{\bar{t}_k}^e),$$

where $j = \sigma(t_k^{m-})$, $i = \sigma(t_k^{M+})$ and $\tilde{\mathbf{\Lambda}}_{\bar{t}_k}^e := \mathbf{\Lambda}_{\bar{t}_k}^e - \bar{\mathbf{\Lambda}}_{\bar{t}_k}^e$;

Case b) $t_k^m = \bar{t}_k$, $t_k^M = t_k$, so that $\Delta t_k := t_k - \bar{t}_k > 0$, and the error at time t_k^{M+}, that is after the k-th couple of switches, is given by $\tilde{\mathbf{x}}_i^e(t_k^{M+}) :=$

$\mathbf{x}_i^e(t_k^{M+}) - \bar{\mathbf{x}}_i^e(t_k^{M+})$, where

$$\begin{aligned}
\mathbf{x}_i^e(t_k^{M+}) &= \mathbf{x}_i^e(t_k^+) = \boldsymbol{\Gamma}_{ij}^e \mathbf{x}_j^e(t_k^-) = \boldsymbol{\Gamma}_{ij}^e e^{\bar{\mathbf{A}}_j^e \Delta t_k} \mathbf{x}_j^e(\bar{t}_k^+) = \\
&= \boldsymbol{\Gamma}_{ij}^e e^{\bar{\mathbf{A}}_j^e \Delta t_k} \mathbf{I}_j^e \mathbf{x}_j^e(\bar{t}_k^-) + \boldsymbol{\Gamma}_{ij}^e e^{\bar{\mathbf{A}}_j^e \Delta t_k} \boldsymbol{\Lambda}_{\bar{t}_k}^e = \\
&= \boldsymbol{\Gamma}_{ij}^e e^{\bar{\mathbf{A}}_j^e \Delta t_k} \mathbf{I}_j^e \tilde{\mathbf{x}}_j^e(\bar{t}_k^-) + \boldsymbol{\Gamma}_{ij}^e e^{\bar{\mathbf{A}}_j^e \Delta t_k} \mathbf{I}_j^e \bar{\mathbf{x}}_j^e(\bar{t}_k^-) + \boldsymbol{\Gamma}_{ij}^e e^{\bar{\mathbf{A}}_j^e \Delta t_k} \boldsymbol{\Lambda}_{\bar{t}_k}^e; \\
\bar{\mathbf{x}}_i^e(t_k^{M+}) &= \bar{\mathbf{x}}_i^e(t_k^+) = \bar{\mathbf{x}}_i^e(t_k^-) = e^{\bar{\mathbf{A}}_i^e \Delta t_k} \bar{\boldsymbol{\Gamma}}_{ij}^e \bar{\mathbf{x}}_j^e(\bar{t}_k^-) + e^{\bar{\mathbf{A}}_i^e \Delta t_k} \bar{\boldsymbol{\Lambda}}_{\bar{t}_k}^e.
\end{aligned}$$

Hence, it follows that

$$\begin{aligned}
\tilde{\mathbf{x}}_i^e(t_k^{M+}) &= \boldsymbol{\Gamma}_{ij}^e e^{\bar{\mathbf{A}}_j^e \Delta t_k} \mathbf{I}_j^e \tilde{\mathbf{x}}_j^e(t_k^{m-}) + (\boldsymbol{\Gamma}_{ij}^e e^{\bar{\mathbf{A}}_j^e \Delta t_k} \mathbf{I}_j^e - e^{\bar{\mathbf{A}}_i^e \Delta t_k} \bar{\boldsymbol{\Gamma}}_{ij}^e) \bar{\mathbf{x}}_j^e(\bar{t}_k^-) + \\
&\quad + (\boldsymbol{\Gamma}_{ij}^e e^{\bar{\mathbf{A}}_j^e \Delta t_k} - e^{\bar{\mathbf{A}}_i^e \Delta t_k}) \bar{\boldsymbol{\Lambda}}_{\bar{t}_k}^e + \boldsymbol{\Gamma}_{ij}^e e^{\bar{\mathbf{A}}_j^e \Delta t_k} \tilde{\boldsymbol{\Lambda}}_{\bar{t}_k}^e =: \\
&=: \mathbf{f}_b(\tilde{\mathbf{x}}_j^e(t_k^{m-}), \Delta t_k, \tilde{\boldsymbol{\Lambda}}_{\bar{t}_k}^e),
\end{aligned}$$

where $j = \sigma(t_k^{m-})$, $i = \sigma(t_k^{M+})$ and $\tilde{\boldsymbol{\Lambda}}_{\bar{t}_k}^e := \boldsymbol{\Lambda}_{\bar{t}_k}^e - \bar{\boldsymbol{\Lambda}}_{\bar{t}_k}^e$.

It is easy to see that $\tilde{\mathbf{x}}_i^e(t_k^{M+})$ is a continuous function in the hyperplane characterized by $\Delta t_k = 0$[3] and if $\tilde{\mathbf{x}}_j^e(t_k^{m-}) = \mathbf{0}, \Delta t_k = 0$ and $\tilde{\boldsymbol{\Lambda}}_{\bar{t}_k}^e = \mathbf{0}$, then $\tilde{\mathbf{x}}_i^e(t_k^{M+}) = \mathbf{0}$. Moreover, it is also possible to show that the function $\tilde{\mathbf{x}}_i^e(t_k^{M+})$ is Lipschitz in its variables $\tilde{\mathbf{x}}_j^e(t_k^{m-}), \Delta t_k$ and $\tilde{\boldsymbol{\Lambda}}_{\bar{t}_k}^e$ in a neighborhood $\boldsymbol{\Upsilon}_0$ of $(\tilde{\mathbf{x}}_j^e(t_k^{m-}) = \mathbf{0}, \Delta t_k = 0, \tilde{\boldsymbol{\Lambda}}_{\bar{t}_k}^e = \mathbf{0})$. In order to prove this, since for $\Delta t_k < 0$ and $\Delta t_k > 0$ the function $\tilde{\mathbf{x}}_i^e(t_k^{M+})$ is clearly analytic, one has to show that

$$\exists M_2 \in \mathbb{R}^+ : \|\mathbf{f}_a(\boldsymbol{v}_1) - \mathbf{f}_b(\boldsymbol{v}_2)\| \leq M_2 \|\boldsymbol{v}_1 - \boldsymbol{v}_2\|,$$

where $\boldsymbol{v}_l := [(\tilde{\mathbf{x}}_j^{eT}(t_k^{m-}))_l, (\Delta t_k)_l, (\tilde{\boldsymbol{\Lambda}}_{\bar{t}_k}^{eT})_l]^T$ and $\boldsymbol{v}_1, \boldsymbol{v}_2 \in \boldsymbol{\Upsilon}_0$ with $(\Delta t_k)_1 \leq 0$

---

[3]By using (6.32), it is easy to show that $\tilde{\mathbf{x}}_i^e(t_k^{M+})|_{\Delta t_k=0} = \bar{\boldsymbol{\Gamma}}_{ij}^e \tilde{\mathbf{x}}_j^e(t_k^{m-}) + \tilde{\boldsymbol{\Lambda}}_{\bar{t}_k}^e$.

and $(\Delta t_k)_2 \geq 0$.

$$\|\mathbf{f}_a(\boldsymbol{v}_1) - \mathbf{f}_b(\boldsymbol{v}_2)\| = \|\mathbf{f}_a(\boldsymbol{v}_1) - \mathbf{f}_a(\boldsymbol{v}_2^*) + \mathbf{f}_a(\boldsymbol{v}_2^*) - \mathbf{f}_b(\boldsymbol{v}_1^*) + \mathbf{f}_b(\boldsymbol{v}_1^*) - \mathbf{f}_b(\boldsymbol{v}_2)\| \leq$$

$$\leq \|\mathbf{f}_a(\boldsymbol{v}_1) - \mathbf{f}_a(\boldsymbol{v}_2^*)\| + \|\mathbf{f}_b(\boldsymbol{v}_2) - \mathbf{f}_b(\boldsymbol{v}_1^*)\| + \|\mathbf{f}_a(\boldsymbol{v}_2^*) - \mathbf{f}_b(\boldsymbol{v}_1^*)\|,$$
$$(6.33)$$

where $\boldsymbol{v}_1^* = \boldsymbol{v}_1|_{(\Delta t_k)_1=0}$ and $\boldsymbol{v}_2^* = \boldsymbol{v}_2|_{(\Delta t_k)_2=0}$. Since functions $\mathbf{f}_a(\cdot)$ and $\mathbf{f}_b(\cdot)$ are Lipschitz the inequality (6.33) can be rewritten as:

$$(6.33) \leq M_{2a}\|\boldsymbol{v}_1 - \boldsymbol{v}_2^*\| + M_{2b}\|\boldsymbol{v}_2 - \boldsymbol{v}_1^*\| + \|\mathbf{f}_a(\boldsymbol{v}_2^*) - \mathbf{f}_b(\boldsymbol{v}_1^*)\|. \qquad (6.34)$$

By the definitions of $\boldsymbol{v}_1^*$ and $\boldsymbol{v}_2^*$, it follows that $\|\boldsymbol{v}_1 - \boldsymbol{v}_2^*\| \leq \|\boldsymbol{v}_1 - \boldsymbol{v}_2\|$ and $\|\boldsymbol{v}_2 - \boldsymbol{v}_1^*\| \leq \|\boldsymbol{v}_1 - \boldsymbol{v}_2\|$. In fact, by using the following well known fact about the norm of a vector $\mathbf{x} = [\mathbf{x}_1, \mathbf{x}_2, \cdots, \mathbf{x}_n]$

$$\|\mathbf{x}\| = \left\| \begin{bmatrix} \|\mathbf{x}_1\| & \|\mathbf{x}_2\| & \cdots & \|\mathbf{x}_n\| \end{bmatrix} \right\|,$$

one has

$$\|\boldsymbol{v}_1 - \boldsymbol{v}_2^*\| = \left\| \begin{bmatrix} (\tilde{\mathbf{x}}_j^e(t_k^{m-}))_1 - (\tilde{\mathbf{x}}_j^e(t_k^{m-}))_2 \\ (\Delta t_k)_1 \\ (\tilde{\boldsymbol{\Lambda}}_{\tilde{t}_k}^e)_1 - (\tilde{\boldsymbol{\Lambda}}_{\tilde{t}_k}^e)_2 \end{bmatrix} \right\| =$$

$$= \sqrt{\|(\tilde{\mathbf{x}}_j^e(t_k^{m-}))_1 - (\tilde{\mathbf{x}}_j^e(t_k^{m-}))_2\|^2 + \|(\tilde{\boldsymbol{\Lambda}}_{\tilde{t}_k}^e)_1 - (\tilde{\boldsymbol{\Lambda}}_{\tilde{t}_k}^e)_2\|^2 + |(\Delta t_k)_1|^2}, (6.35)$$

and

$$\|\boldsymbol{v}_1 - \boldsymbol{v}_2\| = \left\| \begin{bmatrix} (\tilde{\mathbf{x}}_j^e(t_k^{m-}))_1 - (\tilde{\mathbf{x}}_j^e(t_k^{m-}))_2 \\ (\Delta t_k)_1 - (\Delta t_k)_2 \\ (\tilde{\boldsymbol{\Lambda}}_{\tilde{t}_k}^e)_1 - (\tilde{\boldsymbol{\Lambda}}_{\tilde{t}_k}^e)_2 \end{bmatrix} \right\| =$$

$$= \sqrt{\|(\tilde{\mathbf{x}}_j^e(t_k^{m-}))_1 - (\tilde{\mathbf{x}}_j^e(t_k^{m-}))_2\|^2 + \|(\tilde{\boldsymbol{\Lambda}}_{\tilde{t}_k}^e)_1 - (\tilde{\boldsymbol{\Lambda}}_{\tilde{t}_k}^e)_2\|^2 + |(\Delta t_k)_1 - (\Delta t_k)_2|^2} (6.36)$$

Hence,

$$(6.35) \leq (6.36) \Leftrightarrow |(\Delta t_k)_1| \leq |(\Delta t_k)_1 - (\Delta t_k)_2|,$$

where $|(\Delta t_k)_1| \leq |(\Delta t_k)_1 - (\Delta t_k)_2|$ is satisfied since $(\Delta t_k)_1$ and $(\Delta t_k)_2$ have opposite sign. For the sake of brevity, the detailed proof of $\|\boldsymbol{v}_2 - \boldsymbol{v}_1^*\| \leq \|\boldsymbol{v}_1 - \boldsymbol{v}_2\|$ is omitted given that it can be obtained with analogous reasonings.

In (6.34), the last term can be written as follows:

$$\|\mathbf{f}_a(\boldsymbol{v}_2^*) - \mathbf{f}_b(\boldsymbol{v}_1^*)\| = \|\bar{\boldsymbol{\Gamma}}_{ij}^e(\tilde{\mathbf{x}}_j^e(t_k^{m-}))_2 + (\tilde{\boldsymbol{\Lambda}}_{\bar{t}_k}^e)_2 - \bar{\boldsymbol{\Gamma}}_{ij}^e(\tilde{\mathbf{x}}_j^e(t_k^{m-}))_1 - (\tilde{\boldsymbol{\Lambda}}_{\bar{t}_k}^e)_1\| \leq$$
$$\leq \|\bar{\boldsymbol{\Gamma}}_{ij}^e\|\|(\tilde{\mathbf{x}}_j^e(t_k^{m-}))_1 - (\tilde{\mathbf{x}}_j^e(t_k^{m-}))_2\| + \|(\tilde{\boldsymbol{\Lambda}}_{\bar{t}_k}^e)_1 - (\tilde{\boldsymbol{\Lambda}}_{\bar{t}_k}^e)_2\| \leq$$
$$\leq (1 + \|\bar{\boldsymbol{\Gamma}}_{ij}^e\|)\|\boldsymbol{v}_1 - \boldsymbol{v}_2\| =: M_{2ab}\|\boldsymbol{v}_1 - \boldsymbol{v}_2\|. \qquad (6.37)$$

By putting together (6.33),(6.34),(6.35),(6.36) and (6.37), one has for each $\boldsymbol{v}_1, \boldsymbol{v}_2$

$$\|\tilde{\mathbf{x}}_i^e(t_k^{M+})|_{\boldsymbol{v}_1} - \tilde{\mathbf{x}}_i^e(t_k^{M+})|_{\boldsymbol{v}_2}\| \leq M_2\|\boldsymbol{v}_1 - \boldsymbol{v}_2\|,$$

where $M_2 := \max\{M_{2a}, M_{2b}, M_{2ab}\} \in \mathbb{R}^+$. Now, since $(\tilde{\mathbf{x}}_j^e(t_k^{m-}) = \mathbf{0}, \Delta t_k = 0, \tilde{\boldsymbol{\Lambda}}_{\bar{t}_k}^e = \mathbf{0}) \Rightarrow \tilde{\mathbf{x}}_i^e(t_k^{M+}) = \mathbf{0}$ and by using the Lipschitz property for each $(\tilde{\mathbf{x}}_j^e(t_k^{m-}), \Delta t_k, \tilde{\boldsymbol{\Lambda}}_{\bar{t}_k}^e) \in \boldsymbol{\Upsilon}_0$, with $\boldsymbol{\Upsilon}_0$ being a neighborhood of $(\tilde{\mathbf{x}}_j^e(t_k^{m-}) = \mathbf{0}, \Delta t_k = 0, \tilde{\boldsymbol{\Lambda}}_{\bar{t}_k}^e = \mathbf{0})$, one obtains

$$\|\tilde{\mathbf{x}}_i^e(t_k^{M+}) - \mathbf{0}\| \leq M_2 \left\| \begin{bmatrix} \tilde{\mathbf{x}}_j^e(t_k^{m-}) \\ \Delta t_k \\ \tilde{\boldsymbol{\Lambda}}_{\bar{t}_k}^e \end{bmatrix} \right\| \leq M_2\|\tilde{\mathbf{x}}_j^e(t_k^{m-})\| + M_2|\Delta t_k| + M_2\|\tilde{\boldsymbol{\Lambda}}_{\bar{t}_k}^e\|.$$
$$(6.38)$$

Considering that $\|\tilde{\boldsymbol{\Lambda}}_{\bar{t}_k}^e\| = \|\tilde{\boldsymbol{\Lambda}}_{\bar{t}_k}\|$, (6.38) proves (6.18) for each $k \in \mathcal{I}_N$.

Details of the proof of the facts (6.19) and (6.20)

During the free-motion phases the error dynamics $\tilde{\mathbf{x}}_i^e(t)$ are given by

$$
\begin{aligned}
\dot{\tilde{\mathbf{x}}}_i^e(t) = \dot{\mathbf{x}}_i^e(t) - \dot{\bar{\mathbf{x}}}_i^e(t) &= \bar{\mathbf{A}}_i^e \mathbf{x}_i^e(t) + \bar{\mathbf{B}}_i^e(\mathbf{y}(t) - \bar{\mathbf{y}}(t)) - \bar{\mathbf{A}}_i^e \bar{\mathbf{x}}_i^e(t) = \\
&= \bar{\mathbf{A}}_i^e \tilde{\mathbf{x}}_i^e(t) + \bar{\mathbf{B}}_i^e \bar{\mathbf{C}}_i^e \tilde{\mathbf{x}}_i^e(t) = (\bar{\mathbf{A}}_i^e + \bar{\mathbf{B}}_i^e \bar{\mathbf{C}}_i^e)\tilde{\mathbf{x}}_i^e(t) = \\
&= (\mathbf{A}_i^e + \mathbf{B}_i^e \mathbf{K}_i^e)\tilde{\mathbf{x}}_i^e(t),
\end{aligned} \tag{6.39}
$$

where (6.31) have been used and the dynamic matrix $(\mathbf{A}_i^e + \mathbf{B}_i^e \mathbf{K}_i^e)$ is Hurwitz (see 6.3). For later use, the following result is proved.

Lemma 4. *Let η be a positive constant such that all eigenvalues of the Hurwitz matrix $\mathbf{A} \in \mathbb{R}^{n \times n}$ have real part less than or equal to $-\eta$, then*

$$
\|e^{\mathbf{A}t}\| \le L(\eta, t)e^{-\eta t}, \tag{6.40a}
$$

and for each fixed $t = T > 0$, it hold that $\lim_{\eta \to +\infty} L(\eta, T)e^{-\eta T} = 0$, i.e.,

$$
\forall \varepsilon^* > 0, \exists \eta^* > 0 : \eta > \eta^* \Rightarrow L(\eta, T)e^{-\eta T} < \varepsilon^*. \tag{6.40b}
$$

Proof. In the following for the sake of simplicity the assumption of real and distinct eigenvalues will be considered. However, the present result can also be proved when $\mathbf{A}$ has complex and/or repeated eigenvalues by using wholly similar reasonings just needing a more cumbersome notation. The norm of the exponential matrix $e^{\mathbf{A}t}$ can be computed as:

$$
\|e^{\mathbf{A}t}\| = \|\mathcal{L}^{-1}((s\mathbf{I} - \mathbf{A})^{-1})\|, \tag{6.41}
$$

where $\mathcal{L}^{-1}(\cdot)$ denotes the inverse Laplace transform of the expression at argu-

ment. Let $\lambda_1, \lambda_2, \cdots, \lambda_n$ be the eigenvalues of $\mathbf{A}$, so that

$$\det(s\mathbf{I} - \mathbf{A}) = (s - \lambda_1)(s - \lambda_2)\cdots(s - \lambda_n),$$

and

$$(s\mathbf{I} - \mathbf{A})^{-1} = \frac{\mathbf{M}_1}{s - \lambda_1} + \frac{\mathbf{M}_2}{s - \lambda_2} + \cdots + \frac{\mathbf{M}_n}{s - \lambda_n}, \qquad (6.42)$$

where

$$
\begin{aligned}
\mathbf{M}_i &= \left[(s - \lambda_i)(s\mathbf{I} - \mathbf{A})^{-1}\right]\big|_{s=\lambda_i} = \left[(s - \lambda_i)\frac{\mathbf{Adj}(s\mathbf{I} - \mathbf{A})}{\det(s\mathbf{I} - \mathbf{A})}\right]\bigg|_{s=\lambda_i} = \\
&= \left[\frac{\mathbf{Adj}(s\mathbf{I} - \mathbf{A})}{(s - \lambda_1)\cdots(s - \lambda_{i-1})(s - \lambda_{i+1})\cdots(s - \lambda_n)}\right]\bigg|_{s=\lambda_i} = \\
&= \frac{\mathbf{Adj}(\lambda_i\mathbf{I} - \mathbf{A})}{\displaystyle\prod_{\substack{j=1 \\ j \neq i}}^{n}(\lambda_i - \lambda_j)}.
\end{aligned}
\qquad (6.43)
$$

The i-th eigenvalue λ_i can be rewritten in terms of η as $\lambda_i = -\mu_i\eta$ with μ_i being a positive real such that $\mu_i > 1$. It is clear that also the difference between two different eigenvalues can be rewritten in a similar way as $\lambda_i - \lambda_j = -(\mu_i - \mu_j)\eta$. From (6.43) it follows that

$$\mathbf{M}_i = \frac{\mathbf{Adj}(-\mu_i\eta\mathbf{I} - \mathbf{A})}{\displaystyle\prod_{\substack{j=1 \\ j \neq i}}^{n}(-(\mu_i - \mu_j)\eta)} = \gamma_i\frac{\mathbf{Adj}(-\mu_i\eta\mathbf{I} - \mathbf{A})}{\eta^{n-1}}, \qquad (6.44)$$

where $\gamma_i \in \mathbb{R}$. Now, since each element of the adjoint matrix is an algebraic complement of $(-\mu_i\eta\mathbf{I} - \mathbf{A})$, so that it is a polynomial in η of degree less than or equal to $n - 1$, from (6.44) it follows that each element of $\mathbf{M}_i$ is bounded

from above as $\eta \to +\infty$. By putting together (6.41),(6.42) one has

$$
\begin{aligned}
\|e^{\mathbf{A}t}\| &= \left\| \mathcal{L}^{-1} \left(\frac{\mathbf{M}_1}{s - \lambda_1} + \frac{\mathbf{M}_2}{s - \lambda_2} + \cdots + \frac{\mathbf{M}_n}{s - \lambda_n} \right) \right\| = \\
&= \left\| \mathbf{M}_1 e^{-\mu_1 \eta t} + \mathbf{M}_2 e^{-\mu_2 \eta t} + \cdots + \mathbf{M}_n e^{-\mu_n \eta t} \right\| \leq \\
&\leq \|\mathbf{M}_1\| e^{-\mu_1 \eta t} + \|\mathbf{M}_2\| e^{-\mu_2 \eta t} + \cdots + \|\mathbf{M}_n\| e^{-\mu_n \eta t} \leq \\
&\leq \underbrace{(\|\mathbf{M}_1\| + \|\mathbf{M}_2\| + \cdots + \|\mathbf{M}_n\|)}_{L(\eta)} e^{-\eta t}.
\end{aligned}
\tag{6.45}
$$

The boundedness of $L(\eta)$ together with (6.45) prove (6.40). $\qquad\qquad\square$

At this point, from Lemma 4 and (6.39) it follows that

$$
\|\tilde{\mathbf{x}}_i^e(t)\| \leq L(\eta, t - t_k^M) e^{-\eta(t - t_k^M)} \|\tilde{\mathbf{x}}_i^e(t_k^{M+})\|, \quad \forall t \in (t_k^M, t_{k+1}^m),
\tag{6.19}
$$

where $t_k^m := \min\{t_k, \bar{t}_k\}$, $t_k^M := \max\{t_k, \bar{t}_k\}$ and all the eigenvalues of $(\mathbf{A}_i^e + \mathbf{B}_i^e \mathbf{K}_i^e)$ have real part less than or equal to $-\eta$ with $\eta \in \mathbb{R}^+$. Moreover, for each fixed $T > 0$ the following fact holds

$$
\forall \varepsilon^* > 0, \exists \eta^* > 0 : \eta > \eta^* \Rightarrow L(\eta, T) e^{-\eta T} < \varepsilon^*.
\tag{6.20}
$$

Remark 38. If uncertainties are present on the plant description, then the eigenvalues of the actual matrix $(\mathbf{A}_i^e + \mathbf{B}_i^e \mathbf{K}_i^e)$ are in general different from the desired ones assigned by the choice of $\mathbf{K}_i^e$ in (6.3). In this case, a robust eigenvalues assignment has to be considered in order to guarantee that the eigenvalues of the closed-loop dynamic matrix still have real part less than or equal to $-\eta$ and so that the facts (6.19) and (6.20) still hold.

Details of the proof of the fact (6.21)

In presence of uncertainties the relation (6.14) cannot be used, so that in order to estimate the right reset value of the precompensator state vector at time $\bar{t}_k^+$, i.e., $\bar{\mathbf{\Lambda}}_{\bar{t}_k}$, the rule (6.3) is taken into account. From the definition of (6.3)

and by considering the periodicity of the target trajectory it follows that

$$\tilde{\mathbf{\Lambda}}_{\bar{t}_{k+N}} = \mathbf{\Lambda}_{\bar{t}_{k+N}} - \bar{\mathbf{\Lambda}}_{\bar{t}_{k+N}} = e^{-\mathbf{A}_a(\bar{t}_{k+1}-\bar{t}_k)}\mathbf{x}_a(\bar{t}_{k+1}^-) - e^{-\mathbf{A}_a(\bar{t}_{k+1}-\bar{t}_k)}\bar{\mathbf{x}}_a(\bar{t}_{k+1}^-) =$$
$$= e^{-\mathbf{A}_a(\bar{t}_{k+1}-\bar{t}_k)}\tilde{\mathbf{x}}_a(\bar{t}_{k+1}^-),$$

which implies

$$\|\tilde{\mathbf{\Lambda}}_{\bar{t}_{k+N}}\| \le M_a\|\tilde{\mathbf{x}}_a(\bar{t}_{k+1}^-)\|, \tag{6.46}$$

where $M_a := \max_{k \in \mathcal{I}_N}\|e^{-\mathbf{A}_a(\bar{t}_{k+1}-\bar{t}_k)}\| \in \mathbb{R}^+$. For each $k \in \mathcal{I}_N$, one has

$$\exists M_3 \in \mathbb{R}^+ : \|\tilde{\mathbf{\Lambda}}_{\bar{t}_{k+N}}\| \le M_3\|\tilde{\mathbf{x}}_i^e(t_{k+1}^{m-})\|. \tag{6.21}$$

where $i = \sigma(t_{k+1}^{m-})$. The two possible cases are considered separately.

Case a) $t_{k+1}^m = t_{k+1}$ and $t_{k+1}^M = \bar{t}_{k+1}$. From (6.46), one has

$$\|\tilde{\mathbf{\Lambda}}_{\bar{t}_{k+N}}\| \le M_a\|\mathbf{x}_a(\bar{t}_{k+1}^-) - \bar{\mathbf{x}}_a(\bar{t}_{k+1}^-)\| = M_a\|e^{\mathbf{A}_a(t_{k+1}^M - t_{k+1}^m)}\tilde{\mathbf{x}}_a(t_{k+1}^+)\| \le$$
$$\le M_a M_{a,1}\|\tilde{\mathbf{x}}_a(t_{k+1}^-)\| \le M_a M_{a,1}\|\tilde{\mathbf{x}}_i^e(t_{k+1}^-)\| =: M_{3a}\|\tilde{\mathbf{x}}_i^e(t_{k+1}^{m-})\|,$$

where $M_{a,1} := \max_{k \in \mathcal{I}_N}\|e^{-\mathbf{A}_a\Delta t_{k+1}}\|$ with $|\Delta t_{k+1}| < \omega_{k+1} \in \mathbb{R}$ (see step **(i)**) of the proof of Theorem 11).

Case b) $t_{k+1}^m = \bar{t}_{k+1}$ and $t_{k+1}^M = t_{k+1}$. From (6.46), one has

$$\|\tilde{\mathbf{\Lambda}}_{\bar{t}_{k+N}}\| \le M_a\|\tilde{\mathbf{x}}_a(\bar{t}_{k+1}^-)\| \le M_a\|\tilde{\mathbf{x}}_i^e(t_{k+1}^{m-})\|.$$

Therefore, (6.21) follows by choosing $M_3 := \max\{M_{3a}, M_a\}$.

Chapter 7

Conclusions and future works

This thesis focused on the problem of asymptotic trajectory tracking for dynamical systems with discontinuities in the state vector, e.g. mechanical systems subject to impacts.

The Birkhoff elliptical billiard system has been considered as benchmark for theory. In particular, after giving a procedure based on LMIs techniques for determining admissible periodic trajectories inside an elliptical billiards, a tracking control problem taking into account the nonsmooth nature of the considered system has been defined and solved by using a dynamic compensator, whose state is subject to discontinuities and whose structure is based on the internal model principle. First, it was assumed that the plant description is exactly known and the moving mass is not subject to friction. Such assumptions are removed later and the tracking control problem is defined and solved in both cases of *Full-Information* (i.e., the whole plant state vector is accessible) and *Error-Feedback* (i.e., only the position error is available for feedback). In both of them, a solution based on a nonsmooth version of the internal model principle is used and due to the possible presence of uncertainties on the system parameters, an algorithm to estimate the correct jumps for the controller is implemented.

In the second part of this thesis, the results obtained for the elliptical

billiard system have been generalized for a class of switched systems having linear dynamics between switching events and linear reset maps. A numerical examples is also presented in order to show the effectiveness of the proposed control strategy.

In the following, the list of publications that contain the present work is reported:

- A. Potini, A. Tornambè, L. Menini, P. Dorato, C. T. Abdallah *Finite-Time control of linear mechanical systems subject to nonsmooth impacts.* Proc. of 14th Mediter. Conf. on Control and Automation, Ancona. 2006

- S. Galeani, L. Menini, A. Potini, A. Tornambè *Asymptotic tracking of periodic trajectories for a particle in an elliptical billiards.* Proc. of 26th American Control Conf., New York. 2007

- S. Galeani, L. Menini, A. Potini, A. Tornambè *Trajectory tracking for a particle in elliptical billiards.* International Journal of Control. 2007

- S. Galeani, L. Menini, A. Potini, A. Tornambè *Robust asymptotic tracking of periodic trajectories in elliptical billiards.* Proc. of 46th Conf. on Decision and Control, New Orleans. 2007

- S. Galeani, L. Menini, A. Potini *Trajectory tracking in linear hybrid systems: an internal model principle approach.* Submitted to 27th American Control Conf., Seattle. 2008

Further work may be devoted to weaken the requirements, in order to render the approach more amenable to applications. First of all, a global tracking problem (i.e., when no assumption of small initial errors is made) could be considered. Moreover, the class of considered systems should be enlarged by considering more generic hybrid systems (with real discrete dynamics) together with nonlinear switching surfaces and reset maps.

Bibliography

[1] M. Abramowitz and I. Stegun. *Handbook of Mathematical Functions*. Dover, New York, 1964.

[2] P. J. Antsaklis, J. A. Stiver, and M. D. Lemmon. Hybrid system modeling and autonomous control systems. *Lecture Notes in Computer Science*, 736:366–392, 1993.

[3] T. M. Apostol. *Mathematical Analysis* 2nd *ed.* Addison-Wesley, Reading, MA, 1974.

[4] A. Back, J. Guckenheimer, and M. Myers. A dynamical simulation facility for hybrid systems. *Hybrid Systems, Lecture Notes in Computer Science*, 736:255–267, 1993.

[5] M. Berger. *Geometry*. Springer-Verlag, Berlin, 1987.

[6] V. Berry and M. Tabor. Closed orbits and the regular bound spectrum. *Proc. R. Soc. London, Ser. A 349*, page 101123, 1976.

[7] G. D. Birkhoff. Dynamical system. *AMS Coll.*, IX, 1927.

[8] G. A. Bliss. *Lectures on the Calculus of Variations*. University of Chicago Press, Chicago, IL, 1946.

[9] J. M. Bourgeot and B. Brogliato. Tracking control of complementarity Lagrangian systems. *Int. J. of Bifurcation and Chaos*, 15(6):1839–1866, 2005.

[10] M. S. Branicky. *Studies in Hybrid Systems: Modeling, Analysis, and Control.* PhD thesis, Massachusetts Institute of Technology, June 1995.

[11] M. S. Branicky, V. S. Borkar, and S. K. Mitter. A unified framework for hybrid control: Model and optimal control theory. *IEEE Trans. Aut. Control*, 43(1):31–45, 1998.

[12] M. S. Branicky, V. S. Borkar, and S. K. Mitter. A Unified Framework for Hybrid Control: Model and Optimal Control Theory. *IEEE Trans. Aut. Control*, 43(1):31–45, 1998.

[13] R. W. Brockett. Hybrid models for motion control systems. *Essays on Control: Perspectives in the Theory and Its Applications*, pages 29–53, 1993.

[14] B. Brogliato. *Nonsmooth impact mechanics.* Springer-Verlag, London, 1996.

[15] B. Brogliato, S. I. Niculescu, and M. Monteiro-Marques. On tracking control of a class of complementary-slackness hybrid mechanical systems. *Systems and Control Letters*, 39:255–266, 2000.

[16] B. Brogliato, S. I. Niculescu, and P. Orthant. On the control of finite-dimensional mechanical systems with unilateral constraints. *IEEE Transactions on Automatic Control*, 42(2):200–215, 1997.

[17] B. Brogliato and A. Zavala-Rio. On the control of Complementary-Slackness Juggling Mechanical Systems. *IEEE Trans. Aut. Control*, 45(2):235–246, 2000.

[18] M. Buehler, D. E. Koditschek, and P. J. Kindlmann. Planning and control of robotic juggling and catching tasks. *Inter. J. of Robotics Res.*, 13(2):101118, 1994.

[19] J. Buisson. Analysis and characterisation of hybrid systems with Bond-Graphs. In *Proc. IEEE Conf. Syst. Man and Cybernetics*, pages 264–269, Lille, 1993.

[20] J. Buisson and H. Cormerais. Modeling hybrid linear systems with bond-graph using an implicit formulation. *The Bond Graph Digest*, 1, 1997.

[21] A. Cayley. *Geometry*. Springer-Verlag, Berlin, 1987.

[22] S. J. Chang and R. Friedberg. Elliptical billiards and Poncelet's theorem. *J. of Math. Physics*, 29:1537–1550, 1988.

[23] C. T. Chen. *Linear System Theory and Design*. Saunders College Publishing, Fort Worth, TX, 1984.

[24] B. Crespi and S. J. Chang. Elliptical billiards and hyperelliptic functions. *J. of Math. Physics*, 34:2257–2289, 1993.

[25] E. J. Davison. The Output Control of Linear Time-Invariant Multivariable Systems with Unmeasurable Arbitrary Disturbances. *IEEE Trans. Aut. Control*, 17:621–630, 1972.

[26] E. De Santis, M. D. Di Benedetto, and G. Pola. Digital control of continuous-time switching systems with safety constraints. In *Proc. 43rd IEEE Conf. Decision and Control*, pages 1878–1883, Paradise Island, Bahamas, Dec. 2004.

[27] E. De Santis, M. D. Di Benedetto, and G. Pola. Stabilizability based state space reductions for hybrid systems. In *Proc. 2nd IFAC Conf. Analysis and Design of Hybrid Systems*, pages 112–117, Alghero, IT, Jun. 2006. Preprints.

[28] V. Dragovic and M. Radnovic. Conditions of Cayley's type for ellipsoidal billiard. *J. Math. Phys.*, 39(1):355–362, 1998.

[29] V. Dragovic and M. Radnovic. On periodical trajectories of the billiard systems within an ellipsoid in $\mathbb{R}^d$ and generalized Cayley's condition. *J. Math. Phys.*, 39(11):5866–5869, 1998.

[30] V. Dragovic and M. Radnovic. Geometry of integrable billiards and pencils of quadrics. *J. Math. Pures Appl.*, 85:758–790, 2006.

[31] N. H. El-Farra, A. Gani, and P. D. Christofides. A Switched Systems Approach for the Analysis Mode Transitions in Biological Networks. In *Proc. IEEE American Control Conf.*, pages 3247–3252, Portland, OR, USA, June 2005.

[32] S. Galeani, L. Menini, A. Potini, and A. Tornambè. Robust asymptotic tracking of periodic trajectories in elliptical billiards. In *IEEE Conf. on Decision and Control*, New Orleans, LA, Dec. 2007. (to appear).

[33] S. Galeani, L. Menini, A. Potini, and A. Tornambè. Trajectory tracking for a particle in elliptical billiards. *Int. J. of Control*, 2007. (in press).

[34] P. J. Gawthrop. Hybrid Bond Graphs Using Switched I and C Components. *CSC report*, 97005, 1997.

[35] M. Gerard and R. Sepulchre. Stabilization through weak and occasional interactions: a billiard benchmark. In *Proc. of the 4th IFAC Symp. on Nonlinear Control Systems*, pages 73–78, 2004.

[36] H. Goldstein, C. Poole, and J. Safko. *Classical Mechanics*. Addison-Wesley, 2000.

[37] 0. M. Grasselli, S. Longhi, and A. Tornambè. Robust tracking and performance for multivariable systems under physical parameter uncertainties. *Automatica*, 29(1):169–179, 1993.

[38] D. H. Griffel. *Applied Functional Analysis*. Courier Dover Publications, 2002.

[39] P. Griffiths and J. Harris. On cayley's explicit solution to Poncelet's porism. *Enseign. Math.*, 24(1-2):31–40, 1978.

[40] W. P. M. H. Heemels and B. Brogliato. The Complementarity Class of Hybrid Dynamical Systems. *Eur. J. of Control*, 9(2-3):322–360, 2003.

[41] M. F. Heertjes, M. J. G. van den Molengraft, J. J. Kok, and D. H. van Campen. Vibration reduction of a harmonically excited beam with one-sided springs using sliding computed torque control. *Dynamics and control*, 7:361–375, 1997.

[42] D. Henrion and J. B. Lasserre. LMIs for constrained polynomial interpolation with application in trajectory planning. *Systems and Control Letters*, 55(6):473–477, 2006.

[43] D. Henrion, S. Tarbouriech, and V. Kučera. Control of Linear Systems subject to Time-Domain Constraints with Polynomial Pole Placement and LMIs. *IEEE Trans. Aut. Control*, 50(9):1360–1363, 2005.

[44] J. E. Hopcroft and J. D. Ullman. *Introduction to Automata Theory, Languages, and Computation*. Addison-Wesley, Reading, Massachusetts, 1979.

[45] Y. Hurmuzlu, F. Génot, and B. Brogliato. Modelling, stability and control of biped robots – A general framework. *Automatica*, 40:1647–1664, 2004.

[46] T. Izumi and Y. Hitaka. Hitting from any Direction in 3-D Space by a Robot with a Flexible Link Hammer. *IEEE Trans. Robot. & Aut.*, 13(2):296–301, 1997.

[47] K. H. Johansson. *Encyclopedia of Life Support Systems (EOLSS)*, chapter Hybrid Control Systems. H. Unbehauen, Ed., 2004. Theme 6.43: Control Systems, Robotics and Automation. Developed under the auspices of UNESCO.

[48] V. V. Kozlov and D. V. Treshchëv. *Billiards: a genetic introduction to the dynamics of systems with impacts.* American Math. Society, Providence, RI, 1991.

[49] V. Kucera. *Discrete Linear Control: The Polynomial Equation Approach.* John Wiley & Sons, Inc., New York, NY, USA, 1980.

[50] V. Lakshmikantham, D. D. Bainov, and P. S. Simeonov. *Theory of impulsive differential equations*, volume 6. World Scientific, 1989.

[51] H. Lebesgue. *Les coniques.* Gauthier-Villars, Paris, 1942.

[52] M. Levi and S. Tabachnikov. The Poncelet grid and the billiard in an ellipse. *ArXiv Mathematics e-prints*, 2005.

[53] D. Liberzon. *Switching in Systems and Control.* Birkhäuser, 2003.

[54] D. Liberzon and A. S. Morse. Basic Problems in Stability and Design of Switched Systems. *Lecture Notes*, pages 59–70, 1999.

[55] D. G. Luenberger. *Linear and nonlinear programming.* Addison-Wesley, Reading, MA, 1989.

[56] L. Menini and A. Tornambè. Asymptotic Tracking of Periodic Trajectories for a Simple Mechanical System Subject to Nonsmooth Impacts. *IEEE Trans. Aut. Control*, 46:1122–1126, 2001.

[57] G. Meyer. Design of flight vehicle management systems. In *Proc. IEEE Conf. Decision Contr.*, Lake Buena Vista, FL, USA, Dec. 1994. Plenary lecture.

[58] J. K. Mills and D. M. Lokhorst. Control of robotic manipulators during general task execution: a discontinuous control approach. *Int. J. Robotics Res.*, 12(2):146–163, 1993.

[59] J. J. Moreau. *Non-Smooth Mechanics and Applications*, chapter Unilateral contact and dry friction in finite freedom dynamics, pages 1–82. Springer, 1988.

[60] J. J. Moreau. *Topics in Nonsmooth Mechanics*, chapter Bounded variation in time, pages 1–74. Birkhäuser Verlag, 1988.

[61] B. Morris and J. W. Grizzle. A Restricted Poincaré Map for Determining Exponentially Stable Periodic Orbits in Systems with Impulse Effects: Application to Bipedal Robots. *Proc. 44th IEEE Conf. Decision and Control*, pages 4199–4206, 2005.

[62] P. J. Mosterman and G. Biswas. A theory of discontinuities in physical system models. *J. of the Franklin Institute*, 40(6), 1996.

[63] A. Nerode and W. Kohn. Models for hybrid systems: Automata, topologies, controllability, observability. *Lecture Notes in Computer Science*, 736:317–356, 1993.

[64] Y. Nesterov. *Squared Functional Systems and Optimization Problems*. Kluwer Academic Publishers, Dordrecht, 2000.

[65] P. R. Pagilla. Control of Contact Problem in Constrained Euler-Lagrange Systems. *IEEE Trans. Aut. Control*, 46(10):1595–1599, 2001.

[66] T. S. Parker and L. O. Chua. *Practical Numerical Algorithms for Chaotic Systems*. Springer-Verlag, New York, 1989.

[67] F. Pfeiffer and C. Glocker. *Multibody Dynamics with Unilateral Contacts*. Wiley, Chichester, 1996.

[68] J. V. Poncelet. *Traité des Propriétés Projectives des Figures*. (vol. 1-2, 2nd ed., Gauthier-Villars, Paris, 1865-66), Bachelier, Paris, 1822.

[69] P.Pagilla and B. Yu. A stable transition controller for constrained robots. *IEEE/ASME Trans. on Mechatronics*, 6(1):65–74, 2001.

[70] P.Pagilla and B. Yu. An experimental study of a planar impact of a robot manipulator. *IEEE/ASME Trans. on Mechatronics*, 9(1):123–128, 2004.

[71] B. De Schutter, W. P. M. H. Heemels, and A. Bemporad. *Modeling and Control of Hybrid Systems*. Lecture Notes of the DISC Course, 2003.

[72] W. J. Schwind and D. E. Koditschek. Control of Forward Velocity for a Simplified Planar Hopping Robot. In *IEEE Conf. Robotics and Automation*, pages 691–696, 1995.

[73] R. Sepulchre and M. Gerard. Stabilization of periodic orbits in a wedge billiard. In *Proc. of the 42nd IEEE Conf. on Decis. and Contr.*, pages 1568–1573, 2003.

[74] D. Shevitz and B. Paden. Lyapunov stability theory of nonsmooth systems. *IEEE Trans. Automat. Contr.*, 39:1910–1914, 1994.

[75] M. Sieber. Semiclassical transition from an elliptical to an oval billiard. *J. Phys. A: Math. Gen.*, 30:4563–4596, 1997.

[76] J. F. Sturm. Using Sedumi 1.02, a Matlab Toolbox for Optimization over Symmetric Cones. *Optimization Methods and Software*, 11-12:625–653, 1999.

[77] A. Tornambè. Modelling and Control of Impact in Mechanical Systems: Theory and Experimental Results. *IEEE Trans. Aut. Control*, 44(2):294–309, 1999.

[78] F. A. Valentine. *The Problem of Lagrange with Differential Inequalities as Added Side Conditions*. Univ. Chicago Press, Chicago, IL, 1937.

[79] A. van der Schaft. *L2-Gain and Passivity in Nonlinear Control*. Springer-Verlag New York, Inc., Secaucus, NJ, USA, 1999.

[80] T. L. Vincent. Controlling a ball to bounce at a fixed height. *In Proceedings of the American Control Conference*, 1:842–846, 1995.

[81] S. Vorapojpisut. Well-Posedness of a Class of Bimodal Modular Dynamical Systems. *Thammasat Int. J. Sc. Tech.*, 11(3):7–16, 2006.

[82] F. Y. M. Wan. *Introduction To The Calculus of Variations And Its Applications,* 2$^{\text{nd}}$ *ed.* CRC Press, 1995.

[83] P. K. C. Wang and F. Y. Hadaegh. Stability Analysis of Switched Dynamical Systems with State-Space Dilation and Contration. In *AIAA Guid., Navig. and Control Conf.*, Keystone, CO, Aug. 2006.

[84] E. R. Westervelt, J. W. Grizzle, and D. E. Koditschek. Hybrid Zero Dynamics of Planar Biped Walkers. *IEEE Trans. Aut. Control*, 48:42–56, 2003.

[85] E. T. Whittaker and G. N. Watson. *A Course of Modern Analysis.* Cambridge Univ. Press, 1927.

[86] J. Wiersig. Quantum-classical correspondence in polygonal billiards. *Phys. Rev. E*, 64(2):026212, 2001.

[87] L. Zaccarian, D. Nešić, and A. R. Teel. First order reset elements and the Clegg integrator revisited. In *IEEE Amer. Control Conf.*, pages 563–568, Portland, OR, USA, Jun. 2005.

[88] A. Zavala-Rio and B. Brogliato. On the control of a one degree-of-freedom juggling robot. *Dynamics and Control*, 9(7):67–90, 1999.

[89] J. Zhang, A. C. Merchant, and W. D. M. Rae. Geometric derivations of the second constant of motion for an elliptic billiard and other results. *Eur. J. of Phys.*, 15:133138, 1994.